

A CHANDRA-SWIFT VIEW OF POINT SOURCES IN HICKSON COMPACT GROUPS: HIGH AGN FRACTION BUT A DEARTH OF STRONG AGNS

P. TZANAVARIS^{1,2,3}, S. C. GALLAGHER⁴, A. E. HORNSCHEMEIER¹, K. FEDOTOV^{4,5}, M. ERACLEOUS^{5,6}, W. N. BRANDT^{5,6}, T. D. DESJARDINS⁴, J. C. CHARLTON⁵, C. GRONWALL^{5,6}

Accepted by ApJS

ABSTRACT

We present *Chandra* X-ray point source catalogs for 9 Hickson Compact Groups (HCGs, 37 galaxies) at distances 34 – 89 Mpc. We perform detailed X-ray point source detection and photometry, and interpret the point source population by means of simulated hardness ratios. We thus estimate X-ray luminosities (L_X) for all sources, most of which are too weak for reliable spectral fitting. For all sources, we provide catalogs with counts, count rates, power-law indices (Γ), hardness ratios, and L_X , in the full (0.5 – 8.0 keV), soft (0.5 – 2.0 keV) and hard (2.0 – 8.0 keV) bands. We use optical emission-line ratios from the literature to re-classify 24 galaxies as star-forming, accreting onto a supermassive black hole (AGNs), transition objects, or low-ionization nuclear emission regions (LINERs). Two-thirds of our galaxies have nuclear X-ray sources with *Swift*/UVOT counterparts. Two nuclei have $L_{X,0.5-8.0\text{keV}} > 10^{42} \text{ erg s}^{-1}$, are strong multi-wavelength AGNs and follow the known $\alpha_{\text{OX}} - \nu L_{\nu(\text{nearUV})}$ correlation for strong AGNs. Otherwise, most nuclei are X-ray faint, consistent with either a low-luminosity AGN or a nuclear X-ray binary population, and fall in the “non-AGN locus” in $\alpha_{\text{OX}} - \nu L_{\nu(\text{nearUV})}$ space, which also hosts other, normal, galaxies. Our results suggest that HCG X-ray nuclei in high specific star formation rate spiral galaxies are likely dominated by star formation, while those with low specific star formation rates in earlier types likely harbor a weak AGN. The AGN fraction in HCG galaxies with $M_R \leq -20$ and $L_{X,0.5-8.0\text{keV}} \geq 10^{41} \text{ erg s}^{-1}$ is $0.08^{+0.35}_{-0.01}$, somewhat higher than the $\sim 5\%$ fraction in galaxy clusters.

Subject headings: galaxies: nuclei — galaxies: active — ultraviolet: galaxies — X-rays: galaxies — catalogs

1. INTRODUCTION

By virtue of their selection criteria, Hickson Compact Groups (HCGs) constitute a distinct class among small galaxy agglomerations. The Hickson catalog (Hickson 1982; Hickson et al. 1992) comprises 92 spectroscopically confirmed, nearby (median redshift $z_{\text{med}} = 0.03$, ~ 130 Mpc) compact groups with three or more members with accordant redshifts (i.e., within 1000 km s^{-1} of the group mean). The characteristic physical properties of CGs (Hickson et al. 1992) include galaxy separations of the order of a few galaxy radii (median projected separations $\sim 40h^{-1} \text{ kpc}$), low velocity dispersions (radial median $\sim 200 \text{ km s}^{-1}$) and high galaxy number densities (up to $10^8 h^2 \text{ Mpc}^{-2}$). These conditions favor galaxy interactions, as demonstrated by the spectacular examples of HCG 92 (Stephan’s Quintet, e.g. Fedotov et al. 2011) and HCG 31 (Gallagher et al. 2010). It is then natural to ask what influence this interaction-prone environment has on processes related to star-formation or accretion onto a nuclear supermassive black hole.

¹ Laboratory for X-ray Astrophysics, NASA/Goddard Spaceflight Center, Mail Code 662, Greenbelt, Maryland, 20771, USA

² Department of Physics and Astronomy, The Johns Hopkins University, Baltimore, MD 21218, USA

³ NPP Fellow

⁴ Department of Physics and Astronomy, The University of Western Ontario, London, ON N6A 3K7, Canada

⁵ Department of Astronomy and Astrophysics, The Pennsylvania State University, University Park, PA 16802, USA

⁶ The Institute for Gravitation and the Cosmos, The Pennsylvania State University, University Park, PA 16802, USA

⁵ Herzberg Institute Of Astrophysics, Victoria, BC, V9E 2E7, Canada

With regards to star formation, recent work suggests that, compared to non-compact group environments, star formation is accelerated, leading to rapid exhaustion of the gas supply sustaining star forming activity. This result follows from ultraviolet and infrared star-formation estimates that show significant discontinuities in mid-infrared colors and ultraviolet+infrared specific star formation rates (SSFRs, Johnson et al. 2007; Tzanavaris et al. 2010; Walker et al. 2010, 2012). In particular, the discontinuities indicate a bimodality between galaxies with high levels of star formation and those with little star formation. The latter have also been found to exhibit high levels of “H I deficiency”, Def_{HI} , as defined by Verdes-Montenegro et al. (2001). These authors predict an expected H I mass for field galaxies of a given morphological type and compare it to the H I mass of compact group galaxies, thus calculating Def_{HI} . Taken together, the lack of galaxies with intermediate mid-infrared colors and SSFRs, as well as the high Def_{HI} values are suggestive of accelerated and then abruptly truncated star formation.

The importance of accretion onto a nuclear supermassive black hole (SMBH) in compact groups (“AGN”⁸) has not been thoroughly investigated and is not well established. In galaxy clusters Dressler et al. (1985) found fewer AGNs compared to the field (but see also Martini et al. 2006, and below). Compared to clusters, compact groups of galaxies have lower velocity disper-

⁸ In line with common usage in the literature we shall use the acronym “AGN” (active galactic nucleus) to refer to accretion onto a nuclear supermassive black hole. Strictly this is incorrect as nuclear activity can also be due to star formation.

TABLE 1:
Chandra observation log for this HCG sample

HCG ID (1)	Obs. ID (2)	Obs. Start Date (3)	Detector (4)	Obs. time (5) (ks)	Obs. type (6)	PI (7)	References (8)
HCG 7	8171	2007-09-13	ACIS-S	19.4	GTO	Garmire	
HCG 7	9588	2007-09-16	ACIS-S	16.9	GTO	Garmire	
				36.3			Konstantopoulos et al. (2010)
HCG 16	923	2000-11-16	ACIS-S	12.7	GO	Mamon	Jeltema et al. (2008)
HCG 22	8172	2006-11-23	ACIS-S	32.2	GTO	Garmire	Desjardins et al. (2013)
HCG 31	9405	2007-11-15	ACIS-S	36.0	GO	Gallagher	Smith et al. (2012)
HCG 42	3215	2002-03-26	ACIS-S	32.1	GO	Ponman	Jeltema et al. (2008)
HCG 59	9406	2008-04-12	ACIS-S	38.9	GO	Gallagher	Desjardins et al. (2013)
HCG 62	921	2000-01-25	ACIS-S	49.1	GO	Vrtilek	
HCG 62	10462	2009-03-02	ACIS-S	68.0	GO	Rafferty	
HCG 62	10874	2009-03-03	ACIS-S	52.0	GO	Rafferty	
				169.2			Jeltema et al. (2008)
HCG 90	905	2000-07-02	ACIS-I	50.2	GO	Bothun	Jeltema et al. (2008)
HCG 92	7924	2007-08-17	ACIS-S	94.4	GO	Vrtilek	
HCG 92	789	2000-07-09	ACIS-S	20.0	GO	Trinchieri	
				114.4			O'Sullivan et al. (2009)

NOTE. — Columns are: (1) HCG group name; (2) observation ID; (3) start date of observation; (4) detector; (5) exposure time; (6) observation type (Guaranteed Time observing or General Observer proposal); (7) principal investigator; (8) references (first publication using these data). Total exposure times for each group appear in bold.

sions making prolonged close interactions more likely. It is thus possible that the level of AGN activity is different. On the theoretical and computational side, simulation work (e.g. Hopkins & Quataert 2010) suggests that major galaxy mergers are a leading mechanism that can trigger inflow of rotationally supported gas to feed a central SMBH. Note though that this would also provide fuel for intense star formation and could trigger nuclear starbursts (e.g. Mihos & Hernquist 1996). Other feeding mechanisms include supernova winds, minor interactions, and disk instabilities. Several observational surveys have provided insight on the connection between AGNs and galaxy interactions. For instance Kartaltepe et al. (2010) find that AGNs are common in Ultraluminous and Hyperluminous Infrared Galaxies (ULIRGs and HyLIRGs), which are known to result from major mergers. In addition, the AGN fraction in this population increases with infrared luminosity. Recently, Silverman et al. (2011) find increased AGN activity in pairs compared to isolated galaxies. On the other hand, several authors find minor interactions and secular evolution to be most important in triggering AGN activity (e.g. Grogan et al. 2005; Georgakakis et al. 2009; Cisternas et al. 2011; Deng et al. 2013).

In the optical regime, Coziol et al. (1998b,a, 2004) used emission-line ratios in several samples (up to 91 galaxies in 27 compact groups) to determine the type of nuclear activity in compact group galaxies, consistently finding that strong and low-luminosity ($L_{\text{H}\alpha} \lesssim 10^{39} \text{ erg s}^{-1}$) AGNs (LLAGNs) each make up no more than $\sim 10\%$ of the total CG populations (see Coziol et al. 2004, Table 3). Depending on the specific sample, star-forming galaxies represent a fraction up to $\sim 34\%$ of the population, with the remaining galaxies showing no emission lines. Both LLAGNs and AGNs are found mainly in optically luminous early type galaxies with little on-going star formation that are in the centers of evolved groups. This finding was interpreted to indicate that such group cores are old, collapsed systems where star formation activity has ceased. According to this interpretation, high central densities of group cores induced gravitational in-

teractions, which accelerated star formation, rapidly consuming all of the available fuel.

It is important to note that the fractions for “LLAGNs” presented by these authors also include low-ionization nuclear emission regions (LINERs), the nature of which is still a matter of debate. LINERs are characterized by high ratios of narrow optical low ionization oxygen emission lines (Heckman 1980) and are found in about half of all nearby galaxies (Ho et al. 1997). Candidate power sources for LINERs include (1) weak AGNs (e.g. Halpern & Steiner 1983; Ferland & Netzer 1983), (2) hot stars (e.g. Terlevich & Melnick 1985; Filippenko & Terlevich 1992; Shields 1992), and (3) shocks (e.g. Heckman 1980; Dopita et al. 1996). Although weak AGNs have been found in the majority ($\sim 75\%$) of LINERs (e.g. Barth et al. 1998; Ho et al. 2001; Filho et al. 2004; Nagar et al. 2005; Maoz et al. 2005; Flohic et al. 2006; González-Martín et al. 2009), they cannot account for the total LINER emission in the majority of cases (Eracleous et al. 2010a). In fact, for most LINERs Eracleous et al. (2010a) show that there is an energy deficit problem: Star formation and AGN activity are not able to provide a sufficient number of ionizing photons to account for the observed emission lines.

In the most recent optical study Martínez et al. (2010, hereafter M10) compiled a large spectroscopic sample of 280 galaxies in 64 HCGs and used emission-line ratios to classify the type of nuclear activity, providing an estimate for the AGN fraction in HCGs.

They classified 23% of galaxies as AGNs, 10% as transition objects (TO), and 14% as star forming (SF), with the remainder of the galaxies showing no emission lines. According to this study, although AGNs appear to be the most numerous emission-line galaxy class in CGs, they have characteristically low $\text{H}\alpha$ luminosities (median $7.1 \times 10^{39} \text{ erg s}^{-1}$) and virtually no broad emission lines, suggestive of LLAGNs. However, these authors use a restricted set of line ratios that precludes distinguishing between LINERs and AGN.

In this paper we use the Kewley et al. (2006) method

to reclassify the galaxies of M10. This allows us to also identify LINER systems. To stress that this is an optically based classification, we use the designations optAGN, optTO, optSF, optLINER.

Work in different wavelength regimes can provide complementary insight into these questions. Gallagher et al. (2008) used $1 - 24\mu\text{m}$ 2MASS+*Spitzer* nuclear data to probe the nuclear activity in 46 galaxies from 12 nearby HCGs. They found that the spectral index, α_{IRAC} , of a power law fit to the $4.5 - 8.0\mu\text{m}$ IRAC data cleanly separates MIR-active from MIR-inactive HCG nuclei. Unfortunately, the exact origin of activity (whether AGN or star-formation) cannot be deduced by this method. In particular, these authors show that hot dust emission can be responsible for their results, and this can be due either to hard ionizing AGN continua or AGB populations in star forming galaxies. On the other hand, Roche et al. (1991) have shown that MIR-inactivity ($\alpha_{\text{IRAC}} > 0$) is associated with *low-luminosity* AGN activity.

Due to the high-energy emission generated by supermassive black hole accretion, by far the best direct diagnostic for strong AGN activity is nuclear X-ray emission. Compared to the optical, the X-ray regime offers the advantage that the nuclear emission is not diluted by starlight from the host galaxy, while dust obscuration is very significantly mitigated due to the higher, penetrating power of X-ray radiation. Unfortunately, this simple picture is complicated by the combined effect of two factors. First, X-ray starlight sometimes can actually dilute AGN emission. This is because X-ray binary (XRB) populations in circumnuclear star clusters also emit in the X-ray regime, although *individual* XRBs typically have lower luminosities than strong AGNs. Second, as the name implies, LLAGNs emit at low X-ray luminosities. Adopting a fiducial threshold of $L_{X,0.5-8.0\text{keV}} = 10^{41-42} \text{ erg s}^{-1}$, it is only at higher X-ray luminosities that nuclear X-ray emission can be attributed to an AGN with high probability. Thus the situation becomes increasingly ambiguous at progressively fainter luminosities, making it challenging to distinguish between X-ray emission due to unresolved populations of circumnuclear XRBs and that of LLAGNs. In this regime high angular resolution becomes critical for distinguishing nuclear from circumnuclear emission.

Although earlier studies did detect X-ray emission in HCGs, they were hampered by poor angular resolution and the lack of hard X-ray sensitivity, making it difficult to disentangle the contributions from point source (nuclear or extra-nuclear) and diffuse emission, and essentially concentrated on studying the diffuse component. Using *ROSAT* data, Ponman et al. (1996) detected a diffuse IGM in $\sim 75\%$ of a large HCG sample, while Mulchaey et al. (2003), using a low-redshift sample of 109 groups that included poor, compact as well as rich, non-compact systems found diffuse, extended X-ray emission in 61 groups (56%). In an effort to understand the relevance of ram-pressure stripping and strangulation due to a hot IGM in the most H I-deficient HCGs, Rasmussen et al. (2008) also examined the level of nuclear activity in a sample of 8 HCGs, finding no significant enhancement. However, they do not carry out a detailed high angular resolution study to provide more specific results on the nature of nuclear activity in their systems.

The level of AGN activity in galaxy *clusters* has already been systematically investigated in the X-ray regime, leading to differing conclusions (e.g. see Ehlert et al. 2013, for a review). Using a multi-wavelength approach that includes emission lines, X-ray spectral properties and X-ray to visible-wavelength flux ratios in rich clusters, Martini et al. (2006) find that $\sim 5\%$ of cluster galaxies more luminous than $M_R = -20$ host AGNs with $L_{X,0.5-8.0\text{keV}} > 10^{41} \text{ erg s}^{-1}$. They notably also find a discrepancy between the AGN fraction determined from optical spectroscopy and a higher fraction suggested by X-ray luminosities. Interestingly, Shen et al. (2007) compare the environments of poor groups and clusters using a combined optical and X-ray approach. They conclude that poor groups host AGNs that are in an optically dominant phase, whereas those in clusters are dominant in the X-rays, leading to the findings of Martini et al. (2006).

In compact groups there has been to-date no systematic study of nuclear X-ray emission. In this paper we take advantage of the superb angular resolution of the *Chandra* X-ray observatory to carry out detailed point source detection in a sample of 9 compact groups (37 galaxies). This paper has two main goals: First, we make available full X-ray source catalogs based on the *Chandra* observations in 9 compact group fields with detailed information on counts, fluxes, luminosities and hardness ratios. Second, we focus on point sources located in HCG galaxy nuclei. Using *Chandra* and *Swift/Ultra-Violet and Optical Telescope* (UVOT; Roming et al. 2005) data, we combine X-ray and ultraviolet (UV) nuclear photometry, and compare with radio and optical diagnostics to assess the nature of nuclear activity in compact group galaxies. In a separate paper, we discuss the diffuse X-ray emission in the same sample of compact groups (Desjardins et al. 2013). Some of the *Chandra* data have first been presented previously in a different context. We give appropriate references in Table 1.

The structure of the paper is as follows: Section 2 introduces our sample. Section 3 discusses X-ray data and analysis and point source detections. Section 4 presents UV nuclear data and analysis. Section 5 presents multi-wavelength analyses, including new optical emission-line ratio classifications, radio data and a combined X-ray-UV analysis. Section 6 presents estimates on the AGN fraction in HCGs and Section 7 discusses our findings. We conclude with a summary in Section 8.

2. SAMPLE SELECTION

Our original multi-wavelength HCG sample comprises 11 groups compiled from the original HCG catalog of 92 spectroscopically confirmed compact groups (Hickson et al. 1992). This has been the most widely used (“benchmark”, Lee et al. 2004) of all CG catalogs. Although valid concerns regarding selection biases about this catalog have been raised (e.g. Mamon 1994; Ribeiro et al. 1998), comparisons with recent larger catalogs show that many HCG galaxy properties such as surface brightness, or angular and linear diameter are in fact close to median values for the corresponding distributions (Lee et al. 2004).

In order to ensure that our sample would be observable with a range of ground- and space-based instruments for our long-term multi-wavelength campaign, the selection

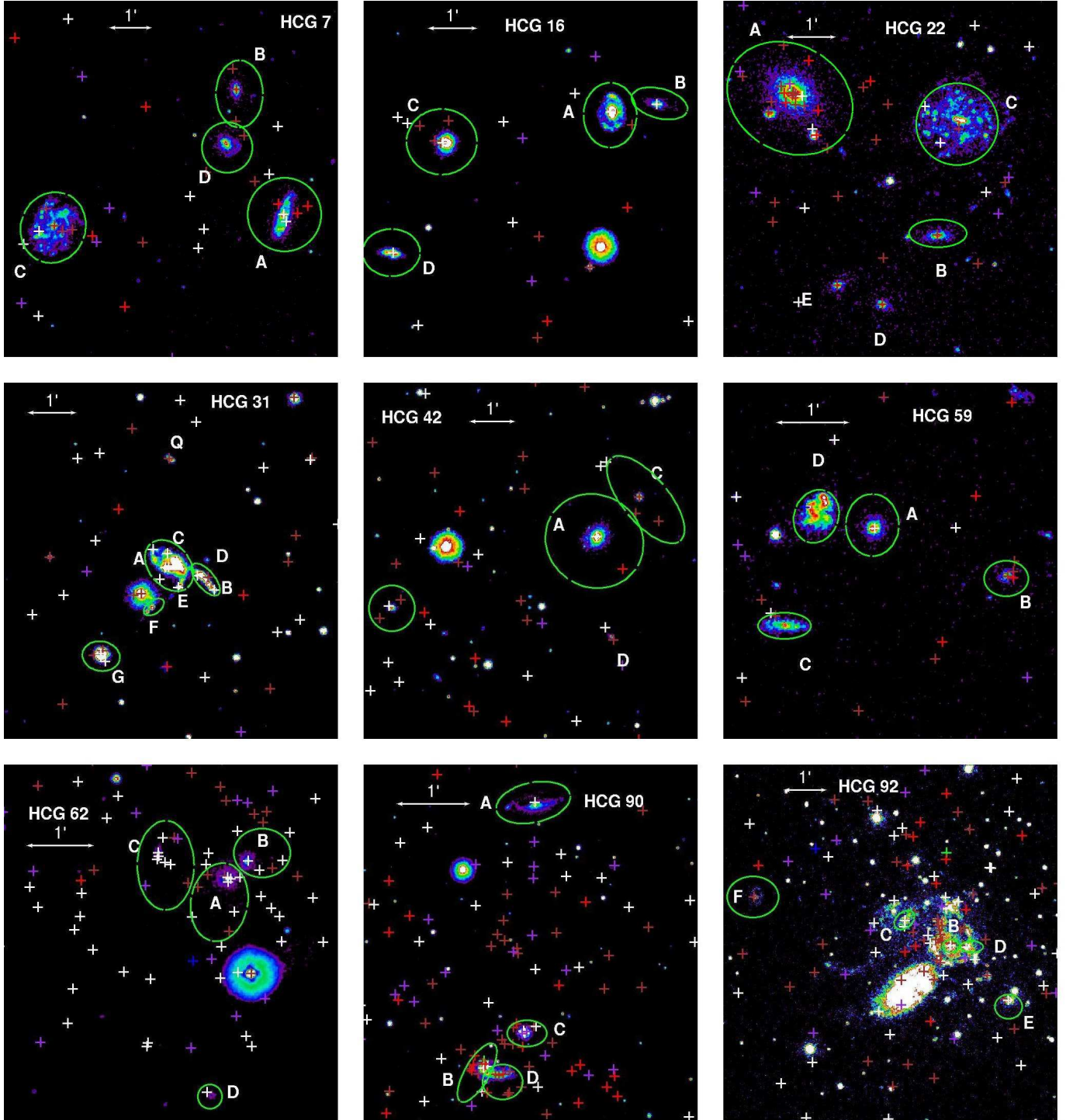


FIG. 1.—: *Swift*-UVOT false color *uvw1* images with *Chandra* X-ray point sources overlaid. UV intensity increases from violet (lowest) to blue to green to red to white (highest). The color coding of source symbols indicates whether they are detected in the full band only (red), the soft band only (green), the hard band only (blue), the full and the hard band (purple), the full and the soft band (brown), the soft and the hard (blue-green) or the full, soft and hard bands (white). The bright source right of center in the HCG 62 field is a foreground star.

was based on membership (a minimum of three giant galaxies with accordant redshifts, i.e., within 1000 km s^{-1} of the group mean), distance ($\lesssim 4500 \text{ km s}^{-1}$), and angular extent ($\lesssim 8'$ in diameter).

In this paper we present 9 of these groups, for which both archival *Chandra* X-ray and *Swift* UVOT ultraviolet data are available. *Swift*/UVOT false color images of the group fields, with detected *Chandra* X-ray point sources overlaid are shown in Fig. 1. An observation log for the *Chandra* data is presented in Table 1. The *Chandra* observations include Guaranteed Time observing (HCGs 7 and 22, P.I. Garmire). An observation log for the *Swift* UVOT data is presented in Tzanavaris et al. (2010). In addition, note that in the present work we have included UVOT data for HCGs 90 and 92 (see below). The group and galaxy ID's, as well as morphological types, can be found in the first two columns of Table 9, which also provides an overview of our multiwavelength results (Sec. 5).

As the nine groups used in this paper represent a small archival sub-sample of the full set of 92 compact groups, we do not a priori expect them to be fully representative of all HCGs. We further investigate this issue by comparing the distributions of a number of characteristic properties, established and tabulated by Hickson (1982) and Hickson et al. (1992), both for the full set and our sub-sample. These include the number of galaxies per group, n , the radial velocity dispersion, σ_v , the median projected separation, D , and the angular diameter, θ_G . The distributions of these properties both for the full sample and our nine-group subsample are shown in Fig. 2. The distribution for n is very similar for the two populations, with means of $\langle n_{92} \rangle = 4.2 \pm 1.0$ and $\langle n_9 \rangle = 3.8 \pm 0.4$ for the 92 and nine HCG samples, respectively. The Kolmogorov-Smirnov (KS) test gives a modestly high probability of 0.005 that the two distributions come from the same parent population. The situation for D is similar ($\langle D_{92} \rangle = (1.6 \pm 0.3) \text{ kpc}$ and $\langle D_9 \rangle = (1.4 \pm 0.2) \text{ kpc}$), with an even higher KS probability (0.2). The σ_v distributions are less similar in terms of their peaks but their means are fully consistent within the uncertainties ($\langle \sigma_{v,92} \rangle = (225 \pm 30) \text{ km s}^{-1}$ and $\langle \sigma_{v,9} \rangle = (212 \pm 31) \text{ km s}^{-1}$). However, the KS probability that the distributions are the same is relatively high (0.3). Finally, the distributions for θ_G are also less similar, and are consistent within 2σ ($\langle \theta_{G,92} \rangle = (3.7 \pm 2.8)'$ and $\langle \theta_{G,9} \rangle = (4.5 \pm 2.2)'$). This is to be expected, as our selection criteria are biased towards more nearby systems. Again though, the KS probability is relatively high (0.3). Thus, overall, we find that the sub-sample used in this paper is reasonably representative of HCGs as a class.

3. X-RAY DATA ANALYSIS

3.1. Point source detection and photometry

Each group was observed at the aim point of the back-illuminated S3 CCD of *Chandra*'s Advanced CCD Imaging Spectrometer (ACIS), with the exception of HCG 90, which was observed with the ACIS-I array. The data were processed using standard *Chandra* X-ray Center aspect solution and grade filtering, from which the level 2 events file was produced. Thanks to *Chandra*'s $\sim 1''$ angular resolution and the proximity of our galaxies, we can detect a multitude of individual point sources in our

fields. We have thus been able to carry out a detailed point source detection and characterization consisting of four stages as follows.

First, the CIAO 4.1.2⁹ wavelet detection tool WAVDETECT (Freeman et al. 2002) was used in the soft (S , 0.5–2.0 keV), hard (H , 2.0–8.0 keV) and full (F , 0.5–8.0 keV) bands to detect candidate point sources in each band. The lower limit of 0.5 keV matches the well-calibrated part of the response, while above 8.0 keV the effective area of the *Chandra* mirrors is known to drop considerably and the particle background increases significantly. The chip field (1024×1024 pixels for S3 and 2048×2048 pixels for I0-I3) was searched with WAVDETECT at the 10^{-5} false-probability threshold in all three energy bands. Although a lower probability threshold (10^{-6} per CCD) is often used to ensure low false positive detections, the situation is more complicated for false negatives, especially near an observation's detection limit (Kim et al. 2004). We thus chose to detect a greater number of spurious sources at this stage, which were excluded at subsequent stages of the analysis as explained below. For comparison, we show the numbers of sources detected with WAVDETECT using these two probability thresholds for each HCG field in the three X-ray bands in Fig. 3. Wavelet scales used were 1, 1.414, 2, 2.828, 4, 5.657 and 8.0 pixels to cover a wide variety of source sizes, as well as to take into account the variation of the point spread function (PSF) size across the ACIS CCD. Source lists produced by WAVDETECT for each band were cross-correlated to produce a single list of positions for candidate point sources in each field. This matching used each source's PSF ellipses, whose size and orientation depend on the detector used (ACIS-S or I), position on the detector and roll angle of observations.

The second stage of the point source analysis involved using the software ACIS EXTRACT (AE, Broos et al. 2010,¹⁰) to perform aperture photometry for sources in the WAVDETECT source list. Some of the features of AE that make it a good choice for ACIS point source extraction include

1. Construction of PSF-shaped aperture extraction regions separately for each source and each observation. These regions encircle $\sim 90 - 60\%$ of the photon energy at 1.5 keV, depending on how crowded a given field region is.
2. Construction of background regions that exclude pixels from neighboring sources, and, where appropriate, a model of the wings of a neighboring source's contaminating emission.
3. Use of the *Chandra* Calibration Database for producing Ancillary Reference Files (ARFs) and Response Matrix Files (RMFs) for each source and observation, appropriately merging these for multiple observations.
4. Aperture corrections by means of calculation of the energy fraction falling inside the PSF region at 5 different energies.

Our initial catalogs included *all* sources detected at the AE stage. We then flagged sources with negative net

⁹ <http://cxc.harvard.edu/ciao>

¹⁰ Package and User's Guide available at http://www.astro.psu.edu/xray/acis/acis_analysis.html

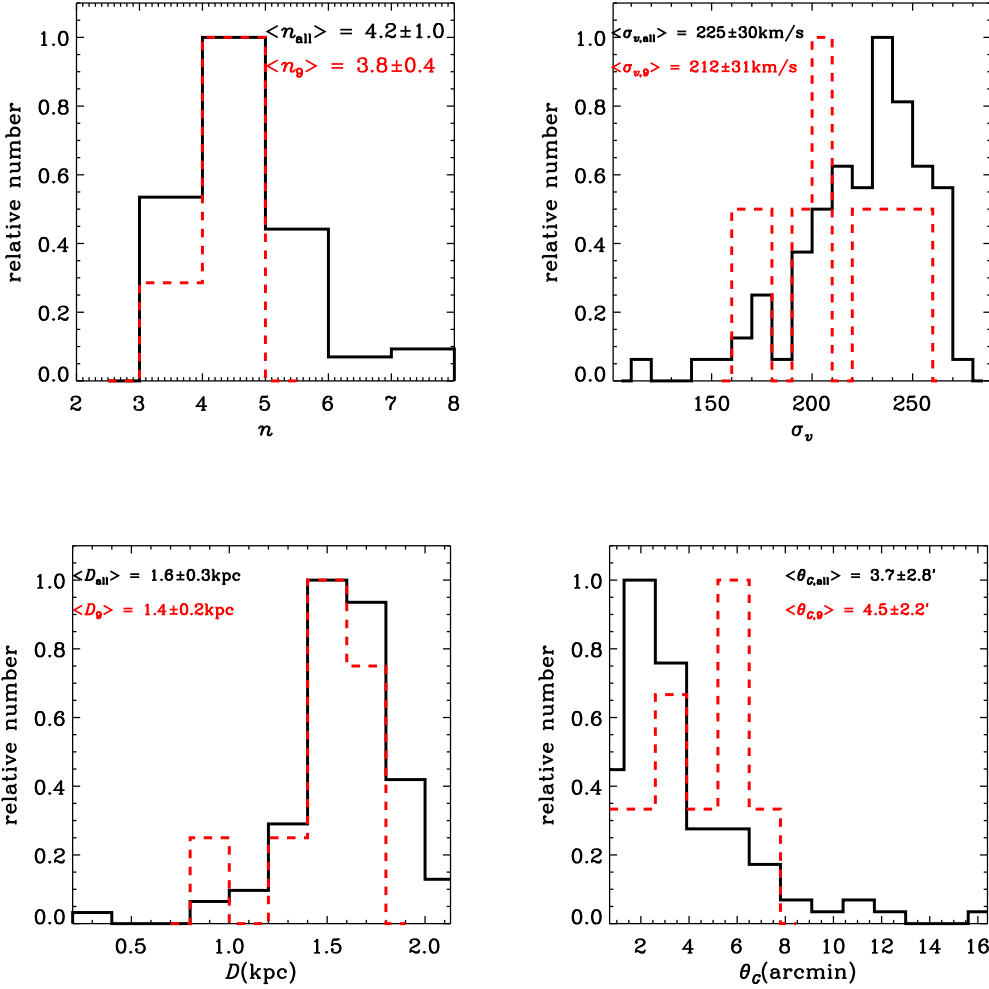


FIG. 2.—: Histograms for physical properties of the nine galaxy groups in this paper (red, dashed lines) and the full sample of 92 Hickson Compact Groups (Hickson 1982; Hickson et al. 1992, black, continuous lines). Clockwise from top left, properties shown are mean number of galaxies per group with accordant redshifts, mean radial velocity dispersion of galaxies per group, mean projected separation, mean angular size of galaxies per group. Mean values and standard deviations are shown in the upper right corner of each panel.

(source – background) counts in a given band as non-detections in that band. Such sources were assigned the detection flag 1 in that band. Further, we obtained Poisson $\pm 1\sigma$ errors on net counts by using the method of Gehrels (1986). If the measured net counts minus the lower 2σ error thus calculated were ≤ 0 , sources were also flagged as non-detections. To distinguish these from the previous type of non-detections, these were assigned the detection flag 5 in that band. For non-detections we estimated upper confidence limits¹¹ for fluxes and confidence levels $\text{CL} = 0.90$ by following Kraft et al. (1991). In this approach, the probability that a source flux, S ,

¹¹ We use the term *upper confidence limit* to stress that this is an estimate of the upper edge of a confidence interval for the source intensity, regardless of the detection procedure. The term *upper limit* should be reserved to characterize the detection process (Kashyap et al. 2010)

lies between S_{min} and S_{max} is given by

$$\text{CL} = \int_{S_{\text{min}}}^{S_{\text{max}}} f_{N,B}(S) dS , \quad (1)$$

where the posterior probability function for parameter S as a function of observed counts N and mean background B is given by

$$f_{N,B}(S) = C \frac{e^{-(S+B)} (S+B)^N}{N!} \quad (2)$$

and C is a normalization constant (equation (8) in Kraft et al. (1991).)

In our catalogs, we also include alternative detection criteria (see below).

Most of our sources have few net counts, precluding reliable spectral fitting. Thus at the third and final stage of the point source analysis, we applied the method of Gallagher et al. (2005), which makes use of hardness ratios to obtain rough estimates of spectral shapes and,

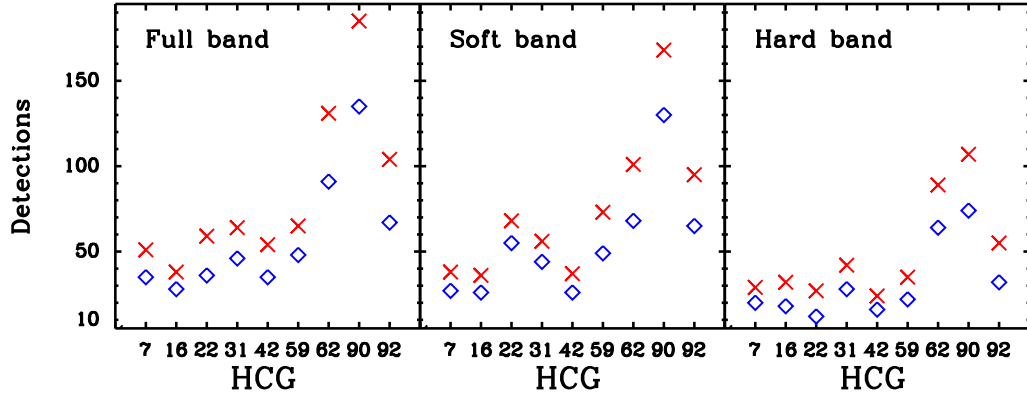


FIG. 3.— Number of sources detected with WAVDETECT in three *Chandra* X-ray bands for each HCG field. Red crosses are for a significance threshold of 10^{-5} and blue diamonds for a significance threshold of 10^{-6} .

hence, fluxes and luminosities for each source. The hardness ratio is defined as

$$\text{HR} \equiv (H - S)/(H + S), \quad (3)$$

where H and S represent net counts in the hard and soft bands, respectively. For each source this method compares the observed hardness ratio to that obtained from simulated spectra, in order to estimate the power-law index Γ (where the photon flux is given by $f_E \propto E^{-\Gamma}$ photon cm $^{-2}$ s $^{-1}$ keV $^{-1}$) and associated X-ray flux and luminosity. We used the X-ray spectral modeling tool XSPEC (Arnaud 1996), version 12.5.0, to construct grids of simulated spectra. For each source, we used the corresponding Galactic column density, $N_{\text{H}}^{\text{gal}}$, as well as the ARFs and RMFs produced by AE. We imposed a simple, absorbed power law model (`tbabs*po` in XSPEC) and varied Γ in the range $-1 \rightarrow +4$ to obtain simulated count rates in the full, soft, and hard band, and, thus, simulated HR values. By comparing with the observed HR, we estimated best Γ values and corresponding fluxes and luminosities. We illustrate this process in Fig. 4. Each panel corresponds to a single X-ray HCG field. For each source detected in at least one band in this field we plot the simulated HR values against corresponding Γ values. Thus, each grey curve in a panel is made up from a set of simulated $\text{HR} - \Gamma$ pairs for a single detected source. Given an *observed* HR value and a simulated $\text{HR} - \Gamma$ curve, there is then a unique Γ value that provides the best *observed* Γ estimate, as indicated by the blue triangles¹².

Due to the simplicity of our model, which assumes no intrinsic absorption ($N_{\text{H}}^{\text{int}} = 0$), it is likely that some Γ values are incorrect. However, Γ and N_{H} are degenerate, so that this should have a minimal effect on luminosity, which is the quantity we are most interested in. As a comparison, for the nucleus of HCG 62 A our method yields luminosities $L_{X,2.0-8.0\text{keV}} = 1.0 \times 10^{39}$ erg s $^{-1}$ and $L_{X,0.5-8.0\text{keV}} = 3.2 \times 10^{39}$ erg s $^{-1}$. These are in a good agreement with the results reported by Rafferty et al. (2013). Using the same *Chandra* data, these authors carry out more detailed spectral fitting that includes both intrinsic and Galactic absorption, as well as a thermal component, and report $L_{X,2.0-10.0\text{keV}} = (1.1 \pm 0.4) \times$

10^{39} erg s $^{-1}$ and $L_{X,0.5-7.0\text{keV}} = 1.5_{-1.0}^{+2.8} \times 10^{39}$ erg s $^{-1}$.

Point source catalogs for all sources are presented in Tables 11 to 28¹³. For completeness, the tables include sources considered both detected and undetected, according to our conservative 2σ criterion above. We have compiled two sets of tables. The first set (Tables 11 to 19) presents Γ values, fluxes and luminosities in the full, soft and hard X-ray bands, derived as explained above, as well as the flux density at 2 keV.

The second set (Tables 20 to 28) presents counts and count rates in the full, soft and hard band.

Apart from the Gehrels detection criterion, for completeness in this second set of tables we also include the two AE detection criteria, namely the *AE significance*, which essentially is a traditional signal-to-noise criterion, as well as the *binomial probability*, P_B , that a source is spurious (Equation 4 below; see Broos et al. 2010, Appendix B for details). Users of our catalogs are left to choose which detection criterion they prefer.

In both sets of tables, we also include two types of detection/non-detection flags for each source. As already mentioned, the first type of flag (columns 17, 18, 19 in Tables 11 to 19; columns 3, 5, 7 in Tables 20 to 28) is related to the relative numbers of source and background counts, and is equal to 1 (net counts negative; no detection in band), 5 (net counts minus Gehrels 2σ error < 0) or 0 otherwise (unambiguous detection in band). The second type of flag (column 16 in Tables 11 to 19 and column 9 in Tables 20 to 28) indicates whether the hardness ratio is an upper or lower limit. From the HR definition (Equation 3) it follows that, if there is a detection in the hard but not the soft band, an HR value is a lower limit (flag value equal to -1). Conversely, if there is a detection in the soft but not in the hard band, an HR value is an upper limit (flag value equal to 1). If there is no detection in either band, this flag is equal to -2 , and if there is a detection in both bands, the flag is equal to 0.

Finally, in both sets of tables, for sources which fall within the boundaries of individual galaxies (defined as explained in Sec. 3.2) an upper-case letter in column 1 (ID) indicates the galaxy they belong to. If these are also nuclear sources, this is indicated by an asterisk next

¹² We stress that there is only one blue triangle per curve, although the high density of curves in Fig. 4 may suggest otherwise.

¹³ These tables are available only in the online version of the journal.

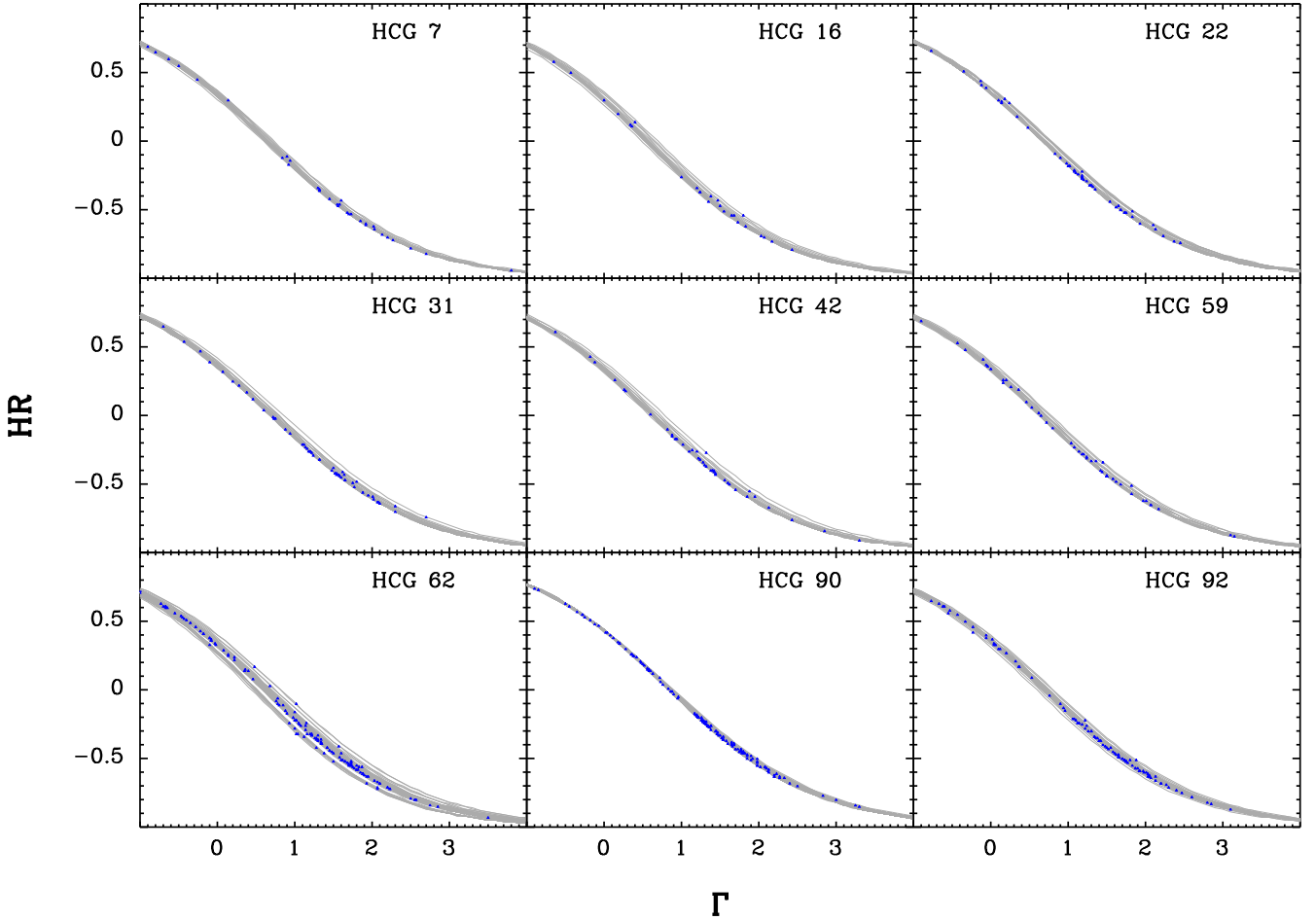


FIG. 4.—: Estimating X-ray spectral slopes for point sources in our fields. Each grey curve is constructed from each detected source’s simulated HR – Γ grid, based on XSPEC simulated spectra that assume a simple absorbed power law, Galactic N_{H} at the source right ascension and declination, as well as ARFs and RMFs specific to the source’s position on the ACIS CCDs. A Γ value that best matches the observed HR can then be obtained for each curve and corresponding source, as indicated by the blue triangles.

to the galaxy’s letter designation.

A summary of key results from the X-ray analysis for all galaxy nuclei in this sample is presented in Table 2. In this table, the ID number in column 2 refers to the master ID running number in column 1 of Tables 11 to 28. For instance, for the nucleus of HCG 7A this number is 6 (first row of Table 2). This indicates that this is the sixth source in the master X-ray catalog of group HCG 7. Since this source belongs to galaxy A and is a nuclear source, it is listed as 6A* in Tables 11 and 20.

Table 2 shows that there appear to be nuclear X-ray detections for 27 out of 37 HCG galaxies. According to column 6, the great majority of X-ray sources associated with galaxy nuclei (24/27 or 89%) are soft ($\text{HR} < 0$). Comparing with column 4, we see that these are also the sources with low luminosities, $L_{X,0.5-8.0\text{keV}} < 10^{41} \text{ erg s}^{-1}$. What about the remaining three sources? The last column indicates whether a galaxy is a good candidate for being a *strong* AGN host, based on whether $L_{X,0.5-8.0\text{keV}} \geq 10^{41} \text{ erg s}^{-1}$. The three remaining

sources (3/27 or 11%) are those that fulfill this condition and are also those that have $\text{HR} > 0$. These trends are also easy to see in Fig. 5. The left and middle panels show histograms for HR and $L_{X,0.5-8.0\text{keV}}$, while the right panel plots HR against $L_{X,0.5-8.0\text{keV}}$. Again, a small minority of positive HR, high $L_{X,0.5-8.0\text{keV}}$ sources are good strong AGN candidates. Note that the last column of Table 2 also appears in Table 9 (its column 8), which combines multiwavelength nuclear activity diagnostics.

3.2. Flux limits and source statistics

Although we detect a large number of X-ray point sources in our fields, we have no a priori information which of these sources are physically associated with HCG galaxies and are not just background AGNs. We assess the effect of AGN background contamination as follows.

The binomial probability, P_B , that a source is spurious

TABLE 2:
 X-ray analysis of HCG nuclear sources

HCG ID (1)	X-ray ID (2)	Γ (3)	$L_{X,0.5-8.0\text{keV}}$ (4)	c(0.5 – 8.0 keV) (5)	HR (6)	Strong AGN? (7)
7A	6	2.0	40.0	102^{+11}_{-10}	$-0.62^{+0.09}_{-0.08}$	n
7B	15	1.9	39.0	9^{+4}_{-3}	$-0.58^{+0.00}_{-0.42}$	n
7C	44	2.1	39.1	12^{+4}_{-3}	$-0.68^{+0.00}_{-0.32}$	n
7D
16A	9	1.2	40.7	134^{+12}_{-11}	$-0.37^{+0.09}_{-0.08}$	n
16B	4	-0.7	41.3	189^{+14}_{-13}	$0.58^{+0.06}_{-0.07}$	y
16C	44	2.0	39.7	24^{+6}_{-4}	$-0.69^{+0.21}_{-0.15}$	n
16D	57	2.4	39.8	37^{+7}_{-6}	$-0.79^{+0.15}_{-0.10}$	n
22A	77,76	1.7(1.1)	38.7(38.7)	$9^{+4}_{-3}(7^{+7}_{-2})$	$-0.50^{+0.00}_{-0.50}(-0.23^{+0.00}_{-0.77})$	n
22B	22	1.2	38.7	7^{+3}_{-2}	$-0.28^{+0.00}_{-0.72}$	n
22C	n
31ACE	40,38	1.3(1.1)	40.1(40.3)	$73^{+9}_{-8}(128^{+11}_{-11})$	$-0.32^{+0.12}_{-0.12}(-0.21^{+0.09}_{-0.09})$	n
31B
31F
31G	63	1.6	40.0	72^{+9}_{-8}	$-0.43^{+0.12}_{-0.11}$	n
31Q	41	1.1	38.9	4^{+3}_{-2}	$-0.23^{+0.00}_{-0.77}$	n
42A	18	3.3	40.3	178^{+14}_{-13}	$-0.91^{+0.04}_{-0.03}$	n
42B
42C	6	2.4	39.3	19^{+5}_{-4}	$-0.76^{+0.00}_{-0.24}$	n
42D
59A	50	0.8	40.1	43^{+7}_{-6}	$-0.09^{+0.17}_{-0.16}$	n
59B	26	1.5	39.3	10^{+4}_{-3}	$-0.44^{+0.00}_{-0.56}$	n
59C
59D
62A	83	2.5	39.5	133^{+12}_{-11}	$-0.79^{+0.07}_{-0.05}$	n
62B	67	2.6	39.4	116^{+11}_{-10}	$-0.80^{+0.07}_{-0.06}$	n
62C	115	1.7	39.0	33^{+6}_{-5}	$-0.54^{+0.18}_{-0.15}$	n
62D
90A	88	-1.1	42.6	23361^{+153}_{-152}	$0.95^{+0.00}_{-0.00}$	y
90B	164	2.3	39.1	31^{+6}_{-5}	$-0.64^{+0.18}_{-0.14}$	n
90C	108	1.5	39.1	23^{+5}_{-4}	$-0.33^{+0.23}_{-0.21}$	n
90D
92B	46	1.8	39.4	19^{+5}_{-4}	$-0.53^{+0.25}_{-0.21}$	n
92C	94	-1.1	42.3	3375^{+59}_{-58}	$0.74^{+0.01}_{-0.01}$	y
92D	36	2.6	39.8	75^{+9}_{-8}	$-0.78^{+0.09}_{-0.07}$	n
92E	22	2.3	39.6	40^{+7}_{-6}	$-0.69^{+0.15}_{-0.12}$	n
92F	145	2.9	39.4	30^{+6}_{-5}	$-0.83^{+0.00}_{-0.17}$	n

NOTE. — Columns are: (1) HCG galaxy ID; (2) X-ray source ID in master list; (3) Γ value from hardness ratio; (4) $\log L_X$ in full band; (5) net counts in full band; (6) hardness ratio; (7) X-rays indicate strong AGN ($L_{X,0.5-8.0\text{keV}} \geq 10^{41} \text{ erg s}^{-1}$).

is given by the binomial function (Broos et al. 2010)

$$P_B = f_b(C_s; C_s + C_b, (1 + A_b/A_s)^{-1}), \quad (4)$$

where C_s and C_b are the number of counts observed in the source and background region in a given energy band, and A_s , A_b are the areas of the source and background regions. In other words, sources with values of P_B less than a given threshold value may be considered as detections. We adopt the threshold $P_B = 0.004$ established by Xue et al. (2011) and use local background information for each detected nuclear source to establish a detectability limit in terms of counts, fluxes and luminosities in the soft and hard band at the location of each galaxy on the ACIS CCD. Each of our nuclear sources has associated background and source extraction regions with measured background counts. The advantage of using these regions, together with measured background counts, is that they have been constructed and

measured by ACIS EXTRACT by taking into account the size of the *Chandra* PSF at the location of the particular source on the CCD. Thus the detection limits that we calculate are local, position-dependent and specific to each galaxy. We fix C_b to the locally measured background counts and start by setting the source counts $C_s = 0$, in which case $P_B \gg 0.004$ (a source with no source counts must be spurious). We then iteratively increase C_s to estimate the minimum number of source counts, $C_{s,\text{lim}}$, required to reach our chosen probability threshold of 0.004. We convert the estimated $C_{s,\text{lim}}$ value to a flux limit by assuming a power law spectrum with $\Gamma = 1.4$ (Hickox & Markevitch 2006; Steffen et al. 2007) and the Galactic N_H value for each galaxy group in PIMMS (Mukai 1993). The flux and corresponding luminosity limits for the soft and hard band are shown in columns 2, 3 (soft band) and 7,8 (hard band) of Table 3. As expected, the estimated limit fluxes are lower in the

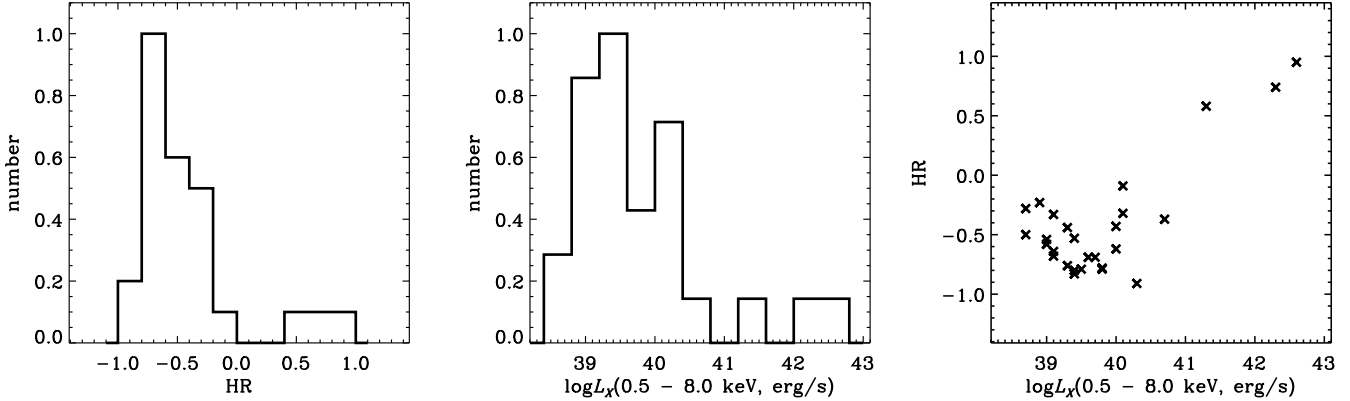


FIG. 5.—: Hardness ratios and X-ray luminosities for nuclear sources (Table 2). The left and middle panels show the normalized distributions of HR and $L_{X,0.5-8.0\text{keV}}$ values for X-ray nuclear detections in HCG galaxies. The right panel plots HR against $L_{X,0.5-8.0\text{keV}}$ for the same sources. With the exception of three sources, HCG nuclei have negative HR values and low luminosities in the X-rays.

soft band, due to the higher sensitivity of ACIS in this regime.

We use these flux limits to estimate how many background AGNs we expect to see inside the galaxy regions of our galaxies. We use the “ $\log N - \log S$ ” relation of Cappelluti et al. (2007) which relates the number of detected point sources per angular area in the soft and hard band as a function of flux, established over 2 deg^2 in the COSMOS field. We thus estimate for each band the expected total number of background AGNs that would be detected over the area of each of our galaxy regions. These regions are determined following Tzanavaris et al. (2010) who use mid-infrared defined galaxy regions (Johnson et al. 2007) for their global galaxy photometry. For each band and galaxy, we then compare the number of expected AGNs to the number of detected sources, $N_{\text{obs,S}}$ and $N_{\text{obs,H}}$ (columns 4 and 9 in Table 3), and calculate the number of detected sources which are in excess of the expected background number, $N_{\text{exc,S}}$ and $N_{\text{exc,H}}$ (columns 5 and 10 in Table 3). The ratio of the number of excess sources over the total number of observed sources is a rough estimate of the probability that a source detected inside a galaxy region is not a background AGN. Although this method cannot tell us whether a *specific* source is likely to be a background source or not, it does provide an overall estimate of whether background contamination may be a serious concern for our galaxies. The probability estimates in Table 3 (columns 6 and 11) are in general quite high. Note that in these columns values equal to zero are simply due to non-detections in one band. Otherwise, rounded values range from 0.7 to 1.0, giving us confidence that our point source detections are likely to be due to HCG galaxies.

4. UV DATA AND DATA ANALYSIS

4.1. Data

For all galaxies in this sample we use 3-band UV data obtained with UVOT on NASA’s *Swift* Gamma-ray Burst Explorer (Gehrels et al. 2004). Details on the telescope, filters, observations, and data reduction can be

found in Tzanavaris et al. (2010). Magnitude limits for each HCG field are estimated using the zero points specific to each UVOT filter (Poole et al. 2008) and shown in Table 4. For quick reference, we mention here that the three UV bands used are $uvw2$, $uvm2$ and $uvw1$, with effective wavelengths 2030, 2231 and 2634 Å, respectively.

As mentioned, in the present work we do include UVOT data for HCG 90. These were excluded in Tzanavaris et al. (2010), as some of the HCG galaxies were not fully covered by the stacked UVOT exposures. A careful re-analysis of the UVOT data for this group reveals that they consist of two exposure “stacks”. The HCG galaxies are not covered by three out of eleven individual exposures in stack 00053602001. We thus combined the eight useful exposures of this stack with the second stack. The corrected total exposure times for HCG 90 and the $uvw2$, $uvm2$ and $uvw1$ filters are now 7387s, 6732s and 5525s (c.f. 8601s, 7946s, 6663s in Tzanavaris et al. (2010, Table 3)).

We also include UVOT data for HCG 92 (Stephan’s Quintet). The UVOT observation ID’s for this group are 00035083005, 00035083007, 00035083008 and 00035083009, with total exposure times for the $uvw2$, $uvm2$ and $uvw1$ filters of 3054s, 3214s and 1007s, respectively.

4.2. UV nuclear photometry

Tzanavaris et al. (2010) carried out galaxy-wide photometry for their HCG galaxies in order to calculate galaxy star formation rates. In this paper we are interested in comparing nuclear fluxes in the UV and X-ray regime and thus perform nuclear photometry as described below.

Using the $uvw1$ ($\sim 2600 \text{ \AA}$) image, we define circular source regions of radius $5''$, centered at the central intensity peak of each galaxy. The choice of radius is dictated both by the UVOT PSF ($2.37''$, FWHM, for $uvw1$, Breeveld et al. 2010) and the fact that the UVOT count rate to flux conversion factors have been calibrated for such a radius. We use the $uvw1$ image because its effective wavelength is closest to the one traditionally used in

TABLE 3:
Flux limit estimates and X-ray point sources associated with galaxies.

ID (1)	$f_{\text{lim,S}}$ (erg cm $^{-2}$ s $^{-1}$) (2)	$L_{X,\text{lim,S}}$ (erg s $^{-1}$) (3)	$N_{\text{obs,S}}$ (4)	$N_{\text{exc,S}}$ (5)	P_S (6)	$f_{\text{lim,H}}$ (erg cm $^{-2}$ s $^{-1}$) (7)	$L_{X,\text{lim,H}}$ (erg s $^{-1}$) (8)	$N_{\text{obs,H}}$ (9)	$N_{\text{exc,H}}$ (10)	P_H (11)
HCG 7 A	5.8×10^{16}	2.2×10^{38}	4	3.5	0.9	2.0×10^{15}	7.6×10^{38}	3	2.3	0.8
HCG 7 B	2.9×10^{16}	1.1×10^{38}	3	2.5	0.8	1.5×10^{15}	5.7×10^{38}	0	-0.5	0.0
HCG 7 C	3.9×10^{16}	1.5×10^{38}	6	5.5	0.9	2.5×10^{15}	9.5×10^{38}	2	1.6	0.8
HCG 16 A	1.9×10^{15}	6.6×10^{38}	2	1.9	0.9	5.8×10^{15}	2.0×10^{39}	2	1.9	0.9
HCG 16 B	1.7×10^{15}	5.7×10^{38}	1	0.9	0.9	7.2×10^{15}	2.5×10^{39}	1	1.0	1.0
HCG 16 C	3.9×10^{15}	1.3×10^{39}	6	5.9	1.0	5.8×10^{15}	2.0×10^{39}	2	1.8	0.9
HCG 16 D	1.4×10^{15}	4.7×10^{38}	1	0.9	0.9	4.4×10^{15}	1.5×10^{39}	1	0.8	0.8
HCG 22 A	4.4×10^{16}	6.9×10^{37}	15	13.9	0.9	1.7×10^{15}	2.7×10^{38}	4	2.7	0.7
HCG 22 B	3.3×10^{16}	5.2×10^{37}	1	0.8	0.8	1.7×10^{15}	2.7×10^{38}	0	-0.2	0.0
HCG 31 ACE	1.1×10^{15}	4.3×10^{38}	9	8.9	1.0	2.6×10^{15}	1.0×10^{39}	9	8.8	1.0
HCG 31 G	5.8×10^{16}	2.3×10^{38}	5	4.9	1.0	2.1×10^{15}	8.3×10^{38}	3	2.9	1.0
HCG 31 Q	2.9×10^{16}	1.2×10^{38}	1	1.0	1.0	1.5×10^{15}	6.2×10^{38}	0	0.0	0.0
HCG 42 A	4.0×10^{15}	1.9×10^{39}	1	0.8	0.8	3.4×10^{15}	1.6×10^{39}	1	0.2	0.2
HCG 42 C	1.2×10^{15}	5.6×10^{38}	4	3.7	0.9	3.4×10^{15}	1.6×10^{39}	1	0.7	0.7
HCG 59 A	5.4×10^{16}	2.6×10^{38}	1	0.9	0.9	1.4×10^{15}	6.9×10^{38}	1	0.8	0.8
HCG 59 B	2.7×10^{16}	1.3×10^{38}	3	2.9	1.0	1.4×10^{15}	6.9×10^{38}	0	-0.1	0.0
HCG 62 A	3.5×10^{15}	1.7×10^{39}	11	10.9	1.0	1.2×10^{15}	5.9×10^{38}	6	5.6	0.9
HCG 62 B	1.2×10^{15}	5.9×10^{38}	6	5.9	1.0	8.7×10^{16}	4.3×10^{38}	4	3.7	0.9
HCG 62 C	2.5×10^{16}	1.2×10^{38}	9	8.7	1.0	6.5×10^{16}	3.2×10^{38}	8	7.5	0.9
HCG 90 A	1.0×10^{15}	1.4×10^{38}	1	0.7	0.7	2.2×10^{14}	3.1×10^{39}	1	1.0	1.0
HCG 90 B	6.7×10^{16}	9.3×10^{37}	7	6.8	1.0	1.7×10^{15}	2.3×10^{38}	2	1.6	0.8
HCG 90 C	4.5×10^{16}	6.2×10^{37}	5	4.8	1.0	1.3×10^{15}	1.8×10^{38}	5	4.8	1.0
HCG 92 B	1.8×10^{16}	1.7×10^{38}	2	1.9	0.9	6.5×10^{16}	6.1×10^{38}	1	0.9	0.9
HCG 92 C	1.3×10^{15}	1.3×10^{39}	2	2.0	1.0	3.1×10^{15}	2.9×10^{39}	2	2.0	1.0
HCG 92 D	2.1×10^{16}	2.0×10^{38}	2	1.9	0.9	8.1×10^{16}	7.6×10^{38}	1	0.9	0.9
HCG 92 E	1.8×10^{16}	1.7×10^{38}	2	1.8	0.9	8.1×10^{16}	7.6×10^{38}	1	0.8	0.8
HCG 92 F	3.7×10^{16}	3.5×10^{38}	1	0.8	0.8	2.9×10^{15}	2.7×10^{39}	0	-0.1	0.0

NOTE. — Columns are: (1) HCG galaxy ID; (2) flux limit estimate in soft band; (3) luminosity limit estimate in soft band; (4) number of detected point sources inside galaxy region; (5) number of point sources in the soft band and inside galaxy region that are in excess of the number expected from the background $\log N - \log S$; (6) probability estimate that in the soft band point sources detected in this galaxy belong to the galaxy and are not background AGN (column (5) / column (4)); (7) as column (2) for the hard band; (8) as column (3) for the hard band; (9) as column (4) for the hard band; (10) as column (5) for the hard band; (11) as column (6) for the hard band.

TABLE 4:
Swift UVOT magnitude limits for HCG fields

HCG ID (1)	$uvw2$ (2030 Å) (2)	$uvm2$ (2231 Å) (3)	$uvw1$ (2634 Å) (4)
7	20.5	20.4	20.6
16	21.6	20.6	20.6
22	20.2	20.7	20.4
31	20.4	20.3	20.5
42	20.5	20.1	20.9
59	20.7	20.2	21.1
62	20.6	20.3	20.9
90	22.6	22.8	21.6
92	20.9	21.0	20.3

NOTE. — Columns are: (1) HCG field ID; (2), (3), (4): magnitude limit estimates for the $uvw2$ (effective wavelength 2030 Å), $uvm2$ (2231 Å), $uvw1$ (2634 Å) UVOT filters.

estimating the X-ray-to-UV spectral index

$$\alpha_{\text{OX}} \equiv 0.380 \log(L_{\nu,2\text{keV}}/L_{\nu,uvw1}), \quad (5)$$

sometimes referred to as “X-ray loudness” (Tananbaum et al. 1979), or X-ray-to-“optical” spectral index¹⁴. Note that, since the effective wavelength of

¹⁴ Note that with this definition, in this paper lower α_{OX} values are more negative.

the $uvw1$ filter is ~ 100 Å redward of 2500 Å, this is very close, but not identical, to frequent definitions of this index which use the 2500 Å luminosity instead. However, given that the spectral slope is essentially flat in the near-to-far UV spectral region (Kennicutt 1998), we expect this discrepancy to have a negligible effect, especially given the scatter in our α_{OX} results (more than an order of magnitude, Sec. 5.3).

At this point we should mention a possible adverse consequence of the UV resolution and photometric aperture. Since the resolution is worse and the aperture larger than the corresponding quantities for the *Chandra* data, and given that we are interested in detecting a possible signature of AGN activity, there is a risk of an AGN signal being diluted if it is weak and there is significant star formation. This issue will be less important for earlier type galaxies, where star formation is unlikely to play a major role. We will come back to this effect later in the paper, but at this point we are cautioning that it is difficult to quantify properly.

To estimate background emission we construct background regions interactively to ensure that no emission either from galaxies or foreground stars was included. In a minority of cases, concentric annuli at radii 50'' and 60'' from the source centers are appropriate. However, compact group galaxies are often very close to each other, so that in most cases we have to construct a back-

TABLE 5:
Swift UVOT nuclear photometry

HCG ID (1)	$f_\nu(2030 \text{ \AA})$ (2)	$f_\nu(2231 \text{ \AA})$ (3)	$f_\nu(2634 \text{ \AA})$ (4)	$\nu L_\nu(2634 \text{ \AA})$ (5)
7A	0.13 ± 0.01	0.16 ± 0.01	0.27 ± 0.01	42.1
7B	0.06 ± 0.00	0.05 ± 0.01	0.17 ± 0.01	41.9
7C	0.20 ± 0.01	0.24 ± 0.01	0.26 ± 0.01	42.1
7D	0.14 ± 0.01	0.16 ± 0.01	0.17 ± 0.01	41.9
16A	0.58 ± 0.03	0.71 ± 0.03	0.97 ± 0.04	42.6
16B	0.04 ± 0.00	0.03 ± 0.01	0.12 ± 0.01	41.7
16C	1.32 ± 0.05	1.52 ± 0.05	1.77 ± 0.07	42.8
16D	0.10 ± 0.01	0.11 ± 0.01	0.20 ± 0.01	41.9
22A	0.12 ± 0.01	0.10 ± 0.01	0.29 ± 0.02	41.7
22B	0.04 ± 0.00	0.04 ± 0.01	0.07 ± 0.01	41.1
22C	0.11 ± 0.01	0.12 ± 0.01	0.10 ± 0.01	41.3
31ACE	2.74 ± 0.13	3.15 ± 0.11	2.59 ± 0.11	43.1
31B	0.35 ± 0.02	0.42 ± 0.02	0.37 ± 0.02	42.2
31F	0.17 ± 0.02	0.19 ± 0.01	0.17 ± 0.01	41.9
31G	1.33 ± 0.07	1.50 ± 0.06	1.28 ± 0.06	42.8
31Q	0.14 ± 0.01	0.15 ± 0.01	0.15 ± 0.01	41.8
42A	0.18 ± 0.01	0.17 ± 0.01	0.36 ± 0.02	42.3
42B	0.05 ± 0.01	0.03 ± 0.01	0.10 ± 0.01	41.7
42C	0.05 ± 0.01	0.04 ± 0.01	0.14 ± 0.01	41.9
42D	0.02 ± 0.00	0.02 ± 0.01	0.05 ± 0.01	41.4
59A	0.06 ± 0.01	0.07 ± 0.01	0.14 ± 0.01	41.9
59B	0.02 ± 0.00	0.02 ± 0.01	0.05 ± 0.01	41.5
59C	0.08 ± 0.01	0.09 ± 0.01	0.09 ± 0.01	41.7
59D	0.19 ± 0.01	0.21 ± 0.01	0.17 ± 0.01	42.0
62A	0.09 ± 0.01	0.08 ± 0.01	0.20 ± 0.01	42.1
62B	0.07 ± 0.01	0.06 ± 0.01	0.17 ± 0.01	42.0
62C	0.03 ± 0.00	0.03 ± 0.01	0.09 ± 0.01	41.7
62D	0.02 ± 0.00	0.02 ± 0.01	0.06 ± 0.01	41.5
90A	0.05 ± 0.00	0.04 ± 0.01	0.11 ± 0.01	41.3
90B	0.15 ± 0.01	0.12 ± 0.01	0.36 ± 0.02	41.8
90C	0.12 ± 0.01	0.10 ± 0.01	0.32 ± 0.02	41.7
90D	0.08 ± 0.01	0.08 ± 0.01	0.14 ± 0.01	41.3
92B	0.04 ± 0.01	0.05 ± 0.01	0.32 ± 0.02	42.5
92C	0.03 ± 0.01	0.04 ± 0.01	0.17 ± 0.01	42.3
92D	0.07 ± 0.01	0.06 ± 0.01	0.38 ± 0.02	42.6
92E	0.04 ± 0.01	0.04 ± 0.01	0.29 ± 0.02	42.5
92F	0.02 ± 0.01	0.02 ± 0.01	0.10 ± 0.01	42.0

NOTE. — Columns are: (1) HCG nucleus ID; (2), (3), (4): flux densities (mJy) for the $uvw2$ (effective wavelength 2030 Å), $uvn2$ (2231 Å), $uvw1$ (2634 Å) UVOT filters (corrected for Galactic extinction only); (5) log luminosity (erg s^{-1}) for $uvw1$ filter.

ground region manually to avoid contamination. We then obtain net count rates in all three UV bands. Finally, using the UVOT-specific flux conversion factors (Poole et al. 2008), we obtain flux and luminosity densities for all galaxies (see Table 5). The tabulated values have been corrected for Galactic extinction, using the maps of Schlegel et al. (1998) and the extinction curve of Cardelli et al. (1989).

For each galaxy, UV fluxes and luminosities have further been corrected for intrinsic extinction by using the UV and $24\mu\text{m}$ SFR components in Tzanavaris et al. (2010) and assuming that $\text{SFR}_{24\mu\text{m}} = \text{SFR}_{\text{UV,unobsured}}$. As HCG 90 and 92 were not analyzed in that work, for these groups we correct for extinction by adopting the highest A_{UV} value for HCG 92 in Xu et al. (2005), i.e. $A_{\text{UV}} = 2$.

5. MULTIWAVELENGTH NUCLEAR ANALYSIS

We investigate the nature of nuclear activity in our HCG galaxies by combining diagnostics using the X-ray, UV, optical and radio regions. An overview of the main multiwavelength results is presented in Table 9, which we discuss in greater detail later.

5.1. Optical

5.1.1. Emission Line Ratio Classifications

M10 have carried out spectroscopic observations and obtained emission line ratios for 200 HCG galaxies. They have also obtained emission line ratios from archival spectra and the literature for a further 70 HCG galaxies, bringing the total to 270. Their primary classification criterion is the location of a galaxy in the [O III]/H β vs. [N II]/H α diagram of K06 (hereafter K06-a; see K06 Figure 1a and 4a and also Baldwin et al. 1981; Veilleux & Osterbrock 1987). As explained by K06, galaxies located below the Kauffmann et al. (2003, hereafter Ka03) line (lower curve) are purely star forming, while galaxies above the Kewley et al. (2001, hereafter Ke01) line are purely AGNs. Galaxies that fall between the two lines are considered composite or transition objects (Ho et al. 1997), in which circumnuclear star formation effectively dilutes the high-ionization emission line ratio signal. Note that this diagram cannot distinguish between LINERs and AGNs in any way. M10 assume that LINERs are just an AGN subcategory and use this diagram to separate SF from AGN systems. Although K06 also consider LINERs to be AGNs, their additional, [O III]/H β vs. [S II]/H α and [O III]/H β vs. [O I]/H α , diagrams can be used to establish a well defined dividing line (their Figures 4b and 4c, hereafter K06-b and K06-c, respectively) separating galaxies dominated by LINER vs. those dominated by Seyfert (i.e. AGN) activity. The distinction between LINERs and AGNs is not a mere matter of semantics for two reasons. First, although a majority of LINERs harbor weak AGNs, not all LINERs have AGNs. Second, the energetics of LINERs cannot be understood in terms of AGN activity, as any weak AGNs in LINERs cannot fully account for the observed emission lines. Thus LINERs, even those that host weak AGNs, are not a scaled-down AGN; in particular, they are not just a LLAGN. They should be considered as an activity class in their own right beside star-forming and AGN systems.

We thus use all three diagnostic diagrams in K06 and the emission line ratios of M10 as our primary criterion for obtaining new nuclear classifications for galaxies in our sample. Our classification scheme explicitly includes LINERs. Our new classifications are presented in Table 6 and Fig. 6. Columns 2, 3 and 4 of this table give the classification based on each of the emission line ratio diagrams K06-a, b and c. As we do not consider LINERs to be just an AGN subclass, we can only use K06-a to classify galaxies as star forming (SF), non star-forming (nonSF, either Seyfert or LINER) or transition objects (TO). We use K06-b and K06-c to classify galaxies as SF, AGN or LINER. Our final classification is given in column 5 and is based on the results of the previous three columns. If in any of the diagrams a galaxy falls on the dividing line, this is a borderline case indicated by a question mark in Table 6.

Finally, for three galaxies in our sample there is only [N II]/H α information. In this case we adopt the classification criterion of M10, who classify galaxies with $\log([\text{N II}]/\text{H}\alpha) \leq -0.4$ as SF, those with $\log([\text{N II}]/\text{H}\alpha) > -0.1$ as AGN, and those in between as TO (Stasińska et al. 2006). Of course, as explained, this precludes the possibility of identifying LINERs. Note

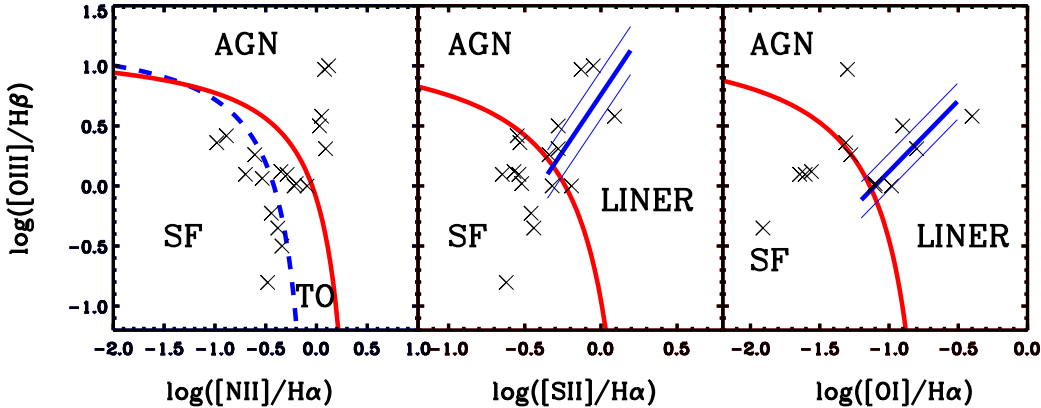


FIG. 6.— Diagnostic optical emission line ratio diagrams for HCG nuclei in this paper. The diagrams are based on the classification scheme of Kewley et al. (2006). See the text for details.

that we include column 5 from Table 6 in Table 9 (its column 7), which presents together multiwavelength nuclear activity diagnostics.

According to Table 6, there exists emission-line ratio information for 22 galaxies in our sample. Out of these 10 are classified optSF (45.5%), 2 are optTO/SF (9%), 1 is optTO (4.5%), 3 are optAGN (13.6%), 1 is optLINER/AGN (4.5%), 1 is opt-nonSF (4.5%), 3 are optTO/LINER (13.6%) and 1 is optLINER (4.5%). Thus, with the caveat of small-number statistics, we see that the most clear result of this classification is that star forming systems represent the most numerous class, followed by AGNs. Otherwise, there appears to be only one clear LINER, as well as a substantial number of mixed classifications.

5.1.2. Optical nuclear excess

For a subset of our galaxy nuclei in seven HCGs, *HST* data are available. An observation log is given in Table 7. The high angular resolution ($\leq 0.1''$) of *HST* may provide a complementary means of identifying nuclear point sources. We identify these sources by examining the median divided image of each galaxy (we use a 13×13 pixel smoothing window and divide the original image by the smoothed one). Additionally, we use GALFIT (Peng et al. 2010) to fit surface brightness profiles and identify nuclear point sources. We compare the GALFIT-derived centers with the central sources detected in median divided images. The findings are summarized in columns 10 and 11 of Table 9. A “y” in column 10 indicates that a nuclear point source in the median-divided image is detected, while a “y” in column 11 indicates that the source coincides with the GALFIT center, within the positional uncertainties (3 pixels). It turns out that, due to the mostly disturbed nature of these galaxies, GALFIT is unable to either converge or provide good fits. We discuss this issue further later (Sec. 5.4).

5.2. Radio

Radio detections of nuclei constitute possible complementary evidence of AGN activity (in the case of radio-loud AGN). Conversely, in star forming galaxies there is a well-known correlation between the 1.4 GHz (21 cm) lu-

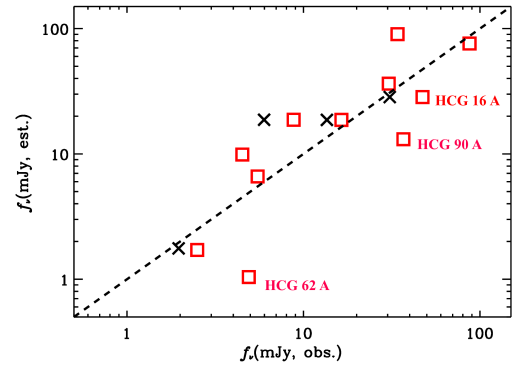


FIG. 7.— 1.4 GHz flux density, estimated from the radio - SFR correlation of Bell (2003), against observed 1.4 GHz flux density. Red squares correspond to NVSS and black crosses to FIRST data (see Table 5). The dashed line is the locus of equal estimated and observed flux densities. The three labeled HCG galaxies that show an excess in observed flux density are all known AGN.

minosity density, $L_{\nu 1.4}$, and SFR (e.g. Bell 2003). Thus, if the SFR is known, one can use this correlation to obtain an estimate for the $L_{\nu 1.4}$, as well as the 1.4 GHz flux density, $f_{\nu 1.4, \text{est}}$. Any significant excess between the observed flux density, $f_{\nu 1.4, \text{obs}}$, and $f_{\nu 1.4, \text{est}}$ may be an indication of AGN activity.

We searched the archives of all publically available major radio surveys, and found detections for 12 of our galaxies in four of the surveys. Details on the radio detections are given in Table 8. As none of the catalogs has full sky coverage, a non-detection does not necessarily imply the lack of radio emission. The catalogs also vary in sensitivity, resolution and positional accuracy. We use both the NVSS and FIRST detections, together with UV+IR SFR values of Tzanavaris et al. (2010) to estimate the $f_{\nu 1.4, \text{est}}$ by means of the Bell (2003) correlation. This correlation has two different forms, depending on whether a galaxy has $M_V > -21$ or not. We estimated $M_V < -21$ for all of our galaxies by using the B and R -band values for HCG galaxies in Hickson et al.

TABLE 6:
Nuclear optical spectroscopic classification.

ID (1)	K06(a) (2)	K06(b) (3)	K06(c) (4)	Type (5)
7A	TO	SF	SF	TO/SF
7B
7C	SF	SF	...	SF
7D	SF	SF	...	SF
16A	nonSF	LNR/AGN	LNR/AGN	LNR/AGN
16B	nonSF	LNR	LNR	LNR
16C	TO	SF	SF	TO/SF
16D	SF	SF	SF	SF
22A	nonSF	AGN	AGN	AGN
22B
22C	SF	SF
31ACE	SF	SF	SF	SF
31B	SF	SF	SF	SF
31F
31G	SF	SF	...	SF
31Q	SF	SF
42A	nonSF	nonSF ¹
42B
42C
42D
59A	TO	LNR	LNR	TO/LNR
59B	TO	TO ¹
59C	SF	SF ¹
59D	SF	SF?	SF?	SF?
62A	TO	SF	LNR/SF	TO/LNR?
62B
62C
62D
90A	nonSF	AGN	AGN	AGN
90B
90C
90D	TO	SF	LNR?	TO/LNR?
92B
92C	nonSF	AGN	...	AGN
92D
92E
92F

NOTE. — Columns give nuclear classification results based on K06 emission line ratio diagrams as follows: (1) [O III]/H β vs. [N II]/H α (K06 - a); (2) [O III]/H β vs. [S II]/H α (K06 - b); (3) [O III]/H β vs. [O I]/H α (K06 - c). Nuclear activity classifications are TO (transition object), SF (star forming), LNR (LINER), AGN (supermassive black hole accretion), nonSF (either LNR or AGN).

¹ Based on [N II]/H α only.

(1989) and the color transformations of Fukugita et al. (1995). Using the Bell (2003) correlation, we thus calculated $f_{\nu 1.4, \text{est}}$. We plot $f_{\nu 1.4, \text{est}}$ against $f_{\nu 1.4, \text{obs}}$ in Fig. 7 for the NVSS and FIRST detected galaxies. For 9 out of 12 galaxies with radio detections the estimated and observed flux density appear to be consistent with each other. The absence of a radio excess for these 9 galaxies is indicated by “n” in column 9 of Table 9. We note though that for galaxies HCG 16 A, 90 A and 62 A, there is an indication of an excess in $f_{\nu 1.4, \text{obs}}$ (“y” in column 9 of Table 9). For the first two this is entirely consistent with their AGN classification in the optical. In addition, HCG 90 A has high X-ray luminosity, further consistent with AGN activity. Our optical classification for the third is LINER, and the radio excess may suggest that it also hosts an AGN (recall that, as mentioned, a majority of LINERs do harbor AGNs). In spite of this consistency, note that for these galaxies $f_{\nu 1.4, \text{est}}$ is still within a factor of ~ 2 from the corresponding $f_{\nu 1.4, \text{obs}}$ value. This

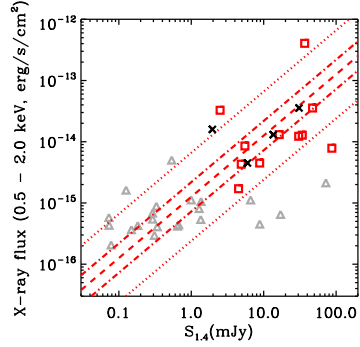


FIG. 8.—: Radio vs. X-ray soft band fluxes for HCG nuclei in this paper. HCG radio fluxes are shown as crosses (FIRST) or red squares (NVSS). Grey triangles are VLA-COSMOS galaxies classified as star-forming by Ranalli et al. (2012, “c1” class from their tables 1 and 2.). The red dashed line is the radio-X-ray correlation of Ranalli et al. (2003, their equation (8) converted to flux using the average distance of our nine HCG nuclei.)

factor also corresponds to the uncertainty of the radio - SFR correlation, so this should not be considered as a robust result. Unfortunately, we are unable to say anything for galaxies for which we do not have any other classification, as none of these are detected in the radio.

We also compare our combined X-ray-radio results for HCG nuclei with the work of Ranalli et al. (2003, 2012) for entire galaxies. Following Ranalli et al. (2012), in Fig. 8 we plot soft band X-ray luminosities against 1.4 GHz fluxes from NVSS and FIRST (red squares and crosses, respectively) for HCG nuclei. We also show the observational X-ray-radio correlation for local star-forming galaxies established by Ranalli et al. (2003) converted to flux using the mean distance of the HCG nuclei. For comparison, we further plot VLA COSMOS sources detected in C-COSMOS and classified as star-forming by Ranalli et al. (2012, class “c1”, their tables 1 and 2). In this figure, HCG nuclei appear to blend smoothly with the lower flux, more distant COSMOS star-forming sources, although with considerable scatter. The topic of X-ray emission in HCGs as a function of star formation rate will be examined in greater detail in a forthcoming publication.

5.3. X-ray – UV

Unlike in the X-rays, each galaxy’s nucleus is well defined in the UV regime as an emission peak in the central region of the galaxy. To identify nuclear X-ray point sources for each galaxy we thus visually inspect all X-ray point sources for spatial coincidence with the central intensity peak of UV sources at 2600 Å. Specifically, we examine the degree of overlap between the AE-determined *Chandra* PSF and a UVOT “PSF”, defined as a circular region 3'' in diameter centered at the $uvw1$ intensity peak. Unlike the case for photometry, the choice of UV circular region size here is solely determined by the $uvw1$ PSF FWHM of 2.37''. Note that the absolute astrometry for both UVOT and *Chandra* is very good, as measured relative to the International Celestial Reference System (ICRS, Ma & Feissel 1998). We

TABLE 7:
HST data for galaxies in this paper.

Group (1)	Galaxy (2)	HST Instrument (3)	Filter (4)	Exp. time (s) (5)	Date (6)	Program ID (7)	PI (8)
HCG 07	A, B, D C	ACS/WFC ACS/WFC	F606W F606W	1230 1230	Sept 2006 Sept 2006	10787	Charlton
HCG 16	A C D A, B B C A	WFPC2 WFPC2 WFPC2 WFPC2 WFPC2 WFPC2 WFPC2	F606W F606W F606W F606W F606W F606W F606W	1900 1900 1900 1900 1900 1900 1900	July 2007 Aug 2007 Aug 2007 Sept 2007 Aug 2007 Sept 2007 Sept 2007		
HCG 22							
HCG 31	A-C, E-H	ACS/WFC	F606W	1230	Aug 2006		
HCG 42	B D	WFPC2 WFPC2	F606W F606W	4200 4200	Dec 2007 Dec 2007		
HCG 59	A, C A, C, D B, I	ACS/WFC ACS/WFC ACS/WFC	F606W F606W F606W	1230 1230 1230	Dec 2007 Nov 2006 Nov 2006		
HCG 62				No HST data			
HCG 90				No HST data			
HCG 92	B, D C, B E	WFC3 WFC3 WFC3	F606W F606W F606W	1395 1395 1395	Aug 2009 Aug 2009 July 2009	11502	Noll

NOTE. — Columns give (1) compact group ID; (2) galaxies observed; (3) instrument used; (4) filter; (5) exposure time; (6) observation date; (7) program ID; (8) program PI.

TABLE 8:
Radio detections of HCG nuclei in this sample.

HCG ID (1)	P (2)	FIRST ^a				NVSS ^b				SUMMS ^c				WISH ^d			
		$f_{20,p}$ (mJy) (3)	\pm (mJy) (4)	$f_{20,i}$ (mJy) (5)	Δpos ($''$) (6)	$f_{20,i}$ (mJy) (7)	\pm (mJy) (8)	Δpos ($''$) (9)	$f_{36,i}$ (mJy) (10)	\pm (mJy) (11)	Δpos ($''$) (12)	$f_{352,p}$ (mJy) (13)	$f_{352,i}$ (mJy) (14)	\pm (mJy) (15)	Δpos ($''$) (16)		
7A	0.014	7.43	0.131	13.57	0.84	16.4	0.7	1.86	
7C	4.5	0.5	8.04	
16A	0.014	12.80	0.159	30.81	2.52	47.3	2.1	1.98	93	100	4.6	4.5		
16B	0.014	1.98	0.158	1.96	0.6	51	53	4.8	0.54		
16C	87.3	3.2	2.04	
16D	34.1	1.1	0.78	
31ACE	30.4	1.6	6.9	
31G	5.5	0.5	4.14	
42A	2.5	0.5	9	
59A	0.014	6.18	0.187	5.98	1.44	8.8	1.0	8.4
62A	4.9	0.5	6.78
90A	36.8	1.5	3.54	45.6	1.7	6.6

NOTE. — Columns are: (1) HCG galaxy ID; (2) FIRST probability that the source is spurious; (3) FIRST peak flux at 20 cm; (4) FIRST error on peak flux; (5) FIRST integrated 20 cm flux; (6) FIRST positional uncertainty in arcseconds; (7) NVSS integrated 20 cm flux; (8) NVSS flux error; (9) NVSS positional uncertainty in arcseconds; (10) SUMMS integrated 36 cm flux; (11) SUMMS flux error; (12) SUMMS positional uncertainty in arcseconds; (13) WISH 352 MHz peak flux; (14) WISH 352 MHz integrated flux; (15) WISH flux error; (16) WISH positional uncertainty in arcseconds.

^a Faint Images of the Radio Sky at Twenty-cm survey (Becker et al. 1995).

^b NRAO-VLA Sky Survey (Condon et al. 1998).

^c Sydney University Molonglo Sky Survey (Bock et al. 1999).

^d Westerbork in the Southern Hemisphere survey (De Breuck et al. 2002),

estimate that in the worst case scenario this could lead to a maximum spurious offset between two coincident sources of $\sim 0.7''$ (combining in quadrature $\sim 0.4''$ from UVOT, Breeveld et al. (2010), and $\sim 0.6''$ from *Chandra*, <http://cxc.harvard.edu/cal/ASPECT/celmon/>).

We also calculate the offset, $\Delta\theta$, in arcseconds between the X-ray and the UV galaxy nucleus as determined by the AE center and UV peak emission, respectively. This is shown in column 3 of Table 9, while column 4 reports if, based on an overlap between the X-ray and UV PSFs, we consider that there exist X-ray – UV nuclear counter-

parts for a given galaxy. Due to the different resolution between the UV and the X-rays, our primary criterion for the existence of counterparts is the PSF overlap, rather than $\Delta\theta$. We do note that all offsets are less than $\sim 3''$. If the PSF overlap criterion indicates that there exist X-ray – UV counterparts, this is indicated by “y” in column 4. There are 22 such cases, which are best candidates for X-ray – UV counterparts. This reduces by 5 the original number of 27 nuclear X-ray sources estimated without strict use of the PSF overlap criterion. Conversely, an “n” indicates no counterparts (10 cases). In two cases

TABLE 9:
Multiwavelength analysis of HCG nuclear sources

HCG ID	Morphology	$\Delta\theta$	X-ray - UV counterparts	α_{OX} (corrected)	α_{OX} (uncorrected)	Optical Type	X-ray Strong AGN	Radio Excess	Optical Nuclear Source	
(1)	(2)	(3)	(4)	(5)	(6)	(7)	(8)	(9)	(10)	(11)
7A	Sb	1.2	y	-2.23	-1.96	TO/SF	n	n	y	y
7B	SB0	1.1	y	-2.31	-2.26	...	n	...	y	y
7C	SBc	0.5	y	-2.39	-2.30	SF	n	n	y	n
7D	SBc	...	n	-2.51	-2.46	SF	n	...	y	y
16A	SBab	3.0	y	-2.16	-1.92	LINER/AGN	n	y	y	...
16B	Sab	0.8	y	-1.68	-1.57	LINER	y	n	y	...
16C	Im	3.0	y	-2.75	-2.35	TO/SF	n	n	y	...
16D	Im	1.1	y	-2.61	-1.96	SF	n	n	y	...
22A	E2	0.8, 0.7	ym	-2.35	-2.33	AGN	n	...	y	...
22B	Sa	1.7	y	-2.13	-2.11	...	n	...	y	...
22C	SBcd	...	n	-2.42	-2.36	SF	n	...	n	...
31ACE	Sdm	1.7, 0.7	ym	-2.50	-2.34	SF	n	n	n	...
31B	Sm	...	n	-2.74	-2.69	SF	n	...	n	...
31F	Im	...	n	-2.57	-2.56	...	n	...	n	...
31G	Im	0.8	y	-2.30	-2.23	SF	n	n	y	...
31Q	Im	2.3	n?	-2.35	-2.32	SF	n	...	n	...
42A	E3	1.8	y	-2.05	-2.01	nonSF	n	n	y	y
42B	SB0	...	n	-2.32	-2.28	...	n	...	y	...
42C	E2	1.0	y	-2.16	-2.14	...	n	...	y	...
42D	E2	...	n	-2.12	-2.09	...	n	...	y	...
59A	Sa	1.8	y	-2.47	-1.90	TO/LINER	n	n	y	n
59B	E0	2.0	y?	-2.01	-1.98	TO	n	...	y	y
59C	Sc	...	n	-2.55	-2.49	SF	n	...	y	y
59D	Im	...	n	-2.63	-2.58	SF?	n	...	n	n
62A	E3	1.1	y	-2.16	-2.14	TO/LINER?	n	y
62B	S0	0.1	y	-2.16	-2.15	...	n
62C	S0	0.4	y	-2.21	-2.20	...	n
62D	E2	...	n	-2.17	-2.08	...	n
90A	Sa	3.3	y	-1.31	-1.01	AGN	y	y
90B	E0	0.4	y	-2.49	-2.18	...	n
90C	E0	0.9	y	-2.49	-2.18	...	n
90D	Im	...	n	-2.91	-2.60	TO/LINER?	n
92B	Sbc	0.6	y	-2.68	-2.37	...	n	...	y	...
92C	Sbc	0.9	y	-1.81	-1.51	AGN	y	...	y	...
92D	E2	0.7	y	-2.54	-2.23	...	n	...	y	...
92E	E1	1.5	y	-2.57	-2.27	...	n	...	y	...
92F	SAB0	2.1	y?	-2.49	-2.19	...	n

NOTE. — Columns are: (1) HCG galaxy ID; (2) Morphological type (Hickson et al. 1989); (3) offset between peak of nuclear UV emission in the UVOT $uvw1$ filter and peak of X-ray emission in the X-rays; (4) X-ray – UV counterparts flag based on PSF overlap: y = detected X-ray – UV overlap; n = no overlapping PSFs - no counterparts; ? = ambiguous; m = multiple X-ray PSFs overlap with UV PSF; (5) α_{OX} value corrected for intrinsic extinction; (6) α_{OX} value uncorrected for intrinsic extinction; (7) nuclear type according to optical spectroscopy classification (Table 6, column 5): SF = star-forming, TO = transition object, ... = no classification; (8) $L_{X,0.5-8.0\text{keV}} \geq 10^{41} \text{ erg s}^{-1}$, suggestive of strong AGN: y = yes, n = no; (9) radio excess flag: y = observed 1.4 GHz flux density in excess of that expected based on the Bell (2003) radio - SFR correlation; (10) *HST* nuclear detection flag for median-divided images: y = central point source detected in *HST* median-divided image; n = no detection; (11) comparison flag for *HST* nuclear detections: y = nuclear point source in *HST* median-divided image coincides with GALFIT center within 3 pixels; n = no coincidence within 3 pixels.

(22A, 31ACE) it is not clear which X-ray source is the best counterpart, as two X-ray PSFs overlap with the UV PSF. This is indicated by an “m” (for “multiple”) in column 3. A question mark indicates that the X-ray – UV counterpart is uncertain, as described in Sec. 5.4 (three cases).

To quantify the relative contributions coming from the X-rays and the UV we calculate the α_{OX} index defined above and tabulate our results in columns 5 and 6 of Table 9, corrected and uncorrected for intrinsic extinction, respectively. The mean α_{OX} values and 1σ standard deviations are $\alpha_{OX} = -2.33 \pm 0.31$ (corrected) and $\alpha_{OX} = -2.17 \pm 0.32$ (uncorrected). Thus, overall, the extinction correction does not significantly affect α_{OX} values. We plot α_{OX} vs. 2600 Å luminosity, $\nu L_{\nu 2600}$, in Fig. 9. The well-known correlation for 333 moderate-to high-luminosity AGNs by Steffen et al. (2006, S06) is shown by the dashed line and the $\pm 3\sigma$ scatter of the

data points on the correlation by the solid lines. The S06 AGNs are shown as black (magenta for upper limits) stars (their tables 1 and 2). We also show the AGNs of Lusso et al. (2010, herafter LC10) as cyan dots. The black open circles are the LINERs of Eracleous et al. (2010b). Our HCG nuclei are shown in color, according to their optical spectroscopic classification (Sec. 5.1.1), or as black crosses if there is no such classification. HCG upper limits are shown by downward pointing arrows. In the interest of clarity, in this and subsequent plots mixed classifications (Table 6, column 5, and Table 9, column 7) have been simplified as follows: AGN? \rightarrow AGN; SF? \rightarrow SF; TO/AGN, TO/SF, TO/LNR \rightarrow TO; LNR/AGN \rightarrow LNR. It can be seen that HCG nuclei do not occupy the same locus as strong AGNs and LINERs. This suggests that HCG nuclei are not likely to harbor strong AGNs or LINERs. To further explore whether this is also consistent with star formation being dominant in HCG nuclei,

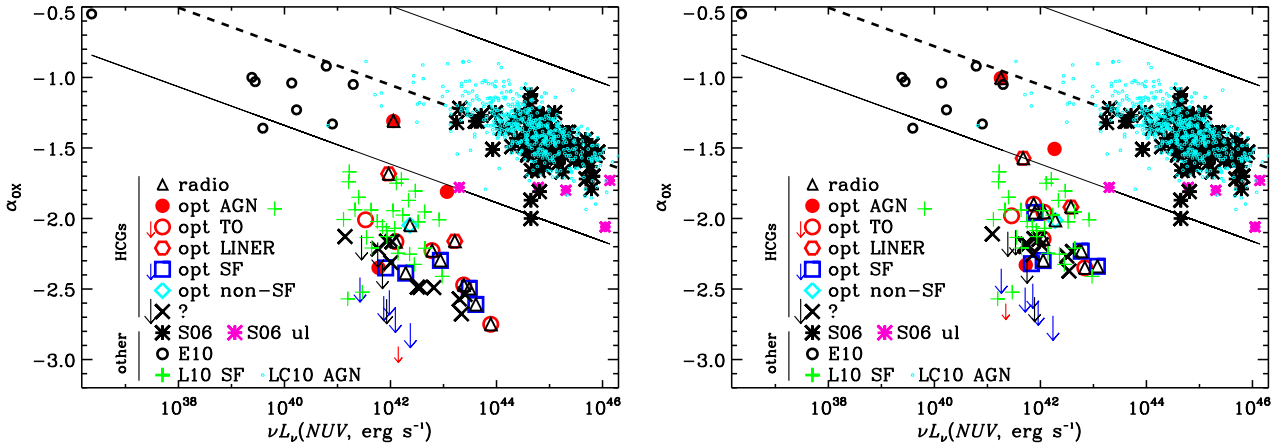


FIG. 9.—: UV-to-X-ray spectral index, α_{OX} , vs. UV luminosity at $\sim 2600\text{\AA}$. The left panel uses values corrected for intrinsic extinction, while the right panel uses uncorrected values. Symbols indicate optical nuclear classification (Sec. 5.1.1) as indicated in the legend: Triangles, large open and filled circles, squares, diamonds, pentagons and crosses are for HCG nuclei. Downward pointing arrows are upper limits for HCG nuclei based on upper limit X-ray flux estimates for X-ray non-detections and are color-coded to indicate optical nuclear classifications (black if there are none). Note that in the interest of clarity, mixed classifications have been simplified, as explained in the text. Non-HCG data points are from Steffen et al. (2006, S06, ul = upper limits), Eracleous et al. (2010b, E10) Lehmer et al. (2010, L10), Lusso et al. (2010, LC10). The dashed line is the correlation for strong AGNs from S06. The two solid lines indicate the $\pm 3\sigma$ region for AGN (S06) and LINERs (E10). The green crosses are star-forming galaxies from L10, with SFRs in the same range as our HCG galaxies. These plots clearly suggest that most HCG nuclei do not follow the correlation for strong AGN but are more similar to star-forming systems.

we compare with star forming galaxies from the compilation of Lehmer et al. (2010, hereafter L10). These authors use multiwavelength criteria to select star forming galaxies among nearby (< 60 Mpc) Luminous Infrared Galaxies (LIRGs). We select a sub-sample of 30 galaxies from this sample whose SFRs are in the range 0.011 to $17 M_{\odot}\text{yr}^{-1}$, matching the SFR range of our HCG galaxies (Tzanavaris et al. 2010). Note that we do not need nuclear photometry of these galaxies in order to test our results. What we wish to investigate is whether the X-ray and UV contributions in a galactic environment dominated by star formation are similar to our findings for the majority of HCG nuclei. We thus calculate α_{OX} for these systems and indicate them in Fig. 9 as green crosses. The mean α_{OX} for these sources is -1.90 ± 0.33 and the figure shows that there is significant overlap with our nuclei. In particular, the most relevant comparison is with HCG nuclei data *not* corrected for intrinsic extinction (right panel in Fig. 9), as L10 did not carry out any such correction. At the same time, compared to strong AGNs, these galaxies seem to occupy a completely different region.

We quantify the comparisons between α_{OX} values for different datasets by carrying out a standard two-sided KS test, the results of which are shown in Fig. 10. The probability that the α_{OX} values for HCG nuclei come from the same distribution as the values for strong AGNs and LINERs is extremely small (8×10^{-28} if corrected and 8×10^{-27} if uncorrected for intrinsic extinction). In contrast, the probability that the α_{OX} values for HCG nuclei uncorrected for intrinsic extinction come from the same distribution as those for the L10 star-forming galaxies is substantially larger at 0.005. This number is not extremely large, as, after all, the L10 sample represents

an extragalactic environment (LIRGs) distinct from compact groups. However this probability may be high enough to suggest that HCG nuclei are at least more similar to star-forming galaxies than they are to strong AGNs. This is also evident from the overlap between the two distributions in the histogram of the rightmost panel in Fig. 10. We thus conclude that, generally speaking, HCG nuclei do not follow the strong AGN correlation and are consistent with star formation being dominant.

Further, in Fig. 9 there is a trend with increasing $\nu L_{\nu 2600}$ and decreasing α_{OX} for nuclei to be both further below the strong AGN locus defined by the correlation and to be optically classified as either SF or TO. To further investigate this possible connection between α_{OX} and star formation, we plot α_{OX} versus SSFR in the top row of Fig. 11 using two different color and symbol schemes. In the left panel symbols are coded to indicate the optically-based nuclear activity classification (where available). In this panel optSFs preferentially occupy the high-SSFR/low- α_{OX} region of parameter space, where $\alpha_{\text{OX}} \lesssim -2.3$. In contrast, optLINERs, opt-nonSFs, optAGNs and some optTOs inhabit the low-SSFR/high- α_{OX} region of parameter space. The fact that two optTOs are found in the optSF region is consistent with their definition, as one would expect transition objects to appear in both regions. If this apparent distribution pattern in α_{OX} – SSFR space is a real effect, then we predict that the nuclei for which there is no optical classification (marked by black crosses or downward pointing arrows in this panel) are most likely AGNs, LINERs or transition objects.

On the other hand, symbols in the right panel indicate the RC3-based morphological classifications of the host galaxies. A value of $\alpha_{\text{OX}} \sim -2.3$ here roughly sep-

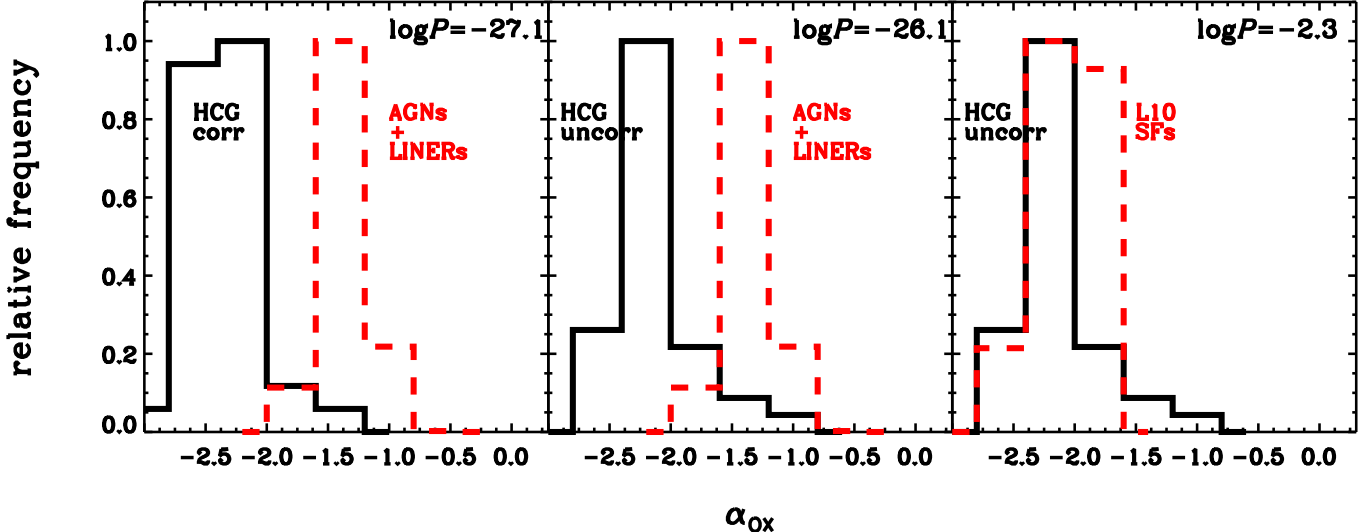


FIG. 10.—: Normalized distributions of X-ray-to-UV spectral index, α_{OX} , and KS probability for different galaxy sample pairs. In all panels, the distribution for HCG nuclei is indicated by the solid black line, corrected for intrinsic extinction in the left panel, and uncorrected in the other two. In the left and middle panels, the red dashed line is for all strong AGNs and LINERs from other samples (S06, LC10, Eracleous 2010a,b). In the right panel, the red dashed line is for the star-forming galaxies of L10. The logarithm of KS probability that two distributions come from the same parent distribution is shown at the top right of each panel.

arates ellipticals (with low SSFRs) from galaxies with progressively more spiral morphologies (and higher SSFRs). This is consistent with our prediction for unknown nuclear activity systems in the left panel, as these nuclei are hosted by morphologically earlier-type systems.

Since SSFR is SFR normalized by stellar mass, M_* , it is interesting to also investigate possible trends of α_{OX} with these quantities separately. In the middle and bottom rows of Fig. 11 we show pairs of plots for α_{OX} versus SFR and α_{OX} versus M_* . Although there is a trend for lower SFR (and higher M_*) systems to have larger values of α_{OX} , this is not as pronounced as the trend with SSFR.

5.4. Multi-wavelength Classifications (Table 9)

Table 9 brings together results on the type of activity of HCG nuclei from different wavelength ranges. The information presented includes X-ray – UV nuclear counterparts (columns 3 and 4, Sec. 5.3), UV-to-X-ray spectral indices (columns 5 and 6, Sec. 5.3), optical emission line ratio classifications (column 7, Sec. 5.1.1), level of X-ray nuclear activity (column 8, Sec. 3.1), radio nuclear excess (column 9, Sec. 5.2) and *HST*- based nuclear detections (columns 10 and 11, Sec. 5.1.2).

Considering this table as a whole, we can draw a number of useful conclusions:

1. For about 60% (22/37) of HCG galaxies we have detected a single, nuclear X-ray point source, as indicated by the overlap between the X-ray and UV PSFs in the central region of a galaxy (“y” in column 4). Two of these galaxies are classified optAGN, one opt-nonSF, one opt-LINER/AGN, one optLINER, two optTO/LINER, two

optTO/SF and three optSF. Nine are have no emission line ratios and are unclassified. Given *Chandra*'s resolution, the detection of these nuclear X-ray sources is consistent with *some* level of AGN activity in these systems, although an XRB origin cannot be excluded (and could, in fact, dominate).

2. For 27% (10/37) of galaxies there is no detected nuclear X-ray emission at all (“n” in column 4). Five of these nuclei are classified optSF, four are unclassified and one is classified optTO/LINER. This is HCG 90 D, which has a very irregular, clumpy appearance, likely related to its close interaction with 90 B. Although we formally identify the center of galaxies with a UV intensity peak, there is likely no well-defined nucleus for such a morphology. Depending on the slit position, it is unclear whether the optical spectroscopic classification corresponds to the same source.

3. For three galaxies ($\sim 8\%$), the identification of counterparts is questionable (“?” in column 4). Specifically, for HCG 31 Q, the *Chandra* PSF overlaps slightly with the UV PSF, but the source positions are also $\sim 2.3''$ apart, so the lack of coincidence is unlikely to be due to astrometric errors (“n?” in column 4). For HCG 59 B and 92 F, the X-ray sources are $\sim 2''$ from the UV intensity peak with little PSF overlap. These can only tentatively be considered as X-ray counterparts to the UV emission (“y?” in column 4).

4. As mentioned, in two cases ($\sim 5\%$) there are two possible X-ray counterparts for a single UV nuclear source. In particular, for HCG 31 ACE, the *Chandra* PSFs for X-ray sources 38 and 40 both overlap with the

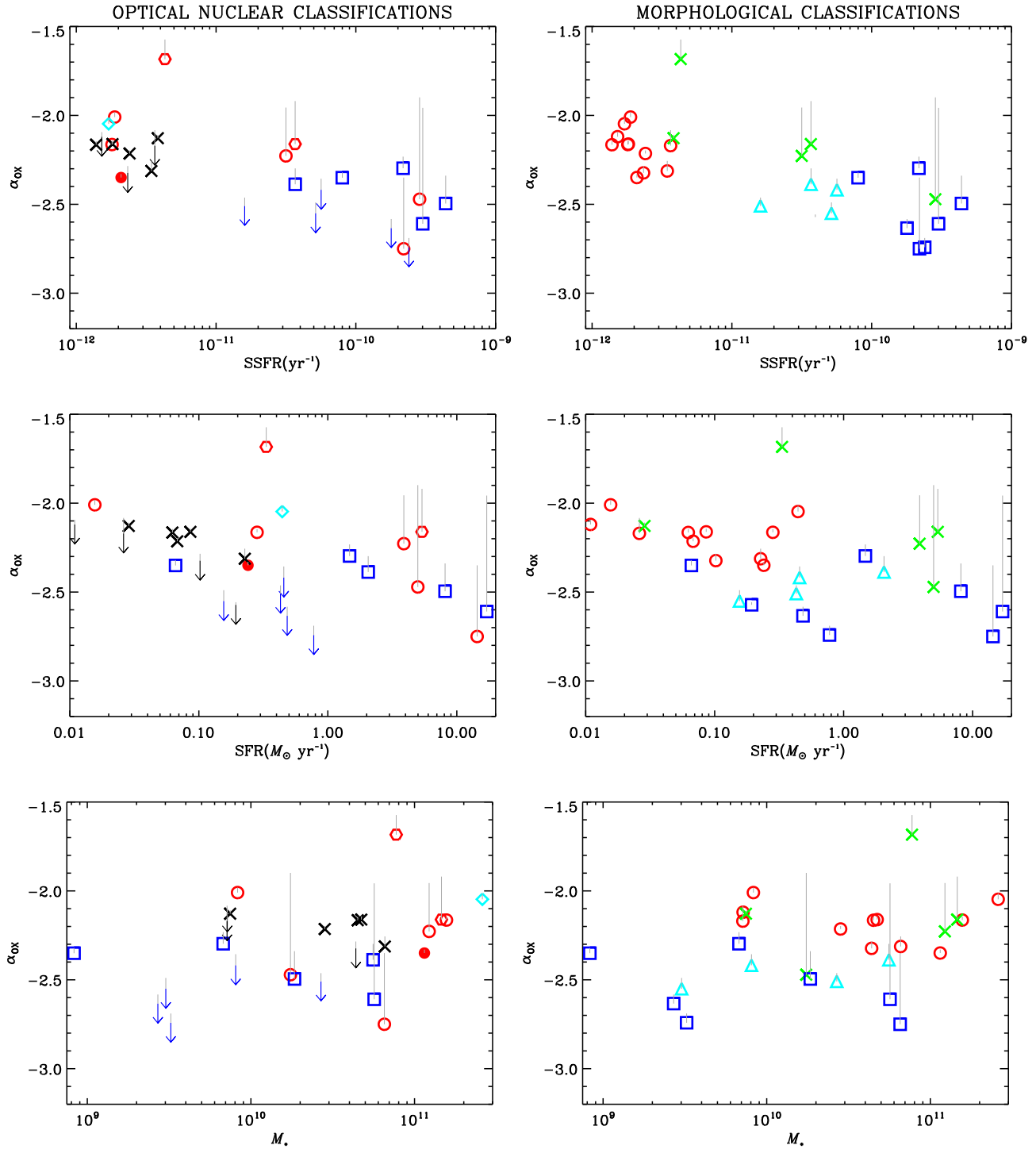


FIG. 11.—: UV-to-X-ray spectral index, α_{OX} , vs SSFR (top panels), SFR (middle panels) and M_{\star} (lower panels). The data points in each panel pair are identical and upper limits are only indicated in the left panel. All symbols use α_{OX} values corrected for intrinsic extinction as explained in the text. The vertical grey lines show the effect of extinction correction (α_{OX} values are more positive if not corrected). *Left*, symbols indicate optical nuclear classifications (same as in Fig. 9). *Right*, symbols indicate morphological T-types, where T increases from ellipticals to spirals to irregulars: Red circles are $T \leq 0$, green crosses are $1 \leq T \leq 3$, cyan triangles are $4 \leq T \leq 7$, blue squares are $T \geq 8$. The SSFR panel pairs suggest that nuclei with lower α_{OX} are highly star-forming and are hosted by later morphological types. This trend is less pronounced in the SFR panels. The M_{\star} panels show that AGNs are hosted by the more massive systems and the earlier morphological types.

UV PSF. Since source 40 is only $0.7''$ away from the UV peak (c.f. $1.7''$ for 38), we chose source 40 as the most likely counterpart. In the case of 22 A both X-ray PSFs are almost symmetrical about the UV peak, so not even a tentative choice is possible.

5. X-ray luminosity is often used as a direct diagnostic for the presence of an AGN, with $\sim 1 \times 10^{41-42}$ erg s $^{-1}$ taken as a fiducial threshold for unambiguously strong AGN activity (e.g. Reynolds & Nowak 2003; Bauer et al. 2004). Using $L_{X,0.5-8.0\text{keV}} = 10^{41}$ erg s $^{-1}$ as our threshold, we see that there are only three sources which are candidates for strong AGNs (column 8 in Table 9). These are HCGs 16 B, 90 A and 92 C. The first is classified as optLINER and the other two optAGN. Thus together with 62 A, HCG 16 B is a second case where a LINER and an AGN may coexist.

7. According to column 7, there is one optLINER/AGN, one optAGN and one opt-nonSF which, according to column 8, are not strong X-ray AGNs. Combining these results, we believe that these are good LLAGN candidates.

8. Columns 10 and 11 suggest that our *HST* data do not help us discriminate clearly between AGN and SF systems. For 22 sources the *HST* median-divided image suggests a nuclear detection ("y" in column 10). However, there is no 1-to-1 correspondence between these 22 sources and the 22 sources for which X-ray – UV counterparts exist. On the one hand, it is encouraging that for four of these, namely the nuclei of HCG 16 A, 22 A, 42 A and 92 C, classified as optLINER/AGN, optAGN, opt-nonSF, and optAGN, respectively (column 7), an optical nuclear source seems to be present in the median-divided image (column 10). However, combining this result with GALFIT is problematic for two main reasons. First, in general GALFIT leads to fits that are poor and in most cases do not converge. This is because most of the galaxies in our sample are disturbed and thus full Sersic profile fitting is usually unable to fit the diffuse light. Second, only one of the AGN candidate galaxies mentioned, HCG 42 A, has a GALFIT center that lies within the 3-pixel positional uncertainty from the median-divided center. For the other three galaxies, we are unable to obtain a satisfactory GALFIT fit. On the other hand, note that five galaxies whose optical classification is not AGN, nevertheless have their GALFIT and median-divided centers within the 3-pixel positional uncertainty. Given the lack of good GALFIT results, it is hard to assess the significance of this result.

6. AGN FRACTION

For the purpose of comparison with galaxy clusters, we calculate the AGN fraction in our compact group sample by following Martini et al. (2006). We estimate 3σ uncertainties using the method of Gehrels (1986). We use *R*-band magnitudes from Hickson et al. (1989) to establish that in our sample there are 26 galaxies with $M_R < -20$. For 4 galaxies for which Hickson et al. (1989) do not provide *R*-band data we obtain magnitude information from the NASA/IPAC Extragalactic Database. We assume that the AGN hosts among these 26 galaxies are those that are optically identified as such (Column 7 in Table 9). This includes mixed (e.g. LINER/AGN) and tentative (AGN?) classifications. The inclusion of these latter cases does not actually matter, as we also use the

TABLE 10:
Physical size estimate (kpc) of areas used for UV and X-ray nuclear photometry.

group ID (1)	<i>Swift</i> -UVOT ($10''$) (2)	<i>Chandra</i> ($1''$) (3)
HCG 7	2.7	0.3
HCG 16	2.6	0.3
HCG 22	1.8	0.2
HCG 31	2.8	0.3
HCG 42	3.0	0.3
HCG 59	3.1	0.3
HCG 62	3.1	0.3
HCG 90	1.6	0.2
HCG 92	4.3	0.4

NOTE. — Columns are: (1) HCG group ID; (2) Extent in kpc of $10''$ at the galaxy group distance. $10''$ is the diameter of the circular regions used for nuclear UVOT photometry. (3) Extent in kpc of $1''$, the on-axis *Chandra* PSF, at the galaxy group distance.

further criterion that $L_{X,0.5-8.0\text{keV}} > 10^{41}$ erg s $^{-1}$. This only leaves two galaxies, which are the two strongest AGN cases, namely HCG 90 A and HCG 92 C. The AGN fraction defined in this way for two out of 26 galaxies is then $f_A(M_R < -20, L_X > 10^{41}) = 0.08^{+0.35}_{-0.01}$. This is close, but higher than the $\sim 5\%$ fraction of Martini et al. (2006) in galaxy clusters.

7. DISCUSSION

The main result of this paper is the significant detection of nuclear X-ray point sources in 60% of the 37 HCG galaxies in this sample. We detect these sources by taking advantage of *Chandra*'s excellent angular resolution, while also taking into account the size of the PSF at each source's detected position on the CCD and the overlap with the UV PSF.

Unfortunately, the mere detection of an X-ray point source that appears to coincide with the UV galactic nucleus is no strong evidence that the origin of the nuclear emission is an AGN, rather than circumnuclear star formation, unless the source also has a high X-ray luminosity. The threshold we use in this paper is $L_{X,0.5-8.0\text{keV}} \geq 10^{41}$ erg s $^{-1}$ and most of our nuclear sources are fainter. We provide a quantitative illustration of this caveat in Table 10, where we give estimates of the physical sizes (in kpc) of the areas used for *Chandra* and UVOT photometry at the distances of our galaxies. Taking the case of *Chandra*, $1''$ at the distances of these galaxies corresponds to physical sizes ranging from ~ 0.16 (for HCG 90, our nearest group) to ~ 0.43 kpc (for HCG 92). The known detections of nuclear star clusters with sizes of this order and ages as young as 10 Myr demonstrates that regions of this physical size can be the sites of compact and intense circumnuclear star formation (e.g. Rossa et al. 2006) that, in turn, can harbor unresolved XRB populations. Since most of our nuclear sources have low L_X estimates, such a possibility should be seriously considered. The optical emission-line ratio classifications for 22 galaxies in the sample are in support of the lack of strong AGN activity and the prevalence of star formation in HCG nuclei. We caution that these are small numbers, but, taken at face value, almost half of our systems (45.5%) are classified as pure optSF, while more are classified as optTO or have mixed classifica-

tions. Only a minority (13.6%) are optAGN, and two of these also have high X-ray luminosities.

Two of the three nuclei that fulfill the X-ray luminosity criterion for harboring strong AGNs have $L_{X,0.5-8.0\text{keV}} > 10^{42} \text{ erg s}^{-1}$ (90 A and 92 C, both also optAGN). The result for HCG 90 A is also independently confirmed by LaMassa et al. (2011) who, using *XMM-Newton* data and detailed spectral fitting, report $L_{X,2.0-10.0\text{keV}} = 10^{42.96} \text{ erg s}^{-1}$ (compare with $L_{X,0.5-8.0\text{keV}} = 10^{42.6} \text{ erg s}^{-1}$ in our Table 2). These are the *only* nuclear sources in our sample that fulfill optical spectroscopic, X-ray luminosity and, for 90 A, radio excess criteria for being unambiguous and strong AGNs.

As X-ray luminosity decreases, so does its discriminative power as an AGN diagnostic. Two nuclei have $10^{40.5} < L_X < 10^{42}$ (16A and 16B, optLINER/AGN and optLINER, respectively), but the optLINER/AGN is the X-ray *fainter* one. The rest of the systems are progressively fainter in the X-rays, precluding any conclusions on the nature of the nuclear activity from X-ray information alone. The conservative conclusion based on X-ray luminosity is to consider these as candidates either for nuclear star clusters and XRB hosts or LLAGN hosts (or, possibly, some combination of the two). Although X-ray faint ($L_{X,2.0-10.0\text{keV}} \sim 10^{38} \text{ erg s}^{-1}$) nuclei have been identified as LLAGNs with *Chandra* data, e.g. in the Palomar sample of Ho et al. (2001), the comparison is not entirely fair as that sample contained early type galaxies where star formation is unlikely to strongly dilute the AGN emission.

We have also combined X-ray and UV nuclear photometry to calculate α_{OX} values and compare with those for strong AGNs and star forming galaxies. The KS test shows that HCG nuclei are completely distinct from strong AGNs and fairly similar, though not identical, to star forming galaxies. The correlation in $\alpha_{\text{OX}} - \nu L_{\nu,2600}$ space (Fig. 9) for strong AGNs is well established over $\sim 4 - 6$ orders of magnitude (Strateva et al. 2005; Steffen et al. 2006; Just et al. 2007). Lusso et al. (2010) also confirm this correlation, slightly extending it to fainter systems. The location of HCG nuclei in Fig. 9 is consistent with their L_X values: The highest L_X nuclei, i.e. those that are more likely to harbor strong AGNs, do, in fact, follow the correlation. For lower nuclear L_X values, nuclei are located further below the correlation. Notably, this region is also inhabited by the normal, star-forming galaxies of L10. Since this latter sample was compiled independently from our HCG sample, as well as the other comparison samples shown in Fig. 9, this result is in support of our conclusion that strong AGN activity is absent and star formation may be dominant in most HCG nuclei.

Taking into account the optical AGN/TO/SF classification information, in Fig. 9 there appears to be a broad transition region at $\alpha_{\text{OX}} \sim -2.3$. At lower α_{OX} values most of the nuclear emission is likely due exclusively to star-formation. This is consistent with the top row of Fig. 11. The left panel shows that it is precisely the high SSFR systems that have $\alpha_{\text{OX}} \lesssim -2.3$, and the right panel shows that these have the most spiral-like morphologies. In addition, the right panel shows a very smooth progression with morphological type towards values of $\alpha_{\text{OX}} \lesssim -2.3$. Although we do not claim

that $\alpha_{\text{OX}} \gtrsim -2.3$ guarantees AGN activity, the fact that these systems are preferentially early type (as well as the most massive, see bottom row of Fig. 11) is consistent with earlier results that AGNs in compact groups are located preferentially in early type galaxies (Coziol et al. 1998b,a). Note also that the trend with decreasing α_{OX} , although still present, is not as clear in the lower two panel rows of Fig. 11. This simply reflects the fact that SSFR is by construction a better discriminator between highly star forming late types and more quiescent (and more massive) early types.

One possible caveat in this work is the mismatch in resolution and, hence, photometric aperture between the X-ray and UV data. The use of a $10''$ diameter for UV photometry, corresponding to physical sizes between 1.6 and 4.3 kpc, means that some of the UV emission may not be co-spatial with emission from the X-ray source inside the smaller X-ray aperture. This would lead to an overestimate of the UV luminosity, and, hence, an underestimate of α_{OX} . In such a case, data points corresponding to the “true” α_{OX} and UV luminosity values in Fig. 9 would be shifted to the left (towards lower $\nu L_{\nu,2600}$ values) and up (towards higher α_{OX}) relatively to the data points shown. Note though that, with the exception of possible nuclear star clusters, the UV aperture mostly traces galactic bulges, where old stellar populations dominate. Contamination from non-nuclear UV emission due to massive young stars might then be not so important. Also, contamination from *old* stars (the so-called UV upturn) is not important at the near-UV wavelengths studied because it only becomes dominant blueward of 2000 Å (O’Connell 1999). These observations are in line with the results of the tests by Grupe et al. (2010) who performed AGN UV photometry with *Swift* UVOT. They performed photometry both with the standard $5''$ -radius UVOT aperture and a narrower $3''$ -radius that included aperture corrections. They found that host galaxy contamination is most serious in the optical UVOT bands, while in the UV bands the magnitude difference was on the order of 0.05 mag. We should caution, however, that since Grupe et al. (2010) had bright AGNs, they were more likely to have the AGNs dominating both in the UV and the X-ray, which is more likely to drive their conclusions. Similarly, the α_{OX} values of our known strong AGN systems do fall close to the strong AGN correlation. Finally, we test the effect of photometric aperture by performing X-ray photometry using the larger UV apertures. This leads, on average to $L_{\nu,2\text{keV}}$ values that are higher by $0.48 \text{ erg s}^{-1} \text{ Hz}^{-1}$ or α_{OX} values that increase by 0.18. Such changes do not significantly affect the results of this work.

We are thus led to the conclusion that the observed trends of α_{OX} with $\nu L_{\nu,2600}$ are telling us two things: First, HCG nuclei *as a class* generally do not harbor strong AGNs. Instead, the UV and X-ray emission we see is in most cases likely dominated by nuclear star formation. Second, considering *early and late-type morphologies*, the most likely interpretation is that low SSFR, early-type, systems are the ones harboring weak AGNs, while high SSFR, late-type, systems are dominated by star formation.

The radio and *HST*-based diagnostics do not provide much additional insight regarding the nuclear activity

in this galaxy sample. For three galaxies, the possible detection of excess radio emission, above that expected from star formation alone, is consistent with the X-ray luminosity (for HCG 90 A), as well as the optAGN classification (for HCG 16 A and 90 A). However, the excess is not greater than the uncertainty in the radio-SFR correlation used. We also have no radio data for any of the galaxies that lack optical classifications. Thus the radio results are not particularly useful.

Using *HST*-data for a subset of our galaxies, we detect what seem to be nuclear sources after subtracting median-smoothed images for 22 galaxies. However, these sources do not correspond to the optical emission line ratio classifications in any systematic way. Due to the disturbed nature of most galaxies, we are also unable to obtain reliable and consistent surface brightness fits with GALFIT in most cases. The fact that some sources have their median divided center within 3-pixels of the GALFIT center is thus of limited significance.

Our AGN fraction result for compact groups suffers from small number statistics and needs to be tested with larger samples. However, taken at face value and given that we have applied the same criteria used by others to obtain the AGN fraction in galaxy clusters, our result is somewhat higher than the one for clusters. This might suggest that the lower velocity dispersions and shorter crossing times in compact groups, which make this environment physically distinct from that of clusters, also have an effect on AGN activity, just as they seem to do for star formation.

We have no emission line ratios, and thus no optical spectroscopic classifications for 15 of our galaxies, indicated by black crosses and arrows in the Figures. These systems include HCG 7B, 22B, 31F, 42B, 42C, 42D, 62B, 62C, 62D, 90B, 90C, 92B, 92D and 92E. Based on the trends discussed above and the morphologies of these systems, we tentatively predict the nature of their nuclear activity. There are two late type systems, HCG 31F (morphological type Im) and HCG 92B (type Sbc). Our prediction is that these will be dominated by star formation. The rest of the systems have elliptical/S0 morphologies, and may harbor a weak LLAGN.

8. CONCLUSIONS

This paper presents the first compilation of X-ray detected point sources in the fields of 9 HCGs, for which we provide an extensive compilation of source characteristics.

We have used multi-wavelength diagnostics (X-ray, UV, optical, and radio) to assess the levels of AGN, SF and LINER activity in the compact group environment. Our main results are the following:

1. In 60% of 37 galaxies we detect single, nuclear X-ray sources that have nuclear UV counterparts. We detect no nuclear X-ray emission for 27% of our galaxies. The rest of the systems have more uncertain X-ray nuclear detections.
2. Out of the 22 galaxies for which emission line ratios are available in the literature, we classify a clear plurality (45.5%) as optSF. Our criteria allow us, for the first time, to also classify five systems as LINERs, although four of these are mixed

(LINER/AGN, TO/LINER). Thus any LINER activity is associated with a minority (22.5%) of systems. Only three nuclei (13.6%) are classified optAGN.

3. Only three systems (HCG 16 B, 90 A, 92 C) are candidates for hosting an X-ray strong AGN ($L_{X,0.5-8.0\text{keV}} \geq 10^{41} \text{ erg s}^{-1}$).
4. When several criteria are taken into account (optical spectroscopic classification, excess radio emission, X-ray luminosity, location in $\alpha_{\text{OX}}-\nu L_{\nu,2600}$ parameter space) only two HCG nuclei (90 A, 92 C) fulfill several criteria and are classified as strong, unambiguous AGNs.
5. In $\alpha_{\text{OX}}-\nu L_{\nu,2600}$ space, HCG nuclei occupy a region which is distinct from that occupied by strong AGNs and largely overlaps with that occupied by other, nearby star-forming galaxies not known to harbor AGNs (Fig. 9). The only exceptions are the two strong AGNs which do fall in the AGN region. We thus tentatively make the prediction that HCG nuclei without optical nuclear-type classifications are dominated by star formation (if they have late-type morphologies) or may harbor *low* luminosity AGNs (especially if they have early-type morphologies).
6. α_{OX} anticorrelates with galaxy-wide SSFR and spiral morphology so that the star formation contribution is strongest in highest SSFR and later type morphology galaxies Fig. 11. The detected anticorrelation (correlation) with SFR (M_*) is weaker.
7. Using the same criterion used in galaxy clusters (Martini et al. 2006), the AGN fraction of HCG galaxies more luminous both than $M_R = -20$ and $L_{X,0.5-8.0\text{keV}} = 10^{41} \text{ erg s}^{-1}$ is $0.08^{+0.35}_{-0.01}$, which is close but higher to that in clusters.

Our general conclusion is that overall the CG environment has a mitigating effect on the level of AGN activity but not AGN numbers. With future expanded X-ray and UV samples as well as deeper observations we will be able to better assess the nature and statistics of HCG nuclei. The comparison with galaxy clusters suggests that environment plays a key role for the overall level of AGN activity. In this respect, it is imperative to carry out detailed comparisons with samples from other group, cluster and field environments.

We gratefully acknowledge the support of the ACIS Instrument Team contract SV4-74018 (PI: G. P. Garmire). P.T. acknowledges support through a NASA Postdoctoral Program Fellowship at NASA Goddard Space Flight Center, administered by Oak Ridge Associated Universities through a contract with NASA. A.H. and P.T. were also supported by NASA ADAP 09-ADP09-0071 (P.I. Hornschemeier). We thank Kip Kuntz for discussions and assistance with matching of sources in three X-ray bands. We thank Bret Lehmer for making his catalog of star forming galaxies available to us. K.F., T.D.D. and S.C.G thank the Natural Science and Engineering

Research Council of Canada and the Ontario Early Researcher Award Program for support. W.N.B. acknowledges support from NASA ADP grant NNX10AC99G. J.C.C. and C.G. acknowledge funding that was provided through *Chandra* Award No. GO8-9124B issued by the *Chandra* X-Ray Observatory Center, which is operated by the Smithsonian Astrophysical Observatory under NASA contract NAS8-03060, grant number HST-GO-10787.15-A from the Space Telescope Science Institute which is operated by AURA, Inc., under NASA contract NAS 5-26555, and by the National Science Foundation under award 090894. The Institute for Gravitation and the Cosmos is supported by the Eberly College of Science

and the Office of the Senior Vice President for Research at the Pennsylvania State University. K.F. acknowledges support from the Queen Elizabeth II Graduate Scholarships in Science and Technology. This research has made use of data obtained from the High Energy Astrophysics Science Archive Research Center (HEASARC), provided by NASA's Goddard Space Flight Center. This research has made use of the NASA/IPAC Extragalactic Database (NED) which is operated by the Jet Propulsion Laboratory, California Institute of Technology, under contract with the National Aeronautics and Space Administration.

Facilities: *Chandra*, *Swift*

REFERENCES

- Arnaud, K. A. 1996, in Astronomical Society of the Pacific Conference Series, Vol. 101, Astronomical Data Analysis Software and Systems V, ed. G. H. Jacoby & J. Barnes, 17
- Baldwin, A., Phillips, M. M., & Terlevich, R. 1981, PASP, 93, 817
- Barth, A. J., Ho, L. C., Filippenko, A. V., & Sargent, W. L. W. 1998, ApJ, 496, 133
- Bauer, F. E., Alexander, D. M., Brandt, W. N., Schneider, D. P., Treister, E., Hornschemeier, A. E., & Garmire, G. P. 2004, AJ, 128, 2048
- Becker, R. H., White, R. L., & Helfand, D. J. 1995, ApJ, 450, 559
- Bell, E. F. 2003, ApJ, 586, 794
- Bock, D. C.-J., Large, M. I., & Sadler, E. M. 1999, AJ, 117, 1578
- Breeveld, A. A., Curran, P. A., Hoversten, E. A., Koch, S., Landsman, W., Marshall, F. E., Page, M. J., Poole, T. S., Roming, P., Smith, P. J., Still, M., Yershov, V., Blustin, A. J., Brown, P. J., Gronwall, C., Holland, S. T., Kuin, N. P. M., McGowan, K., Rosen, S., Boyd, P., Broos, P., Carter, M., Chester, M. M., Hancock, B., Huckle, H., Immel, S., Ivanushkina, M., Kennedy, T., Mason, K. O., Morgan, A. N., Oates, S., de Pasquale, M., Schady, P., Siegel, M., & vanden Berk, D. 2010, MNRAS, 406, 1687
- Broos, P. S., Townsley, L. K., Feigelson, E. D., Getman, K. V., Bauer, F. E., & Garmire, G. P. 2010, ApJ, 714, 1582
- Cappelluti, N., Hasinger, G., Brusa, M., Comastri, A., Zamorani, G., Böhringer, H., Brunner, H., Civano, F., Finoguenov, A., Fiore, F., Gilli, R., Griffiths, R. E., Mainieri, V., Matute, I., Miyaji, T., & Silverman, J. 2007, ApJS, 172, 341
- Cardelli, J. A., Clayton, G. C., & Mathis, J. S. 1989, ApJ, 345, 245
- Cisternas, M., Jahnke, K., Inskip, K. J., Kartaltepe, J., Koekemoer, A. M., Lisker, T., Robaina, A. R., Scodéggi, M., Sheth, K., Trump, J. R., Andrae, R., Miyaji, T., Lusso, E., Brusa, M., Capak, P., Cappelluti, N., Civano, F., Ilbert, O., Impey, C. D., Leauthaud, A., Lilly, S. J., Salvato, M., Scoville, N. Z., & Taniguchi, Y. 2011, ApJ, 726, 57
- Condon, J. J., Cotton, W. D., Greisen, E. W., Yin, Q. F., Perley, R. A., Taylor, G. B., & Broderick, J. J. 1998, AJ, 115, 1693
- Coziol, R., Brinks, E., & Bravo-Alfaro, H. 2004, AJ, 128, 68
- Coziol, R., de Carvalho, R. R., Capelato, H. V., & Ribeiro, A. L. B. 1998a, ApJ, 506, 545
- Coziol, R., Ribeiro, A. L. B., de Carvalho, R. R., & Capelato, H. V. 1998b, ApJ, 493, 563
- De Breuck, C., Tang, Y., de Bruyn, A. G., Röttgering, H., & van Breugel, W. 2002, A&A, 394, 59
- Deng, X.-F., Yu, G., & Jiang, P. 2013, PASA, 30, 18
- Desjardins, T. D., Gallagher, S. C., Tzanavaris, P., Mulchaey, J. S., Brandt, W. N., Charlton, J. C., Garmire, G. P., Gronwall, C., Hornschemeier, A. E., Johnson, K. E., Konstantopoulos, I. S., & Zabludoff, A. I. 2013, ApJ, 763, 121
- Dopita, M. A., Koratkar, A. P., Evans, I. N., Allen, M., Bicknell, G. V., Sutherland, R. S., Hawley, J. F., & Sadler, E. 1996, in Astronomical Society of the Pacific Conference Series, Vol. 103, The Physics of Liners in View of Recent Observations, ed. M. Eracleous, A. Koratkar, C. Leitherer, & L. Ho, 44
- Dressler, A., Thompson, I. B., & Shectman, S. A. 1985, ApJ, 288, 481
- Ehlert, S., Allen, S. W., Brandt, W. N., Xue, Y. Q., Luo, B., von der Linden, A., Mantz, A., & Morris, R. G. 2013, MNRAS, 428, 3509
- Eracleous, M., Hwang, J. A., & Flohic, H. M. L. G. 2010a, ApJ, 711, 796
- . 2010b, ApJS, 187, 135
- Fedotov, K., Gallagher, S. C., Konstantopoulos, I. S., Chandar, R., Bastian, N., Charlton, J. C., Whitmore, B., & Tranco, G. 2011, AJ, 142, 42
- Ferland, G. J., & Netzer, H. 1983, ApJ, 264, 105
- Filho, M. E., Fraternali, F., Markoff, S., Nagar, N. M., Barthel, P. D., Ho, L. C., & Yuan, F. 2004, A&A, 418, 429
- Filippenko, A. V., & Terlevich, R. 1992, ApJ, 397, L79
- Flohic, H. M. L. G., Eracleous, M., Chartas, G., Shields, J. C., & Moran, E. C. 2006, ApJ, 647, 140
- Freeman, P. E., Kashyap, V., Rosner, R., & Lamb, D. Q. 2002, ApJS, 138, 185
- Fukugita, M., Shimasaku, K., & Ichikawa, T. 1995, PASP, 107, 945
- Gallagher, S. C., Durrell, P. R., Elmegreen, D. M., Chandar, R., English, J., Charlton, J. C., Gronwall, C., Young, J., Tzanavaris, P., Johnson, K. E., Mendes de Oliveira, C., Whitmore, B., Hornschemeier, A. E., Maybhate, A., & Zabludoff, A. 2010, AJ, 139, 545
- Gallagher, S. C., Johnson, K. E., Hornschemeier, A. E., Charlton, J. C., & Hibbard, J. E. 2008, ApJ, 673, 730
- Gallagher, S. C., Richards, G. T., Hall, P. B., Brandt, W. N., Schneider, D. P., & Vanden Berk, D. E. 2005, AJ, 129, 567
- Gehrels, N. 1986, ApJ, 303, 336
- Gehrels, N., Chincarini, G., Giommi, P., Mason, K. O., Nosek, J. A., Wells, A. A., White, N. E., Barthelmy, S. D., Burrows, D. N., Cominsky, L. R., Hurley, K. C., Marshall, F. E., Mészáros, P., Roming, P. W. A., Angelini, L., Barbier, L. M., Belloni, T., Campana, S., Caraveo, P. A., Chester, M. M., Citterio, O., Cline, T. L., Cropper, M. S., Cummings, J. R., Dean, A. J., Feigelson, E. D., Fenimore, E. E., Frail, D. A., Fruchter, A. S., Garmire, G. P., Gendreau, K., Ghisellini, G., Greiner, J., Hill, J. E., Hunsberger, S. D., Krimm, H. A., Kulkarni, S. R., Kumar, P., Lebrun, F., Lloyd-Ronning, N. M., Markwardt, C. B., Mattson, B. J., Mushotzky, R. F., Norris, J. P., Osborne, J., Paczynski, B., Palmer, D. M., Park, H.-S., Parsons, A. M., Paul, J., Rees, M. J., Reynolds, C. S., Rhoads, J. E., Sasseen, T. P., Schaefer, B. E., Short, A. T., Smale, A. P., Smith, I. A., Stella, L., Tagliaferri, G., Takahashi, T., Tashiro, M., Townsley, L. K., Tueller, J., Turner, M. J. L., Vietri, M., Voges, W., Ward, M. J., Willingale, R., Zerbi, F. M., & Zhang, W. W. 2004, ApJ, 611, 1005
- Georgakakis, A., Coil, A. L., Laird, E. S., Griffith, R. L., Nandra, K., Lotz, J. M., Pierce, C. M., Cooper, M. C., Newman, J. A., & Koekemoer, A. M. 2009, MNRAS, 397, 623
- González-Martín, O., Masegosa, J., Márquez, I., Guainazzi, M., & Jiménez-Bailón, E. 2009, A&A, 506, 1107
- Grogan, N. A., Conselice, C. J., Chatzichristou, E., Alexander, D. M., Bauer, F. E., Hornschemeier, A. E., Jogee, S., Koekemoer, A. M., Laidler, V. G., Livio, M., Lucas, R. A., Paolillo, M., Ravindranath, S., Schreier, E. J., Simmons, B. D., & Urry, C. M. 2005, ApJ, 627, L97
- Grupe, D., Komossa, S., Leighly, K. M., & Page, K. L. 2010, ApJS, 187, 64
- Halpern, J. P., & Steiner, J. E. 1983, ApJ, 269, L37
- Heckman, T. M. 1980, A&A, 87, 152
- Hickox, R. C., & Markevitch, M. 2006, ApJ, 645, 95
- Hickox, P. 1982, ApJ, 259, 930
- Hickox, P., Kindl, E., & Auman, J. R. 1989, ApJS, 70, 687
- Hickox, P., Mendes de Oliveira, C., Huchra, J. P., & Palumbo, G. G. 1992, ApJ, 399, 353
- Ho, L. C., Feigelson, E. D., Townsley, L. K., Sambruna, R. M., Garmire, G. P., Brandt, W. N., Filippenko, A. V., Griffiths, R. E., Ptak, A. F., & Sargent, W. L. W. 2001, ApJ, 549, L51
- Ho, L. C., Filippenko, A. V., & Sargent, W. L. W. 1997, ApJ, 487, 568
- Hopkins, P. F., & Quataert, E. 2010, MNRAS, 407, 1529
- Jeltema, T. E., Binder, B., & Mulchaey, J. S. 2008, ApJ, 679, 1162
- Johnson, K. E., Hibbard, J. E., Gallagher, S. C., Charlton, J. C., Hornschemeier, A. E., Jarrett, T. H., & Reines, A. E. 2007, AJ, 134, 1522
- Just, D. W., Brandt, W. N., Shemmer, O., Steffen, A. T., Schneider, D. P., Chartas, G., & Garmire, G. P. 2007, ApJ, 665, 1004

- Kartaltepe, J. S., Sanders, D. B., Le Floc'h, E., Frayer, D. T., Aussel, H., Arnouts, S., Ilbert, O., Salvato, M., Scoville, N. Z., Surace, J., Yan, L., Capak, P., Caputi, K., Carollo, C. M., Cassata, P., Civano, F., Hasinger, G., Koekemoer, A. M., Le Fèvre, O., Lilly, S., Liu, C. T., McCracken, H. J., Schinnerer, E., Smolčić, V., Taniguchi, Y., Thompson, D. J., Trump, J., Baldassare, V. F., & Fiorenza, S. L. 2010, *ApJ*, 721, 98
- Kashyap, V. L., van Dyk, D. A., Connors, A., Freeman, P. E., Siemiginowska, A., Xu, J., & Zezas, A. 2010, *ApJ*, 719, 900
- Kauffmann, G., Heckman, T. M., Tremonti, C., Brinchmann, J., Charlot, S., White, S. D. M., Ridgway, S. E., Brinkmann, J., Fukugita, M., Hall, P. B., Ivezić, Ž., Richards, G. T., & Schneider, D. P. 2003, *MNRAS*, 346, 1055
- Kennicutt, R. C. 1998, *ARA&A*, 36, 189
- Kewley, L. J., Dopita, M. A., Sutherland, R. S., Heisler, C. A., & Trevena, J. 2001, *ApJ*, 556, 121
- Kewley, L. J., Groves, B., Kauffmann, G., & Heckman, T. 2006, *MNRAS*, 372, 961
- Kim, D.-W., Cameron, R. A., Drake, J. J., Evans, N. R., Freeman, P., Gaetz, T. J., Ghosh, H., Green, P. J., Harnden, Jr., F. R., Karovska, M., Kashyap, V., Maksym, P. W., Ratzlaff, P. W., Schlegel, E. M., Silverman, J. D., Tananbaum, H. D., Vikhlinin, A. A., Wilkes, B. J., & Grimes, J. P. 2004, *ApJS*, 150, 19
- Konstantopoulos, I. S., Gallagher, S. C., Fedotov, K., Durrell, P. R., Heiderman, A., Elmegreen, D. M., Charlton, J. C., Hibbard, J. E., Tzanavaris, P., Chandar, R., Johnson, K. E., Maybhate, A., Zabludoff, A. E., Gronwall, C., Szathmary, D., Hornschemeier, A. E., English, J., Whitmore, B., Mendes de Oliveira, C., & Mulchaey, J. S. 2010, *ApJ*, 723, 197
- Kraft, R. P., Burrows, D. N., & Nousek, J. A. 1991, *ApJ*, 374, 344
- LaMassa, S. M., Heckman, T. M., Ptak, A., Martins, L., Wild, V., Sonnenrucker, P., & Hornschemeier, A. 2011, *ApJ*, 729, 52
- Lee, B. C., Allam, S. S., Tucker, D. L., Annis, J., Johnston, D. E., Scranton, R., Acebo, Y., Bahcall, N. A., Bartelmann, M., Böhringer, H., Ellman, N., Grebel, E. K., Infante, L., Loveday, J., McKay, T. A., Prada, F., Schneider, D. P., Stoughton, C., Szalay, A. S., Vogeley, M. S., Voges, W., & Yanny, B. 2004, *AJ*, 127, 1811
- Lehmer, B. D., Alexander, D. M., Bauer, F. E., Brandt, W. N., Goulding, A. D., Jenkins, L. P., Ptak, A., & Roberts, T. P. 2010, *ApJ*, 724, 559
- Lusso, E., Comastri, A., Vignali, C., Zamorani, G., Brusa, M., Gilli, R., Iwasawa, K., Salvato, M., Civano, F., Elvis, M., Merlin, A., Bongiorno, A., Trump, J. R., Koekemoer, A. M., Schinnerer, E., Le Floc'h, E., Cappelluti, N., Jahnke, K., Sargent, M., Silverman, J., Mainieri, V., Fiore, F., Bolzonella, M., Le Fèvre, O., Garilli, B., Iovino, A., Kneib, J. P., Lamareille, F., Lilly, S., Mignoli, M., Scodéggi, M., & Vergani, D. 2010, *A&A*, 512, A34
- Ma, C., & Feissel, M. 1998, *VizieR Online Data Catalog*, 1251, 0
- Mamon, G. A. 1994, in *Clusters of Galaxies*, ed. F. Durret, A. Mazure, & J. Tran Thanh Van, 291
- Maoz, D., Nagar, N. M., Falcke, H., & Wilson, A. S. 2005, *ApJ*, 625, 699
- Martínez, M. A., Del Olmo, A., Coziol, R., & Perea, J. 2010, *AJ*, 139, 1199
- Martini, P., Kelson, D. D., Kim, E., Mulchaey, J. S., & Athey, A. A. 2006, *ApJ*, 644, 116
- Mihos, J. C., & Hernquist, L. 1996, *ApJ*, 464, 641
- Mukai, K. 1993, *Legacy*, vol. 3, p.21-31, 3, 21
- Mulchaey, J. S., Davis, D. S., Mushotzky, R. F., & Burstein, D. 2003, *ApJS*, 145, 39
- Nagar, N. M., Falcke, H., & Wilson, A. S. 2005, *A&A*, 435, 521
- O'Connell, R. W. 1999, *ARA&A*, 37, 603
- O'Sullivan, E., Giacintucci, S., Vrtilek, J. M., Raychaudhury, S., & David, L. P. 2009, *ApJ*, 701, 1560
- Peng, C. Y., Ho, L. C., Impey, C. D., & Rix, H.-W. 2010, *AJ*, 139, 2097
- Ponman, T. J., Bourner, P. D. J., Ebeling, H., & Böhringer, H. 1996, *MNRAS*, 283, 690
- Poole, T. S., Breeveld, A. A., Page, M. J., Landsman, W., Holland, S. T., Roming, P., Kuin, N. P. M., Brown, P. J., Gronwall, C., Hunsberger, S., Koch, S., Mason, K. O., Schady, P., vanden Berk, D., Blustin, A. J., Boyd, P., Broos, P., Carter, M., Chester, M. M., Cucchiara, A., Hancock, B., Huckle, H., Immler, S., Ivanushkina, M., Kennedy, T., Marshall, F., Morgan, A., Pandey, S. B., de Pasquale, M., Smith, P. J., & Still, M. 2008, *MNRAS*, 383, 627
- Rafferty, D. A., Birzan, L., Nulsen, P. E. J., McNamara, B. R., Brandt, W. N., Wise, M. W., & Röttgering, H. J. A. 2013, *MNRAS*, 428, 58
- Ranalli, P., Comastri, A., & Setti, G. 2003, *A&A*, 399, 39
- Ranalli, P., Comastri, A., Zamorani, G., Cappelluti, N., Civano, F., Georgantopoulos, I., Gilli, R., Schinnerer, E., Smolčić, V., & Vignali, C. 2012, *A&A*, 542, A16
- Rasmussen, J., Ponman, T. J., Verdes-Montenegro, L., Yun, M. S., & Borthakur, S. 2008, *MNRAS*, 388, 1245
- Reynolds, C. S., & Nowak, M. A. 2003, *Phys. Rep.*, 377, 389
- Ribeiro, A. L. B., de Carvalho, R. R., Capelato, H. V., & Zepf, S. E. 1998, *ApJ*, 497, 72
- Roche, P. F., Aitken, D. K., Smith, C. H., & Ward, M. J. 1991, *MNRAS*, 248, 606
- Roming, P. W. A., Kennedy, T. E., Mason, K. O., Nousek, J. A., Ahn, L., Bingham, R. E., Broos, P. S., Carter, M. J., Hancock, B. K., Huckle, H. E., Hunsberger, S. D., Kawakami, H., Killough, R., Koch, T. S., McLellan, M. K., Smith, K., Smith, P. J., Soto, J. C., Boyd, P. T., Breeveld, A. A., Holland, S. T., Ivanushkina, M., Pryzby, M. S., Still, M. D., & Stock, J. 2005, *Space Science Reviews*, 120, 95
- Rossa, J., van der Marel, R. P., Böker, T., Gerssen, J., Ho, L. C., Rix, H.-W., Shields, J. C., & Walcher, C.-J. 2006, *AJ*, 132, 1074
- Schlegel, D. J., Finkbeiner, D. P., & Davis, M. 1998, *ApJ*, 500, 525
- Shen, Y., Mulchaey, J. S., Raychaudhury, S., Rasmussen, J., & Ponman, T. J. 2007, *ApJ*, 654, L115
- Shields, J. C. 1992, *ApJ*, 399, L27
- Silverman, J. D., Kampczyk, P., Jahnke, K., Andrae, R., Lilly, S. J., Elvis, M., Civano, F., Mainieri, V., Vignali, C., Zamorani, G., Nair, P., Le Fèvre, O., de Ravel, L., Bardelli, S., Bongiorno, A., Bolzonella, M., Cappi, A., Caputi, K., Carollo, C. M., Contini, T., Coppa, G., Cucciati, O., de la Torre, S., Franzetti, P., Garilli, B., Halliday, C., Hasinger, G., Iovino, A., Knobel, C., Koekemoer, A. M., Kovač, K., Lamareille, F., Le Borgne, J.-F., Le Brun, V., Maier, C., Mignoli, M., Pello, R., Pérez-Montero, E., Ricciardelli, E., Peng, Y., Scodéggi, M., Tanaka, M., Tasca, L., Tresse, L., Vergani, D., Zucca, E., Brusa, M., Cappelluti, N., Comastri, A., Finoguenov, A., Fu, H., Gilli, R., Hao, H., Ho, L. C., & Salvato, M. 2011, *ApJ*, 743, 2
- Smith, B. J., Swartz, D. A., Miller, O., Burleson, J. A., Nowak, M. A., & Struck, C. 2012, *AJ*, 143, 144
- Stasińska, G., Cid Fernandes, R., Mateus, A., Sodré, L., & Asari, N. V. 2006, *MNRAS*, 371, 972
- Steffen, A. T., Brandt, W. N., Alexander, D. M., Gallagher, S. C., & Lehmer, B. D. 2007, *ApJ*, 667, L25
- Steffen, A. T., Strateva, I., Brandt, W. N., Alexander, D. M., Koekemoer, A. M., Lehmer, B. D., Schneider, D. P., & Vignali, C. 2006, *AJ*, 131, 2826
- Strateva, I. V., Brandt, W. N., Schneider, D. P., Vanden Berk, D. G., & Vignali, C. 2005, *AJ*, 130, 387
- Tananbaum, H., Avni, Y., Branduardi, G., Elvis, M., Fabbiano, G., Feigelson, E., Giacconi, R., Henry, J. P., Pye, J. P., Soltan, A., & Zamorani, G. 1979, *ApJ*, 234, L9
- Terlevich, R., & Melnick, J. 1985, *MNRAS*, 213, 841
- Tzanavaris, P., Hornschemeier, A. E., Gallagher, S. C., Johnson, K. E., Gronwall, C., Immler, S., Reines, A. E., Hoversten, E., & Charlton, J. C. 2010, *ApJ*, 716, 556
- Veilleux, S., & Osterbrock, D. E. 1987, *ApJS*, 63, 295
- Verdes-Montenegro, L., Yun, M. S., Williams, B. A., Huchtmeier, W. K., Del Olmo, A., & Perea, J. 2001, *A&A*, 377, 812
- Walker, L. M., Johnson, K. E., Gallagher, S. C., Charlton, J. C., Hornschemeier, A. E., & Hibbard, J. E. 2012, *AJ*, 143, 69
- Walker, L. M., Johnson, K. E., Gallagher, S. C., Hibbard, J. E., Hornschemeier, A. E., Tzanavaris, P., Charlton, J. C., & Jarrett, T. H. 2010, *AJ*, 140, 1254
- Xu, C. K., Iglesias-Páramo, J., Burgarella, D., Rich, R. M., Neff, S. G., Lauger, S., Barlow, T. A., Bianchi, L., Byun, Y.-I., Förster, K., Friedman, P. G., Heckman, T. M., Jelinsky, P. N., Lee, Y.-W., Madore, B. F., Malina, R. F., Martin, D. C., Milliard, B., Morrissey, P., Schiminovich, D., Siegmund, O. H. W., Small, T., Szalay, A. S., Welsh, B. Y., & Wyder, T. K. 2005, *ApJ*, 619, L95
- Xue, Y. Q., Luo, B., Brandt, W. N., Bauer, F. E., Lehmer, B. D., Broos, P. S., Schneider, D. P., Alexander, D. M., Brusa, M., Comastri, A., Fabian, A. C., Gilli, R., Hasinger, G., Hornschemeier, A. E., Koekemoer, A., Liu, T., Mainieri, V., Paolillo, M., Rafferty, D. A., Rosati, P., Shemmer, O., Silverman, J. D., Smail, I., Tozzi, P., & Vignali, C. 2011, *ApJS*, 195, 10

TABLE 11:
Derived quantities and detection codes for X-ray point sources in HCG 7 (online only).

ID (1)	Γ (2)	L_X										lim									
		+	-	f_F (5)	\pm (6)	f_S (7)	\pm (8)	f_H (9)	\pm (10)	F (11)	S (12)	H (13)	$f_{\nu,2\text{keV}}$ (14)	\pm (15)	HR (16)	F (17)	S (18)	H (19)	EEF (20)	RA (21)	DEC (22)
1	1.0	0.0	-0.0	-15.0	0.0	-15.7	0.0	-15.1	0.0	38.6	37.9	38.5	-33.2	0.0	-2	5	1	5	0.9	9.7884	0.8779
2A	0.7	0.0	-0.0	-14.6	0.2	-15.4	0.0	-14.7	0.0	39.0	38.1	38.9	-32.9	0.2	-2	0	5	5	0.9	9.7965	0.8677
3	1.0	0.0	-0.0	-15.0	0.0	-15.7	0.0	-15.1	0.0	38.6	37.9	38.5	-33.3	0.0	-2	5	5	1	0.9	9.8001	0.8911
4A	0.7	0.0	-0.0	-14.5	0.2	-15.4	0.0	-14.6	0.0	39.0	38.2	39.0	-32.9	0.2	-2	0	5	5	0.9	9.8005	0.8649
5A	0.9	0.1	-0.1	-13.1	0.0	-13.9	0.0	-13.2	0.0	40.4	39.7	40.3	-31.4	0.0	0	0	0	0	0.9	9.8050	0.8617
6A*	2.0	0.2	-0.2	-13.6	0.0	-13.9	0.0	-13.9	0.0	40.0	39.7	39.7	-31.7	0.0	0	0	0	0	0.9	9.8059	0.8643
7A	0.7	0.0	-0.0	-14.7	0.2	-15.5	0.0	-14.7	0.0	38.9	38.1	38.9	-33.0	0.2	-2	0	5	5	0.9	9.8081	0.8685
8	1.6	0.4	-0.4	-14.0	0.1	-14.4	0.1	-14.2	0.1	39.6	39.1	39.4	-32.2	0.1	0	0	0	0	0.9	9.8082	0.8986
9A	2.0	0.4	-0.4	-14.0	0.1	-14.3	0.1	-14.3	0.1	39.6	39.3	39.3	-32.1	0.1	0	0	0	0	0.9	9.8116	0.8800
10	1.0	0.0	-0.0	-15.0	0.0	-15.7	0.0	-15.1	0.0	38.6	37.9	38.5	-33.3	0.0	-2	5	5	1	0.9	9.8132	0.8967
11	1.0	0.0	-0.0	-15.0	0.0	-15.7	0.0	-15.1	0.0	38.6	37.9	38.5	-33.3	0.0	-2	5	5	5	0.9	9.8162	0.8568
12A	1.3	3.1	-0.0	-14.6	0.2	-15.2	0.2	-14.8	0.0	39.0	38.4	38.8	-32.8	0.2	1	0	0	5	0.9	9.8172	0.8770
13D	1.3	3.1	-0.0	-14.6	0.2	-15.1	0.2	-14.7	0.0	39.0	38.5	38.9	-32.7	0.2	1	0	0	5	0.9	9.8213	0.8950
14	1.0	0.0	-0.0	-15.0	0.0	-15.7	0.0	-15.1	0.0	38.6	37.9	38.5	-33.3	0.0	-2	5	1	5	0.9	9.8219	0.8435
15B*	1.9	2.5	-0.0	-14.6	0.2	-14.9	0.2	-14.8	0.0	39.0	38.6	38.7	-32.7	0.2	1	0	0	5	0.9	9.8243	0.9128
16B	3.8	0.6	-0.0	-13.8	0.0	-13.8	0.0	-14.9	0.0	39.8	39.8	38.7	-32.3	0.0	1	0	0	5	0.9	9.8244	0.9005
17B	1.9	1.9	-0.0	-14.5	0.1	-14.8	0.1	-14.8	0.0	39.1	38.8	38.8	-32.6	0.1	1	0	0	5	0.9	9.8257	0.9207
18	1.0	0.0	-0.0	-15.0	0.0	-15.7	0.0	-15.1	0.0	38.5	37.8	38.4	-33.3	0.0	-2	5	5	1	0.9	9.8271	0.8846
19	1.0	0.0	-0.0	-15.0	0.0	-15.7	0.0	-15.1	0.0	38.6	37.9	38.5	-33.3	0.0	-2	5	5	5	0.9	9.8273	0.8128
20	1.0	0.0	-0.0	-15.0	0.0	-15.7	0.0	-15.1	0.0	38.6	37.9	38.5	-33.3	0.0	-2	5	5	1	0.9	9.8275	0.8605
21D	2.5	1.3	-0.0	-14.3	0.1	-14.5	0.1	-14.8	0.0	39.3	39.1	38.8	-32.5	0.1	1	0	0	5	0.9	9.8361	0.8807
22	-0.5	0.5	-0.6	-13.7	0.1	-15.2	0.1	-13.7	0.1	39.9	38.4	39.9	-32.5	0.1	0	0	0	0	0.9	9.8370	0.8586
23	1.7	0.3	-0.3	-13.7	0.1	-14.0	0.1	-13.9	0.1	39.9	39.5	39.7	-31.8	0.1	0	0	0	0	0.9	9.8390	0.8513
24	2.2	0.3	-0.3	-13.7	0.1	-14.0	0.1	-14.1	0.1	39.8	39.6	39.5	-31.9	0.1	0	0	0	0	0.9	9.8422	0.8714
25	1.0	0.0	-0.0	-15.0	0.0	-15.7	0.0	-15.1	0.0	38.5	37.8	38.5	-33.3	0.0	-2	5	1	5	0.9	9.8484	0.9095
26	-1.1	0.3	-0.0	-13.6	0.1	-15.5	0.0	-13.6	0.1	40.0	38.1	40.0	-32.7	0.1	-1	0	5	0	0.9	9.8491	0.8088
27	1.0	0.0	-0.0	-15.0	0.0	-15.7	0.0	-15.1	0.0	38.6	37.9	38.5	-33.3	0.0	-2	5	5	1	0.9	9.8574	0.8385
28	0.8	0.2	-0.2	-13.4	0.1	-14.2	0.1	-13.5	0.1	40.2	39.4	40.1	-31.7	0.1	0	0	0	0	0.9	9.8577	0.7919
29	0.6	0.0	-0.0	-14.6	0.2	-15.5	0.0	-14.6	0.0	39.0	38.1	38.9	-32.9	0.2	-2	0	5	5	0.9	9.8594	0.9060
30	1.4	2.4	-0.0	-14.6	0.2	-15.1	0.2	-14.7	0.0	39.0	38.5	38.8	-32.7	0.2	1	0	0	5	0.9	9.8606	0.8535
31	1.0	0.0	-0.0	-15.0	0.0	-15.7	0.0	-15.1	0.0	38.5	37.9	38.5	-33.3	0.0	-2	5	1	5	0.9	9.8648	0.9242
32	0.6	0.0	-0.0	-14.5	0.2	-15.4	0.0	-14.6	0.0	39.1	38.2	39.0	-32.9	0.2	-2	0	5	5	0.9	9.8675	0.8284
33	1.0	0.0	-0.0	-15.0	0.0	-15.7	0.0	-15.1	0.0	38.6	37.9	38.5	-33.3	0.0	-2	5	5	5	0.9	9.8705	0.9308
34	-0.6	0.0	-0.5	-13.9	0.1	-15.5	0.0	-13.9	0.1	39.7	38.1	39.7	-32.8	0.1	-1	0	5	0	0.9	9.8737	0.8667
35	1.0	0.0	-0.0	-15.0	0.0	-15.7	0.0	-15.1	0.0	38.6	37.9	38.5	-33.3	0.0	-2	5	5	5	0.9	9.8763	0.8612
36	-0.3	0.0	-0.8	-14.2	0.2	-15.5	0.0	-14.2	0.2	39.4	38.0	39.4	-32.8	0.2	-1	0	5	0	0.9	9.8785	0.8536
37	0.6	0.0	-0.0	-14.6	0.2	-15.5	0.0	-14.7	0.0	38.9	38.0	38.9	-33.0	0.2	-2	0	5	5	0.9	9.8801	0.8561
38	2.3	1.5	-0.0	-14.4	0.1	-14.6	0.1	-14.8	0.0	39.2	39.0	38.8	-32.5	0.1	1	0	0	5	0.9	9.8839	0.8028
39	-0.9	0.0	-0.2	-13.8	0.1	-15.6	0.0	-13.8	0.1	39.7	38.0	39.7	-32.8	0.1	-1	0	1	0	0.9	9.8842	0.9178
40C	1.6	2.2	-0.0	-14.5	0.2	-15.0	0.2	-14.7	0.0	39.0	38.6	38.8	-32.7	0.2	1	0	0	5	0.9	9.8879	0.8585
41	1.7	0.6	-0.6	-14.2	0.1	-14.7	0.1	-14.5	0.1	39.3	38.9	39.1	-32.4	0.1	0	0	0	0	0.9	9.8894	0.9401
42C	2.7	1.1	-0.0	-14.2	0.1	-14.4	0.1	-14.8	0.0	39.4	39.2	38.8	-32.4	0.1	1	0	0	5	0.9	9.8917	0.8577
43	1.0	0.0	-0.0	-15.0	0.0	-15.7	0.0	-15.1	0.0	38.6	37.9	38.5	-33.3	0.0	-2	5	5	5	0.9	9.8935	0.8392
44C*	2.1	2.3	-0.0	-14.5	0.1	-14.8	0.1	-14.8	0.0	39.1	38.8	38.7	-32.6	0.1	1	0	0	5	0.9	9.8947	0.8600
45	1.0	0.0	-0.0	-15.0	0.0	-15.7	0.0	-15.1	0.0	38.6	37.9	38.5	-33.3	0.0	-2	5	1	5	0.9	9.8969	0.8864
46C	1.7	2.1	-0.0	-14.7	0.2	-15.1	0.2	-14.9	0.0	38.9	38.5	38.7	-32.8	0.2	1	0	0	1	0.9	9.8979	0.8667
47	1.0	0.0	-0.0	-15.0	0.0	-15.7	0.0	-15.1	0.0	38.6	37.9	38.5	-33.3	0.0	-2	5	5	1	0.9	9.9006	0.9317
48C	1.3	0.5	-0.4	-14.0	0.1	-14.6	0.1	-14.1	0.1	39.6	39.0	39.4	-32.2	0.1	0	0	0	0	0.9	9.9008	0.8578
49	1.6	0.3	-0.3	-13.6	0.1	-14.1	0.1	-13.8	0.1	39.9	39.5	39.8	-31.8	0.1	0	0	0	0	0.9	9.9009	0.8250
50	1.0	0.0	-0.0	-15.0	0.0	-15.7	0.0	-15.1	0.0	38.6	37.9	38.5	-33.3	0.0	-2	5	5	5	0.9	9.9051	0.8854
51C	1.9	0.1	-0.1	-12.9	0.0	-13.2	0.0	-13.2	0.0	40.7	40.3	40.4	-31.0	0.0	0	0	0	0	0.9	9.9067	0.8528

TABLE 11:
Derived quantities and detection codes for X-ray point sources in HCG 7 (online only).

52	-0.8	0.0	-0.3	-13.8	0.1	-15.5	0.0	-13.8	0.1	39.7	38.0	39.7	-32.8	0.1	-1	0	5	0	0.9	9.9078	0.8299
53	0.7	0.0	-0.0	-14.7	0.3	-15.6	0.0	-14.8	0.0	38.9	38.0	38.8	-33.0	0.3	-2	0	5	5	0.9	9.9102	0.9327
54	1.0	0.0	-0.0	-15.0	0.0	-15.7	0.0	-15.1	0.0	38.6	37.9	38.5	-33.2	0.0	-2	5	1	5	0.9	9.9110	0.8737
55	1.0	0.0	-0.0	-14.6	0.0	-15.3	0.0	-14.7	0.0	38.9	38.2	38.8	-32.9	0.0	-2	5	5	1	0.9	9.9134	0.9404
56	1.0	0.0	-0.0	-15.0	0.0	-15.7	0.0	-15.1	0.0	38.6	37.9	38.5	-33.2	0.0	-2	1	5	1	0.9	9.9151	0.8095
57	0.1	0.0	-1.2	-14.6	0.3	-15.7	0.0	-14.6	0.3	39.0	37.9	39.0	-33.1	0.3	-1	0	1	0	0.9	9.9169	0.9048
58	0.9	0.8	-0.7	-14.4	0.2	-15.1	0.2	-14.5	0.2	39.2	38.5	39.1	-32.6	0.2	0	0	0	0	0.9	9.9179	0.8771
59	1.6	0.3	-0.3	-13.7	0.1	-14.2	0.1	-13.9	0.1	39.8	39.4	39.6	-31.9	0.1	0	0	0	0	0.9	9.9212	0.9077
60	0.7	0.0	-0.0	-14.7	0.2	-15.5	0.0	-14.7	0.0	38.9	38.1	38.8	-33.0	0.2	-2	0	5	5	0.9	9.9230	0.8966
61	0.9	0.6	-0.6	-14.2	0.1	-14.9	0.1	-14.3	0.1	39.4	38.6	39.3	-32.5	0.1	0	0	0	0	0.9	9.9285	0.8067

NOTE. — Columns are: (1) source ID (for sources inside galaxy regions, the galaxy is indicated by an upper case letter); (2) Γ power law index; (3) upper error in Γ ; (4) lower error in Γ ; (5) log of full band flux ($\text{erg cm}^{-2} \text{s}^{-1}$); (6) error; (7) log of soft band flux ($\text{erg cm}^{-2} \text{s}^{-1}$); (8) error; (9) log of hard band flux ($\text{erg cm}^{-2} \text{s}^{-1}$); (10) error; (11) $L_X(\text{erg s}^{-1})$ (full band); (12) $L_X(\text{erg s}^{-1})$ (soft band); (13) $L_X(\text{erg s}^{-1})$ (hard band); (14) log of flux density at 2 keV ($\text{erg cm}^{-2} \text{s}^{-1} \text{Hz}^{-1}$); (15) error; (16) detection code for hardness ratio: 0 (detection in both hard and soft bands); -1 (detection in hard but not soft band; HR is a lower limit); 1 (detection in soft but not hard band; HR is an upper limit); -2 (no detection in either hard or soft band); (17) detection code for full band: 0 (detection in band); 1 (no detection in band because net counts < 0); 5 (no detection in band because net counts - Gehrels 2σ error < 0); (18) as previous column but for the soft band; (19) as previous column but for the hard band; (20) encircled energy fraction by AE PSF at 1.5 keV; (21) right ascension; (22) declination;

TABLE 12:
Derived quantities and detection codes for X-ray point sources in HCG 16 (online only).

ID (1)	Γ (2)	L_X										lim									
		f_F (5)	\pm (6)	f_S (7)	\pm (8)	f_H (9)	\pm (10)	F (11)	S (12)	H (13)	$f_{\nu, 2\text{keV}}$ (14)	\pm (15)	HR	F (17)	S (18)	H (19)	EEF (20)	RA (21)	DEC (22)		
1	0.3	0.5	-0.6	-13.5	0.1	-14.6	0.1	-13.6	0.1	40.0	39.0	40.0	-32.0	0.1	0	0	0	0	0.9	32.3125	-10.2028
2	0.4	0.8	-0.8	-13.8	0.2	-14.8	0.2	-13.8	0.2	39.7	38.7	39.7	-32.3	0.2	0	0	0	0	0.9	32.3261	-10.2070
3	1.0	0.0	-0.0	-14.6	0.0	-15.3	0.0	-14.7	0.0	38.9	38.2	38.8	-32.9	0.0	-2	5	1	5	0.9	32.3344	-10.1731
4B*	-0.7	0.2	-0.2	-12.2	0.0	-13.8	0.0	-12.2	0.0	41.3	39.7	41.3	-31.1	0.0	0	0	0	0	0.9	32.3370	-10.1332
5	1.5	2.8	-0.0	-14.0	0.1	-14.5	0.1	-14.2	0.0	39.5	39.0	39.3	-32.2	0.1	1	0	0	5	0.9	32.3422	-10.2364
6	1.6	2.8	-0.0	-14.1	0.2	-14.5	0.2	-14.3	0.0	39.5	39.0	39.3	-32.2	0.2	1	0	0	5	0.9	32.3454	-10.1402
7	0.6	0.0	-0.0	-14.2	0.3	-15.1	0.0	-14.3	0.0	39.3	38.4	39.3	-32.6	0.3	-2	0	5	5	0.9	32.3472	-10.1683
8	1.0	0.0	-0.0	-14.6	0.0	-15.3	0.0	-14.7	0.0	39.0	38.3	38.9	-32.8	0.0	-2	5	5	1	0.9	32.3518	-10.1864
9A*	1.2	0.2	-0.2	-12.9	0.0	-13.4	0.0	-13.0	0.0	40.7	40.1	40.5	-31.1	0.0	0	0	0	0	0.9	32.3527	-10.1359
10	0.0	0.0	-1.1	-14.1	0.3	-15.3	0.0	-14.1	0.3	39.5	38.3	39.5	-32.6	0.3	-1	0	1	0	0.9	32.3581	-10.1173
11	1.0	0.0	-0.0	-14.3	0.0	-15.0	0.0	-14.4	0.0	39.2	38.5	39.1	-32.6	0.0	-2	5	5	5	0.9	32.3587	-10.2055
12	1.0	2.8	-0.0	-14.3	0.3	-15.0	0.3	-14.4	0.0	39.2	38.5	39.1	-32.6	0.3	1	0	0	1	0.9	32.3601	-10.1884
13	1.0	0.0	-0.0	-14.6	0.0	-15.3	0.0	-14.6	0.0	39.0	38.3	38.9	-32.8	0.0	-2	5	5	1	0.9	32.3613	-10.2332
14	1.0	0.0	-0.0	-14.5	0.0	-15.2	0.0	-14.6	0.0	39.0	38.3	38.9	-32.8	0.0	-2	5	5	5	0.9	32.3634	-10.2215
15A	1.6	0.3	-0.3	-13.4	0.1	-13.8	0.1	-13.6	0.1	40.1	39.7	39.9	-31.5	0.1	0	0	0	0	0.9	32.3650	-10.1296
16	1.0	0.0	-0.0	-14.4	0.0	-15.1	0.0	-14.5	0.0	39.2	38.5	39.1	-32.6	0.0	-2	5	1	5	0.9	32.3691	-10.1869
17	1.0	0.0	-0.0	-14.5	0.0	-15.2	0.0	-14.6	0.0	39.0	38.3	38.9	-32.8	0.0	-2	5	5	1	0.9	32.3726	-10.2018
18	0.5	0.0	-0.0	-14.0	0.2	-14.9	0.0	-14.1	0.0	39.5	38.6	39.5	-32.4	0.2	-2	0	5	5	0.9	32.3747	-10.2068
19	1.7	2.1	-0.0	-14.2	0.2	-14.6	0.2	-14.4	0.0	39.4	39.0	39.1	-32.3	0.2	1	0	0	1	0.9	32.3776	-10.1780
20	2.1	1.7	-0.0	-13.8	0.1	-14.1	0.1	-14.2	0.0	39.7	39.4	39.4	-32.0	0.1	1	0	0	5	0.9	32.3782	-10.2124
21	-1.1	4.9	-0.0	-12.6	0.1	-14.5	0.0	-12.7	0.1	40.9	39.0	40.9	-31.7	0.1	-1	0	5	0	0.9	32.3801	-10.1932
22	1.0	0.0	-0.0	-14.5	0.0	-15.2	0.0	-14.6	0.0	39.0	38.3	38.9	-32.8	0.0	-2	5	1	5	0.9	32.3806	-10.2387
23	1.0	0.0	-0.0	-14.6	0.0	-15.3	0.0	-14.7	0.0	38.9	38.2	38.9	-32.8	0.0	-2	5	1	5	0.9	32.3806	-10.2068
24	1.0	0.0	-0.0	-14.5	0.0	-15.2	0.0	-14.6	0.0	39.0	38.3	38.9	-32.8	0.0	-2	5	5	5	0.9	32.3812	-10.1642
25	1.0	0.0	-0.0	-14.6	0.0	-15.2	0.0	-14.6	0.0	39.0	38.3	38.9	-32.8	0.0	-2	5	1	5	0.9	32.3829	-10.2504
26	-0.4	0.0	-0.7	-13.6	0.2	-15.1	0.0	-13.6	0.2	40.0	38.5	39.9	-32.3	0.2	-1	0	5	0	0.9	32.3831	-10.1448
27	0.2	0.5	-0.6	-13.5	0.1	-14.6	0.1	-13.5	0.1	40.0	38.9	40.0	-32.0	0.1	0	0	0	0	0.9	32.3867	-10.1734
28	1.0	0.0	-0.0	-14.5	0.0	-15.2	0.0	-14.6	0.0	39.1	38.4	39.0	-32.7	0.0	-2	5	1	5	0.9	32.3871	-10.1896
29	1.0	0.0	-0.0	-14.5	0.0	-15.2	0.0	-14.6	0.0	39.0	38.3	38.9	-32.8	0.0	-2	5	1	5	0.9	32.3871	-10.2107
30	1.0	0.0	-0.0	-14.5	0.0	-15.2	0.0	-14.6	0.0	39.0	38.3	38.9	-32.8	0.0	-2	5	1	5	0.9	32.3870	-10.1691
31	1.0	0.0	-0.0	-14.4	0.0	-15.1	0.0	-14.5	0.0	39.1	38.4	39.0	-32.7	0.0	-2	5	5	5	0.9	32.3881	-10.1908
32	1.2	0.4	-0.3	-13.5	0.1	-14.1	0.1	-13.6	0.1	40.1	39.5	39.9	-31.7	0.1	0	0	0	0	0.9	32.3898	-10.1392
33	1.0	0.0	-0.0	-14.5	0.0	-15.2	0.0	-14.6	0.0	39.0	38.3	38.9	-32.8	0.0	-2	5	1	5	0.9	32.3904	-10.2501
34	1.0	0.0	-0.0	-14.5	0.0	-15.2	0.0	-14.6	0.0	39.0	38.3	38.9	-32.8	0.0	-2	5	5	5	0.9	32.3916	-10.2450
35	1.0	0.0	-0.0	-14.5	0.0	-15.2	0.0	-14.6	0.0	39.0	38.3	38.9	-32.8	0.0	-2	5	1	5	0.9	32.3954	-10.2410
36	1.0	0.0	-0.0	-14.6	0.0	-15.3	0.0	-14.7	0.0	38.9	38.2	38.8	-32.9	0.0	-2	5	5	5	0.9	32.4047	-10.1491
37	1.0	0.0	-0.0	-14.6	0.0	-15.3	0.0	-14.7	0.0	39.0	38.3	38.9	-32.8	0.0	-2	5	1	5	0.9	32.4063	-10.1554
38	1.0	0.0	-0.0	-14.6	0.0	-15.3	0.0	-14.7	0.0	38.9	38.2	38.8	-32.9	0.0	-2	5	5	1	0.9	32.4074	-10.1504
39	1.0	0.0	-0.0	-14.6	0.0	-15.3	0.0	-14.7	0.0	38.9	38.2	38.8	-32.9	0.0	-2	1	1	1	0.9	32.4076	-10.1489
40	0.5	0.0	-0.0	-14.2	0.3	-15.1	0.0	-14.2	0.0	39.4	38.4	39.3	-32.6	0.3	-2	0	5	5	0.9	32.4079	-10.2255
41	1.0	0.0	-0.0	-14.5	0.0	-15.2	0.0	-14.6	0.0	39.0	38.3	38.9	-32.8	0.0	-2	5	5	1	0.8	32.4079	-10.1499
42	1.0	0.0	-0.0	-14.5	0.0	-15.2	0.0	-14.6	0.0	39.0	38.3	38.9	-32.8	0.0	-2	5	5	1	0.9	32.4085	-10.1647
43C	1.4	2.9	-0.0	-14.1	0.2	-14.6	0.2	-14.2	0.0	39.5	38.9	39.3	-32.2	0.2	1	0	0	5	0.9	32.4089	-10.1388
44C*	2.0	0.7	-0.6	-13.8	0.1	-14.1	0.1	-14.1	0.1	39.7	39.4	39.4	-31.9	0.1	0	0	0	0	0.6	32.4107	-10.1464
45	1.0	0.0	-0.0	-14.6	0.0	-15.3	0.0	-14.7	0.0	38.9	38.2	38.8	-32.9	0.0	-2	5	5	1	0.9	32.4107	-10.1490
46C	1.4	2.5	-0.0	-14.3	0.2	-14.8	0.2	-14.4	0.0	39.3	38.7	39.1	-32.5	0.2	1	0	0	1	0.4	32.4115	-10.1465
47	1.0	0.0	-0.0	-14.6	0.0	-15.3	0.0	-14.7	0.0	38.9	38.2	38.8	-32.9	0.0	-2	5	5	1	0.9	32.4120	-10.1515
48C	1.7	2.6	-0.0	-14.0	0.1	-14.5	0.1	-14.3	0.0	39.5	39.1	39.3	-32.2	0.1	1	0	0	5	0.9	32.4135	-10.1455
49	1.0	0.0	-0.0	-14.3	0.0	-15.0	0.0	-14.4	0.0	39.2	38.5	39.1	-32.6	0.0	-2	5	1	5	0.9	32.4182	-10.1812
50C	1.5	2.3	-0.0	-14.3	0.2	-14.8	0.2	-14.5	0.0	39.2	38.7	39.1	-32.5	0.2	1	0	0	1	0.9	32.4189	-10.1405
51	2.2	0.6	-0.5	-13.8	0.1	-14.0	0.1	-14.1	0.1	39.8	39.5	39.4	-31.9	0.1	0	0	0	0	0.9	32.4193	-10.2081

TABLE 12:
Derived quantities and detection codes for X-ray point sources in HCG 16 (online only).

52	1.0	0.0	-0.0	-14.6	0.0	-15.3	0.0	-14.7	0.0	39.0	38.3	38.9	-32.8	0.0	-2	5	1	5	0.9	32.4210	-10.2028
53C	0.4	0.6	-0.6	-13.6	0.1	-14.6	0.1	-13.7	0.1	39.9	38.9	39.9	-32.0	0.1	0	0	0	0	0.9	32.4230	-10.1397
54	1.0	0.0	-0.0	-14.5	0.0	-15.2	0.0	-14.6	0.0	39.0	38.3	38.9	-32.8	0.0	-2	5	5	1	0.9	32.4229	-10.1619
55	1.8	0.5	-0.4	-13.7	0.1	-14.0	0.1	-13.9	0.1	39.9	39.5	39.6	-31.8	0.1	0	0	0	0	0.9	32.4263	-10.1376
56	1.0	0.0	-0.0	-14.5	0.0	-15.2	0.0	-14.6	0.0	39.1	38.4	39.0	-32.7	0.0	-2	5	1	5	0.9	32.4271	-10.1950
57D*	2.4	0.6	-0.5	-13.7	0.1	-13.9	0.1	-14.2	0.1	39.8	39.6	39.4	-31.8	0.1	0	0	0	0	0.9	32.4280	-10.1836
58	1.0	0.0	-0.0	-14.5	0.0	-15.2	0.0	-14.6	0.0	39.0	38.3	38.9	-32.8	0.0	-2	5	5	1	0.9	32.4320	-10.1864
59	1.0	0.0	-0.0	-14.5	0.0	-15.2	0.0	-14.6	0.0	39.0	38.3	38.9	-32.8	0.0	-2	5	5	1	0.9	32.4350	-10.1818
60	1.2	0.3	-0.3	-13.2	0.1	-13.8	0.1	-13.3	0.1	40.3	39.8	40.2	-31.4	0.1	0	0	0	0	0.9	32.4414	-10.1931
61	1.8	2.5	-0.0	-13.8	0.1	-14.1	0.1	-14.0	0.0	39.8	39.4	39.5	-31.9	0.1	1	0	0	5	0.9	32.4444	-10.1836

TABLE 13:
Derived quantities and detection codes for X-ray point sources in HCG 22 (online only).

ID (1)	Γ (2)	L_X										lim									
		f_F (5)	\pm (6)	f_S (7)	\pm (8)	f_H (9)	\pm (10)	F (11)	S (12)	H (13)	$f_{\nu,2\text{keV}}$ (14)	\pm (15)	HR	F (17)	S (18)	H (19)	EEF (20)	RA (21)	DEC (22)		
1	1.0	0.0	-0.0	-15.0	0.0	-15.7	0.0	-15.1	0.0	38.2	37.5	38.1	-33.2	0.0	-2	5	5	5	0.9	45.8077	-15.5924
2	1.8	2.0	-0.0	-14.5	0.2	-14.9	0.2	-14.8	0.0	38.7	38.3	38.4	-32.7	0.2	1	0	0	5	0.9	45.8096	-15.6824
3	1.0	0.0	-0.0	-15.0	0.0	-15.7	0.0	-15.1	0.0	38.2	37.5	38.1	-33.2	0.0	-2	5	5	5	0.9	45.8175	-15.6480
4	2.1	0.6	-0.6	-14.2	0.1	-14.5	0.1	-14.5	0.1	39.0	38.7	38.7	-32.3	0.1	0	0	0	0	0.9	45.8261	-15.5570
5	1.2	0.8	-0.7	-14.3	0.1	-14.9	0.1	-14.5	0.1	38.9	38.3	38.7	-32.5	0.1	0	0	0	0	0.9	45.8268	-15.5977
6	1.0	0.0	-0.0	-14.9	0.0	-15.6	0.0	-15.0	0.0	38.3	37.6	38.2	-33.2	0.0	-2	5	5	5	0.9	45.8312	-15.6053
7	0.1	0.0	-1.2	-14.5	0.3	-15.7	0.0	-14.5	0.3	38.7	37.5	38.7	-33.0	0.3	-1	0	1	0	0.9	45.8338	-15.6422
8	1.0	0.0	-0.0	-15.0	0.0	-15.7	0.0	-15.1	0.0	38.2	37.5	38.1	-33.2	0.0	-2	5	5	5	0.9	45.8340	-15.5516
9	1.3	3.1	-0.0	-14.7	0.2	-15.3	0.2	-14.9	0.0	38.5	37.9	38.3	-32.9	0.2	1	0	0	5	0.9	45.8351	-15.6438
10	-0.1	0.0	-1.0	-14.1	0.2	-15.4	0.0	-14.1	0.2	39.1	37.8	39.1	-32.7	0.2	-1	0	5	0	0.9	45.8352	-15.5746
11	0.1	0.0	-1.2	-14.5	0.2	-15.6	0.0	-14.5	0.2	38.7	37.6	38.7	-33.0	0.2	-1	0	1	0	0.9	45.8376	-15.6544
12	1.8	0.6	-0.5	-14.2	0.1	-14.5	0.1	-14.4	0.1	39.0	38.7	38.8	-32.3	0.1	0	0	0	0	0.9	45.8419	-15.6471
13	1.0	2.8	-0.0	-14.5	0.2	-15.2	0.2	-14.6	0.0	38.7	38.0	38.6	-32.7	0.2	1	0	0	5	0.9	45.8448	-15.6715
14	2.2	0.7	-0.6	-14.2	0.1	-14.5	0.1	-14.6	0.1	39.0	38.7	38.6	-32.4	0.1	0	0	0	0	0.9	45.8458	-15.5906
15	1.0	0.0	-0.0	-14.7	0.0	-15.4	0.0	-14.8	0.0	38.5	37.8	38.4	-32.9	0.0	-2	1	1	5	0.9	45.8497	-15.5489
16	1.0	0.0	-0.0	-14.9	0.0	-15.6	0.0	-15.0	0.0	38.3	37.6	38.2	-33.2	0.0	-2	5	5	5	0.9	45.8515	-15.5516
17C	1.3	3.1	-0.0	-14.6	0.2	-15.2	0.2	-14.8	0.0	38.6	38.0	38.4	-32.8	0.2	1	0	0	5	0.9	45.8515	-15.6257
18	1.6	0.7	-0.6	-14.3	0.1	-14.7	0.1	-14.5	0.1	38.9	38.5	38.7	-32.4	0.1	0	0	0	0	0.9	45.8547	-15.5747
19	1.0	0.0	-0.0	-14.9	0.0	-15.6	0.0	-15.0	0.0	38.2	37.5	38.2	-33.2	0.0	-2	5	1	5	0.9	45.8558	-15.6043
20	-0.1	0.0	-1.0	-14.2	0.2	-15.5	0.0	-14.2	0.2	39.0	37.7	39.0	-32.8	0.2	-1	0	5	0	0.9	45.8579	-15.5601
21C	1.7	0.4	-0.4	-14.0	0.1	-14.3	0.1	-14.2	0.1	39.2	38.9	39.0	-32.1	0.1	0	0	0	0	0.9	45.8581	-15.6303
22B*	1.2	3.2	-0.0	-14.5	0.2	-15.1	0.2	-14.6	0.0	38.7	38.1	38.6	-32.7	0.2	1	0	0	5	0.9	45.8591	-15.6617
23	0.5	0.8	-0.8	-14.2	0.2	-15.2	0.2	-14.3	0.2	39.0	38.0	38.9	-32.7	0.2	0	0	0	0	0.9	45.8634	-15.6179
24	1.0	0.0	-0.0	-15.0	0.0	-15.7	0.0	-15.0	0.0	38.2	37.5	38.1	-33.2	0.0	-2	5	5	1	0.9	45.8645	-15.6626
25	1.0	0.0	-0.0	-14.9	0.0	-15.6	0.0	-15.0	0.0	38.3	37.6	38.2	-33.2	0.0	-2	5	5	5	0.9	45.8680	-15.6399
26	1.0	0.0	-0.0	-14.9	0.0	-15.6	0.0	-15.0	0.0	38.3	37.6	38.2	-33.2	0.0	-2	5	5	1	0.9	45.8680	-15.6330
27	1.0	0.0	-0.0	-14.9	0.0	-15.6	0.0	-15.0	0.0	38.3	37.6	38.2	-33.2	0.0	-2	5	5	5	0.9	45.8741	-15.6049
28	1.0	0.0	-0.0	-14.9	0.0	-15.6	0.0	-15.0	0.0	38.3	37.6	38.2	-33.2	0.0	-2	5	5	1	0.9	45.8744	-15.6246
29	1.0	0.0	-0.0	-15.0	0.0	-15.7	0.0	-15.1	0.0	38.2	37.5	38.1	-33.2	0.0	-2	5	1	5	0.9	45.8762	-15.6718
30	0.2	0.0	-1.3	-14.4	0.2	-15.5	0.0	-14.4	0.2	38.8	37.7	38.8	-32.9	0.2	-1	0	5	0	0.9	45.8762	-15.5651
31	1.9	2.5	-0.0	-14.5	0.1	-14.8	0.1	-14.8	0.0	38.7	38.4	38.4	-32.6	0.1	1	0	0	5	0.9	45.8765	-15.6173
32	0.7	0.0	-0.0	-14.6	0.2	-15.5	0.0	-14.7	0.0	38.6	37.7	38.5	-33.0	0.2	-2	0	5	5	0.9	45.8774	-15.5783
33	1.7	2.7	-0.0	-14.6	0.2	-15.0	0.2	-14.8	0.0	38.6	38.2	38.4	-32.7	0.2	1	0	0	5	0.9	45.8781	-15.6695
34	1.0	0.0	-0.0	-15.0	0.0	-15.7	0.0	-15.1	0.0	38.2	37.5	38.1	-33.2	0.0	-2	5	5	1	0.9	45.8783	-15.6803
35	1.0	0.0	-0.0	-14.9	0.0	-15.6	0.0	-15.0	0.0	38.3	37.6	38.2	-33.2	0.0	-2	5	5	5	0.9	45.8783	-15.5895
36	2.5	1.4	-0.0	-14.4	0.1	-14.6	0.1	-14.9	0.0	38.8	38.6	38.3	-32.6	0.1	1	0	0	5	0.9	45.8786	-15.6852
37	1.0	0.0	-0.0	-15.0	0.0	-15.7	0.0	-15.1	0.0	38.2	37.5	38.1	-33.2	0.0	-2	5	5	1	0.9	45.8788	-15.6819
38	1.0	0.0	-0.0	-15.0	0.0	-15.7	0.0	-15.1	0.0	38.2	37.5	38.1	-33.3	0.0	-2	5	5	5	0.9	45.8789	-15.6841
39	1.2	3.2	-0.0	-14.6	0.2	-15.2	0.2	-14.7	0.0	38.6	38.0	38.5	-32.8	0.2	1	0	0	5	0.9	45.8807	-15.6293
40	1.0	0.0	-0.0	-14.9	0.0	-15.6	0.0	-15.0	0.0	38.3	37.6	38.2	-33.2	0.0	-2	5	5	5	0.9	45.8817	-15.6845
41	1.0	0.0	-0.0	-14.8	0.0	-15.5	0.0	-14.9	0.0	38.4	37.7	38.3	-33.1	0.0	-2	5	1	5	0.9	45.8825	-15.7063
42	1.2	3.3	-0.0	-14.8	0.3	-15.4	0.3	-14.9	0.0	38.4	37.8	38.3	-33.0	0.3	1	0	0	5	0.9	45.8826	-15.5721
43	0.7	0.0	-0.0	-14.7	0.3	-15.5	0.0	-14.7	0.0	38.5	37.7	38.5	-33.0	0.3	-2	0	5	5	0.9	45.8827	-15.6095
44	1.7	2.7	-0.0	-14.7	0.2	-15.1	0.2	-14.9	0.0	38.5	38.1	38.3	-32.8	0.2	1	0	0	1	0.9	45.8852	-15.6115
45	1.0	0.0	-0.0	-14.9	0.0	-15.6	0.0	-15.0	0.0	38.3	37.6	38.2	-33.2	0.0	-2	5	5	1	0.9	45.8860	-15.5750
46	1.0	0.0	-0.0	-14.9	0.0	-15.6	0.0	-15.0	0.0	38.3	37.6	38.2	-33.2	0.0	-2	5	5	1	0.9	45.8860	-15.6276
47	1.0	0.0	-0.0	-14.9	0.0	-15.6	0.0	-15.0	0.0	38.3	37.6	38.2	-33.2	0.0	-2	5	5	1	0.9	45.8882	-15.6012
48	1.0	0.0	-0.0	-14.9	0.0	-15.6	0.0	-15.0	0.0	38.3	37.6	38.2	-33.2	0.0	-2	5	5	5	0.9	45.8883	-15.6171
49	2.1	2.4	-0.0	-14.6	0.1	-14.9	0.1	-14.9	0.0	38.6	38.3	38.3	-32.7	0.1	1	0	0	5	0.9	45.8911	-15.5743
50	1.0	0.0	-0.0	-14.9	0.0	-15.6	0.0	-15.0	0.0	38.2	37.5	38.2	-33.2	0.0	-2	5	5	1	0.9	45.8924	-15.6882
51	1.0	0.0	-0.0	-15.0	0.0	-15.7	0.0	-15.1	0.0	38.2	37.5	38.1	-33.2	0.0	-2	5	5	1	0.9	45.8935	-15.6864

TABLE 13:
Derived quantities and detection codes for X-ray point sources in HCG 22 (online only).

52	1.0	0.0	-0.0	-15.0	0.0	-15.7	0.0	-15.1	0.0	38.2	37.5	38.1	-33.2	0.0	-2	5	1	5	0.9	45.8941	-15.5966
53	1.5	2.9	-0.0	-14.7	0.2	-15.2	0.2	-14.9	0.0	38.5	38.0	38.3	-32.8	0.2	1	0	0	1	0.9	45.8941	-15.6485
54	1.4	3.0	-0.0	-14.7	0.2	-15.3	0.2	-14.9	0.0	38.5	37.9	38.3	-32.9	0.2	1	0	0	1	0.9	45.8945	-15.6787
55	1.0	0.0	-0.0	-14.9	0.0	-15.6	0.0	-15.0	0.0	38.2	37.5	38.2	-33.2	0.0	-2	5	5	5	0.9	45.8976	-15.6839
56A	1.1	3.3	-0.0	-14.7	0.2	-15.3	0.2	-14.8	0.0	38.5	37.9	38.4	-32.9	0.2	1	0	0	5	0.9	45.8979	-15.6323
57	1.0	0.0	-0.0	-15.0	0.0	-15.7	0.0	-15.0	0.0	38.2	37.5	38.1	-33.2	0.0	-2	5	5	5	0.9	45.8989	-15.6801
58	1.0	0.0	-0.0	-14.9	0.0	-15.6	0.0	-15.0	0.0	38.3	37.6	38.2	-33.2	0.0	-2	5	1	5	0.9	45.8999	-15.6629
59	1.0	0.0	-0.0	-14.9	0.0	-15.6	0.0	-15.0	0.0	38.3	37.6	38.2	-33.1	0.0	-2	5	5	1	0.9	45.9010	-15.6375
60A	0.7	0.0	-0.0	-14.7	0.3	-15.5	0.0	-14.7	0.0	38.5	37.7	38.5	-33.0	0.3	-2	0	5	5	0.9	45.9011	-15.6194
61A	0.7	0.0	-0.0	-14.7	0.3	-15.5	0.0	-14.7	0.0	38.5	37.7	38.5	-33.0	0.3	-2	0	5	5	0.9	45.9018	-15.6278
62	1.0	0.0	-0.0	-14.9	0.0	-15.6	0.0	-15.0	0.0	38.3	37.6	38.2	-33.2	0.0	-2	5	5	1	0.9	45.9025	-15.6912
63A	-0.8	0.6	-0.3	-13.5	0.1	-15.2	0.1	-13.5	0.1	39.7	38.0	39.7	-32.4	0.1	0	0	0	0	0.9	45.9030	-15.6258
64A	0.7	0.0	-0.0	-14.6	0.2	-15.4	0.0	-14.6	0.0	38.6	37.8	38.6	-32.9	0.2	-2	0	5	5	0.9	45.9045	-15.6025
65	1.6	0.6	-0.5	-14.2	0.1	-14.6	0.1	-14.4	0.1	39.0	38.6	38.8	-32.4	0.1	0	0	0	0	0.9	45.9058	-15.6526
66A	1.0	3.4	-0.0	-14.7	0.2	-15.3	0.2	-14.8	0.0	38.5	37.9	38.4	-32.9	0.2	1	0	0	5	0.9	45.9061	-15.6178
67A	0.9	0.6	-0.5	-14.1	0.1	-14.8	0.1	-14.2	0.1	39.1	38.4	39.0	-32.4	0.1	0	0	0	0	0.9	45.9068	-15.6146
68	1.0	0.0	-0.0	-14.9	0.0	-15.6	0.0	-15.0	0.0	38.3	37.6	38.2	-33.2	0.0	-2	5	5	1	0.9	45.9068	-15.6250
69	1.0	0.0	-0.0	-14.9	0.0	-15.6	0.0	-15.0	0.0	38.3	37.6	38.2	-33.1	0.0	-2	5	5	5	0.9	45.9069	-15.6071
70	0.8	0.5	-0.5	-13.9	0.1	-14.7	0.1	-14.0	0.1	39.3	38.5	39.2	-32.2	0.1	0	0	0	0	0.9	45.9081	-15.6844
71	1.0	0.0	-0.0	-14.9	0.0	-15.6	0.0	-15.0	0.0	38.3	37.6	38.2	-33.2	0.0	-2	5	5	5	0.9	45.9082	-15.6219
72A	1.3	3.1	-0.0	-14.7	0.2	-15.2	0.2	-14.8	0.0	38.5	38.0	38.4	-32.9	0.2	1	0	0	5	0.9	45.9091	-15.6141
73	1.0	0.0	-0.0	-14.9	0.0	-15.6	0.0	-15.0	0.0	38.3	37.6	38.2	-33.2	0.0	-2	5	5	5	0.9	45.9092	-15.6154
74A	1.8	2.6	-0.0	-14.6	0.2	-15.0	0.2	-14.8	0.0	38.6	38.2	38.4	-32.7	0.2	1	0	0	5	0.9	45.9092	-15.6175
75	1.0	0.0	-0.0	-14.9	0.0	-15.6	0.0	-15.0	0.0	38.3	37.6	38.2	-33.2	0.0	-2	5	1	5	0.9	45.9096	-15.6951
76A*	1.1	3.3	-0.0	-14.5	0.2	-15.1	0.2	-14.6	0.0	38.7	38.1	38.6	-32.7	0.2	1	0	0	5	0.8	45.9099	-15.6137
77A*	1.7	2.7	-0.0	-14.5	0.2	-14.9	0.2	-14.7	0.0	38.7	38.3	38.5	-32.7	0.2	1	0	0	5	0.9	45.9100	-15.6133
78A	2.4	2.0	-0.0	-14.3	0.1	-14.5	0.1	-14.7	0.0	38.9	38.7	38.5	-32.4	0.1	1	0	0	5	0.9	45.9101	-15.6144
79A	1.0	0.0	-0.0	-14.9	0.0	-15.6	0.0	-15.0	0.0	38.3	37.6	38.2	-33.2	0.0	-2	5	0	1	0.9	45.9106	-15.6130
80	1.0	0.0	-0.0	-15.0	0.0	-15.7	0.0	-15.1	0.0	38.2	37.5	38.1	-33.2	0.0	-2	5	5	1	0.9	45.9112	-15.6222
81A	0.3	0.0	-1.4	-14.4	0.2	-15.4	0.0	-14.4	0.2	38.8	37.8	38.8	-32.8	0.2	-1	0	5	0	0.9	45.9111	-15.6104
82	1.0	0.0	-0.0	-14.9	0.0	-15.6	0.0	-15.0	0.0	38.3	37.6	38.2	-33.1	0.0	-2	5	5	5	0.9	45.9115	-15.6428
83A	0.7	0.0	-0.0	-14.6	0.2	-15.4	0.0	-14.6	0.0	38.6	37.8	38.6	-32.9	0.2	-2	0	5	5	0.9	45.9125	-15.6169
84A	0.7	0.0	-0.0	-14.5	0.2	-15.3	0.0	-14.5	0.0	38.7	37.9	38.7	-32.8	0.2	-2	0	5	5	0.9	45.9130	-15.6135
85	1.0	0.0	-0.0	-14.8	0.0	-15.5	0.0	-14.9	0.0	38.4	37.7	38.3	-33.1	0.0	-2	5	1	5	0.9	45.9133	-15.6438
86A	1.2	2.6	-0.0	-14.8	0.3	-15.4	0.3	-15.0	0.0	38.4	37.8	38.2	-33.0	0.3	1	0	0	1	0.9	45.9133	-15.5973
87A	1.1	3.3	-0.0	-14.7	0.2	-15.3	0.2	-14.8	0.0	38.5	37.9	38.4	-32.9	0.2	1	0	0	5	0.9	45.9141	-15.6112
88	1.0	0.0	-0.0	-15.0	0.0	-15.7	0.0	-15.1	0.0	38.2	37.5	38.1	-33.2	0.0	-2	5	5	1	0.9	45.9143	-15.6127
89	1.0	0.0	-0.0	-14.9	0.0	-15.6	0.0	-15.0	0.0	38.3	37.6	38.2	-33.1	0.0	-2	5	5	1	0.9	45.9144	-15.6044
90	1.0	3.4	-0.0	-14.6	0.2	-15.3	0.2	-14.7	0.0	38.6	37.9	38.5	-32.8	0.2	1	0	0	5	0.9	45.9163	-15.6507
91	1.3	3.1	-0.0	-14.6	0.2	-15.2	0.2	-14.8	0.0	38.6	38.0	38.4	-32.8	0.2	1	0	0	5	0.9	45.9171	-15.6572
92A	1.2	3.2	-0.0	-14.8	0.3	-15.4	0.3	-14.9	0.0	38.4	37.8	38.3	-33.0	0.3	1	0	0	1	0.9	45.9176	-15.6165
93A	1.1	3.3	-0.0	-14.4	0.2	-15.1	0.2	-14.5	0.0	38.8	38.1	38.7	-32.6	0.2	1	0	0	5	0.9	45.9187	-15.6200
94	-0.3	0.0	-0.8	-14.0	0.2	-15.4	0.0	-14.0	0.2	39.2	37.8	39.2	-32.7	0.2	-1	0	5	0	0.9	45.9230	-15.6472
95	0.2	0.0	-1.3	-14.3	0.2	-15.4	0.0	-14.3	0.2	38.9	37.8	38.9	-32.8	0.2	-1	0	5	0	0.9	45.9273	-15.5839
96A	1.0	3.4	-0.0	-14.5	0.2	-15.2	0.2	-14.6	0.0	38.7	38.0	38.6	-32.8	0.2	1	0	0	5	0.9	45.9278	-15.6078
97A	0.1	0.0	-1.2	-14.2	0.2	-15.3	0.0	-14.2	0.2	39.0	37.9	39.0	-32.7	0.2	-1	0	5	0	0.9	45.9287	-15.6061
98	1.0	0.0	-0.0	-15.0	0.0	-15.7	0.0	-15.0	0.0	38.2	37.5	38.1	-33.2	0.0	-2	5	5	1	0.9	45.9306	-15.6115
99	1.0	0.0	-0.0	-14.9	0.0	-15.6	0.0	-15.0	0.0	38.3	37.6	38.2	-33.2	0.0	-2	5	1	5	0.9	45.9325	-15.5894
100	1.2	3.2	-0.0	-14.8	0.3	-15.4	0.3	-14.9	0.0	38.4	37.8	38.3	-33.0	0.3	1	0	0	1	0.9	45.9364	-15.6282
101	-0.1	0.0	-1.0	-14.1	0.2	-15.3	0.0	-14.1	0.2	39.1	37.9	39.1	-32.7	0.2	-1	0	5	0	0.9	45.9391	-15.6034
102	1.0	0.0	-0.0	-14.4	0.0	-15.1	0.0	-14.5	0.0	38.8	38.1	38.7	-32.6	0.0	-2	5	5	5	0.9	45.9411	-15.5795
103	1.0	0.0	-0.0	-14.9	0.0	-15.6	0.0	-15.0	0.0	38.3	37.6	38.2	-33.2	0.0	-2	5	0	1	0.9	45.9514	-15.5871

TABLE 14:
Derived quantities and detection codes for X-ray point sources in HCG 31 (online only).

ID (1)	Γ (2)	L_X										lim									
		+	-	f_F (5)	\pm (6)	f_S (7)	\pm (8)	f_H (9)	\pm (10)	F (11)	S (12)	H (13)	$f_{\nu, 2\text{keV}}$ (14)	\pm (15)	HR	F (17)	S (18)	H (19)	EEF (20)	RA (21)	DEC (22)
1	1.8	0.6	-0.5	-14.2	0.1	-14.6	0.1	-14.4	0.1	39.4	39.0	39.2	-32.3	0.1	0	0	0	0	0.9	75.3102	-4.2743
2	0.7	0.8	-0.8	-14.3	0.2	-15.1	0.2	-14.4	0.2	39.3	38.5	39.2	-32.6	0.2	0	0	0	0	0.9	75.3159	-4.2936
3	0.9	0.8	-0.7	-14.3	0.1	-15.0	0.1	-14.4	0.1	39.3	38.6	39.2	-32.6	0.1	0	0	0	0	0.4	75.3268	-4.2817
4	1.0	0.0	-0.0	-14.6	0.0	-15.3	0.0	-14.7	0.0	39.0	38.3	38.9	-32.9	0.0	-2	5	0	1	0.4	75.3269	-4.2817
5	-0.1	0.0	-1.0	-14.3	0.2	-15.5	0.0	-14.3	0.2	39.3	38.1	39.3	-32.9	0.2	-1	0	5	0	0.9	75.3348	-4.3111
6	1.6	2.2	-0.0	-14.6	0.2	-15.1	0.2	-14.8	0.0	39.0	38.5	38.8	-32.8	0.2	1	0	0	5	0.9	75.3411	-4.2934
7	0.7	0.0	-0.0	-14.6	0.2	-15.5	0.0	-14.7	0.0	39.0	38.1	38.9	-33.0	0.2	-2	0	5	5	0.9	75.3468	-4.2624
8	1.0	0.0	-0.0	-15.0	0.0	-15.7	0.0	-15.1	0.0	38.6	37.9	38.5	-33.2	0.0	-2	5	1	5	0.9	75.3514	-4.2629
9	1.5	0.4	-0.4	-13.9	0.1	-14.4	0.1	-14.1	0.1	39.7	39.2	39.5	-32.1	0.1	0	0	0	0	0.9	75.3527	-4.2447
10	2.3	2.3	-0.0	-14.5	0.1	-14.7	0.1	-14.9	0.0	39.1	38.9	38.7	-32.7	0.1	1	0	0	5	0.9	75.3617	-4.2222
11	1.6	0.6	-0.6	-14.2	0.1	-14.7	0.1	-14.4	0.1	39.4	38.9	39.2	-32.4	0.1	0	0	0	0	0.9	75.3624	-4.2228
12	0.2	0.0	-1.3	-14.4	0.2	-15.5	0.0	-14.4	0.2	39.2	38.1	39.2	-32.9	0.2	-1	0	5	0	0.9	75.3640	-4.3251
13	1.0	0.0	-0.0	-15.0	0.0	-15.7	0.0	-15.1	0.0	38.6	37.9	38.5	-33.2	0.0	-2	5	5	1	0.9	75.3655	-4.2463
14	1.9	0.2	-0.2	-13.5	0.0	-13.8	0.0	-13.8	0.0	40.1	39.8	39.8	-31.6	0.0	0	0	0	0	0.9	75.3657	-4.2770
15	1.0	0.0	-0.0	-15.0	0.0	-15.7	0.0	-15.1	0.0	38.6	37.9	38.5	-33.2	0.0	-2	5	5	5	0.9	75.3663	-4.2229
16	1.1	2.7	-0.0	-14.6	0.2	-15.2	0.2	-14.7	0.0	39.0	38.4	38.9	-32.8	0.2	1	0	0	5	0.9	75.3671	-4.2484
17	2.7	2.0	-0.0	-14.4	0.1	-14.5	0.1	-14.9	0.0	39.2	39.1	38.7	-32.6	0.1	1	0	0	5	0.9	75.3676	-4.2018
18	1.2	2.6	-0.0	-14.8	0.3	-15.4	0.3	-15.0	0.0	38.8	38.2	38.6	-33.1	0.3	1	0	0	1	0.9	75.3697	-4.2573
19	1.5	0.6	-0.5	-14.2	0.1	-14.7	0.1	-14.4	0.1	39.4	38.9	39.2	-32.3	0.1	0	0	0	0	0.9	75.3708	-4.3351
20	2.1	0.6	-0.5	-14.2	0.1	-14.5	0.1	-14.5	0.1	39.4	39.1	39.1	-32.3	0.1	0	0	0	0	0.9	75.3730	-4.3207
21	1.6	0.4	-0.4	-13.9	0.1	-14.4	0.1	-14.2	0.1	39.7	39.2	39.5	-32.1	0.1	0	0	0	0	0.9	75.3734	-4.2812
22	0.6	0.8	-0.8	-14.3	0.2	-15.2	0.2	-14.3	0.2	39.3	38.4	39.3	-32.6	0.2	0	0	0	0	0.9	75.3742	-4.3319
23	2.0	1.8	-0.0	-14.6	0.2	-14.9	0.2	-14.9	0.0	39.0	38.7	38.7	-32.7	0.2	1	0	0	1	0.9	75.3758	-4.3004
24	2.0	0.4	-0.4	-13.9	0.1	-14.2	0.1	-14.2	0.1	39.7	39.4	39.4	-32.0	0.1	0	0	0	0	0.9	75.3781	-4.2254
25	1.0	0.0	-0.0	-15.0	0.0	-15.7	0.0	-15.1	0.0	38.6	37.9	38.5	-33.3	0.0	-2	5	5	5	0.9	75.3814	-4.2842
26	0.7	0.0	-0.0	-14.5	0.2	-15.4	0.0	-14.6	0.0	39.1	38.2	39.0	-32.9	0.2	-2	0	5	5	0.9	75.3849	-4.2685
27	0.3	0.0	-1.4	-14.6	0.3	-15.6	0.0	-14.6	0.3	39.0	38.0	39.0	-33.1	0.3	-1	0	5	0	0.9	75.3859	-4.3151
28	1.0	0.0	-0.0	-15.0	0.0	-15.7	0.0	-15.1	0.0	38.6	37.9	38.5	-33.2	0.0	-2	5	1	5	0.9	75.3912	-4.1931
29B	0.5	0.8	-0.8	-14.3	0.2	-15.3	0.2	-14.3	0.2	39.3	38.4	39.3	-32.7	0.2	0	0	0	0	0.9	75.3950	-4.2670
30B	1.6	2.2	-0.0	-14.6	0.2	-15.0	0.2	-14.8	0.0	39.1	38.6	38.9	-32.7	0.2	1	0	0	5	0.9	75.3971	-4.2626
31	0.1	0.6	-0.6	-13.9	0.1	-15.1	0.1	-13.9	0.1	39.7	38.5	39.7	-32.4	0.1	0	0	0	0	0.9	75.3980	-4.2966
32	1.0	0.0	-0.0	-15.0	0.0	-15.7	0.0	-15.1	0.0	38.6	37.9	38.5	-33.3	0.0	-2	5	5	1	0.9	75.3982	-4.2860
33B	1.2	0.2	-0.2	-13.4	0.0	-14.0	0.0	-13.5	0.0	40.3	39.6	40.1	-31.6	0.0	0	0	0	0	0.9	75.4007	-4.2620
34	-0.7	0.5	-0.4	-13.4	0.1	-15.0	0.1	-13.4	0.1	40.2	38.6	40.2	-32.3	0.1	0	0	0	0	0.9	75.4011	-4.2100
35	1.0	0.0	-0.0	-14.9	0.0	-15.6	0.0	-15.0	0.0	38.7	38.0	38.6	-33.2	0.0	-2	5	5	5	0.9	75.4042	-4.1919
36	-0.2	0.6	-0.7	-13.9	0.1	-15.2	0.1	-13.9	0.1	39.7	38.4	39.7	-32.6	0.1	0	0	0	0	0.9	75.4064	-4.2025
37ACE	1.2	0.2	-0.2	-13.3	0.0	-13.9	0.0	-13.4	0.0	40.3	39.8	40.2	-31.5	0.0	0	0	0	0	0.9	75.4072	-4.2661
38ACE*	1.1	0.2	-0.2	-13.3	0.0	-13.9	0.0	-13.4	0.0	40.3	39.7	40.2	-31.5	0.0	0	0	0	0	0.9	75.4073	-4.2582
39ACE	1.6	0.3	-0.3	-13.8	0.1	-14.2	0.1	-14.0	0.1	39.8	39.4	39.6	-32.0	0.1	0	0	0	0	0.9	75.4076	-4.2571
40ACE*	1.3	0.3	-0.2	-13.6	0.1	-14.1	0.1	-13.7	0.1	40.1	39.5	39.9	-31.7	0.1	0	0	0	0	0.9	75.4077	-4.2579
41Q*	1.1	2.7	-0.0	-14.7	0.2	-15.3	0.2	-14.8	0.0	38.9	38.3	38.8	-32.9	0.2	1	0	0	5	0.9	75.4103	-4.2223
42ACE	0.9	0.7	-0.6	-14.2	0.1	-15.0	0.1	-14.3	0.1	39.4	38.7	39.3	-32.5	0.1	0	0	0	0	0.9	75.4105	-4.2592
43ACE	1.6	0.3	-0.2	-13.6	0.1	-14.0	0.1	-13.8	0.1	40.0	39.6	39.8	-31.7	0.1	0	0	0	0	0.9	75.4108	-4.2545
44	0.7	0.0	-0.0	-14.7	0.3	-15.6	0.0	-14.8	0.0	38.9	38.0	38.8	-33.1	0.3	-2	0	5	5	0.9	75.4109	-4.2929
45	1.6	0.2	-0.2	-13.4	0.0	-13.8	0.0	-13.6	0.0	40.2	39.8	40.0	-31.6	0.0	0	0	0	0	0.9	75.4111	-4.3503
46ACE	2.1	0.3	-0.3	-13.8	0.1	-14.1	0.1	-14.1	0.1	39.8	39.5	39.5	-31.9	0.1	0	0	0	0	0.9	75.4114	-4.2593
47	1.0	0.0	-0.0	-14.9	0.0	-15.6	0.0	-15.0	0.0	38.7	38.0	38.6	-33.2	0.0	-2	5	1	5	0.9	75.4115	-4.2873
48	1.0	0.0	-0.0	-15.0	0.0	-15.7	0.0	-15.1	0.0	38.6	37.9	38.5	-33.2	0.0	-2	5	1	0	0.9	75.4116	-4.2933
49	1.0	0.0	-0.0	-15.0	0.0	-15.7	0.0	-15.1	0.0	38.6	37.9	38.5	-33.3	0.0	-2	5	1	5	0.9	75.4116	-4.2079
50	1.0	0.0	-0.0	-15.0	0.0	-15.7	0.0	-15.1	0.0	38.6	37.9	38.5	-33.3	0.0	-2	5	1	0	0.9	75.4118	-4.2580
51ACE	2.1	0.4	-0.3	-13.8	0.1	-14.1	0.1	-14.2	0.1	39.8	39.5	39.4	-32.0	0.1	0	0	0	0	0.9	75.4135	-4.2633

TABLE 14:
Derived quantities and detection codes for X-ray point sources in HCG 31 (online only).

52	1.0	0.0	-0.0	-15.0	0.0	-15.7	0.0	-15.1	0.0	38.6	37.9	38.5	-33.3	0.0	-2	5	5	5	0.9	75.4138	-4.2993
53	1.0	0.0	-0.0	-14.9	0.0	-15.6	0.0	-15.0	0.0	38.7	38.0	38.6	-33.2	0.0	-2	5	5	1	0.9	75.4147	-4.2570
54ACE	0.7	0.3	-0.3	-13.6	0.1	-14.5	0.1	-13.7	0.1	40.0	39.1	39.9	-32.0	0.1	0	0	0	0	0.9	75.4157	-4.2533
55	1.0	0.0	-0.0	-14.9	0.0	-15.6	0.0	-15.0	0.0	38.7	38.0	38.6	-33.2	0.0	-2	5	5	5	0.9	75.4169	-4.3478
56	1.2	2.6	-0.0	-14.8	0.3	-15.4	0.3	-14.9	0.0	38.8	38.2	38.7	-33.0	0.3	1	0	0	1	0.9	75.4198	-4.2682
57	1.0	0.0	-0.0	-15.0	0.0	-15.7	0.0	-15.1	0.0	38.6	37.9	38.5	-33.3	0.0	-2	5	5	1	0.9	75.4203	-4.2897
58	1.3	2.5	-0.0	-14.7	0.2	-15.2	0.2	-14.8	0.0	38.9	38.4	38.8	-32.9	0.2	1	0	0	5	0.9	75.4223	-4.2687
59	1.2	2.6	-0.0	-14.8	0.3	-15.4	0.3	-14.9	0.0	38.8	38.2	38.7	-33.0	0.3	1	0	0	1	0.9	75.4229	-4.2122
60	0.7	0.0	-0.0	-14.7	0.3	-15.5	0.0	-14.7	0.0	38.9	38.1	38.9	-33.0	0.3	-2	0	5	5	0.9	75.4274	-4.2395
61G	1.8	0.3	-0.3	-13.7	0.1	-14.0	0.1	-13.9	0.1	40.0	39.6	39.7	-31.8	0.1	0	0	0	0	0.9	75.4320	-4.2912
62G	2.3	1.5	-0.0	-14.4	0.1	-14.6	0.1	-14.8	0.0	39.2	39.0	38.8	-32.5	0.1	1	0	0	5	0.9	75.4328	-4.2875
63G*	1.6	0.3	-0.3	-13.6	0.1	-14.1	0.1	-13.8	0.1	40.0	39.5	39.8	-31.8	0.1	0	0	0	0	0.9	75.4336	-4.2886
64G	1.5	0.3	-0.3	-13.6	0.1	-14.1	0.1	-13.8	0.1	40.0	39.5	39.8	-31.8	0.1	0	0	0	0	0.9	75.4336	-4.2893
65	1.5	0.8	-0.7	-14.4	0.1	-14.8	0.1	-14.5	0.1	39.3	38.8	39.1	-32.5	0.1	0	0	0	0	0.9	75.4339	-4.2206
66	1.0	0.0	-0.0	-14.8	0.0	-15.5	0.0	-14.9	0.0	38.8	38.1	38.7	-33.1	0.0	-2	5	1	5	0.9	75.4346	-4.2196
67	0.4	0.5	-0.6	-14.0	0.1	-15.0	0.1	-14.0	0.1	39.6	38.6	39.6	-32.4	0.1	0	0	0	0	0.9	75.4353	-4.2502
68G	1.9	1.9	-0.0	-14.6	0.2	-14.9	0.2	-14.8	0.0	39.0	38.7	38.8	-32.7	0.2	1	0	0	5	0.9	75.4359	-4.2892
69	1.0	0.0	-0.0	-15.0	0.0	-15.7	0.0	-15.1	0.0	38.6	37.9	38.5	-33.2	0.0	-2	5	1	5	0.9	75.4374	-4.3201
70	-0.4	0.0	-0.7	-13.9	0.1	-15.3	0.0	-13.9	0.1	39.8	38.3	39.7	-32.6	0.1	-1	0	5	0	0.9	75.4383	-4.2608
71	1.0	0.0	-0.0	-14.9	0.0	-15.6	0.0	-15.0	0.0	38.7	38.0	38.6	-33.2	0.0	-2	5	5	5	0.9	75.4385	-4.2339
72	1.5	0.7	-0.6	-14.3	0.1	-14.8	0.1	-14.5	0.1	39.3	38.8	39.1	-32.5	0.1	0	0	0	0	0.9	75.4414	-4.2224
73	1.0	0.0	-0.0	-14.9	0.0	-15.6	0.0	-15.0	0.0	38.7	38.0	38.6	-33.2	0.0	-2	5	1	5	0.9	75.4432	-4.3167
74	0.7	0.5	-0.5	-14.0	0.1	-14.8	0.1	-14.0	0.1	39.6	38.8	39.6	-32.3	0.1	0	0	0	0	0.9	75.4462	-4.2686
75	1.8	2.8	-0.0	-14.7	0.2	-15.1	0.2	-15.0	0.0	38.9	38.5	38.6	-32.9	0.2	1	0	0	1	0.9	75.4467	-4.3057
76	1.0	0.0	-0.0	-15.0	0.0	-15.7	0.0	-15.1	0.0	38.6	37.9	38.5	-33.3	0.0	-2	5	1	5	0.9	75.4507	-4.2589
77	1.2	2.6	-0.0	-14.8	0.3	-15.4	0.3	-14.9	0.0	38.8	38.2	38.7	-33.0	0.3	1	0	0	1	0.9	75.4508	-4.2558
78	0.8	0.8	-0.7	-14.3	0.2	-15.1	0.2	-14.4	0.2	39.3	38.5	39.2	-32.6	0.2	0	0	0	0	0.9	75.4569	-4.2754
79	0.7	0.0	-0.0	-14.5	0.2	-15.4	0.0	-14.6	0.0	39.1	38.2	39.0	-32.9	0.2	-2	0	5	5	0.9	75.4743	-4.2592

TABLE 15:
Derived quantities and detection codes for X-ray point sources in HCG 42 (online only).

ID (1)	Γ (2)	LX										lim								RA (21)	DEC (22)
		$+$ (3)	$-$ (4)	f_F (5)	\pm (6)	f_S (7)	\pm (8)	f_H (9)	\pm (10)	F (11)	S (12)	H (13)	$f_{\nu, \text{2keV}}$ (14)	\pm (15)	HR	F (17)	S (18)	H (19)	EEF (20)		
1	1.2	0.8	-0.7	-14.4	0.2	-15.0	0.2	-14.5	0.2	39.3	38.7	39.2	-32.6	0.2	0	0	0	0	0.9	150.0048	-19.6321
2	1.0	0.0	-0.0	-14.9	0.0	-15.6	0.0	-15.0	0.0	38.8	38.1	38.7	-33.1	0.0	-2	5	5	5	0.9	150.0286	-19.6759
3C	1.4	2.4	-0.0	-14.7	0.2	-15.2	0.2	-14.9	0.0	39.0	38.5	38.8	-32.9	0.2	1	0	0	1	0.9	150.0355	-19.6309
4	1.0	0.0	-0.0	-15.0	0.0	-15.7	0.0	-15.1	0.0	38.7	38.0	38.6	-33.3	0.0	-2	5	1	5	0.9	150.0412	-19.6145
5	1.0	0.0	-0.0	-15.0	0.0	-15.7	0.0	-15.1	0.0	38.7	38.0	38.6	-33.2	0.0	-2	5	5	1	0.9	150.0416	-19.6763
6C*	2.4	1.4	-0.0	-14.3	0.1	-14.5	0.1	-14.8	0.0	39.3	39.1	38.9	-32.5	0.1	1	0	0	5	0.9	150.0430	-19.6221
7	0.7	0.0	-0.0	-14.5	0.2	-15.4	0.0	-14.6	0.0	39.2	38.3	39.1	-32.9	0.2	-2	0	5	5	0.9	150.0430	-19.7098
8C	1.6	2.2	-0.0	-14.7	0.2	-15.1	0.2	-14.9	0.0	39.0	38.5	38.8	-32.8	0.2	1	0	0	1	0.9	150.0445	-19.6279
9	1.0	0.0	-0.0	-15.0	0.0	-15.7	0.0	-15.1	0.0	38.7	38.0	38.6	-33.3	0.0	-2	5	5	1	0.9	150.0444	-19.6119
10A	0.6	0.0	-0.0	-14.6	0.3	-15.5	0.0	-14.7	0.0	39.0	38.1	39.0	-33.0	0.3	-2	0	5	5	0.9	150.0494	-19.6482
11	-0.1	0.0	-1.0	-14.2	0.2	-15.5	0.0	-14.2	0.2	39.5	38.2	39.4	-32.8	0.2	-1	0	5	0	0.9	150.0494	-19.6829
12	1.0	0.0	-0.0	-15.0	0.0	-15.7	0.0	-15.1	0.0	38.7	38.0	38.6	-33.2	0.0	-2	5	5	1	0.9	150.0501	-19.6684
13D	1.4	2.4	-0.0	-14.6	0.2	-15.1	0.2	-14.8	0.0	39.1	38.5	38.9	-32.8	0.2	1	0	0	5	0.9	150.0526	-19.6736
14	1.1	0.5	-0.5	-14.1	0.1	-14.7	0.1	-14.2	0.1	39.6	39.0	39.5	-32.3	0.1	0	0	0	0	0.9	150.0530	-19.7176
15C	1.9	0.1	-0.1	-13.2	0.0	-13.5	0.0	-13.4	0.0	40.5	40.2	40.2	-31.3	0.0	0	0	0	0	0.9	150.0554	-19.6094
16D	0.6	0.8	-0.8	-14.3	0.2	-15.2	0.2	-14.4	0.2	39.3	38.4	39.3	-32.7	0.2	0	0	0	0	0.9	150.0558	-19.6692
17	1.3	0.2	-0.2	-13.4	0.0	-13.9	0.0	-13.5	0.0	40.3	39.7	40.1	-31.6	0.0	0	0	0	0	0.9	150.0576	-19.6109
18A*	3.3	0.4	-0.3	-13.4	0.0	-13.5	0.0	-14.3	0.0	40.3	40.2	39.4	-31.7	0.0	0	0	0	0	0.9	150.0592	-19.6364
19	1.0	0.0	-0.0	-15.0	0.0	-15.7	0.0	-15.1	0.0	38.7	38.0	38.6	-33.2	0.0	-2	5	5	1	0.9	150.0610	-19.6682
20	1.4	2.4	-0.0	-14.8	0.2	-15.3	0.2	-15.0	0.0	38.9	38.4	38.7	-33.0	0.2	1	0	0	1	0.9	150.0640	-19.5825
21	1.4	0.5	-0.5	-14.1	0.1	-14.6	0.1	-14.2	0.1	39.6	39.1	39.4	-32.2	0.1	0	0	0	0	0.9	150.0670	-19.7030
22	1.0	0.0	-0.0	-15.0	0.0	-15.7	0.0	-15.1	0.0	38.7	38.0	38.6	-33.2	0.0	-2	5	5	1	0.9	150.0728	-19.6505
23	0.1	0.0	-1.2	-14.5	0.3	-15.7	0.0	-14.5	0.3	39.2	38.0	39.1	-33.1	0.3	-1	0	1	0	0.9	150.0802	-19.6678
24	1.0	0.0	-0.0	-14.9	0.0	-15.6	0.0	-15.0	0.0	38.8	38.1	38.7	-33.1	0.0	-2	5	5	5	0.9	150.0805	-19.7136
25	1.0	0.0	-0.0	-15.0	0.0	-15.7	0.0	-15.1	0.0	38.7	38.0	38.6	-33.2	0.0	-2	5	5	1	0.9	150.0818	-19.6698
26	1.4	2.4	-0.0	-14.8	0.2	-15.3	0.2	-14.9	0.0	38.9	38.4	38.8	-32.9	0.2	1	0	0	1	0.9	150.0827	-19.5802
27	1.0	0.0	-0.0	-15.0	0.0	-15.7	0.0	-15.1	0.0	38.7	38.0	38.6	-33.2	0.0	-2	5	5	5	0.9	150.0844	-19.5759
28	1.4	0.3	-0.3	-13.7	0.1	-14.3	0.1	-13.9	0.1	39.9	39.4	39.8	-31.9	0.1	0	0	0	0	0.9	150.0857	-19.6866
29	1.3	2.5	-0.0	-14.7	0.2	-15.3	0.2	-14.9	0.0	38.9	38.4	38.8	-32.9	0.2	1	0	0	1	0.9	150.0859	-19.6667
30	0.3	0.0	-1.4	-14.4	0.2	-15.5	0.0	-14.4	0.2	39.3	38.2	39.3	-32.9	0.2	-1	0	5	0	0.9	150.0862	-19.7137
31	0.9	2.9	-0.0	-14.5	0.2	-15.2	0.2	-14.6	0.0	39.2	38.4	39.1	-32.8	0.2	1	0	0	5	0.9	150.0869	-19.6191
32	2.9	0.9	-0.0	-14.2	0.1	-14.3	0.1	-14.8	0.0	39.5	39.4	38.8	-32.4	0.1	1	0	0	5	0.9	150.0876	-19.6072
33	0.9	2.9	-0.0	-14.5	0.2	-15.3	0.2	-14.6	0.0	39.1	38.4	39.0	-32.8	0.2	1	0	0	5	0.9	150.0883	-19.6595
34	1.0	0.0	-0.0	-15.0	0.0	-15.7	0.0	-15.1	0.0	38.7	38.0	38.6	-33.2	0.0	-2	5	5	5	0.9	150.0935	-19.6275
35	0.6	0.0	-0.0	-14.6	0.3	-15.5	0.0	-14.7	0.0	39.0	38.1	39.0	-33.0	0.3	-2	0	5	5	0.9	150.0941	-19.7031
36	1.7	0.4	-0.4	-13.9	0.1	-14.3	0.1	-14.1	0.1	39.8	39.4	39.6	-32.0	0.1	0	0	0	0	0.9	150.1047	-19.6428
37	0.6	0.0	-0.0	-14.6	0.3	-15.5	0.0	-14.7	0.0	39.0	38.1	39.0	-33.0	0.3	-2	0	5	5	0.9	150.1060	-19.6804
38	1.1	2.7	-0.0	-14.5	0.2	-15.1	0.2	-14.6	0.0	39.2	38.6	39.1	-32.7	0.2	1	0	0	5	0.9	150.1065	-19.6995
39	0.6	0.0	-0.0	-14.6	0.3	-15.5	0.0	-14.7	0.0	39.0	38.1	39.0	-33.0	0.3	-2	0	5	5	0.9	150.1083	-19.6976
40	0.3	0.0	-1.4	-14.5	0.2	-15.5	0.0	-14.5	0.2	39.2	38.1	39.2	-32.9	0.2	-1	0	5	0	0.9	150.1088	-19.6471
41	0.6	0.0	-0.0	-14.5	0.2	-15.4	0.0	-14.6	0.0	39.2	38.3	39.1	-32.9	0.2	-2	0	5	5	0.9	150.1118	-19.6271
42	0.9	2.9	-0.0	-14.4	0.2	-15.1	0.2	-14.5	0.0	39.3	38.5	39.2	-32.7	0.2	1	0	0	5	0.9	150.1124	-19.6457
43	1.0	0.0	-0.0	-15.0	0.0	-15.7	0.0	-15.1	0.0	38.7	38.0	38.6	-33.2	0.0	-2	5	1	5	0.9	150.1135	-19.6668
44	1.0	0.0	-0.0	-14.9	0.0	-15.6	0.0	-15.0	0.0	38.8	38.1	38.7	-33.1	0.0	-2	5	5	5	0.9	150.1205	-19.6867
45	2.1	2.3	-0.0	-14.4	0.1	-14.7	0.1	-14.8	0.0	39.2	39.0	38.9	-32.6	0.1	1	0	0	5	0.9	150.1212	-19.6133
46	0.9	0.4	-0.4	-13.8	0.1	-14.6	0.1	-13.9	0.1	39.8	39.1	39.7	-32.1	0.1	0	0	0	0	0.9	150.1229	-19.6681
47	1.9	0.6	-0.6	-14.2	0.1	-14.5	0.1	-14.5	0.1	39.4	39.1	39.2	-32.3	0.1	0	0	0	0	0.9	150.1247	-19.5845
48	0.6	0.0	-0.0	-14.6	0.3	-15.5	0.0	-14.7	0.0	39.0	38.1	39.0	-33.0	0.3	-2	0	5	5	0.9	150.1255	-19.6638
49	1.0	0.0	-0.0	-15.0	0.0	-15.7	0.0	-15.1	0.0	38.7	38.0	38.6	-33.2	0.0	-2	5	1	5	0.9	150.1260	-19.6944
50	1.0	0.2	-0.2	-13.3	0.0	-14.0	0.0	-13.4	0.0	40.4	39.7	40.3	-31.5	0.0	0	0	0	0	0.9	150.1268	-19.6370
51	1.0	0.0	-0.0	-15.0	0.0	-15.7	0.0	-15.1	0.0	38.7	38.0	38.6	-33.2	0.0	-2	5	5	5	0.9	150.1307	-19.6330

TABLE 15:
Derived quantities and detection codes for X-ray point sources in HCG 42 (online only).

52B	1.2	2.6	-0.0	-14.6	0.2	-15.2	0.2	-14.8	0.0	39.0	38.5	38.9	-32.8	0.2	1	0	0	5	0.9	150.1345	-19.6592
53	1.6	0.2	-0.2	-13.3	0.0	-13.7	0.0	-13.5	0.0	40.4	40.0	40.2	-31.4	0.0	0	0	0	0	0.9	150.1350	-19.6890
54	1.4	2.4	-0.0	-14.6	0.2	-15.1	0.2	-14.8	0.0	39.1	38.5	38.9	-32.8	0.2	1	0	0	5	0.9	150.1363	-19.6461
55B	0.8	0.8	-0.8	-14.3	0.2	-15.1	0.2	-14.4	0.2	39.3	38.5	39.2	-32.7	0.2	0	0	0	0	0.9	150.1389	-19.6614
56	1.3	0.7	-0.7	-14.3	0.1	-14.9	0.1	-14.5	0.1	39.3	38.8	39.2	-32.5	0.1	0	0	0	0	0.9	150.1393	-19.6818
57B	1.2	2.6	-0.0	-14.6	0.2	-15.2	0.2	-14.8	0.0	39.0	38.4	38.9	-32.8	0.2	1	0	0	5	0.9	150.1425	-19.6658
58	1.3	3.3	-0.0	-14.6	0.2	-15.2	0.2	-14.8	0.0	39.1	38.5	38.9	-32.8	0.2	1	0	0	5	0.9	150.1449	-19.6023
59	1.6	0.2	-0.2	-13.5	0.0	-13.9	0.0	-13.7	0.0	40.2	39.7	40.0	-31.6	0.0	0	0	0	0	0.9	150.1462	-19.6922
60	1.9	2.6	-0.0	-14.5	0.1	-14.8	0.1	-14.8	0.0	39.2	38.8	38.9	-32.6	0.1	1	0	0	5	0.9	150.1524	-19.6330
61	-0.2	0.0	-0.9	-14.1	0.2	-15.5	0.0	-14.2	0.2	39.5	38.2	39.5	-32.8	0.2	-1	0	5	0	0.9	150.1561	-19.6761
62	-0.6	0.0	-0.5	-13.8	0.1	-15.4	0.0	-13.8	0.1	39.9	38.3	39.9	-32.6	0.1	-1	0	5	0	0.9	150.1564	-19.6869
63	0.7	0.0	-0.0	-14.6	0.2	-15.4	0.0	-14.6	0.0	39.1	38.2	39.1	-32.9	0.2	-2	0	5	5	0.9	150.1596	-19.6923
64	1.0	0.0	-0.0	-14.9	0.0	-15.6	0.0	-15.0	0.0	38.8	38.1	38.7	-33.2	0.0	-2	5	5	1	0.9	150.1659	-19.6559
65	0.7	0.0	-0.0	-14.7	0.3	-15.5	0.0	-14.7	0.0	39.0	38.2	38.9	-33.0	0.3	-2	0	5	5	0.9	150.1710	-19.6837

TABLE 16:
Derived quantities and detection codes for X-ray point sources in HCG 59 (online only).

ID (1)	Γ (2)	L_X										lim									
		+	-	f_F (5)	\pm (6)	f_S (7)	\pm (8)	f_H (9)	\pm (10)	F (11)	S (12)	H (13)	$f_{\nu,2\text{keV}}$ (14)	\pm (15)	HR	F (17)	S (18)	H (19)	EEF (20)	RA (21)	DEC (22)
1	1.0	0.0	-0.0	-14.9	0.0	-15.6	0.0	-15.0	0.0	38.8	38.1	38.7	-33.1	0.0	-2	5	1	5	0.9	177.0392	12.7376
2	1.0	0.0	-0.0	-14.7	0.0	-15.4	0.0	-14.8	0.0	39.0	38.3	38.9	-32.9	0.0	-2	5	5	5	0.9	177.0435	12.7450
3	1.0	0.0	-0.0	-15.0	0.0	-15.7	0.0	-15.1	0.0	38.7	38.0	38.6	-33.2	0.0	-2	5	5	1	0.9	177.0456	12.7168
4	1.2	3.2	-0.0	-14.5	0.2	-15.1	0.2	-14.6	0.0	39.2	38.6	39.1	-32.7	0.2	1	0	0	5	0.9	177.0500	12.7112
5	1.0	0.0	-0.0	-14.9	0.0	-15.6	0.0	-15.0	0.0	38.8	38.1	38.7	-33.2	0.0	-2	5	1	5	0.9	177.0528	12.7024
6	-0.9	0.0	-0.2	-13.7	0.1	-15.4	0.0	-13.7	0.1	40.0	38.2	40.0	-32.7	0.1	-1	0	1	0	0.9	177.0570	12.7208
7	0.7	0.0	-0.0	-14.4	0.2	-15.2	0.0	-14.4	0.0	39.3	38.5	39.2	-32.7	0.2	-2	0	5	5	0.9	177.0631	12.7514
8	1.0	0.0	-0.0	-15.0	0.0	-15.7	0.0	-15.1	0.0	38.7	38.0	38.6	-33.3	0.0	-2	5	5	1	0.9	177.0669	12.7091
9	0.7	0.0	-1.8	-14.3	0.2	-15.2	0.0	-14.4	0.2	39.4	38.5	39.3	-32.7	0.2	-1	0	5	0	0.9	177.0684	12.6981
10	0.6	0.0	-0.0	-14.4	0.2	-15.3	0.0	-14.4	0.0	39.3	38.4	39.2	-32.8	0.2	-2	0	5	5	0.9	177.0686	12.7164
11	1.0	0.0	-0.0	-15.0	0.0	-15.7	0.0	-15.1	0.0	38.7	38.0	38.6	-33.3	0.0	-2	5	5	1	0.9	177.0734	12.7317
12	0.2	0.0	-1.3	-14.4	0.2	-15.5	0.0	-14.4	0.2	39.3	38.2	39.3	-32.9	0.2	-1	0	5	0	0.9	177.0736	12.7679
13	1.0	0.0	-0.0	-15.0	0.0	-15.7	0.0	-15.1	0.0	38.7	38.0	38.6	-33.3	0.0	-2	5	5	5	0.9	177.0751	12.7461
14	1.0	0.0	-0.0	-15.0	0.0	-15.7	0.0	-15.1	0.0	38.7	38.0	38.6	-33.3	0.0	-2	5	5	1	0.9	177.0752	12.7370
15	1.0	0.0	-0.0	-15.0	0.0	-15.7	0.0	-15.1	0.0	38.7	38.0	38.6	-33.3	0.0	-2	5	5	5	0.9	177.0771	12.7467
16	0.2	0.0	-1.3	-14.4	0.3	-15.6	0.0	-14.5	0.3	39.2	38.1	39.2	-33.0	0.3	-1	0	1	0	0.9	177.0791	12.6937
17	1.0	0.0	-0.0	-15.0	0.0	-15.7	0.0	-15.1	0.0	38.7	38.0	38.6	-33.3	0.0	-2	5	5	5	0.9	177.0802	12.7359
18	1.0	0.0	-0.0	-14.8	0.0	-15.5	0.0	-14.9	0.0	38.9	38.2	38.8	-33.1	0.0	-2	5	5	5	0.9	177.0810	12.6788
19	0.7	0.0	-0.0	-14.5	0.2	-15.4	0.0	-14.6	0.0	39.2	38.3	39.1	-32.8	0.2	-2	0	5	5	0.9	177.0813	12.7692
20	1.0	0.0	-0.0	-15.0	0.0	-15.7	0.0	-15.1	0.0	38.7	38.0	38.6	-33.3	0.0	-2	5	5	5	0.9	177.0815	12.7330
21B	1.5	2.9	-0.0	-14.6	0.2	-15.1	0.2	-14.8	0.0	39.1	38.6	38.9	-32.8	0.2	1	0	0	1	0.9	177.0821	12.7198
22B	0.6	0.0	-0.0	-14.5	0.2	-15.4	0.0	-14.5	0.0	39.2	38.3	39.1	-32.8	0.2	-2	0	5	5	0.9	177.0824	12.7162
23B	1.5	2.9	-0.0	-14.6	0.2	-15.1	0.2	-14.8	0.0	39.1	38.6	38.9	-32.8	0.2	1	0	0	1	0.9	177.0824	12.7177
24	1.0	0.0	-0.0	-15.0	0.0	-15.7	0.0	-15.1	0.0	38.7	38.0	38.6	-33.2	0.0	-2	5	5	5	0.9	177.0828	12.6784
25	0.7	0.0	-0.0	-14.4	0.2	-15.3	0.0	-14.5	0.0	39.3	38.4	39.2	-32.7	0.2	-2	0	5	5	0.9	177.0827	12.7558
26B*	1.5	2.9	-0.0	-14.3	0.1	-14.8	0.1	-14.5	0.0	39.3	38.9	39.2	-32.5	0.1	1	0	0	5	0.9	177.0837	12.7166
27	1.0	0.0	-0.0	-15.0	0.0	-15.7	0.0	-15.1	0.0	38.7	38.0	38.6	-33.3	0.0	-2	5	1	5	0.9	177.0857	12.7499
28	0.7	0.0	-0.0	-14.6	0.3	-15.4	0.0	-14.6	0.0	39.1	38.2	39.1	-32.9	0.3	-2	0	5	5	0.9	177.0863	12.6743
29	1.0	0.0	-0.0	-15.1	0.0	-15.8	0.0	-15.2	0.0	38.6	37.9	38.5	-33.3	0.0	-2	5	5	1	0.9	177.0894	12.7450
30	1.0	0.0	-0.0	-15.0	0.0	-15.7	0.0	-15.1	0.0	38.7	38.0	38.6	-33.3	0.0	-2	5	5	1	0.9	177.0896	12.7081
31	1.0	0.0	-0.0	-15.1	0.0	-15.8	0.0	-15.2	0.0	38.6	37.9	38.5	-33.3	0.0	-2	5	5	1	0.9	177.0907	12.7424
32	0.6	0.0	-0.0	-14.6	0.3	-15.4	0.0	-14.6	0.0	39.1	38.2	39.1	-32.9	0.3	-2	0	5	5	0.9	177.0910	12.7347
33	1.0	0.0	-0.0	-15.0	0.0	-15.7	0.0	-15.1	0.0	38.7	38.0	38.6	-33.3	0.0	-2	5	5	1	0.9	177.0946	12.6731
34	1.8	0.5	-0.4	-13.9	0.1	-14.3	0.1	-14.2	0.1	39.7	39.4	39.5	-32.1	0.1	0	0	0	0	0.9	177.0957	12.7274
35	-0.0	0.0	-1.1	-14.1	0.2	-15.3	0.0	-14.1	0.2	39.6	38.3	39.6	-32.7	0.2	-1	0	5	0	0.9	177.0982	12.7648
36	1.0	0.0	-0.0	-15.0	0.0	-15.7	0.0	-15.1	0.0	38.7	38.0	38.6	-33.3	0.0	-2	5	5	5	0.9	177.0987	12.7401
37	0.7	0.0	-0.0	-14.6	0.3	-15.4	0.0	-14.6	0.0	39.1	38.2	39.1	-32.9	0.3	-2	0	5	5	0.9	177.0988	12.7016
38	1.0	0.0	-0.0	-15.0	0.0	-15.7	0.0	-15.1	0.0	38.7	38.0	38.6	-33.3	0.0	-2	5	5	1	0.9	177.0997	12.6865
39	0.7	3.8	-0.0	-14.3	0.2	-15.2	0.2	-14.4	0.0	39.4	38.5	39.3	-32.7	0.2	1	0	0	5	0.9	177.1004	12.6978
40	1.0	0.0	-0.0	-15.0	0.0	-15.7	0.0	-15.1	0.0	38.7	38.0	38.6	-33.3	0.0	-2	5	5	1	0.9	177.1009	12.7237
41	1.0	0.0	-0.0	-15.0	0.0	-15.7	0.0	-15.1	0.0	38.7	38.0	38.6	-33.3	0.0	-2	5	5	1	0.9	177.1027	12.7126
42	1.0	0.0	-0.0	-15.0	0.0	-15.7	0.0	-15.1	0.0	38.7	38.0	38.6	-33.3	0.0	-2	5	5	5	0.9	177.1030	12.7208
43	1.0	0.0	-0.0	-15.0	0.0	-15.7	0.0	-15.1	0.0	38.7	38.0	38.6	-33.2	0.0	-2	5	5	1	0.9	177.1041	12.7211
44	1.0	0.0	-0.0	-15.0	0.0	-15.7	0.0	-15.1	0.0	38.7	38.0	38.6	-33.3	0.0	-2	5	5	1	0.9	177.1058	12.7067
45	1.0	0.0	-0.0	-15.0	0.0	-15.7	0.0	-15.1	0.0	38.7	38.0	38.6	-33.3	0.0	-2	5	5	1	0.9	177.1068	12.7334
46	1.0	0.0	-0.0	-15.1	0.0	-15.8	0.0	-15.2	0.0	38.6	37.9	38.5	-33.4	0.0	-2	5	5	1	0.9	177.1100	12.7247
47	2.1	2.3	-0.0	-14.5	0.1	-14.8	0.1	-14.8	0.0	39.2	38.9	38.9	-32.6	0.1	1	0	0	1	0.9	177.1124	12.7570
48	1.0	0.0	-0.0	-15.0	0.0	-15.7	0.0	-15.1	0.0	38.7	38.0	38.6	-33.3	0.0	-2	5	5	1	0.9	177.1128	12.7154
49	1.0	0.0	-0.0	-15.0	0.0	-15.7	0.0	-15.1	0.0	38.7	38.0	38.6	-33.2	0.0	-2	5	5	1	0.9	177.1130	12.7149
50A*	0.8	0.3	-0.3	-13.6	0.1	-14.3	0.1	-13.6	0.1	40.1	39.3	40.1	-31.9	0.1	0	0	0	0	0.9	177.1147	12.7274
51	1.0	0.0	-0.0	-15.0	0.0	-15.7	0.0	-15.1	0.0	38.7	38.0	38.6	-33.2	0.0	-2	5	5	5	0.9	177.1147	12.6843

TABLE 16:
Derived quantities and detection codes for X-ray point sources in HCG 59 (online only).

52	1.0	0.0	-0.0	-15.1	0.0	-15.8	0.0	-15.2	0.0	38.6	37.9	38.5	-33.3	0.0	-2	5	5	5	0.9	177.1151	12.7503
53	-0.4	0.0	-0.7	-13.9	0.2	-15.4	0.0	-13.9	0.2	39.8	38.3	39.7	-32.7	0.2	-1	0	5	0	0.9	177.1152	12.7702
54	1.0	0.0	-0.0	-15.0	0.0	-15.7	0.0	-15.1	0.0	38.7	38.0	38.6	-33.2	0.0	-2	5	1	5	0.9	177.1173	12.6773
55	1.0	0.0	-0.0	-15.1	0.0	-15.8	0.0	-15.2	0.0	38.6	37.9	38.5	-33.3	0.0	-2	5	5	1	0.9	177.1178	12.7269
56	1.1	3.3	-0.0	-14.7	0.3	-15.3	0.3	-14.8	0.0	39.0	38.4	38.9	-32.9	0.3	1	0	0	1	0.9	177.1183	12.6861
57	1.0	0.0	-0.0	-15.0	0.0	-15.7	0.0	-15.1	0.0	38.7	38.0	38.6	-33.2	0.0	-2	5	5	5	0.9	177.1199	12.6786
58	1.0	0.0	-0.0	-15.0	0.0	-15.7	0.0	-15.1	0.0	38.7	38.0	38.6	-33.3	0.0	-2	5	5	1	0.9	177.1223	12.7310
59	1.3	0.5	-0.4	-13.9	0.1	-14.5	0.1	-14.0	0.1	39.8	39.2	39.6	-32.1	0.1	0	0	0	0	0.9	177.1226	12.7926
60	0.5	0.6	-0.6	-14.0	0.1	-14.9	0.1	-14.0	0.1	39.7	38.8	39.7	-32.4	0.1	0	0	0	0	0.9	177.1238	12.7474
61	1.0	0.0	-0.0	-15.1	0.0	-15.8	0.0	-15.2	0.0	38.6	37.9	38.5	-33.3	0.0	-2	5	5	1	0.9	177.1243	12.6454
62	1.0	0.0	-0.0	-15.0	0.0	-15.7	0.0	-15.1	0.0	38.7	38.0	38.6	-33.3	0.0	-2	5	5	1	0.9	177.1244	12.7309
63	1.0	0.0	-0.0	-15.1	0.0	-15.8	0.0	-15.2	0.0	38.6	37.9	38.5	-33.3	0.0	-2	5	5	1	0.9	177.1262	12.7350
64	1.0	0.0	-0.0	-15.0	0.0	-15.7	0.0	-15.1	0.0	38.7	38.0	38.6	-33.3	0.0	-2	5	5	1	0.9	177.1273	12.6847
65	1.0	0.0	-0.0	-15.1	0.0	-15.8	0.0	-15.2	0.0	38.6	37.9	38.5	-33.3	0.0	-2	5	5	1	0.9	177.1277	12.7303
66D	1.0	0.0	-0.0	-15.1	0.0	-15.8	0.0	-15.2	0.0	38.6	37.9	38.5	-33.3	0.0	-2	5	1	0	0.9	177.1308	12.7321
67	1.0	0.0	-0.0	-15.0	0.0	-15.7	0.0	-15.1	0.0	38.7	38.0	38.6	-33.3	0.0	-2	5	5	1	0.9	177.1329	12.7185
68	1.0	0.0	-0.0	-15.0	0.0	-15.7	0.0	-15.1	0.0	38.7	38.0	38.6	-33.3	0.0	-2	5	5	5	0.9	177.1367	12.6868
69	2.0	2.4	-0.0	-14.5	0.2	-14.8	0.2	-14.8	0.0	39.2	38.9	38.9	-32.6	0.2	1	0	0	1	0.9	177.1375	12.7075
70C	0.5	0.5	-0.5	-13.8	0.1	-14.8	0.1	-13.9	0.1	39.9	38.9	39.8	-32.2	0.1	0	0	0	0	0.9	177.1386	12.7081
71	1.0	0.0	-0.0	-15.1	0.0	-15.8	0.0	-15.2	0.0	38.6	37.9	38.5	-33.3	0.0	-2	5	5	1	0.9	177.1393	12.6805
72	1.4	0.7	-0.6	-14.2	0.1	-14.7	0.1	-14.3	0.1	39.5	39.0	39.3	-32.4	0.1	0	0	0	0	0.9	177.1406	12.7918
73	1.4	3.0	-0.0	-14.5	0.2	-15.0	0.2	-14.6	0.0	39.2	38.7	39.0	-32.6	0.2	1	0	0	5	0.9	177.1408	12.7111
74	1.0	0.0	-0.0	-15.1	0.0	-15.8	0.0	-15.2	0.0	38.6	37.9	38.5	-33.3	0.0	-2	5	5	5	0.9	177.1423	12.6586
75	0.4	0.7	-0.8	-14.1	0.2	-15.1	0.2	-14.1	0.2	39.6	38.6	39.5	-32.5	0.2	0	0	0	0	0.9	177.1429	12.6664
76	1.2	0.6	-0.6	-14.1	0.1	-14.7	0.1	-14.2	0.1	39.6	39.0	39.5	-32.3	0.1	0	0	0	0	0.9	177.1436	12.7855
77	1.7	0.3	-0.3	-13.6	0.1	-14.0	0.1	-13.8	0.1	40.1	39.7	39.9	-31.7	0.1	0	0	0	0	0.9	177.1439	12.7741
78	1.0	0.0	-0.0	-15.1	0.0	-15.8	0.0	-15.2	0.0	38.6	37.9	38.5	-33.3	0.0	-2	5	1	5	0.9	177.1443	12.6614
79	1.0	3.4	-0.0	-14.4	0.2	-15.1	0.2	-14.5	0.0	39.2	38.6	39.1	-32.7	0.2	1	0	0	5	0.9	177.1445	12.6881
80	0.0	0.0	-1.1	-14.3	0.2	-15.6	0.0	-14.3	0.2	39.4	38.1	39.3	-32.9	0.2	-1	0	1	0	0.9	177.1447	12.7210
81	2.2	0.5	-0.4	-13.9	0.1	-14.1	0.1	-14.2	0.1	39.8	39.5	39.4	-32.0	0.1	0	0	0	0	0.9	177.1452	12.6935
82	1.0	0.0	-0.0	-15.1	0.0	-15.8	0.0	-15.1	0.0	38.6	37.9	38.5	-33.3	0.0	-2	5	5	5	0.9	177.1461	12.6597
83	0.3	0.0	-1.4	-14.2	0.2	-15.3	0.0	-14.2	0.2	39.5	38.4	39.5	-32.7	0.2	-1	0	5	0	0.9	177.1463	12.7238
84	1.1	0.4	-0.4	-13.8	0.1	-14.4	0.1	-13.9	0.1	39.9	39.3	39.8	-32.0	0.1	0	0	0	0	0.9	177.1466	12.7344
85	1.4	2.4	-0.0	-14.5	0.2	-15.1	0.2	-14.7	0.0	39.1	38.6	39.0	-32.7	0.2	1	0	0	5	0.9	177.1485	12.6686
86	1.0	0.0	-0.0	-15.0	0.0	-15.7	0.0	-15.1	0.0	38.7	38.0	38.6	-33.3	0.0	-2	5	5	5	0.9	177.1487	12.6627
87	1.4	0.6	-0.5	-14.1	0.1	-14.6	0.1	-14.3	0.1	39.6	39.1	39.4	-32.3	0.1	0	0	0	0	0.9	177.1491	12.6587
88	-0.1	0.0	-1.0	-14.1	0.2	-15.4	0.0	-14.1	0.2	39.6	38.3	39.6	-32.7	0.2	-1	0	5	0	0.9	177.1530	12.7183
89	1.0	0.0	-0.0	-15.1	0.0	-15.8	0.0	-15.2	0.0	38.6	37.9	38.5	-33.3	0.0	-2	5	1	5	0.9	177.1555	12.7241
90	0.6	0.6	-0.6	-14.0	0.1	-14.9	0.1	-14.1	0.1	39.7	38.8	39.6	-32.4	0.1	0	0	0	0	0.9	177.1592	12.7272
91	2.1	0.6	-0.5	-14.0	0.1	-14.3	0.1	-14.4	0.1	39.7	39.4	39.3	-32.2	0.1	0	0	0	0	0.9	177.1599	12.7801
92	1.0	0.0	-0.0	-15.0	0.0	-15.7	0.0	-15.1	0.0	38.7	38.0	38.6	-33.3	0.0	-2	5	5	1	0.9	177.1622	12.7482
93	1.6	0.2	-0.2	-13.3	0.0	-13.7	0.0	-13.5	0.0	40.4	40.0	40.2	-31.4	0.0	0	0	0	0	0.9	177.1626	12.7566
94	3.1	0.3	-0.4	-13.4	0.0	-13.5	0.0	-14.2	0.0	40.2	40.1	39.5	-31.7	0.0	0	0	0	0	0.9	177.1655	12.7158
95	1.6	0.5	-0.5	-14.0	0.1	-14.4	0.1	-14.2	0.1	39.7	39.3	39.5	-32.1	0.1	0	0	0	0	0.9	177.1657	12.7402
96	2.0	0.2	-0.3	-13.4	0.0	-13.7	0.0	-13.7	0.0	40.2	39.9	39.9	-31.6	0.0	0	0	0	0	0.9	177.1673	12.7329
97	1.0	0.0	-0.0	-14.6	0.0	-15.3	0.0	-14.7	0.0	39.1	38.4	39.0	-32.9	0.0	-2	5	5	5	0.9	177.1708	12.7859
98	1.2	3.2	-0.0	-14.6	0.2	-15.2	0.2	-14.8	0.0	39.0	38.5	38.9	-32.8	0.2	1	0	0	5	0.9	177.1711	12.7298
99	1.0	0.0	-0.0	-15.0	0.0	-15.7	0.0	-15.1	0.0	38.6	37.9	38.5	-33.3	0.0	-2	5	5	5	0.9	177.1718	12.6831
100	1.0	0.0	-0.0	-15.0	0.0	-15.7	0.0	-15.1	0.0	38.7	38.0	38.6	-33.3	0.0	-2	5	5	1	0.9	177.1729	12.6885
101	1.0	0.0	-0.0	-15.1	0.0	-15.8	0.0	-15.2	0.0	38.6	37.9	38.5	-33.3	0.0	-2	1	1	5	0.9	177.1745	12.7743
102	1.2	3.2	-0.0	-14.6	0.2	-15.2	0.2	-14.7	0.0	39.1	38.5	39.0	-32.8	0.2	1	0	0	5	0.9	177.1810	12.7322
103	1.0	0.0	-0.0	-15.0	0.0	-15.7	0.0	-15.1	0.0	38.6	38.0	38.6	-33.3	0.0	-2	5	5	5	0.9	177.1856	12.6964
104	-0.1	0.3	-0.3	-13.1	0.1	-14.4	0.1	-13.2	0.1	40.5	39.2	40.5	-31.8	0.1	0	0	0	0	0.9	177.1877	12.7183
105	0.8	0.0	-0.0	-14.5	0.2	-15.3	0.0	-14.6	0.0	39.2	38.4	39.1	-32.8	0.2	-2	0	5	5	0.9	177.1878	12.7052
106	0.2	0.0	-1.3	-14.4	0.3	-15.5	0.0	-14.4	0.3	39.3	38.1	39.3	-32.9	0.3	-1	0	5	0	0.5	177.1883	12.7535
107	1.0	0.0	-0.0	-14.7	0.0	-15.4	0.0	-14.8	0.0	39.0	38.3	38.9	-33.0	0.0	-2	5	5	5	0.4	177.1884	12.7557
108	3.1	0.6	-0.5	-13.6	0.1	-13.7	0.1	-14.4	0.1	40.0	40.0	39.3	-31.9	0.1	0	0	0	0	0.9	177.1885	12.7485

TABLE 16:
Derived quantities and detection codes for X-ray point sources in HCG 59 (online only).

109	1.8	0.6	-0.6	-14.2	0.1	-14.5	0.1	-14.4	0.1	39.5	39.2	39.3	-32.3	0.1	0	0	0	0.9	177.1896	12.7080	
110	-0.3	0.0	-0.8	-14.2	0.2	-15.6	0.0	-14.2	0.2	39.5	38.1	39.5	-32.9	0.2	-1	0	1	0	0.9	177.1985	12.7574

TABLE 17:
Derived quantities and detection codes for X-ray point sources in HCG 62 (online only).

Tzanavaris et al.

ID (1)	Γ (2)	L_X										lim						EEF (20)	RA (21)	DEC (22)	
		+	-	f_F (5)	\pm (6)	f_S (7)	\pm (8)	f_H (9)	\pm (10)	F (11)	S (12)	H (13)	$f_{\nu,2\text{keV}}$ (14)	\pm (15)	HR	F (17)	S (18)	H (19)			
1	0.7	0.4	-0.4	-14.5	0.1	-15.3	0.1	-14.5	0.1	39.2	38.4	39.2	-32.8	0.1	0	0	0	0	0.9	193.1794	-9.2492
2	0.5	0.6	-0.7	-14.8	0.1	-15.7	0.1	-14.8	0.1	38.9	38.0	38.9	-33.2	0.1	0	0	0	0	0.9	193.1884	-9.2188
3	0.4	0.4	-0.3	-14.3	0.1	-15.3	0.1	-14.4	0.1	39.4	38.4	39.3	-32.8	0.1	0	0	0	0	0.9	193.1889	-9.2643
4	1.0	0.0	-0.0	-15.4	0.0	-16.1	0.0	-15.5	0.0	38.3	37.6	38.2	-33.7	0.0	-2	5	5	1	0.9	193.1988	-9.1934
5	0.8	0.3	-0.3	-14.2	0.1	-15.0	0.1	-14.3	0.1	39.5	38.7	39.4	-32.5	0.1	0	0	0	0	0.9	193.2010	-9.2535
6	1.1	0.4	-0.4	-14.5	0.1	-15.2	0.1	-14.6	0.1	39.2	38.5	39.1	-32.7	0.1	0	0	0	0	0.9	193.2026	-9.2236
7	1.7	0.2	-0.2	-14.1	0.0	-14.5	0.0	-14.3	0.0	39.6	39.2	39.3	-32.3	0.0	0	0	0	0	0.9	193.2058	-9.2073
8	1.9	0.3	-0.3	-14.4	0.1	-14.7	0.1	-14.7	0.1	39.3	39.0	39.0	-32.5	0.1	0	0	0	0	0.9	193.2071	-9.1961
9	1.0	0.8	-0.7	-15.0	0.2	-15.7	0.2	-15.1	0.2	38.7	38.0	38.6	-33.3	0.2	0	0	0	0	0.9	193.2074	-9.1769
10	1.6	0.6	-0.5	-14.9	0.1	-15.3	0.1	-15.1	0.1	38.8	38.4	38.6	-33.0	0.1	0	0	0	0	0.9	193.2089	-9.1821
11	1.6	0.2	-0.2	-13.9	0.0	-14.4	0.0	-14.1	0.0	39.8	39.3	39.6	-32.1	0.0	0	0	0	0	0.9	193.2092	-9.2580
12	1.8	0.5	-0.4	-14.7	0.1	-15.0	0.1	-14.9	0.1	39.0	38.7	38.8	-32.8	0.1	0	0	0	0	0.9	193.2168	-9.2673
13	0.2	0.5	-0.5	-14.6	0.1	-15.7	0.1	-14.6	0.1	39.1	38.0	39.1	-33.1	0.1	0	0	0	0	0.9	193.2172	-9.2614
14	2.9	0.9	-0.0	-14.9	0.1	-15.0	0.1	-15.5	0.0	38.8	38.7	38.2	-33.1	0.1	1	0	0	1	0.9	193.2196	-9.2283
15	1.0	0.0	-0.0	-15.8	0.0	-16.5	0.0	-15.9	0.0	37.9	37.2	37.8	-34.1	0.0	-2	5	5	1	0.9	193.2219	-9.1628
16	0.7	0.0	-0.0	-15.4	0.3	-16.3	0.0	-15.5	0.0	38.3	37.4	38.2	-33.8	0.3	-2	0	5	5	0.9	193.2243	-9.1571
17	0.7	0.0	-0.0	-15.2	0.2	-16.1	0.0	-15.3	0.0	38.5	37.6	38.4	-33.6	0.2	-2	0	5	5	0.9	193.2247	-9.1678
18	1.8	2.0	-0.0	-15.2	0.2	-15.6	0.2	-15.5	0.0	38.5	38.1	38.2	-33.3	0.2	1	0	0	5	0.9	193.2266	-9.2112
19	-0.5	0.6	-0.7	-14.4	0.1	-15.9	0.1	-14.4	0.1	39.3	37.8	39.3	-33.1	0.1	0	0	0	0	0.9	193.2272	-9.2328
20	1.1	0.5	-0.5	-14.8	0.1	-15.4	0.1	-14.9	0.1	38.9	38.3	38.8	-33.0	0.1	0	0	0	0	0.9	193.2289	-9.1543
21	0.2	0.6	-0.7	-14.7	0.1	-15.8	0.1	-14.7	0.1	39.0	37.9	39.0	-33.2	0.1	0	0	0	0	0.9	193.2297	-9.1999
22	-1.1	0.3	-0.0	-14.3	0.1	-16.2	0.0	-14.3	0.1	39.4	37.5	39.4	-33.4	0.1	-1	0	5	0	0.9	193.2317	-9.2089
23	1.0	0.0	-0.0	-15.8	0.0	-16.5	0.0	-15.9	0.0	37.8	37.1	37.7	-34.1	0.0	-2	5	5	5	0.9	193.2344	-9.1436
24	1.0	0.0	-0.0	-15.8	0.0	-16.5	0.0	-15.9	0.0	37.8	37.1	37.7	-34.1	0.0	-2	5	1	0	0.9	193.2368	-9.1709
25	-0.0	0.4	-0.4	-14.3	0.1	-15.6	0.1	-14.3	0.1	39.4	38.1	39.4	-32.9	0.1	0	0	0	0	0.9	193.2371	-9.2215
26	-0.4	0.0	-0.7	-14.7	0.2	-16.1	0.0	-14.7	0.2	39.0	37.5	39.0	-33.4	0.2	-1	0	5	0	0.9	193.2400	-9.2189
27	1.7	2.1	-0.0	-15.5	0.2	-15.9	0.2	-15.7	0.0	38.2	37.8	38.0	-33.6	0.2	1	0	0	1	0.8	193.2400	-9.2176
28	1.0	0.0	-0.0	-15.8	0.0	-16.5	0.0	-15.9	0.0	37.9	37.2	37.8	-34.1	0.0	-2	5	5	5	0.9	193.2403	-9.1381
29	2.1	1.7	-0.0	-15.0	0.1	-15.3	0.1	-15.4	0.0	38.6	38.4	38.3	-33.2	0.1	1	0	0	5	0.9	193.2409	-9.2622
30	1.6	2.7	-0.0	-15.3	0.2	-15.8	0.2	-15.5	0.0	38.3	37.9	38.2	-33.5	0.2	1	0	0	1	0.9	193.2436	-9.1952
31	1.6	2.2	-0.0	-15.5	0.2	-15.9	0.2	-15.7	0.0	38.2	37.8	38.0	-33.6	0.2	1	0	0	1	0.9	193.2436	-9.1860
32	1.0	0.0	-0.0	-15.9	0.0	-16.6	0.0	-16.0	0.0	37.8	37.1	37.7	-34.1	0.0	-2	5	5	1	0.9	193.2470	-9.1652
33	1.0	0.0	-0.0	-15.9	0.0	-16.6	0.0	-16.0	0.0	37.8	37.1	37.7	-34.2	0.0	-2	5	5	1	0.9	193.2471	-9.1332
34	1.3	0.6	-0.5	-14.9	0.1	-15.4	0.1	-15.0	0.1	38.8	38.3	38.7	-33.1	0.1	0	0	0	0	0.9	193.2481	-9.1406
35	2.2	0.6	-0.5	-14.8	0.1	-15.0	0.1	-15.1	0.1	38.9	38.7	38.6	-32.9	0.1	0	0	0	0	0.9	193.2497	-9.2199
36	-1.1	0.0	-0.0	-13.6	0.0	-15.5	0.0	-13.6	0.0	40.1	38.2	40.1	-32.7	0.0	0	0	0	0	0.9	193.2516	-9.1845
37	-0.1	0.6	-0.6	-14.5	0.1	-15.8	0.1	-14.5	0.1	39.2	37.9	39.1	-33.1	0.1	0	0	0	0	0.9	193.2523	-9.2090
38	-1.1	0.5	-0.0	-13.9	0.1	-15.8	0.1	-13.9	0.1	39.8	37.9	39.8	-33.0	0.1	0	0	0	0	0.9	193.2538	-9.1614
39	1.0	0.0	-0.0	-15.9	0.0	-16.6	0.0	-16.0	0.0	37.8	37.1	37.7	-34.2	0.0	-2	5	5	5	0.9	193.2559	-9.1240
40	1.8	2.5	-0.0	-15.1	0.1	-15.5	0.1	-15.3	0.0	38.6	38.2	38.4	-33.2	0.1	1	0	0	5	0.9	193.2562	-9.2038
41	0.1	0.0	-1.2	-15.3	0.3	-16.4	0.0	-15.3	0.3	38.4	37.2	38.4	-33.8	0.3	-1	0	1	0	0.9	193.2570	-9.1666
42	-0.1	0.0	-1.0	-15.2	0.3	-16.5	0.0	-15.2	0.3	38.5	37.2	38.5	-33.9	0.3	-1	0	1	0	0.9	193.2579	-9.1608
43	1.9	0.3	-0.3	-14.4	0.1	-14.7	0.1	-14.6	0.1	39.3	39.0	39.0	-32.5	0.1	0	0	0	0	0.9	193.2581	-9.1929
44B	0.8	0.4	-0.4	-14.6	0.1	-15.4	0.1	-14.7	0.1	39.1	38.3	39.0	-32.9	0.1	0	0	0	0	0.9	193.2598	-9.1998
45	1.0	0.0	-0.0	-15.9	0.0	-16.6	0.0	-16.0	0.0	37.8	37.1	37.7	-34.1	0.0	-2	5	5	1	0.9	193.2598	-9.2070
46	1.7	0.1	-0.1	-12.9	0.0	-13.3	0.0	-13.1	0.0	40.8	40.4	40.6	-31.0	0.0	0	0	0	0	0.9	193.2601	-9.2198
47	-0.0	0.5	-0.6	-14.5	0.1	-15.7	0.1	-14.5	0.1	39.2	38.0	39.2	-33.1	0.1	0	0	0	0	0.9	193.2606	-9.2136
48	-1.1	0.3	-0.0	-14.3	0.1	-16.2	0.0	-14.3	0.1	39.4	37.5	39.4	-33.4	0.1	-1	0	5	0	0.9	193.2622	-9.1826
49B	2.0	2.3	-0.0	-15.0	0.1	-15.3	0.1	-15.3	0.0	38.7	38.4	38.3	-33.2	0.1	1	0	0	5	0.9	193.2624	-9.2017
50	1.9	0.1	-0.1	-13.6	0.0	-13.9	0.0	-13.8	0.0	40.1	39.8	39.8	-31.7	0.0	0	0	0	0	0.9	193.2627	-9.2115
51	1.1	3.2	-0.0	-15.2	0.2	-15.9	0.2	-15.4	0.0	38.5	37.8	38.3	-33.5	0.2	1	0	0	5	0.9	193.2638	-9.1876

TABLE 17:
Derived quantities and detection codes for X-ray point sources in HCG 62 (online only).

52	0.1	0.0	-1.2	-14.9	0.1	-16.0	0.0	-14.9	0.1	38.8	37.7	38.8	-33.4	0.1	-1	0	5	0	0.9	193.2641	-9.2338
53	1.0	0.0	-0.0	-15.9	0.0	-16.6	0.0	-16.0	0.0	37.8	37.1	37.7	-34.1	0.0	-2	5	1	5	0.9	193.2646	-9.1594
54	1.9	2.4	-0.0	-15.2	0.2	-15.6	0.2	-15.5	0.0	38.5	38.1	38.2	-33.4	0.2	1	0	0	5	0.9	193.2647	-9.1732
55B	1.9	2.4	-0.0	-15.1	0.1	-15.4	0.1	-15.4	0.0	38.6	38.2	38.3	-33.2	0.1	1	0	0	5	0.9	193.2648	-9.1903
56	2.1	0.4	-0.3	-14.5	0.1	-14.8	0.1	-14.8	0.1	39.2	38.9	38.9	-32.6	0.1	0	0	0	0	0.9	193.2653	-9.2086
57B	1.4	0.3	-0.2	-14.3	0.1	-14.8	0.1	-14.5	0.1	39.4	38.9	39.2	-32.5	0.1	0	0	0	0	0.9	193.2656	-9.2021
58	1.0	0.7	-0.7	-15.0	0.2	-15.7	0.2	-15.1	0.2	38.7	38.0	38.6	-33.3	0.2	0	0	0	0	0.9	193.2656	-9.1249
59	1.4	0.2	-0.2	-14.1	0.0	-14.6	0.0	-14.2	0.0	39.6	39.1	39.5	-32.2	0.0	0	0	0	0	0.9	193.2661	-9.1360
60	0.3	0.5	-0.5	-14.6	0.1	-15.6	0.1	-14.6	0.1	39.1	38.1	39.1	-33.0	0.1	0	0	0	0	0.9	193.2664	-9.1506
61	1.3	0.5	-0.4	-14.7	0.1	-15.3	0.1	-14.9	0.1	39.0	38.4	38.8	-32.9	0.1	0	0	0	0	0.9	193.2667	-9.1270
62	2.2	2.1	-0.0	-15.1	0.1	-15.3	0.1	-15.4	0.0	38.6	38.4	38.3	-33.2	0.1	1	0	0	5	0.9	193.2669	-9.1883
63	1.7	0.1	-0.1	-13.8	0.0	-14.2	0.0	-14.0	0.0	39.9	39.5	39.7	-31.9	0.0	0	0	0	0	0.9	193.2670	-9.3016
64	0.4	0.3	-0.3	-14.1	0.1	-15.2	0.1	-14.2	0.1	39.6	38.5	39.5	-32.6	0.1	0	0	0	0	0.9	193.2674	-9.2954
65	-0.1	0.6	-0.7	-14.6	0.1	-15.9	0.1	-14.6	0.1	39.1	37.8	39.0	-33.2	0.1	0	0	0	0	0.9	193.2675	-9.2455
66	4.2	0.1	-0.0	-13.3	0.0	-13.3	0.0	-14.7	0.0	40.4	40.4	39.0	-32.0	0.0	1	0	0	5	0.9	193.2677	-9.2276
67B*	2.6	0.3	-0.3	-14.3	0.0	-14.4	0.0	-14.8	0.0	39.4	39.3	38.9	-32.4	0.0	0	0	0	0	0.9	193.2685	-9.1998
68	-0.1	0.0	-1.0	-15.0	0.2	-16.3	0.0	-15.1	0.2	38.7	37.4	38.6	-33.7	0.2	-1	0	1	0	0.9	193.2687	-9.1855
69	1.0	0.4	-0.4	-14.6	0.1	-15.2	0.1	-14.7	0.1	39.1	38.5	39.0	-32.8	0.1	0	0	0	0	0.9	193.2690	-9.2429
70	1.0	0.0	-0.0	-15.9	0.0	-16.6	0.0	-16.0	0.0	37.8	37.1	37.7	-34.1	0.0	-2	1	1	5	0.9	193.2691	-9.2100
71	0.9	3.3	-0.0	-15.5	0.3	-16.2	0.3	-15.6	0.0	38.2	37.5	38.1	-33.8	0.3	1	0	0	1	0.9	193.2693	-9.1459
72A	-0.2	0.6	-0.6	-14.5	0.1	-15.8	0.1	-14.5	0.1	39.2	37.8	39.2	-33.2	0.1	0	0	0	0	0.9	193.2705	-9.2039
73	1.0	0.4	-0.4	-14.6	0.1	-15.3	0.1	-14.7	0.1	39.1	38.4	39.0	-32.9	0.1	0	0	0	0	0.9	193.2709	-9.2784
74	1.6	0.1	-0.1	-13.8	0.0	-14.2	0.0	-14.0	0.0	39.9	39.4	39.7	-32.0	0.0	0	0	0	0	0.9	193.2710	-9.2274
75B	1.0	0.6	-0.5	-14.8	0.1	-15.5	0.1	-14.9	0.1	38.8	38.1	38.7	-33.1	0.1	0	0	0	0	0.9	193.2711	-9.1925
76	0.1	0.0	-1.2	-15.0	0.2	-16.1	0.0	-15.0	0.2	38.7	37.6	38.7	-33.5	0.2	-1	0	5	0	0.9	193.2712	-9.1849
77	-0.7	0.0	-0.5	-14.8	0.2	-16.4	0.0	-14.8	0.2	38.9	37.3	38.9	-33.7	0.2	-1	0	1	0	0.9	193.2713	-9.2382
78A	1.1	0.2	-0.1	-13.9	0.0	-14.5	0.0	-14.0	0.0	39.8	39.2	39.7	-32.1	0.0	0	0	0	0	0.9	193.2719	-9.2124
79	1.9	0.1	-0.2	-13.8	0.0	-14.1	0.0	-14.1	0.0	39.9	39.6	39.6	-31.9	0.0	0	0	0	0	0.9	193.2723	-9.1399
80A	2.1	0.3	-0.3	-14.4	0.1	-14.6	0.1	-14.7	0.1	39.3	39.1	39.0	-32.5	0.1	0	0	0	0	0.9	193.2728	-9.2043
81A	1.9	2.4	-0.0	-15.2	0.2	-15.5	0.2	-15.5	0.0	38.5	38.2	38.2	-33.3	0.2	1	0	0	5	0.9	193.2732	-9.2172
82A	2.5	0.3	-0.3	-14.3	0.0	-14.4	0.0	-14.8	0.0	39.4	39.3	38.9	-32.4	0.0	0	0	0	0	0.9	193.2735	-9.2050
83A*	2.5	0.3	-0.3	-14.2	0.0	-14.4	0.0	-14.7	0.0	39.5	39.3	39.0	-32.3	0.0	0	0	0	0	0.9	193.2736	-9.2040
84	1.5	2.8	-0.0	-15.1	0.2	-15.6	0.2	-15.3	0.0	38.5	38.1	38.4	-33.3	0.2	1	0	0	5	0.9	193.2740	-9.1850
85A	3.5	0.8	-0.0	-14.5	0.1	-14.5	0.1	-15.5	0.0	39.2	39.1	38.2	-32.9	0.1	1	0	0	1	0.9	193.2744	-9.2036
86	1.1	3.1	-0.0	-15.4	0.2	-16.0	0.2	-15.5	0.0	38.3	37.7	38.2	-33.6	0.2	1	0	0	1	0.9	193.2748	-9.1468
87	1.3	3.0	-0.0	-15.4	0.2	-16.0	0.2	-15.5	0.0	38.3	37.7	38.2	-33.6	0.2	1	0	0	1	0.9	193.2749	-9.1750
88	1.2	0.1	-0.1	-13.6	0.0	-14.2	0.0	-13.7	0.0	40.1	39.5	40.0	-31.8	0.0	0	0	0	0	0.9	193.2751	-9.2211
89	0.9	0.1	-0.1	-13.6	0.0	-14.3	0.0	-13.7	0.0	40.1	39.3	40.0	-31.9	0.0	0	0	0	0	0.9	193.2754	-9.2287
90	2.2	2.1	-0.0	-15.0	0.1	-15.2	0.1	-15.3	0.0	38.7	38.5	38.3	-33.1	0.1	1	0	0	5	0.9	193.2754	-9.1816
91	-0.6	0.0	-0.6	-14.9	0.2	-16.5	0.0	-15.0	0.2	38.8	37.2	38.7	-33.8	0.2	-1	0	1	0	0.9	193.2776	-9.2240
92	0.9	0.7	-0.7	-15.0	0.2	-15.8	0.2	-15.1	0.2	38.7	37.9	38.6	-33.3	0.2	0	0	0	0	0.9	193.2780	-9.1683
93	1.0	0.3	-0.3	-14.4	0.1	-15.1	0.1	-14.5	0.1	39.3	38.6	39.2	-32.6	0.1	0	0	0	0	0.9	193.2784	-9.1980
94A	1.3	3.0	-0.0	-15.3	0.2	-15.8	0.2	-15.4	0.0	38.4	37.9	38.3	-33.5	0.2	1	0	0	5	0.9	193.2786	-9.2033
95D	-0.5	0.5	-0.6	-14.3	0.1	-15.8	0.1	-14.3	0.1	39.4	37.9	39.4	-33.0	0.1	0	0	0	0	0.9	193.2787	-9.2571
96	1.4	0.3	-0.3	-14.5	0.1	-15.0	0.1	-14.7	0.1	39.2	38.7	39.0	-32.7	0.1	0	0	0	0	0.9	193.2790	-9.2007
97	0.6	0.0	-0.0	-15.4	0.3	-16.3	0.0	-15.4	0.0	38.3	37.4	38.3	-33.8	0.3	-2	0	5	5	0.9	193.2808	-9.1558
98A	1.7	2.6	-0.0	-15.1	0.2	-15.5	0.2	-15.3	0.0	38.6	38.2	38.3	-33.3	0.2	1	0	0	5	0.9	193.2810	-9.2063
99	1.0	0.0	-0.0	-15.6	0.0	-16.3	0.0	-15.7	0.0	38.1	37.4	38.0	-33.8	0.0	-2	5	1	0	0.9	193.2822	-9.2247
100A	1.3	0.6	-0.5	-14.8	0.1	-15.4	0.1	-15.0	0.1	38.9	38.3	38.7	-33.0	0.1	0	0	0	0	0.9	193.2824	-9.2137
101	1.5	2.8	-0.0	-15.5	0.2	-15.9	0.2	-15.6	0.0	38.2	37.8	38.1	-33.6	0.2	1	0	0	1	0.9	193.2826	-9.1782
102	-0.7	0.0	-0.4	-14.5	0.1	-16.1	0.0	-14.5	0.1	39.2	37.6	39.2	-33.4	0.1	-1	0	5	0	0.9	193.2828	-9.2460
103A	1.3	3.0	-0.0	-15.6	0.3	-16.1	0.3	-15.7	0.0	38.1	37.6	38.0	-33.8	0.3	1	0	0	1	0.9	193.2834	-9.2053
104	1.0	0.0	-0.0	-15.9	0.0	-16.6	0.0	-16.0	0.0	37.8	37.1	37.7	-34.2	0.0	-2	5	0	1	0.9	193.2844	-9.1429
105C	-0.3	0.0	-0.8	-14.7	0.2	-16.1	0.0	-14.7	0.2	39.0	37.6	39.0	-33.4	0.2	-1	0	5	0	0.9	193.2861	-9.1944
106C	1.9	2.5	-0.0	-15.3	0.1	-15.7	0.1	-15.6	0.0	38.4	38.0	38.1	-33.4	0.1	1	0	0	1	0.9	193.2869	-9.1941
107C	1.2	0.6	-0.5	-14.9	0.1	-15.5	0.1	-15.0	0.1	38.8	38.2	38.7	-33.1	0.1	0	0	0	0	0.9	193.2878	-9.2007
108	1.3	0.5	-0.4	-14.7	0.1	-15.2	0.1	-14.8	0.1	39.0	38.5	38.9	-32.9	0.1	0	0	0	0	0.9	193.2883	-9.2828

TABLE 17:
Derived quantities and detection codes for X-ray point sources in HCG 62 (online only).

109C	1.4	0.6	-0.5	-14.9	0.1	-15.4	0.1	-15.0	0.1	38.8	38.3	38.7	-33.0	0.1	0	0	0	0	0.9	193.2893	-9.2003
110	0.6	0.0	-0.0	-15.4	0.3	-16.3	0.0	-15.5	0.0	38.3	37.4	38.2	-33.8	0.3	-2	0	5	5	0.9	193.2896	-9.1673
111	1.4	3.0	-0.0	-15.2	0.1	-15.7	0.1	-15.3	0.0	38.5	38.0	38.4	-33.4	0.1	1	0	0	5	0.9	193.2897	-9.1691
112C	1.7	0.5	-0.5	-14.7	0.1	-15.1	0.1	-15.0	0.1	38.9	38.6	38.7	-32.9	0.1	0	0	0	0	0.9	193.2898	-9.1942
113	-0.1	0.0	-1.0	-14.8	0.1	-16.1	0.0	-14.8	0.1	38.9	37.6	38.9	-33.5	0.1	-1	0	5	0	0.9	193.2903	-9.1463
114C	2.8	0.7	-0.5	-14.6	0.1	-14.8	0.1	-15.2	0.1	39.1	38.9	38.5	-32.8	0.1	0	0	0	0	0.9	193.2908	-9.1987
115C*	1.7	0.4	-0.4	-14.7	0.1	-15.1	0.1	-14.9	0.1	39.0	38.6	38.8	-32.8	0.1	0	0	0	0	0.9	193.2909	-9.1978
116C	1.1	0.4	-0.4	-14.6	0.1	-15.3	0.1	-14.7	0.1	39.1	38.4	39.0	-32.9	0.1	0	0	0	0	0.9	193.2912	-9.1995
117	1.0	0.2	-0.2	-13.9	0.0	-14.6	0.0	-14.0	0.0	39.8	39.1	39.7	-32.2	0.0	0	0	0	0	0.9	193.2916	-9.3135
118	0.6	0.0	-0.0	-15.4	0.3	-16.3	0.0	-15.5	0.0	38.3	37.4	38.2	-33.8	0.3	-2	0	5	5	0.9	193.2918	-9.1679
119	1.0	0.0	-0.0	-15.9	0.0	-16.6	0.0	-16.0	0.0	37.8	37.1	37.7	-34.2	0.0	-2	5	5	1	0.9	193.2927	-9.1512
120	2.2	0.5	-0.5	-14.7	0.1	-14.9	0.1	-15.1	0.1	39.0	38.8	38.6	-32.8	0.1	0	0	0	0	0.9	193.2929	-9.2290
121	1.7	0.1	-0.1	-13.9	0.0	-14.3	0.0	-14.1	0.0	39.8	39.4	39.6	-32.0	0.0	0	0	0	0	0.9	193.2935	-9.1731
122	-0.7	0.4	-0.4	-14.0	0.1	-15.6	0.1	-14.0	0.1	39.7	38.1	39.7	-32.9	0.1	0	0	0	0	0.7	193.2935	-9.2447
123	-1.0	0.0	-0.1	-14.5	0.2	-16.3	0.0	-14.5	0.2	39.2	37.4	39.2	-33.5	0.2	-1	0	1	0	0.9	193.2937	-9.1762
124	1.3	0.3	-0.3	-14.3	0.1	-14.9	0.1	-14.5	0.1	39.3	38.8	39.2	-32.5	0.1	0	0	0	0	0.8	193.2938	-9.2456
125C	-0.7	0.0	-0.4	-14.6	0.2	-16.2	0.0	-14.6	0.2	39.1	37.5	39.1	-33.4	0.2	-1	0	5	0	0.9	193.2942	-9.2059
126	1.7	0.4	-0.4	-14.6	0.1	-15.0	0.1	-14.8	0.1	39.1	38.7	38.9	-32.7	0.1	0	0	0	0	0.9	193.2944	-9.2844
127	-1.1	0.0	-0.0	-13.6	0.0	-15.5	0.0	-13.6	0.0	40.1	38.2	40.1	-32.7	0.0	-1	0	5	0	0.9	193.2964	-9.1881
128	1.2	3.1	-0.0	-15.5	0.3	-16.2	0.3	-15.7	0.0	38.1	37.5	38.0	-33.8	0.3	1	0	0	1	0.9	193.2965	-9.1646
129	1.6	0.1	-0.1	-13.9	0.0	-14.3	0.0	-14.1	0.0	39.8	39.4	39.6	-32.0	0.0	0	0	0	0	0.9	193.2995	-9.2272
130	1.3	0.1	-0.1	-13.7	0.0	-14.3	0.0	-13.9	0.0	40.0	39.4	39.8	-31.9	0.0	0	0	0	0	0.9	193.2996	-9.2849
131	0.5	0.5	-0.5	-14.6	0.1	-15.6	0.1	-14.6	0.1	39.1	38.1	39.1	-33.0	0.1	0	0	0	0	0.9	193.3009	-9.1839
132	0.8	0.6	-0.6	-14.8	0.1	-15.6	0.1	-14.9	0.1	38.9	38.1	38.8	-33.1	0.1	0	0	0	0	0.9	193.3038	-9.1894
133	1.2	3.1	-0.0	-15.6	0.3	-16.2	0.3	-15.7	0.0	38.1	37.5	38.0	-33.8	0.3	1	0	0	1	0.9	193.3069	-9.2021
134	1.6	0.6	-0.5	-14.8	0.1	-15.2	0.1	-15.0	0.1	38.9	38.5	38.7	-33.0	0.1	0	0	0	0	0.9	193.3072	-9.2218
135	1.1	3.2	-0.0	-15.3	0.2	-16.0	0.2	-15.4	0.0	38.4	37.7	38.2	-33.6	0.2	1	0	0	5	0.9	193.3074	-9.1753
136	1.0	3.2	-0.0	-15.1	0.1	-15.8	0.1	-15.2	0.0	38.6	37.9	38.5	-33.4	0.1	1	0	0	5	0.9	193.3095	-9.1526
137	-0.2	0.6	-0.7	-14.5	0.1	-15.9	0.1	-14.6	0.1	39.1	37.8	39.1	-33.2	0.1	0	0	0	0	0.9	193.3101	-9.2078
138	0.6	0.0	-0.0	-15.2	0.2	-16.1	0.0	-15.3	0.0	38.5	37.6	38.4	-33.6	0.2	-2	0	5	5	0.9	193.3102	-9.2046
139	0.8	0.6	-0.6	-14.8	0.1	-15.6	0.1	-14.9	0.1	38.9	38.0	38.8	-33.2	0.1	0	0	0	0	0.9	193.3104	-9.2136
140	1.8	0.2	-0.2	-14.3	0.0	-14.6	0.0	-14.5	0.0	39.4	39.1	39.2	-32.4	0.0	0	0	0	0	0.9	193.3106	-9.2716
141	1.8	0.3	-0.3	-14.3	0.1	-14.7	0.1	-14.5	0.1	39.4	39.0	39.1	-32.4	0.1	0	0	0	0	0.9	193.3110	-9.1803
142	-0.1	0.1	-0.1	-13.3	0.0	-14.6	0.0	-13.3	0.0	40.4	39.1	40.4	-31.9	0.0	0	0	0	0	0.9	193.3118	-9.2168
143	1.8	0.4	-0.3	-14.5	0.1	-14.9	0.1	-14.8	0.1	39.2	38.8	38.9	-32.7	0.1	0	0	0	0	0.9	193.3122	-9.2313
144	1.0	0.0	-0.0	-15.9	0.0	-16.6	0.0	-16.0	0.0	37.8	37.1	37.7	-34.1	0.0	-2	5	1	5	0.9	193.3125	-9.2006
145	-0.3	0.2	-0.1	-13.4	0.0	-14.8	0.0	-13.4	0.0	40.3	38.9	40.3	-32.1	0.0	0	0	0	0	0.9	193.3135	-9.2399
146	1.3	0.5	-0.4	-14.7	0.1	-15.2	0.1	-14.8	0.1	39.0	38.5	38.9	-32.9	0.1	0	0	0	0	0.9	193.3151	-9.2702
147	-0.4	0.0	-0.7	-14.8	0.1	-16.2	0.0	-14.8	0.1	38.9	37.5	38.9	-33.5	0.1	-1	0	5	0	0.9	193.3204	-9.2447
148	1.2	0.6	-0.5	-14.9	0.1	-15.5	0.1	-15.0	0.1	38.8	38.2	38.7	-33.1	0.1	0	0	0	0	0.9	193.3209	-9.2113
149	1.8	2.5	-0.0	-15.3	0.1	-15.7	0.1	-15.5	0.0	38.4	38.0	38.2	-33.4	0.1	1	0	0	5	0.9	193.3211	-9.1814
150	-0.2	0.0	-0.9	-14.9	0.2	-16.2	0.0	-14.9	0.2	38.8	37.5	38.8	-33.6	0.2	-1	0	5	0	0.9	193.3221	-9.2025
151	1.9	0.2	-0.2	-14.0	0.0	-14.3	0.0	-14.3	0.0	39.7	39.3	39.4	-32.1	0.0	0	0	0	0	0.9	193.3230	-9.2062
152	1.0	0.0	-0.0	-15.9	0.0	-16.6	0.0	-16.0	0.0	37.8	37.1	37.7	-34.1	0.0	-2	5	5	5	0.9	193.3263	-9.2027
153	-0.7	0.0	-0.4	-14.6	0.2	-16.2	0.0	-14.6	0.2	39.1	37.5	39.1	-33.5	0.2	-1	0	5	0	0.9	193.3298	-9.1877
154	1.0	0.0	-0.0	-15.6	0.0	-16.2	0.0	-15.6	0.0	38.1	37.4	38.0	-33.8	0.0	-2	5	5	5	0.9	193.3305	-9.2527
155	0.8	0.6	-0.5	-14.8	0.1	-15.5	0.1	-14.8	0.1	38.9	38.2	38.8	-33.1	0.1	0	0	0	0	0.9	193.3307	-9.2209
156	1.7	0.6	-0.5	-14.9	0.1	-15.3	0.1	-15.1	0.1	38.8	38.4	38.6	-33.0	0.1	0	0	0	0	0.9	193.3308	-9.2265
157	1.0	0.0	-0.0	-15.9	0.0	-16.6	0.0	-16.0	0.0	37.8	37.1	37.7	-34.2	0.0	-2	5	5	5	0.9	193.3313	-9.1755
158	1.0	0.0	-0.0	-15.9	0.0	-16.6	0.0	-16.0	0.0	37.8	37.1	37.7	-34.2	0.0	-2	5	5	1	0.9	193.3343	-9.1742
159	-0.7	0.0	-0.5	-14.6	0.2	-16.2	0.0	-14.6	0.2	39.1	37.5	39.1	-33.5	0.2	-1	0	5	0	0.9	193.3383	-9.2019
160	-0.7	0.0	-0.4	-14.5	0.1	-16.1	0.0	-14.5	0.1	39.2	37.6	39.2	-33.4	0.1	-1	0	5	0	0.9	193.3470	-9.1925
161	1.0	3.2	-0.0	-15.3	0.2	-16.0	0.2	-15.4	0.0	38.4	37.7	38.3	-33.6	0.2	1	0	0	1	0.9	193.3490	-9.1625
162	0.5	0.0	-0.0	-15.1	0.2	-16.0	0.0	-15.1	0.0	38.6	37.7	38.6	-33.5	0.2	-2	0	5	5	0.9	193.3508	-9.1859
163	2.1	2.1	-0.0	-15.1	0.1	-15.4	0.1	-15.4	0.0	38.6	38.3	38.3	-33.2	0.1	1	0	0	5	0.9	193.3508	-9.1727
164	1.5	0.5	-0.5	-14.8	0.1	-15.3	0.1	-15.0	0.1	38.9	38.4	38.7	-33.0	0.1	0	0	0	0	0.9	193.3518	-9.1797
165	2.1	1.7	-0.0	-15.0	0.1	-15.3	0.1	-15.4	0.0	38.7	38.4	38.3	-33.2	0.1	1	0	0	5	0.9	193.3642	-9.1783

TABLE 17:
Derived quantities and detection codes for X-ray point sources in HCG 62 (online only).

TABLE 18:
Derived quantities and detection codes for X-ray point sources in HCG 90 (online only).

ID (1)	Γ (2)	L_X										lim									
		$+$ (3)	$-$ (4)	f_F (5)	\pm (6)	f_S (7)	\pm (8)	f_H (9)	\pm (10)	F (11)	S (12)	H (13)	$f_{\nu,2\text{keV}}$ (14)	\pm (15)	HR	F (17)	S (18)	H (19)	EEF (20)	RA (21)	DEC (22)
1	2.0	0.5	-0.5	-14.1	0.1	-14.4	0.1	-14.3	0.1	39.1	38.8	38.8	-32.2	0.1	0	0	0	0	0.9	330.3675	-32.0938
2	2.1	0.4	-0.3	-13.7	0.1	-14.0	0.1	-14.0	0.1	39.4	39.1	39.1	-31.8	0.1	0	0	0	0	0.9	330.3732	-31.9535
3	-0.1	0.3	-0.3	-13.4	0.1	-14.7	0.1	-13.4	0.1	39.8	38.5	39.7	-32.0	0.1	0	0	0	0	0.9	330.3733	-31.8821
4	1.9	0.2	-0.2	-13.5	0.0	-13.8	0.0	-13.8	0.0	39.6	39.3	39.3	-31.6	0.0	0	0	0	0	0.9	330.3776	-31.9212
5	1.8	0.5	-0.5	-14.1	0.1	-14.4	0.1	-14.3	0.1	39.1	38.7	38.8	-32.2	0.1	0	0	0	0	0.9	330.3796	-32.0583
6	1.8	0.6	-0.5	-14.1	0.1	-14.5	0.1	-14.4	0.1	39.0	38.7	38.8	-32.2	0.1	0	0	0	0	0.9	330.3834	-31.8770
7	1.8	0.4	-0.4	-14.0	0.1	-14.3	0.1	-14.2	0.1	39.2	38.8	38.9	-32.1	0.1	0	0	0	0	0.9	330.3838	-31.9160
8	0.7	0.5	-0.5	-14.0	0.1	-14.8	0.1	-14.0	0.1	39.2	38.3	39.1	-32.3	0.1	0	0	0	0	0.9	330.3868	-32.0294
9	1.8	0.3	-0.3	-13.6	0.1	-14.0	0.1	-13.9	0.1	39.5	39.2	39.3	-31.7	0.1	0	0	0	0	0.9	330.3886	-31.8629
10	1.5	0.2	-0.2	-13.3	0.0	-13.7	0.0	-13.5	0.0	39.9	39.4	39.7	-31.4	0.0	0	0	0	0	0.9	330.3915	-31.9358
11	1.0	0.9	-0.9	-14.4	0.2	-15.1	0.2	-14.5	0.2	38.7	38.0	38.6	-32.7	0.2	0	0	0	0	0.9	330.3921	-31.8955
12	1.0	0.0	-0.0	-15.0	0.0	-15.7	0.0	-15.1	0.0	38.2	37.5	38.1	-33.2	0.0	-2	5	5	5	0.9	330.3926	-31.9844
13	2.1	2.6	-0.0	-14.5	0.2	-14.8	0.2	-14.9	0.0	38.6	38.3	38.3	-32.7	0.2	1	0	0	5	0.9	330.3939	-31.8878
14	1.5	3.2	-0.0	-14.7	0.2	-15.2	0.2	-14.9	0.0	38.4	38.0	38.3	-32.9	0.2	1	0	0	5	0.9	330.3957	-31.9440
15	0.2	0.3	-0.3	-13.3	0.1	-14.4	0.1	-13.3	0.1	39.8	38.7	39.8	-31.8	0.1	0	0	0	0	0.9	330.4006	-31.8901
16	1.6	3.0	-0.0	-14.5	0.2	-14.9	0.2	-14.7	0.0	38.6	38.2	38.4	-32.7	0.2	1	0	0	5	0.9	330.4013	-32.0404
17	0.9	0.0	-0.0	-14.8	0.3	-15.5	0.0	-14.8	0.0	38.4	37.6	38.3	-33.1	0.3	-2	0	5	5	0.9	330.4052	-31.9324
18	1.8	0.2	-0.2	-13.5	0.0	-13.9	0.0	-13.8	0.0	39.6	39.2	39.4	-31.7	0.0	0	0	0	0	0.9	330.4088	-31.8615
19	1.7	0.4	-0.4	-13.9	0.1	-14.3	0.1	-14.1	0.1	39.3	38.9	39.1	-32.0	0.1	0	0	0	0	0.9	330.4117	-32.0952
20	0.9	0.0	-0.0	-14.6	0.2	-15.4	0.0	-14.7	0.0	38.5	37.8	38.5	-32.9	0.2	-2	0	5	5	0.9	330.4179	-31.9324
21	1.8	0.6	-0.5	-14.2	0.1	-14.6	0.1	-14.4	0.1	38.9	38.6	38.7	-32.3	0.1	0	0	0	0	0.9	330.4225	-31.9327
22	2.0	0.2	-0.2	-13.2	0.0	-13.5	0.0	-13.5	0.0	39.9	39.6	39.6	-31.3	0.0	0	0	0	0	0.9	330.4250	-31.9140
23	2.8	1.9	-0.0	-14.3	0.1	-14.4	0.1	-14.9	0.0	38.9	38.7	38.2	-32.5	0.1	1	0	0	5	0.9	330.4253	-32.0653
24	1.4	0.5	-0.5	-14.1	0.1	-14.6	0.1	-14.3	0.1	39.0	38.5	38.9	-32.3	0.1	0	0	0	0	0.9	330.4256	-32.0117
25	3.2	1.4	-0.0	-14.1	0.1	-14.1	0.1	-14.9	0.0	39.1	39.0	38.2	-32.4	0.1	1	0	0	5	0.9	330.4448	-32.1073
26	1.6	3.0	-0.0	-14.5	0.2	-15.0	0.2	-14.7	0.0	38.6	38.2	38.4	-32.7	0.2	1	0	0	5	0.9	330.4474	-31.9261
27	1.4	2.4	-0.0	-14.9	0.3	-15.4	0.3	-15.1	0.0	38.3	37.8	38.1	-33.1	0.3	1	0	0	1	0.9	330.4504	-31.8733
28	1.0	0.0	-0.0	-15.0	0.0	-15.7	0.0	-15.1	0.0	38.1	37.4	38.0	-33.3	0.0	-2	5	1	5	0.9	330.4505	-31.9273
29	1.8	2.9	-0.0	-14.5	0.2	-14.9	0.2	-14.8	0.0	38.6	38.2	38.4	-32.7	0.2	1	0	0	5	0.9	330.4508	-31.9533
30	1.0	0.0	-0.0	-15.0	0.0	-15.7	0.0	-15.1	0.0	38.1	37.4	38.0	-33.3	0.0	-2	5	5	1	0.9	330.4536	-31.9582
31	0.9	0.0	-0.0	-14.6	0.2	-15.3	0.0	-14.7	0.0	38.6	37.8	38.5	-32.9	0.2	-2	0	5	5	0.9	330.4537	-32.0297
32	1.0	0.0	-0.0	-15.0	0.0	-15.7	0.0	-15.1	0.0	38.1	37.4	38.0	-33.3	0.0	-2	5	1	5	0.9	330.4539	-31.9128
33	2.4	0.6	-0.6	-14.1	0.1	-14.3	0.1	-14.5	0.1	39.0	38.8	38.6	-32.2	0.1	0	0	0	0	0.9	330.4576	-31.9169
34	1.0	0.0	-0.0	-15.0	0.0	-15.7	0.0	-15.1	0.0	38.2	37.5	38.1	-33.2	0.0	-2	5	5	1	0.9	330.4619	-31.9438
35	1.0	0.0	-0.0	-15.0	0.0	-15.7	0.0	-15.1	0.0	38.2	37.5	38.1	-33.2	0.0	-2	5	5	1	0.9	330.4619	-31.9416
36	1.0	0.0	-0.0	-14.9	0.0	-15.6	0.0	-15.0	0.0	38.2	37.5	38.1	-33.2	0.0	-2	5	1	5	0.9	330.4628	-31.9806
37	0.9	0.0	-0.0	-14.6	0.2	-15.4	0.0	-14.7	0.0	38.5	37.8	38.5	-32.9	0.2	-2	0	5	5	0.9	330.4637	-32.0026
38	1.0	0.0	-0.0	-15.1	0.0	-15.8	0.0	-15.1	0.0	38.1	37.4	38.0	-33.3	0.0	-2	5	1	0	0.9	330.4637	-32.0352
39	1.0	0.0	-0.0	-15.0	0.0	-15.7	0.0	-15.1	0.0	38.1	37.4	38.0	-33.3	0.0	-2	5	5	1	0.9	330.4649	-31.9719
40	-0.2	0.0	-0.9	-14.1	0.2	-15.5	0.0	-14.2	0.2	39.0	37.7	39.0	-32.8	0.2	-1	0	5	0	0.9	330.4653	-31.8981
41	0.9	0.0	-0.0	-14.7	0.2	-15.5	0.0	-14.8	0.0	38.4	37.7	38.4	-33.0	0.2	-2	0	5	5	0.9	330.4653	-32.0225
42	0.8	0.0	-0.0	-14.7	0.2	-15.5	0.0	-14.8	0.0	38.4	37.7	38.4	-33.0	0.2	-2	0	5	5	0.9	330.4654	-31.9936
43	-0.3	0.0	-0.8	-14.1	0.2	-15.5	0.0	-14.2	0.2	39.0	37.6	39.0	-32.9	0.2	-1	0	1	0	0.9	330.4658	-31.9904
44	1.0	0.0	-0.0	-15.0	0.0	-15.7	0.0	-15.1	0.0	38.1	37.4	38.0	-33.3	0.0	-2	5	5	5	0.9	330.4662	-32.0648
45	1.0	0.0	-0.0	-15.1	0.0	-15.8	0.0	-15.2	0.0	38.1	37.4	38.0	-33.3	0.0	-2	5	5	1	0.9	330.4665	-31.9187
46	1.2	3.4	-0.0	-14.7	0.2	-15.3	0.2	-14.8	0.0	38.5	37.9	38.3	-32.9	0.2	1	0	0	5	0.9	330.4683	-31.9889
47	0.8	0.0	-0.0	-14.5	0.2	-15.3	0.0	-14.6	0.0	38.6	37.8	38.5	-32.8	0.2	-2	0	5	5	0.9	330.4695	-31.9983
48	1.6	3.0	-0.0	-14.6	0.2	-15.1	0.2	-14.8	0.0	38.5	38.1	38.3	-32.8	0.2	1	0	0	5	0.9	330.4710	-31.9540
49	1.0	0.0	-0.0	-15.0	0.0	-15.7	0.0	-15.1	0.0	38.1	37.4	38.0	-33.3	0.0	-2	5	5	5	0.9	330.4719	-31.9369
50	1.8	0.5	-0.5	-14.1	0.1	-14.5	0.1	-14.3	0.1	39.0	38.7	38.8	-32.2	0.1	0	0	0	0	0.9	330.4724	-31.9037
51	1.0	0.0	-0.0	-14.9	0.0	-15.6	0.0	-15.0	0.0	38.2	37.5	38.1	-33.2	0.0	-2	5	5	5	0.9	330.4745	-31.9292

TABLE 18:
Derived quantities and detection codes for X-ray point sources in HCG 90 (online only).

52	0.5	0.0	-1.6	-14.5	0.2	-15.5	0.0	-14.6	0.2	38.6	37.7	38.6	-32.9	0.2	-1	0	5	0	0.9	330.4789	-31.9930
53	1.0	0.0	-0.0	-15.1	0.0	-15.8	0.0	-15.2	0.0	38.1	37.4	38.0	-33.3	0.0	-2	5	1	5	0.9	330.4793	-31.9243
54	0.8	0.0	-0.0	-14.6	0.2	-15.4	0.0	-14.7	0.0	38.5	37.8	38.5	-32.9	0.2	-2	0	5	5	0.9	330.4807	-31.9146
55	1.0	0.0	-0.0	-15.0	0.0	-15.7	0.0	-15.1	0.0	38.1	37.5	38.1	-33.2	0.0	-2	5	5	1	0.9	330.4820	-31.9759
56	1.0	0.0	-0.0	-15.0	0.0	-15.7	0.0	-15.1	0.0	38.1	37.4	38.0	-33.3	0.0	-2	5	5	1	0.9	330.4833	-31.8875
57	0.9	0.0	-0.0	-14.7	0.2	-15.5	0.0	-14.8	0.0	38.4	37.7	38.4	-33.0	0.2	-2	0	5	5	0.9	330.4836	-31.9883
58	1.2	0.8	-0.7	-14.4	0.2	-15.0	0.2	-14.5	0.2	38.8	38.2	38.6	-32.6	0.2	0	0	0	0	0.9	330.4842	-31.9441
59	0.8	0.0	-0.0	-14.7	0.2	-15.5	0.0	-14.8	0.0	38.4	37.7	38.4	-33.0	0.2	-2	0	5	5	0.9	330.4844	-32.0054
60	1.0	0.0	-0.0	-15.0	0.0	-15.7	0.0	-15.1	0.0	38.2	37.5	38.1	-33.2	0.0	-2	5	1	5	0.9	330.4853	-31.9952
61	1.0	0.0	-0.0	-15.0	0.0	-15.7	0.0	-15.1	0.0	38.2	37.5	38.1	-33.2	0.0	-2	5	1	5	0.9	330.4870	-31.9978
62	1.3	0.5	-0.4	-14.0	0.1	-14.6	0.1	-14.2	0.1	39.1	38.6	39.0	-32.2	0.1	0	0	0	0	0.9	330.4876	-32.0729
63	0.9	0.0	-0.0	-14.7	0.2	-15.5	0.0	-14.8	0.0	38.4	37.7	38.4	-33.0	0.2	-2	0	5	5	0.9	330.4881	-31.9911
64	0.2	0.0	-1.3	-14.5	0.2	-15.6	0.0	-14.5	0.2	38.6	37.5	38.6	-33.0	0.2	-1	0	1	0	0.9	330.4897	-32.0424
65	1.0	0.0	-0.0	-15.1	0.0	-15.8	0.0	-15.2	0.0	38.1	37.4	38.0	-33.3	0.0	-2	5	5	1	0.9	330.4909	-32.0337
66	0.3	0.0	-1.4	-14.6	0.2	-15.6	0.0	-14.6	0.2	38.6	37.5	38.5	-33.0	0.2	-1	0	1	0	0.9	330.4910	-31.9455
67	1.7	0.3	-0.3	-13.7	0.1	-14.1	0.1	-13.9	0.1	39.4	39.0	39.2	-31.9	0.1	0	0	0	0	0.9	330.4912	-31.9030
68	1.3	0.4	-0.4	-13.9	0.1	-14.5	0.1	-14.1	0.1	39.2	38.7	39.1	-32.1	0.1	0	0	0	0	0.9	330.4940	-31.8930
69	1.0	0.0	-0.0	-15.1	0.0	-15.8	0.0	-15.2	0.0	38.1	37.4	38.0	-33.3	0.0	-2	5	5	1	0.9	330.4940	-31.9895
70	0.8	0.0	-0.0	-14.7	0.2	-15.5	0.0	-14.8	0.0	38.4	37.7	38.4	-33.0	0.2	-2	0	5	5	0.9	330.4950	-31.9523
71	2.0	2.6	-0.0	-14.5	0.2	-14.8	0.2	-14.8	0.0	38.6	38.3	38.3	-32.7	0.2	1	0	0	5	0.9	330.4963	-31.9286
72	1.0	0.0	-0.0	-15.0	0.0	-15.7	0.0	-15.1	0.0	38.2	37.5	38.1	-33.2	0.0	-2	1	5	1	0.9	330.4966	-31.8446
73	1.2	3.4	-0.0	-14.6	0.2	-15.2	0.2	-14.7	0.0	38.5	37.9	38.4	-32.8	0.2	1	0	0	5	0.9	330.4970	-31.9101
74	1.2	3.4	-0.0	-14.7	0.2	-15.3	0.2	-14.8	0.0	38.5	37.8	38.3	-32.9	0.2	1	0	0	5	0.9	330.4986	-31.9783
75	1.3	3.3	-0.0	-14.8	0.2	-15.4	0.2	-15.0	0.0	38.3	37.8	38.2	-33.0	0.2	1	0	0	1	0.9	330.4987	-32.0196
76	1.0	0.0	-0.0	-15.0	0.0	-15.7	0.0	-15.1	0.0	38.2	37.5	38.1	-33.2	0.0	-2	5	5	5	0.9	330.5005	-31.9583
77	1.3	3.3	-0.0	-14.8	0.2	-15.4	0.2	-15.0	0.0	38.3	37.8	38.2	-33.0	0.2	1	0	0	1	0.9	330.5015	-32.0107
78	0.6	0.0	-1.7	-14.4	0.2	-15.3	0.0	-14.4	0.2	38.8	37.8	38.7	-32.8	0.2	-1	0	5	0	0.9	330.5024	-31.9841
79	1.0	0.0	-0.0	-15.1	0.0	-15.8	0.0	-15.2	0.0	38.1	37.4	38.0	-33.3	0.0	-2	5	5	1	0.9	330.5042	-31.9979
80	1.0	0.0	-0.0	-15.1	0.0	-15.8	0.0	-15.2	0.0	38.1	37.4	38.0	-33.3	0.0	-2	5	5	1	0.9	330.5054	-31.9711
81	1.8	2.9	-0.0	-14.6	0.2	-14.9	0.2	-14.8	0.0	38.6	38.2	38.3	-32.7	0.2	1	0	0	5	0.9	330.5052	-32.0901
82	1.0	0.0	-0.0	-14.9	0.0	-15.6	0.0	-15.0	0.0	38.2	37.5	38.1	-33.2	0.0	-2	5	5	1	0.9	330.5059	-31.9762
83	1.7	0.6	-0.5	-14.2	0.1	-14.6	0.1	-14.4	0.1	39.0	38.6	38.8	-32.3	0.1	0	0	0	0	0.9	330.5061	-31.9984
84	1.0	0.0	-0.0	-14.8	0.0	-15.5	0.0	-14.9	0.0	38.3	37.6	38.2	-33.1	0.0	-2	5	5	1	0.9	330.5063	-31.9515
85C	0.8	0.8	-0.8	-14.4	0.2	-15.2	0.2	-14.5	0.2	38.7	38.0	38.7	-32.7	0.2	0	0	0	0	0.9	330.5073	-31.9708
86	-0.9	0.0	-0.2	-13.7	0.1	-15.5	0.0	-13.7	0.1	39.4	37.7	39.4	-32.7	0.1	-1	0	5	0	0.9	330.5074	-31.8452
87	0.9	0.5	-0.5	-14.0	0.1	-14.8	0.1	-14.1	0.1	39.1	38.4	39.1	-32.3	0.1	0	0	0	0	0.9	330.5075	-31.9451
88A*	-1.1	0.0	-0.0	-10.5	0.0	-12.4	0.0	-10.5	0.0	42.6	40.7	42.6	-29.6	0.0	0	0	0	0	0.9	330.5079	-31.8696
89	1.0	0.0	-0.0	-inf	0.0	-inf	0.0	-inf	0.0	-inf	-inf	-inf	-inf	0.0	-2	5	5	5	0.9	330.5080	-31.8778
90	-0.3	0.0	-0.8	-14.1	0.2	-15.5	0.0	-14.1	0.2	39.0	37.6	39.0	-32.8	0.2	-1	0	1	0	0.9	330.5082	-31.8874
91C	1.5	3.1	-0.0	-14.8	0.2	-15.2	0.2	-14.9	0.0	38.4	37.9	38.2	-32.9	0.2	1	0	0	1	0.9	330.5084	-31.9706
92	-0.5	0.0	-0.7	-14.0	0.2	-15.5	0.0	-14.0	0.2	39.1	37.7	39.1	-32.8	0.2	-1	0	5	0	0.9	330.5084	-31.8987
93	1.0	0.0	-0.0	-15.1	0.0	-15.8	0.0	-15.2	0.0	38.1	37.4	38.0	-33.3	0.0	-2	5	1	5	0.9	330.5086	-31.9094
94	-0.2	0.0	-0.8	-14.1	0.2	-15.5	0.0	-14.1	0.2	39.0	37.7	39.0	-32.8	0.2	-1	0	5	0	0.9	330.5086	-31.9042
95	1.0	0.0	-0.0	-15.1	0.0	-15.8	0.0	-15.2	0.0	38.1	37.4	38.0	-33.3	0.0	-2	5	1	5	0.9	330.5090	-31.9413
96	1.0	0.0	-0.0	-15.1	0.0	-15.8	0.0	-15.2	0.0	38.1	37.4	38.0	-33.3	0.0	-2	5	1	5	0.9	330.5092	-31.9214
97	0.6	0.0	-1.7	-14.6	0.2	-15.5	0.0	-14.6	0.2	38.6	37.6	38.5	-33.0	0.2	-1	0	5	0	0.9	330.5092	-31.9298
98	1.0	0.0	-0.0	-15.1	0.0	-15.8	0.0	-15.2	0.0	38.1	37.4	38.0	-33.3	0.0	-2	5	1	5	0.9	330.5095	-31.9493
99	1.0	0.0	-0.0	-15.1	0.0	-15.8	0.0	-15.2	0.0	38.1	37.4	38.0	-33.3	0.0	-2	5	1	5	0.9	330.5097	-31.9554
100	1.5	3.1	-0.0	-14.8	0.2	-15.2	0.2	-14.9	0.0	38.4	37.9	38.2	-32.9	0.2	1	0	0	1	0.9	330.5109	-31.9891
101	1.0	0.0	-0.0	-15.1	0.0	-15.8	0.0	-15.2	0.0	38.1	37.4	38.0	-33.3	0.0	-2	5	5	1	0.9	330.5110	-31.9572
102	1.0	0.0	-0.0	-15.1	0.0	-15.8	0.0	-15.2	0.0	38.1	37.4	38.0	-33.3	0.0	-2	5	5	1	0.9	330.5114	-31.9956
103	1.0	0.0	-0.0	-15.0	0.0	-15.7	0.0	-15.1	0.0	38.1	37.4	38.0	-33.3	0.0	-2	5	1	5	0.9	330.5116	-32.0057
104	1.0	0.0	-0.0	-15.0	0.0	-15.7	0.0	-15.1	0.0	38.1	37.4	38.0	-33.3	0.0	-2	5	5	5	0.9	330.5118	-31.8898
105C	0.1	0.0	-1.2	-14.2	0.2	-15.4	0.0	-14.2	0.2	38.9	37.8	38.9	-32.8	0.2	-1	0	5	0	0.9	330.5121	-31.9733
106	1.0	0.0	-0.0	-15.1	0.0	-15.8	0.0	-15.2	0.0	38.1	37.4	38.0	-33.3	0.0	-2	5	5	1	0.9	330.5123	-31.9768
107	1.3	0.5	-0.4	-14.0	0.1	-14.6	0.1	-14.1	0.1	39.1	38.5	39.0	-32.2	0.1	0	0	0	0	0.9	330.5133	-32.0842
108C*	1.5	0.5	-0.4	-14.1	0.1	-14.6	0.1	-14.2	0.1	39.1	38.6	38.9	-32.2	0.1	0	0	0	0	0.9	330.5132	-31.9738

TABLE 18:
Derived quantities and detection codes for X-ray point sources in HCG 90 (online only).

109C	1.3	0.8	-0.7	-14.4	0.2	-14.9	0.2	-14.5	0.2	38.8	38.2	38.6	-32.6	0.2	0	0	0	0	0	0.9	330.5138	-31.9731
110	1.3	0.4	-0.4	-14.0	0.1	-14.5	0.1	-14.1	0.1	39.2	38.6	39.0	-32.2	0.1	0	0	0	0	0	0.9	330.5143	-32.0622
111C	0.8	0.0	-0.0	-14.7	0.2	-15.5	0.0	-14.8	0.0	38.4	37.7	38.4	-33.0	0.2	-2	0	5	5	0	0.9	330.5144	-31.9803
112C	-0.1	0.0	-1.0	-14.2	0.2	-15.4	0.0	-14.2	0.2	39.0	37.7	39.0	-32.8	0.2	-1	0	5	0	0	0.9	330.5146	-31.9742
113	1.3	3.3	-0.0	-14.8	0.2	-15.4	0.2	-14.9	0.0	38.3	37.8	38.2	-33.0	0.2	0	-2	5	5	1	0.9	330.5149	-31.9982
114	1.0	0.0	-0.0	-14.8	0.0	-15.5	0.0	-14.9	0.0	38.4	37.7	38.3	-33.0	0.0	-2	5	5	1	0.9	330.5154	-31.9626	
115	1.0	0.0	-0.0	-15.0	0.0	-15.7	0.0	-15.1	0.0	38.1	37.4	38.0	-33.3	0.0	-2	5	5	1	0.9	330.5168	-31.9853	
116	1.2	3.4	-0.0	-14.6	0.2	-15.2	0.2	-14.7	0.0	38.5	37.9	38.4	-32.8	0.2	1	0	0	5	0	0.9	330.5170	-31.9378
117	1.0	0.0	-0.0	-15.0	0.0	-15.7	0.0	-15.1	0.0	38.1	37.4	38.0	-33.3	0.0	-2	5	5	1	0.9	330.5170	-31.9932	
118	2.2	2.4	-0.0	-14.3	0.1	-14.6	0.1	-14.7	0.0	38.8	38.6	38.5	-32.4	0.1	1	0	0	5	0	0.9	330.5174	-31.9356
119	1.0	0.0	-0.0	-15.0	0.0	-15.7	0.0	-15.1	0.0	38.1	37.4	38.0	-33.3	0.0	-2	5	5	1	0.9	330.5174	-31.9561	
120C	0.8	0.0	-0.0	-14.5	0.2	-15.3	0.0	-14.6	0.0	38.6	37.8	38.5	-32.8	0.2	-2	0	5	5	0	0.9	330.5176	-31.9697
121	1.5	2.3	-0.0	-14.8	0.2	-15.3	0.2	-15.0	0.0	38.3	37.8	38.1	-33.0	0.2	1	0	0	1	0.9	330.5176	-31.8517	
122	1.0	0.0	-0.0	-15.0	0.0	-15.7	0.0	-15.1	0.0	38.1	37.4	38.0	-33.3	0.0	-2	5	5	1	0.9	330.5184	-31.9905	
123	1.0	0.0	-0.0	-15.0	0.0	-15.7	0.0	-15.1	0.0	38.1	37.4	38.0	-33.3	0.0	-2	5	5	1	0.9	330.5187	-31.9756	
124	0.6	0.0	-1.7	-14.5	0.2	-15.5	0.0	-14.6	0.2	38.6	37.7	38.5	-32.9	0.2	-1	0	5	0	0.9	330.5193	-31.9372	
125C	1.3	3.3	-0.0	-14.8	0.2	-15.4	0.2	-14.9	0.0	38.3	37.8	38.2	-33.0	0.2	1	0	0	1	0.9	330.5194	-31.9714	
126	1.0	0.0	-0.0	-15.0	0.0	-15.7	0.0	-15.1	0.0	38.1	37.4	38.0	-33.3	0.0	-2	5	5	1	0.9	330.5196	-31.9555	
127	1.3	3.3	-0.0	-14.9	0.3	-15.4	0.3	-15.0	0.0	38.3	37.7	38.1	-33.1	0.3	1	0	0	1	0.9	330.5196	-31.9791	
128	0.1	0.0	-1.2	-14.4	0.2	-15.6	0.0	-14.5	0.2	38.7	37.5	38.7	-33.0	0.2	-1	0	1	0	0.9	330.5204	-32.0724	
129D	1.5	3.1	-0.0	-14.8	0.2	-15.2	0.2	-14.9	0.0	38.4	37.9	38.2	-32.9	0.2	1	0	0	1	0.9	330.5214	-31.9914	
130D	1.8	2.9	-0.0	-14.5	0.2	-14.9	0.2	-14.7	0.0	38.7	38.3	38.4	-32.6	0.2	1	0	0	5	0.9	330.5214	-32.0008	
131	0.9	0.7	-0.7	-14.2	0.1	-15.0	0.1	-14.3	0.1	38.9	38.1	38.8	-32.5	0.1	0	0	0	0	0.9	330.5217	-32.0447	
132	1.0	0.0	-0.0	-15.0	0.0	-15.7	0.0	-15.1	0.0	38.2	37.5	38.1	-33.2	0.0	-2	5	5	1	0.9	330.5222	-31.9735	
133D	1.3	3.3	-0.0	-14.6	0.2	-15.1	0.2	-14.7	0.0	38.6	38.0	38.5	-32.8	0.2	1	0	0	5	0.9	330.5224	-32.0017	
134	1.5	0.7	-0.6	-14.3	0.1	-14.8	0.1	-14.5	0.1	38.8	38.3	38.7	-32.5	0.1	0	0	0	0	0.9	330.5225	-31.8969	
135	1.3	3.3	-0.0	-14.7	0.2	-15.2	0.2	-14.8	0.0	38.5	37.9	38.4	-32.9	0.2	1	0	0	5	0.9	330.5224	-31.9111	
136	1.0	0.0	-0.0	-15.0	0.0	-15.7	0.0	-15.1	0.0	38.1	37.4	38.0	-33.3	0.0	-2	5	5	1	0.9	330.5226	-31.9943	
137	1.0	0.0	-0.0	-15.0	0.0	-15.7	0.0	-15.1	0.0	38.1	37.4	38.0	-33.3	0.0	-2	5	5	1	0.9	330.5227	-31.9263	
138	1.3	0.8	-0.7	-14.4	0.2	-15.0	0.2	-14.5	0.2	38.7	38.2	38.6	-32.6	0.2	0	0	0	0	0.9	330.5228	-32.0311	
139	0.8	0.0	-0.0	-14.6	0.2	-15.4	0.0	-14.7	0.0	38.5	37.8	38.5	-32.9	0.2	-2	0	5	5	0.9	330.5235	-32.0262	
140	2.1	2.5	-0.0	-14.6	0.2	-14.9	0.2	-14.9	0.0	38.5	38.3	38.2	-32.7	0.2	1	0	0	1	0.9	330.5238	-32.0281	
141	1.7	2.9	-0.0	-14.4	0.1	-14.8	0.1	-14.7	0.0	38.7	38.3	38.5	-32.6	0.1	1	0	0	5	0.9	330.5239	-31.9789	
142	1.0	0.0	-0.0	-15.1	0.0	-15.8	0.0	-15.2	0.0	38.1	37.4	38.0	-33.3	0.0	-2	5	5	1	0.9	330.5240	-31.9967	
143	2.0	2.6	-0.0	-14.4	0.1	-14.7	0.1	-14.7	0.0	38.8	38.5	38.5	-32.5	0.1	1	0	0	5	0.9	330.5240	-31.9322	
144	1.0	0.0	-0.0	-15.0	0.0	-15.7	0.0	-15.1	0.0	38.2	37.5	38.1	-33.2	0.0	-2	5	5	1	0.9	330.5245	-31.9896	
145	1.4	3.2	-0.0	-14.5	0.2	-15.0	0.2	-14.7	0.0	38.6	38.1	38.5	-32.7	0.2	1	0	0	5	0.9	330.5245	-31.9229	
146D	0.8	0.0	-0.0	-14.7	0.2	-15.4	0.0	-14.7	0.0	38.5	37.7	38.4	-32.9	0.2	-2	0	5	5	0.9	330.5247	-31.9925	
147	0.0	0.0	-1.1	-14.4	0.2	-15.6	0.0	-14.4	0.2	38.8	37.6	38.7	-33.0	0.2	-1	0	1	0	0.9	330.5247	-32.0403	
148	2.2	2.4	-0.0	-14.3	0.1	-14.6	0.1	-14.7	0.0	38.8	38.6	38.4	-32.5	0.1	1	0	0	5	0.9	330.5253	-31.9769	
149D	2.2	2.4	-0.0	-14.5	0.2	-14.8	0.2	-14.9	0.0	38.6	38.4	38.3	-32.7	0.2	1	0	0	1	0.9	330.5269	-31.9930	
150	2.0	2.6	-0.0	-14.6	0.2	-14.9	0.2	-14.9	0.0	38.5	38.2	38.2	-32.7	0.2	1	0	0	1	0.9	330.5278	-31.9293	
151	2.0	2.7	-0.0	-14.6	0.2	-14.9	0.2	-14.9	0.0	38.5	38.2	38.3	-32.7	0.2	1	0	0	5	0.9	330.5274	-32.0813	
152	0.8	0.0	-1.9	-14.4	0.2	-15.3	0.0	-14.5	0.2	38.7	37.9	38.6	-32.8	0.2	-1	0	5	0	0.9	330.5279	-31.9728	
153D	1.9	2.8	-0.0	-14.5	0.2	-14.9	0.2	-14.8	0.0	38.6	38.3	38.4	-32.7	0.2	1	0	0	5	0.9	330.5288	-31.9925	
154	1.0	0.0	-0.0	-14.7	0.0	-15.4	0.0	-14.8	0.0	38.4	37.7	38.3	-33.0	0.0	-2	5	5	5	0.9	330.5293	-31.9945	
155	0.9	3.6	-0.0	-14.5	0.2	-15.3	0.2	-14.6	0.0	38.6	37.9	38.5	-32.8	0.2	1	0	0	5	0.9	330.5312	-31.9347	
156	1.0	0.0	-0.0	-14.8	0.0	-15.5	0.0	-14.9	0.0	38.4	37.7	38.3	-33.0	0.0	-2	5	5	1	0.9	330.5314	-31.9917	
157	1.4	0.8	-0.7	-14.4	0.1	-14.9	0.1	-14.5	0.1	38.8	38.2	38.6	-32.6	0.1	0	0	0	0	0.9	330.5324	-31.9603	
158	1.0	0.0	-0.0	-14.9	0.0	-15.6	0.0	-15.0	0.0	38.3	37.6	38.2	-33.1	0.0	-2	5	1	5	0.9	330.5326	-31.9039	
159B	1.2	0.3	-0.3	-13.7	0.1	-14.2	0.1	-13.8	0.1	39.5	38.9	39.4	-31.9	0.1	0	0	0	0	0.9	330.5329	-31.9891	
160B	1.3	3.3	-0.0	-14.7	0.2	-15.2	0.2	-14.8	0.0	38.5	37.9	38.3	-32.9	0.2	1	0	0	5	0.9	330.5331	-31.9899	
161	0.8	0.0	-0.0	-14.5	0.2	-15.3	0.0	-14.6	0.0	38.6	37.8	38.5	-32.8	0.2	-2	0	5	5	0.9	330.5332	-32.0009	
162B	0.8	0.0	-0.0	-14.6	0.2	-15.4	0.0	-14.7	0.0	38.5	37.8	38.5	-32.9	0.2	-2	0	5	5	0.9	330.5344	-31.9880	
163B	1.0	0.0	-0.0	-15.1	0.0	-15.8	0.0	-15.2	0.0	38.1	37.4	38.0	-33.3	0.0	-2	5	0	1	0.9	330.5351	-31.9864	
164B*	2.3	0.5	-0.5	-14.1	0.1	-14.3	0.1	-14.4	0.1	39.1	38.9	38.7	-32.2	0.1	0	0	0	0	0.9	330.5352	-31.9898	
165	1.0	0.0	-0.0	-15.1	0.0	-15.8	0.0	-15.2	0.0	38.1	37.4	38.0	-33.3	0.0	-2	5	5	1	0.9	330.5355	-31.9888	

TABLE 18:
Derived quantities and detection codes for X-ray point sources in HCG 90 (online only).

166B	1.3	3.3	-0.0	-14.6	0.2	-15.1	0.2	-14.7	0.0	38.6	38.0	38.5	-32.8	0.2	1	0	0	5	0.9	330.5357	-31.9876
167	1.0	0.0	-0.0	-15.0	0.0	-15.7	0.0	-15.1	0.0	38.2	37.5	38.1	-33.2	0.0	-2	5	5	1	0.9	330.5358	-31.8357
168	1.2	0.8	-0.7	-14.4	0.2	-15.0	0.2	-14.5	0.2	38.8	38.2	38.6	-32.6	0.2	0	0	0	0	0.9	330.5360	-32.0004
169	1.0	0.0	-0.0	-15.1	0.0	-15.8	0.0	-15.2	0.0	38.1	37.4	38.0	-33.3	0.0	-2	5	5	1	0.9	330.5366	-31.9873
170	1.0	0.0	-0.0	-15.0	0.0	-15.7	0.0	-15.1	0.0	38.1	37.4	38.0	-33.3	0.0	-2	5	5	1	0.9	330.5367	-31.9912
171B	1.3	3.3	-0.0	-14.5	0.2	-15.1	0.2	-14.7	0.0	38.6	38.0	38.5	-32.7	0.2	1	0	0	5	0.9	330.5381	-31.9922
172	0.4	0.5	-0.5	-13.8	0.1	-14.8	0.1	-13.9	0.1	39.3	38.3	39.3	-32.3	0.1	0	0	0	0	0.9	330.5383	-32.0630
173	1.0	0.0	-0.0	-15.1	0.0	-15.8	0.0	-15.1	0.0	38.1	37.4	38.0	-33.3	0.0	-2	5	5	5	0.9	330.5393	-31.9848
174	-0.3	0.0	-0.8	-13.9	0.1	-15.3	0.0	-13.9	0.1	39.2	37.8	39.2	-32.6	0.1	-1	0	5	0	0.9	330.5393	-31.8976
175	1.9	0.7	-0.6	-14.3	0.1	-14.6	0.1	-14.6	0.1	38.8	38.5	38.6	-32.4	0.1	0	0	0	0	0.9	330.5394	-31.9162
176	1.7	2.1	-0.0	-14.6	0.2	-15.0	0.2	-14.8	0.0	38.6	38.2	38.4	-32.7	0.2	1	0	0	5	0.9	330.5395	-32.0659
177B	0.8	0.0	-0.0	-14.7	0.2	-15.5	0.0	-14.8	0.0	38.4	37.7	38.4	-33.0	0.2	-2	0	5	5	0.9	330.5399	-31.9841
178B	0.8	0.0	-0.0	-14.7	0.2	-15.5	0.0	-14.8	0.0	38.4	37.7	38.4	-33.0	0.2	-2	0	5	5	0.9	330.5406	-31.9883
179B	0.8	0.0	-0.0	-14.6	0.2	-15.4	0.0	-14.7	0.0	38.5	37.8	38.5	-32.9	0.2	-2	0	5	5	0.9	330.5415	-31.9910
180	0.7	0.0	-1.8	-14.4	0.2	-15.3	0.0	-14.5	0.2	38.7	37.9	38.6	-32.8	0.2	-1	0	5	0	0.9	330.5416	-32.0070
181	1.3	3.3	-0.0	-14.7	0.2	-15.3	0.2	-14.8	0.0	38.4	37.9	38.3	-32.9	0.2	1	0	0	5	0.9	330.5417	-32.0280
182	1.0	0.0	-0.0	-15.0	0.0	-15.7	0.0	-15.1	0.0	38.1	37.4	38.0	-33.3	0.0	-2	5	5	1	0.9	330.5421	-31.9742
183	1.0	0.0	-0.0	-15.0	0.0	-15.7	0.0	-15.1	0.0	38.2	37.5	38.1	-33.2	0.0	-2	5	5	1	0.9	330.5420	-31.9707
184B	1.2	3.4	-0.0	-14.5	0.2	-15.1	0.2	-14.7	0.0	38.6	38.0	38.5	-32.8	0.2	1	0	0	5	0.9	330.5425	-31.9899
185	1.0	0.0	-0.0	-14.9	0.0	-15.6	0.0	-15.0	0.0	38.2	37.5	38.1	-33.2	0.0	-2	5	5	1	0.9	330.5437	-31.9689
186	1.3	3.3	-0.0	-14.4	0.2	-15.0	0.2	-14.6	0.0	38.7	38.1	38.6	-32.6	0.2	1	0	0	5	0.9	330.5473	-31.9813
187	1.0	0.0	-0.0	-14.8	0.0	-15.5	0.0	-14.9	0.0	38.3	37.6	38.2	-33.1	0.0	-2	5	1	5	0.9	330.5475	-31.9438
188	0.8	0.0	-0.0	-14.7	0.2	-15.5	0.0	-14.8	0.0	38.4	37.7	38.4	-33.0	0.2	-2	0	5	5	0.9	330.5479	-32.0232
189	1.0	0.0	-0.0	-15.0	0.0	-15.7	0.0	-15.1	0.0	38.1	37.4	38.0	-33.3	0.0	-2	5	5	1	0.9	330.5498	-31.9933
190	1.0	0.0	-0.0	-15.1	0.0	-15.8	0.0	-15.1	0.0	38.1	37.4	38.0	-33.3	0.0	-2	5	5	1	0.9	330.5511	-32.0448
191	-0.8	0.0	-0.2	-13.8	0.1	-15.5	0.0	-13.8	0.1	39.4	37.6	39.4	-32.7	0.1	-1	0	1	0	0.9	330.550	-32.0443
192	0.4	0.0	-1.5	-14.6	0.2	-15.6	0.0	-14.6	0.2	38.6	37.5	38.5	-33.0	0.2	-1	0	1	0	0.9	330.5554	-31.9465
193	1.4	0.5	-0.5	-14.1	0.1	-14.6	0.1	-14.2	0.1	39.1	38.5	38.9	-32.3	0.1	0	0	0	0	0.9	330.5578	-31.9856
194	0.9	0.0	-0.0	-14.5	0.2	-15.3	0.0	-14.6	0.0	38.6	37.9	38.6	-32.8	0.2	-2	0	5	5	0.9	330.5593	-32.0408
195	1.0	0.0	-0.0	-14.9	0.0	-15.6	0.0	-15.0	0.0	38.3	37.6	38.2	-33.1	0.0	-2	5	5	5	0.9	330.5597	-31.9948
196	0.9	0.0	-0.0	-14.7	0.2	-15.5	0.0	-14.8	0.0	38.4	37.7	38.4	-33.0	0.2	-2	0	5	5	0.9	330.5599	-31.8569
197	1.0	0.0	-0.0	-15.0	0.0	-15.7	0.0	-15.1	0.0	38.1	37.4	38.0	-33.3	0.0	-2	5	5	5	0.9	330.5618	-32.0737
198	1.2	3.4	-0.0	-14.7	0.2	-15.3	0.2	-14.8	0.0	38.5	37.9	38.3	-32.9	0.2	1	0	0	5	0.9	330.5624	-31.9516
199	0.3	0.0	-1.4	-14.6	0.2	-15.6	0.0	-14.6	0.2	38.6	37.5	38.5	-33.1	0.2	-1	0	1	0	0.9	330.5637	-32.0577
200	0.4	0.0	-1.5	-14.6	0.2	-15.6	0.0	-14.6	0.2	38.5	37.5	38.5	-33.0	0.2	-1	0	1	0	0.9	330.5646	-31.9225
201	0.5	0.7	-0.7	-14.1	0.1	-15.1	0.1	-14.2	0.1	39.0	38.0	38.9	-32.5	0.1	0	0	0	0	0.9	330.5652	-31.8808
202	1.0	0.0	-0.0	-15.1	0.0	-15.8	0.0	-15.2	0.0	38.1	37.4	38.0	-33.3	0.0	-2	5	5	5	0.9	330.5658	-32.0358
203	0.9	3.7	-0.0	-14.5	0.2	-15.2	0.2	-14.6	0.0	38.7	37.9	38.6	-32.8	0.2	1	0	0	5	0.9	330.5662	-31.9694
204	2.1	0.3	-0.3	-13.6	0.0	-13.8	0.0	-13.9	0.0	39.6	39.3	39.2	-31.7	0.0	0	0	0	0	0.9	330.5668	-32.0048
205	1.3	0.7	-0.6	-14.3	0.1	-14.9	0.1	-14.4	0.1	38.9	38.3	38.7	-32.5	0.1	0	0	0	0	0.9	330.5689	-32.0156
206	2.1	0.6	-0.5	-14.2	0.1	-14.4	0.1	-14.5	0.1	39.0	38.7	38.6	-32.3	0.1	0	0	0	0	0.9	330.5689	-31.8407
207	1.5	0.3	-0.2	-13.6	0.1	-14.1	0.1	-13.8	0.1	39.5	39.1	39.4	-31.8	0.1	0	0	0	0	0.9	330.5694	-31.9325
208	0.6	0.0	-1.7	-14.3	0.2	-15.2	0.0	-14.3	0.2	38.9	37.9	38.8	-32.7	0.2	-1	0	5	0	0.9	330.5722	-31.9597
209	0.9	0.0	-0.0	-14.7	0.2	-15.5	0.0	-14.8	0.0	38.4	37.7	38.4	-33.0	0.2	-2	0	5	5	0.9	330.5748	-31.9210
210	0.4	0.0	-1.5	-14.5	0.2	-15.6	0.0	-14.6	0.2	38.6	37.6	38.6	-33.0	0.2	-1	0	5	0	0.9	330.5761	-32.0696
211	0.4	0.0	-1.5	-14.6	0.2	-15.6	0.0	-14.6	0.2	38.6	37.5	38.5	-33.0	0.2	-1	0	1	0	0.9	330.5775	-31.9526
212	0.6	0.8	-0.8	-14.3	0.2	-15.2	0.2	-14.3	0.2	38.9	37.9	38.8	-32.7	0.2	0	0	0	0	0.9	330.5796	-31.8880
213	1.0	0.0	-0.0	-15.0	0.0	-15.7	0.0	-15.1	0.0	38.1	37.4	38.0	-33.3	0.0	-2	5	5	1	0.9	330.5806	-32.0125
214	0.9	0.0	-0.0	-14.5	0.2	-15.3	0.0	-14.6	0.0	38.6	37.8	38.5	-32.8	0.2	-2	0	5	5	0.9	330.5808	-31.9591
215	1.8	0.4	-0.4	-13.9	0.1	-14.3	0.1	-14.2	0.1	39.2	38.9	39.0	-32.1	0.1	0	0	0	0	0.9	330.5809	-31.8268
216	1.0	0.0	-0.0	-15.0	0.0	-15.7	0.0	-15.0	0.0	38.2	37.5	38.1	-33.2	0.0	-2	5	5	1	0.9	330.5821	-31.9741
217	0.6	0.0	-1.7	-14.4	0.2	-15.3	0.0	-14.5	0.2	38.7	37.8	38.7	-32.8	0.2	-1	0	5	0	0.9	330.5824	-31.9565
218	1.0	0.0	-0.0	-14.8	0.0	-15.5	0.0	-14.9	0.0	38.4	37.7	38.3	-33.0	0.0	-2	5	1	5	0.9	330.5826	-31.9620
219	1.3	3.3	-0.0	-14.7	0.2	-15.3	0.2	-14.9	0.0	38.4	37.8	38.3	-32.9	0.2	1	0	0	5	0.9	330.5854	-32.0003
220	0.9	0.0	-0.0	-14.6	0.2	-15.3	0.0	-14.6	0.0	38.6	37.8	38.5	-32.9	0.2	-2	0	5	5	0.9	330.5855	-31.9050
221	0.9	0.0	-0.0	-14.7	0.2	-15.4	0.0	-14.7	0.0	38.5	37.7	38.4	-32.9	0.2	-2	0	5	5	0.9	330.5854	-31.9283
222	-0.5	0.0	-0.6	-14.0	0.2	-15.5	0.0	-14.0	0.2	39.1	37.6	39.1	-32.8	0.2	-1	0	1	0	0.9	330.5864	-32.0502

TABLE 18:
Derived quantities and detection codes for X-ray point sources in HCG 90 (online only).

223	0.9	0.0	-0.0	-14.7	0.2	-15.4	0.0	-14.7	0.0	38.5	37.7	38.4	-32.9	0.2	-2	0	5	5	0.9	330.5870	-32.0102
224	1.9	0.3	-0.3	-13.7	0.1	-14.1	0.1	-14.0	0.1	39.4	39.1	39.2	-31.8	0.1	0	0	0	0	0.9	330.5935	-31.9157
225	0.5	0.0	-1.6	-14.4	0.2	-15.4	0.0	-14.5	0.2	38.7	37.7	38.7	-32.9	0.2	-1	0	5	0	0.9	330.5954	-32.0655
226	2.5	2.1	-0.0	-14.3	0.1	-14.5	0.1	-14.8	0.0	38.8	38.7	38.4	-32.5	0.1	1	0	0	5	0.9	330.5960	-31.9154
227	1.2	0.6	-0.5	-14.2	0.1	-14.8	0.1	-14.3	0.1	39.0	38.4	38.9	-32.4	0.1	0	0	0	0	0.9	330.5973	-31.9680
228	1.6	0.8	-0.7	-14.4	0.1	-14.8	0.1	-14.6	0.1	38.8	38.4	38.6	-32.5	0.1	0	0	0	0	0.9	330.6008	-31.9613
229	0.4	0.0	-1.5	-14.7	0.3	-15.7	0.0	-14.7	0.3	38.5	37.5	38.4	-33.1	0.3	-1	0	1	0	0.9	330.6007	-31.9767
230	1.6	3.0	-0.0	-14.7	0.2	-15.1	0.2	-14.9	0.0	38.4	38.0	38.2	-32.8	0.2	1	0	0	5	0.9	330.6044	-32.0617
231	1.3	0.6	-0.5	-14.1	0.1	-14.7	0.1	-14.3	0.1	39.0	38.4	38.9	-32.3	0.1	0	0	0	0	0.9	330.6077	-31.8675
232	1.0	0.0	-0.0	-15.0	0.0	-15.7	0.0	-15.1	0.0	38.1	37.4	38.0	-33.3	0.0	-2	5	5	1	0.9	330.6116	-32.0003
233	1.7	0.3	-0.3	-13.7	0.1	-14.1	0.1	-14.0	0.1	39.4	39.0	39.2	-31.9	0.1	0	0	0	0	0.9	330.6117	-31.9739
234	1.0	0.0	-0.0	-15.0	0.0	-15.7	0.0	-15.1	0.0	38.1	37.4	38.0	-33.3	0.0	-2	5	0	1	0.9	330.6132	-31.9182
235	1.0	0.0	-0.0	-14.9	0.0	-15.6	0.0	-15.0	0.0	38.2	37.5	38.1	-33.2	0.0	-2	5	5	5	0.9	330.6212	-31.9693
236	3.3	0.3	-0.3	-13.3	0.0	-13.4	0.0	-14.2	0.0	39.8	39.8	39.0	-31.6	0.0	0	0	0	0	0.9	330.6221	-32.0705
237	1.4	0.7	-0.6	-14.3	0.1	-14.8	0.1	-14.4	0.1	38.9	38.4	38.7	-32.4	0.1	0	0	0	0	0.9	330.6233	-32.0663
238	1.4	2.4	-0.0	-14.5	0.2	-15.0	0.2	-14.7	0.0	38.6	38.1	38.4	-32.7	0.2	1	0	0	5	0.9	330.6243	-31.9876
239	1.0	0.0	-0.0	-15.0	0.0	-15.7	0.0	-15.1	0.0	38.1	37.4	38.0	-33.3	0.0	-2	5	1	5	0.9	330.6321	-32.0844
240	0.5	0.7	-0.7	-14.2	0.1	-15.1	0.1	-14.2	0.1	39.0	38.0	38.9	-32.6	0.1	0	0	0	0	0.9	330.6321	-31.9432
241	2.2	2.5	-0.0	-14.4	0.1	-14.7	0.1	-14.8	0.0	38.7	38.5	38.3	-32.6	0.1	1	0	0	5	0.9	330.6355	-32.0540
242	2.3	0.6	-0.5	-14.1	0.1	-14.3	0.1	-14.5	0.1	39.1	38.8	38.7	-32.2	0.1	0	0	0	0	0.9	330.6369	-31.9110
243	1.4	0.5	-0.4	-14.0	0.1	-14.5	0.1	-14.2	0.1	39.1	38.6	39.0	-32.2	0.1	0	0	0	0	0.9	330.6378	-31.9629
244	1.0	0.0	-0.0	-15.0	0.0	-15.7	0.0	-15.1	0.0	38.2	37.5	38.1	-33.2	0.0	-2	5	1	5	0.9	330.6389	-31.9730
245	0.0	0.0	-1.1	-14.4	0.2	-15.6	0.0	-14.4	0.2	38.7	37.5	38.7	-33.0	0.2	-1	0	1	0	0.9	330.6413	-31.8567
246	0.9	0.0	-0.0	-14.7	0.2	-15.5	0.0	-14.8	0.0	38.4	37.7	38.4	-33.0	0.2	-2	0	5	5	0.9	330.6457	-31.9453
247	1.0	0.0	-0.0	-15.0	0.0	-15.7	0.0	-15.1	0.0	38.2	37.5	38.1	-33.2	0.0	-2	5	5	5	0.9	330.6483	-31.9589
248	0.2	0.7	-0.8	-14.1	0.1	-15.2	0.1	-14.1	0.1	39.1	38.0	39.1	-32.6	0.1	0	0	0	0	0.9	330.6526	-32.0298
249	1.9	0.6	-0.6	-14.2	0.1	-14.5	0.1	-14.5	0.1	38.9	38.6	38.7	-32.3	0.1	0	0	0	0	0.9	330.6530	-32.0923
250	2.3	2.4	-0.0	-14.5	0.2	-14.7	0.2	-14.9	0.0	38.6	38.4	38.2	-32.7	0.2	1	0	0	1	0.9	330.6545	-32.0373
251	1.9	0.1	-0.1	-13.0	0.0	-13.3	0.0	-13.2	0.0	40.2	39.8	39.9	-31.1	0.0	0	0	0	0	0.9	330.6585	-32.0154
252	2.1	2.6	-0.0	-14.5	0.1	-14.7	0.1	-14.8	0.0	38.7	38.4	38.3	-32.6	0.1	1	0	0	5	0.9	330.6625	-31.9548
253	2.1	0.3	-0.3	-13.6	0.1	-13.9	0.1	-14.0	0.1	39.5	39.2	39.2	-31.7	0.1	0	0	0	0	0.9	330.6666	-31.9462
254	1.4	0.3	-0.3	-13.6	0.1	-14.1	0.1	-13.8	0.1	39.5	39.0	39.4	-31.8	0.1	0	0	0	0	0.9	330.6672	-31.9415
255	1.8	0.5	-0.4	-14.0	0.1	-14.3	0.1	-14.2	0.1	39.2	38.8	38.9	-32.1	0.1	0	0	0	0	0.9	330.6768	-31.9509
256	3.0	0.5	-0.5	-13.8	0.1	-13.9	0.1	-14.5	0.1	39.4	39.3	38.7	-32.0	0.1	0	0	0	0	0.9	330.6862	-31.9978

TABLE 19:
Derived quantities and detection codes for X-ray point sources in HCG 92 (online only).

ID (1)	Γ (2)	L_X										lim									
		+	-	f_F (5)	\pm (6)	f_S (7)	\pm (8)	f_H (9)	\pm (10)	F (11)	S (12)	H (13)	$f_{\nu,2\text{keV}}$ (14)	\pm (15)	HR	F (17)	S (18)	H (19)	EEF (20)	RA (21)	DEC (22)
1	1.1	3.3	-0.0	-15.1	0.2	-15.7	0.2	-15.2	0.0	38.9	38.3	38.8	-33.3	0.2	1	0	0	5	0.9	338.9142	33.9697
2	1.0	0.0	-0.0	-15.5	0.0	-16.2	0.0	-15.6	0.0	38.4	37.7	38.3	-33.8	0.0	-2	5	0	1	0.9	338.9196	33.9596
3	1.1	3.3	-0.0	-14.9	0.2	-15.5	0.2	-15.0	0.0	39.1	38.4	39.0	-33.1	0.2	1	0	0	5	0.9	338.9382	33.9753
4	-0.7	0.0	-0.4	-14.2	0.1	-15.8	0.0	-14.2	0.1	39.8	38.2	39.8	-33.1	0.1	-1	0	5	0	0.9	338.9413	33.9651
5	1.1	3.3	-0.0	-15.1	0.2	-15.7	0.2	-15.2	0.0	38.9	38.3	38.8	-33.3	0.2	1	0	0	5	0.9	338.9429	33.9902
6	0.5	0.8	-0.9	-14.7	0.2	-15.6	0.2	-14.7	0.2	39.3	38.4	39.3	-33.1	0.2	0	0	0	0	0.9	338.9438	33.9632
7	0.2	0.0	-1.3	-14.6	0.2	-15.8	0.0	-14.7	0.2	39.3	38.2	39.3	-33.2	0.2	-1	0	5	0	0.9	338.9442	33.9478
8	1.0	0.0	-0.0	-15.3	0.0	-16.0	0.0	-15.4	0.0	38.6	37.9	38.5	-33.6	0.0	-2	5	5	1	0.9	338.9473	34.0095
9	1.6	2.1	-0.0	-15.0	0.2	-15.4	0.2	-15.2	0.0	39.0	38.6	38.8	-33.1	0.2	1	0	0	5	0.9	338.9488	33.9476
10	1.2	0.4	-0.4	-14.2	0.1	-14.8	0.1	-14.3	0.1	39.7	39.1	39.6	-32.4	0.1	0	0	0	0	0.9	338.9501	33.9505
11	1.5	2.9	-0.0	-15.0	0.2	-15.5	0.2	-15.2	0.0	39.0	38.5	38.8	-33.2	0.2	1	0	0	5	0.9	338.9508	33.9885
12	1.0	0.0	-0.0	-15.1	0.0	-15.8	0.0	-15.2	0.0	38.9	38.2	38.8	-33.4	0.0	-2	5	1	5	0.9	338.9517	34.0284
13	1.0	0.6	-0.6	-14.5	0.1	-15.3	0.1	-14.6	0.1	39.4	38.7	39.3	-32.8	0.1	0	0	0	0	0.9	338.9540	33.9861
14	0.1	0.0	-1.2	-14.7	0.2	-15.9	0.0	-14.7	0.2	39.3	38.1	39.3	-33.3	0.2	-1	0	5	0	0.9	338.9556	33.9660
15	1.0	0.0	-0.0	-15.5	0.0	-16.2	0.0	-15.6	0.0	38.4	37.7	38.3	-33.8	0.0	-2	5	1	5	0.9	338.9572	33.9503
16	1.0	0.0	-0.0	-15.6	0.0	-16.3	0.0	-15.7	0.0	38.4	37.7	38.3	-33.8	0.0	-2	5	1	5	0.9	338.9599	33.9872
17	0.7	0.0	-0.0	-15.0	0.2	-15.8	0.0	-15.0	0.0	39.0	38.2	39.0	-33.3	0.2	-2	0	5	5	0.9	338.9600	34.0087
18	1.2	0.6	-0.6	-14.5	0.1	-15.1	0.1	-14.7	0.1	39.5	38.9	39.3	-32.7	0.1	0	0	0	0	0.9	338.9606	33.9197
19	0.9	0.3	-0.4	-14.1	0.1	-14.9	0.1	-14.2	0.1	39.9	39.1	39.8	-32.4	0.1	0	0	0	0	0.9	338.9624	34.0310
20	1.3	3.2	-0.0	-15.1	0.2	-15.7	0.2	-15.3	0.0	38.9	38.3	38.7	-33.3	0.2	1	0	0	1	0.9	338.9639	33.9339
21	2.0	0.1	-0.1	-13.4	0.0	-13.7	0.0	-13.7	0.0	40.6	40.3	40.3	-31.5	0.0	0	0	0	0	0.9	338.9662	34.0182
22E*	2.3	0.5	-0.4	-14.4	0.1	-14.6	0.1	-14.8	0.1	39.6	39.4	39.2	-32.5	0.1	0	0	0	0	0.9	338.9665	33.9450
23E	1.4	3.0	-0.0	-15.0	0.2	-15.5	0.2	-15.1	0.0	39.0	38.5	38.9	-33.1	0.2	1	0	0	5	0.9	338.9684	33.9455
24	1.0	0.0	-0.0	-15.5	0.0	-16.2	0.0	-15.6	0.0	38.4	37.7	38.3	-33.8	0.0	-2	5	5	5	0.9	338.9683	33.9480
25	1.3	0.5	-0.5	-14.4	0.1	-15.0	0.1	-14.6	0.1	39.6	39.0	39.4	-32.6	0.1	0	0	0	0	0.9	338.9719	33.9304
26	1.3	0.2	-0.2	-13.6	0.0	-14.1	0.0	-13.7	0.0	40.4	39.8	40.2	-31.8	0.0	0	0	0	0	0.9	338.9746	33.9963
27	1.2	0.5	-0.5	-14.4	0.1	-15.0	0.1	-14.6	0.1	39.5	38.9	39.4	-32.7	0.1	0	0	0	0	0.9	338.9751	33.9965
28	2.2	2.2	-0.0	-14.8	0.1	-15.0	0.1	-15.2	0.0	39.2	38.9	38.8	-32.9	0.1	1	0	0	5	0.9	338.9763	33.9545
29	1.9	2.5	-0.0	-15.0	0.2	-15.3	0.2	-15.2	0.0	39.0	38.7	38.8	-33.1	0.2	1	0	0	5	0.9	338.9771	33.9686
30	1.0	0.0	-0.0	-15.6	0.0	-16.3	0.0	-15.7	0.0	38.4	37.7	38.3	-33.8	0.0	-2	5	1	5	0.9	338.9805	33.9949
31	1.6	0.1	-0.1	-13.1	0.0	-13.6	0.0	-13.3	0.0	40.8	40.4	40.6	-31.3	0.0	0	0	0	0	0.9	338.9821	33.9608
32	1.8	2.6	-0.0	-15.1	0.2	-15.4	0.2	-15.3	0.0	38.9	38.5	38.7	-33.2	0.2	1	0	0	1	0.9	338.9831	33.9860
33	1.0	0.0	-0.0	-15.5	0.0	-16.2	0.0	-15.6	0.0	38.4	37.7	38.3	-33.8	0.0	-2	5	5	1	0.9	338.9835	33.9864
34	1.1	3.3	-0.0	-15.0	0.2	-15.6	0.2	-15.1	0.0	39.0	38.4	38.9	-33.2	0.2	1	0	0	5	0.9	338.9846	34.0113
35	1.6	0.7	-0.6	-14.6	0.1	-15.1	0.1	-14.8	0.1	39.3	38.9	39.1	-32.8	0.1	0	0	0	0	0.9	338.9854	33.9512
36D*	2.6	0.4	-0.4	-14.1	0.1	-14.3	0.1	-14.7	0.1	39.8	39.7	39.3	-32.3	0.1	0	0	0	0	0.9	338.9862	33.9656
37	0.7	0.0	-0.0	-14.9	0.2	-15.8	0.0	-15.0	0.0	39.0	38.2	39.0	-33.3	0.2	-2	0	5	5	0.9	338.9863	33.9802
38	0.1	0.0	-1.2	-14.6	0.2	-15.8	0.0	-14.6	0.2	39.4	38.2	39.3	-33.2	0.2	-1	0	5	0	0.9	338.9868	33.9612
39	2.0	2.4	-0.0	-14.8	0.1	-15.1	0.1	-15.2	0.0	39.1	38.8	38.8	-33.0	0.1	1	0	0	5	0.9	338.9874	33.9730
40D	2.5	1.9	-0.0	-14.8	0.1	-15.0	0.1	-15.2	0.0	39.2	39.0	38.7	-32.9	0.1	1	0	0	5	0.9	338.9880	33.9663
41	2.4	2.0	-0.0	-14.8	0.1	-15.0	0.1	-15.2	0.0	39.2	39.0	38.8	-32.9	0.1	1	0	0	5	0.9	338.9891	33.9719
42	1.4	0.2	-0.2	-13.9	0.1	-14.4	0.1	-14.1	0.1	40.1	39.5	39.9	-32.1	0.1	0	0	0	0	0.9	338.9900	33.9833
43	1.3	3.1	-0.0	-15.1	0.2	-15.7	0.2	-15.3	0.0	38.8	38.3	38.7	-33.3	0.2	1	0	0	1	0.9	338.9902	34.0180
44	-0.4	0.0	-0.7	-14.2	0.1	-15.7	0.0	-14.2	0.1	39.7	38.3	39.7	-33.0	0.1	-1	0	5	0	0.9	338.9918	33.9301
45B	2.1	2.3	-0.0	-14.9	0.1	-15.1	0.1	-15.2	0.0	39.1	38.8	38.8	-33.0	0.1	1	0	0	5	0.9	338.9931	33.9671
46B*	1.8	0.7	-0.6	-14.6	0.1	-15.0	0.1	-14.8	0.1	39.4	39.0	39.1	-32.7	0.1	0	0	0	0	0.9	338.9934	33.9661
47	0.7	0.0	-0.0	-15.0	0.2	-15.8	0.0	-15.0	0.0	39.0	38.2	39.0	-33.3	0.2	-2	0	5	5	0.9	338.9953	34.0251
48	1.0	0.0	-0.0	-15.6	0.0	-16.3	0.0	-15.7	0.0	38.4	37.7	38.3	-33.8	0.0	-2	5	0	1	0.9	338.9954	34.0022
49	1.7	0.6	-0.5	-14.5	0.1	-14.9	0.1	-14.8	0.1	39.4	39.0	39.2	-32.7	0.1	0	0	0	0	0.9	338.9957	33.9805
50	0.7	0.0	-0.0	-14.9	0.2	-15.8	0.0	-15.0	0.0	39.0	38.2	39.0	-33.3	0.2	-2	0	5	5	0.9	338.9958	33.9995
51	0.8	0.5	-0.5	-14.4	0.1	-15.2	0.1	-14.4	0.1	39.6	38.8	39.5	-32.7	0.1	0	0	0	0	0.9	338.9960	33.9849

TABLE 19:
Derived quantities and detection codes for X-ray point sources in HCG 92 (online only).

52	0.1	0.4	-0.4	-13.9	0.1	-15.1	0.1	-14.0	0.1	40.0	38.9	40.0	-32.5	0.1	0	0	0	0	0.9	338.9969	33.9545	
53	1.6	2.8	-0.0	-14.9	0.2	-15.3	0.2	-15.1	0.0	39.1	38.6	38.9	-33.0	0.2	1	0	0	5	0.9	338.9974	33.9680	
54	1.7	2.7	-0.0	-14.9	0.2	-15.3	0.2	-15.1	0.0	39.1	38.7	38.8	-33.1	0.2	1	0	0	5	0.9	338.9975	33.9739	
55	1.0	0.0	-0.0	-15.6	0.0	-16.2	0.0	-15.6	0.0	38.4	37.7	38.3	-33.8	0.0	-2	5	5	1	0.9	338.9976	33.9432	
56	-0.2	0.0	-0.9	-14.4	0.2	-15.7	0.0	-14.4	0.2	39.6	38.3	39.6	-33.0	0.2	-1	0	5	0	0.9	338.9976	33.9816	
57	1.8	2.6	-0.0	-15.0	0.2	-15.4	0.2	-15.2	0.0	39.0	38.6	38.8	-33.1	0.2	1	0	0	5	0.9	338.9977	33.9674	
58	1.6	2.8	-0.0	-15.0	0.2	-15.5	0.2	-15.2	0.0	39.0	38.5	38.8	-33.2	0.2	1	0	0	5	0.9	338.9982	33.9622	
59	1.9	2.5	-0.0	-15.0	0.2	-15.4	0.2	-15.3	0.0	39.0	38.6	38.7	-33.1	0.2	1	0	0	1	0.9	338.9984	33.9706	
60	2.8	1.6	-0.0	-14.6	0.1	-14.8	0.1	-15.3	0.0	39.3	39.2	38.7	-32.8	0.1	1	0	0	5	0.9	338.9984	33.9595	
61	1.8	2.6	-0.0	-15.0	0.2	-15.4	0.2	-15.3	0.0	39.0	38.6	38.7	-33.1	0.2	1	0	0	1	0.9	338.9988	33.9723	
62	1.5	2.9	-0.0	-14.9	0.2	-15.3	0.2	-15.1	0.0	39.1	38.6	38.9	-33.0	0.2	1	0	0	5	0.9	338.9992	33.9741	
63	1.0	0.0	-0.0	-15.6	0.0	-16.3	0.0	-15.7	0.0	38.4	37.7	38.3	-33.8	0.0	-2	5	5	1	0.9	338.9996	33.9723	
64	2.2	2.2	-0.0	-14.8	0.1	-15.1	0.1	-15.2	0.0	39.1	38.9	38.8	-33.0	0.1	1	0	0	5	0.9	338.9997	33.9763	
65	2.0	2.4	-0.0	-14.9	0.1	-15.2	0.1	-15.2	0.0	39.1	38.8	38.8	-33.0	0.1	1	0	0	5	0.9	339.0000	33.9606	
66	1.0	0.0	-0.0	-15.6	0.0	-16.3	0.0	-15.7	0.0	38.4	37.7	38.3	-33.8	0.0	-2	5	1	5	0.9	339.0001	34.0017	
67	0.7	0.0	-0.0	-14.9	0.2	-15.7	0.0	-14.9	0.0	39.1	38.3	39.1	-33.2	0.2	-2	0	0	5	5	0.9	339.0003	33.9902
68	2.1	2.3	-0.0	-14.8	0.1	-15.1	0.1	-15.1	0.0	39.2	38.9	38.8	-32.9	0.1	1	0	0	5	0.9	339.0003	33.9684	
69	-0.5	0.6	-0.6	-14.1	0.1	-15.6	0.1	-14.1	0.1	39.9	38.4	39.9	-32.9	0.1	0	0	0	0	0.9	339.0011	33.9930	
70	2.0	2.4	-0.0	-14.9	0.2	-15.2	0.2	-15.3	0.0	39.0	38.8	38.7	-33.1	0.2	1	0	0	1	0.9	339.0013	33.9531	
71	1.8	2.7	-0.0	-14.9	0.2	-15.3	0.2	-15.2	0.0	39.0	38.7	38.8	-33.1	0.2	1	0	0	5	0.9	339.0010	33.9148	
72	0.7	0.0	-0.0	-15.0	0.2	-15.8	0.0	-15.0	0.0	39.0	38.2	39.0	-33.3	0.2	-2	0	0	5	5	0.9	339.0028	33.9369
73	1.8	0.2	-0.2	-13.8	0.0	-14.2	0.0	-14.1	0.0	40.1	39.8	39.9	-32.0	0.0	0	0	0	0	0.9	339.0031	33.9671	
74	1.9	0.6	-0.5	-14.6	0.1	-14.9	0.1	-14.8	0.1	39.4	39.1	39.1	-32.7	0.1	0	0	0	0	0.9	339.0040	33.9702	
75	-0.1	0.0	-1.0	-14.7	0.2	-15.9	0.0	-14.7	0.2	39.3	38.1	39.3	-33.3	0.2	-1	0	5	0	0.9	339.0056	34.0341	
76	1.4	3.0	-0.0	-15.0	0.2	-15.6	0.2	-15.2	0.0	38.9	38.4	38.8	-33.2	0.2	1	0	0	5	0.9	339.0060	33.9683	
77	2.3	2.1	-0.0	-14.9	0.1	-15.1	0.1	-15.3	0.0	39.1	38.9	38.7	-33.0	0.1	1	0	0	1	0.9	339.0059	33.9563	
78	0.7	0.0	-0.0	-14.9	0.2	-15.7	0.0	-14.9	0.0	39.1	38.3	39.1	-33.2	0.2	-2	0	0	5	5	0.9	339.0076	34.0140
79	1.0	0.0	-0.0	-15.6	0.0	-16.2	0.0	-15.6	0.0	38.4	37.7	38.3	-33.8	0.0	-2	5	5	5	5	0.9	339.0087	33.9971
80	0.7	0.0	-0.0	-14.9	0.2	-15.8	0.0	-15.0	0.0	39.0	38.2	39.0	-33.3	0.2	-2	0	0	5	5	0.9	339.0099	33.9659
81	-0.1	0.0	-1.0	-14.5	0.2	-15.8	0.0	-14.5	0.2	39.5	38.2	39.4	-33.1	0.2	-1	0	0	5	0	0.9	339.0103	33.9746
82	1.7	2.7	-0.0	-15.0	0.2	-15.4	0.2	-15.2	0.0	39.0	38.6	38.8	-33.1	0.2	1	0	0	5	0.9	339.0105	33.9794	
83	0.7	0.0	-0.0	-14.9	0.2	-15.8	0.0	-15.0	0.0	39.0	38.2	39.0	-33.3	0.2	-2	0	0	5	5	0.9	339.0110	34.0084
84	1.4	3.0	-0.0	-14.9	0.2	-15.4	0.2	-15.1	0.0	39.1	38.6	38.9	-33.1	0.2	1	0	0	5	0.9	339.0111	33.9713	
85	0.0	0.0	-1.1	-14.9	0.3	-16.1	0.0	-14.9	0.3	39.1	37.9	39.1	-33.5	0.3	-1	0	1	0	0.9	339.0115	34.0408	
86	2.0	2.5	-0.0	-14.9	0.2	-15.2	0.2	-15.2	0.0	39.0	38.7	38.7	-33.0	0.2	1	0	0	5	0.9	339.0135	33.9201	
87	0.7	0.0	-0.0	-14.9	0.2	-15.8	0.0	-15.0	0.0	39.0	38.2	39.0	-33.3	0.2	-2	0	0	5	5	0.9	339.0137	33.9973
88	1.0	0.0	-0.0	-15.5	0.0	-16.2	0.0	-15.6	0.0	38.4	37.7	38.3	-33.8	0.0	-2	5	5	5	0.9	339.0138	33.9533	
89	1.4	0.2	-0.2	-13.9	0.1	-14.4	0.1	-14.1	0.1	40.1	39.5	39.9	-32.1	0.1	0	0	0	0	0.9	339.0142	33.9482	
90	3.1	1.3	-0.0	-14.5	0.1	-14.6	0.1	-15.3	0.0	39.4	39.3	38.7	-32.8	0.1	1	0	0	5	0.9	339.0143	34.0091	
91	1.7	0.3	-0.3	-14.2	0.1	-14.6	0.1	-14.4	0.1	39.8	39.4	39.6	-32.3	0.1	0	0	0	0	0.9	339.0144	33.9474	
92	0.3	0.0	-1.4	-14.8	0.2	-15.9	0.0	-14.9	0.2	39.1	38.1	39.1	-33.3	0.2	-1	0	0	5	0	0.9	339.0147	34.0255
93	0.7	0.0	-0.0	-14.9	0.2	-15.8	0.0	-15.0	0.0	39.0	38.2	39.0	-33.3	0.2	-2	0	0	5	5	0.9	339.0147	33.9637
94C*	-1.1	0.6	-0.0	-11.7	0.0	-13.5	0.0	-11.7	0.0	42.3	40.5	42.3	-30.7	0.0	0	0	0	0	0.9	339.0149	33.9759	
95C	1.6	0.2	-0.2	-13.7	0.0	-14.1	0.0	-13.9	0.0	40.3	39.8	40.0	-31.9	0.0	0	0	0	0	0.9	339.0152	33.9736	
96	1.0	0.0	-0.0	-15.6	0.0	-16.2	0.0	-15.6	0.0	38.4	37.7	38.3	-33.8	0.0	-2	5	5	5	0.9	339.0154	33.9811	
97	1.1	0.6	-0.6	-14.6	0.1	-15.2	0.1	-14.7	0.1	39.4	38.7	39.3	-32.8	0.1	0	0	0	0	0.9	339.0160	34.0119	
98	1.3	3.1	-0.0	-15.1	0.2	-15.7	0.2	-15.2	0.0	38.9	38.3	38.7	-33.3	0.2	1	0	0	5	0.9	339.0166	33.9528	
99	0.0	0.0	-1.1	-14.7	0.2	-15.9	0.0	-14.7	0.2	39.3	38.1	39.3	-33.3	0.2	-1	0	5	0	0.9	339.0166	33.9432	
100	1.9	2.5	-0.0	-14.9	0.2	-15.2	0.2	-15.2	0.0	39.1	38.7	38.8	-33.0	0.2	1	0	0	5	0.9	339.0187	33.9986	
101	1.0	0.0	-0.0	-15.5	0.0	-16.2	0.0	-15.6	0.0	38.5	37.8	38.4	-33.8	0.0	-2	5	5	1	0.9	339.0188	33.9821	
102	0.1	0.4	-0.5	-14.0	0.1	-15.2	0.1	-14.1	0.1	40.0	38.8	39.9	-32.6	0.1	0	0	0	0	0.9	339.0199	34.0088	
103	1.1	0.3	-0.3	-13.9	0.1	-14.6	0.1	-14.0	0.1	40.0	39.4	39.9	-32.2	0.1	0	0	0	0	0.9	339.0200	33.9837	
104	2.1	2.4	-0.0	-14.9	0.1	-15.1	0.1	-15.2	0.0	39.1	38.8	38.8	-33.0	0.1	1	0	0	5	0.9	339.0205	33.9116	
105	1.4	0.3	-0.3	-14.2	0.1	-14.7	0.1	-14.3	0.1	39.8	39.3	39.7	-32.3	0.1	0	0	0	0	0.9	339.0217	33.9317	
106	1.9	0.3	-0.2	-13.9	0.0	-14.2	0.0	-14.2	0.0	40.1	39.7	39.8	-32.0	0.0	0	0	0	0	0.9	339.0224	33.8989	
107	1.7	0.1	-0.1	-13.3	0.0	-13.7	0.0	-13.5	0.0	40.7	40.3	40.5	-31.4	0.0	0	0	0	0	0.9	339.0271	33.9406	
108	1.9	0.6	-0.5	-14.5	0.1	-14.8	0.1	-14.8	0.1	39.5	39.1	39.2	-32.6	0.1	0	0	0	0	0.9	339.0279	34.0185	

TABLE 19:
Derived quantities and detection codes for X-ray point sources in HCG 92 (online only).

109	1.8	0.7	-0.6	-14.7	0.1	-15.1	0.1	-14.9	0.1	39.3	38.9	39.1	-32.8	0.1	0	0	0	0	0.9	339.0287	33.9635
110	1.5	0.2	-0.2	-13.6	0.0	-14.1	0.0	-13.8	0.0	40.4	39.9	40.2	-31.8	0.0	0	0	0	0	0.9	339.0293	33.9749
111	1.0	0.0	-0.0	-15.5	0.0	-16.2	0.0	-15.6	0.0	38.4	37.7	38.3	-33.8	0.0	-2	5	5	1	0.9	339.0297	33.9936
112	0.0	0.0	-1.1	-14.5	0.2	-15.7	0.0	-14.6	0.2	39.4	38.2	39.4	-33.1	0.2	-1	0	5	0	0.9	339.0310	33.9723
113	-0.6	0.0	-0.6	-14.2	0.1	-15.8	0.0	-14.3	0.1	39.7	38.2	39.7	-33.1	0.1	-1	0	5	0	0.9	339.0308	33.8728
114	1.0	0.0	-0.0	-15.5	0.0	-16.2	0.0	-15.6	0.0	38.5	37.8	38.4	-33.7	0.0	-2	5	5	1	0.9	339.0318	34.0120
115	2.0	1.8	-0.0	-15.0	0.2	-15.3	0.2	-15.3	0.0	39.0	38.7	38.7	-33.1	0.2	1	0	0	1	0.9	339.0322	34.0222
116	2.0	1.8	-0.0	-14.8	0.1	-15.1	0.1	-15.1	0.0	39.2	38.9	38.9	-32.9	0.1	1	0	0	5	0.9	339.0324	33.9212
117	1.0	0.0	-0.0	-15.5	0.0	-16.2	0.0	-15.6	0.0	38.5	37.8	38.4	-33.8	0.0	-2	5	1	5	0.9	339.0338	34.0202
118	1.0	0.0	-0.0	-15.5	0.0	-16.2	0.0	-15.6	0.0	38.4	37.7	38.3	-33.8	0.0	-2	5	1	5	0.9	339.0368	33.9513
119	-0.2	0.0	-0.9	-14.7	0.2	-16.1	0.0	-14.7	0.2	39.3	37.9	39.2	-33.4	0.2	-1	0	1	0	0.9	339.0381	33.8761
120	1.0	0.0	-0.0	-15.5	0.0	-16.2	0.0	-15.6	0.0	38.5	37.8	38.4	-33.8	0.0	-2	1	5	1	0.9	339.0410	34.0260
121	-0.3	0.0	-0.8	-14.3	0.1	-15.7	0.0	-14.3	0.1	39.7	38.3	39.7	-33.0	0.1	-1	0	5	0	0.9	339.0427	33.9549
122	1.0	0.0	-0.0	-15.5	0.0	-16.2	0.0	-15.6	0.0	38.4	37.7	38.3	-33.8	0.0	-2	5	5	5	0.9	339.0443	33.9911
123	-1.1	0.6	-0.0	-13.9	0.1	-15.8	0.0	-13.9	0.1	40.1	38.2	40.0	-33.0	0.1	-1	0	5	0	0.9	339.0468	34.0070
124	1.0	0.0	-0.0	-15.5	0.0	-16.2	0.0	-15.6	0.0	38.4	37.7	38.3	-33.8	0.0	-2	5	5	5	0.9	339.0472	33.9733
125	1.6	3.0	-0.0	-15.1	0.2	-15.5	0.2	-15.3	0.0	38.9	38.4	38.7	-33.2	0.2	1	0	0	5	0.9	339.0479	34.0228
126	1.0	0.0	-0.0	-15.2	0.0	-15.9	0.0	-15.3	0.0	38.8	38.1	38.7	-33.4	0.0	-2	5	5	5	0.9	339.0483	34.0360
127	0.4	0.8	-0.8	-14.6	0.2	-15.6	0.2	-14.6	0.2	39.4	38.4	39.4	-33.0	0.2	0	0	0	0	0.9	339.0507	34.0007
128	0.4	0.0	-1.5	-14.7	0.2	-15.7	0.0	-14.7	0.2	39.3	38.3	39.2	-33.1	0.2	-1	0	5	0	0.9	339.0517	33.9860
129	1.8	2.6	-0.0	-15.0	0.2	-15.4	0.2	-15.2	0.0	39.0	38.6	38.8	-33.1	0.2	1	0	0	1	0.9	339.0534	33.9667
130	1.0	0.0	-0.0	-15.5	0.0	-16.2	0.0	-15.6	0.0	38.4	37.7	38.3	-33.8	0.0	-2	5	5	1	0.9	339.0549	33.9524
131	1.0	0.0	-0.0	-15.5	0.0	-16.2	0.0	-15.6	0.0	38.4	37.7	38.3	-33.8	0.0	-2	5	1	0	0.9	339.0566	34.0038
132	1.7	2.1	-0.0	-15.0	0.2	-15.4	0.2	-15.2	0.0	39.0	38.6	38.8	-33.1	0.2	1	0	0	5	0.9	339.0571	33.9558
133	-0.6	0.0	-0.5	-14.3	0.2	-15.9	0.0	-14.3	0.2	39.7	38.1	39.7	-33.1	0.2	-1	0	1	0	0.9	339.0577	33.9323
134	1.4	0.5	-0.5	-14.5	0.1	-15.0	0.1	-14.6	0.1	39.5	39.0	39.4	-32.6	0.1	0	0	0	0	0.9	339.0581	33.9209
135	1.2	0.6	-0.6	-14.6	0.1	-15.1	0.1	-14.7	0.1	39.4	38.8	39.3	-32.8	0.1	0	0	0	0	0.9	339.0606	33.8995
136	1.0	0.0	-0.0	-15.5	0.0	-16.2	0.0	-15.6	0.0	38.4	37.7	38.3	-33.8	0.0	-2	5	5	1	0.9	339.0638	33.9804
137	1.0	0.0	-0.0	-15.5	0.0	-16.2	0.0	-15.6	0.0	38.4	37.7	38.3	-33.8	0.0	-2	5	5	1	0.9	339.0646	33.9903
138	2.0	1.8	-0.0	-15.0	0.2	-15.3	0.2	-15.3	0.0	38.9	38.6	38.6	-33.2	0.2	1	0	0	1	0.9	339.0687	33.9503
139	-0.8	0.0	-0.3	-14.1	0.1	-15.7	0.0	-14.1	0.1	39.9	38.2	39.9	-33.0	0.1	-1	0	5	0	0.9	339.0694	33.9990
140	0.9	0.4	-0.4	-14.3	0.1	-15.0	0.1	-14.4	0.1	39.7	39.0	39.6	-32.6	0.1	0	0	0	0	0.9	339.0729	33.9126
141	1.0	0.0	-0.0	-15.5	0.0	-16.2	0.0	-15.6	0.0	38.4	37.7	38.3	-33.8	0.0	-2	5	1	5	0.9	339.0770	33.9970
142	1.0	0.0	-0.0	-15.5	0.0	-16.2	0.0	-15.6	0.0	38.4	37.7	38.3	-33.8	0.0	-2	1	5	1	0.9	339.0804	33.9975
143	0.6	0.0	-0.0	-14.9	0.2	-15.8	0.0	-15.0	0.0	39.0	38.2	39.0	-33.3	0.2	-2	0	5	5	0.9	339.0836	33.9973
144	1.0	0.0	-0.0	-15.4	0.0	-16.1	0.0	-15.5	0.0	38.6	37.9	38.5	-33.6	0.0	-2	1	1	1	0.6	0.0000	0.0000
145F	2.9	0.9	-0.0	-14.6	0.1	-14.7	0.1	-15.2	0.0	39.4	39.3	38.8	-32.8	0.1	1	0	0	5	0.9	339.0854	33.9850
146	-0.6	0.6	-0.5	-14.0	0.1	-15.5	0.1	-14.0	0.1	40.0	38.4	40.0	-32.8	0.1	0	0	0	0	0.9	339.0874	34.0131
147	1.9	2.5	-0.0	-14.9	0.1	-15.2	0.1	-15.2	0.0	39.1	38.8	38.8	-33.0	0.1	1	0	0	5	0.9	339.0908	33.9631
148	1.7	0.3	-0.3	-14.1	0.1	-14.5	0.1	-14.3	0.1	39.9	39.5	39.6	-32.2	0.1	0	0	0	0	0.9	339.0927	33.9478
149	1.0	0.0	-0.0	-15.5	0.0	-16.2	0.0	-15.6	0.0	38.5	37.8	38.4	-33.8	0.0	-2	1	1	5	0.9	339.0947	33.9789

TABLE 20:
Counts, count rates and AE detection significance and no-source probabilities for X-ray point sources in HCG 7 (online only).

ID (1)	c(FB) (2)	lim _F (3)	c(SB) (4)	lim _S (5)	c(HB) (6)	lim _S (7)	HR (8)	lim _{HR} (9)	cr(FB) (10)	cr(SB) (11)	cr(HB) (12)	AE(sig) (13)	AE(<i>P</i>) (14)
1	2 ₋₂ ⁺⁰	5	2 ₋₂ ⁺⁰	1	2 ₋₂ ⁺⁰	5	0.00 _{-0.00} ^{+0.00}	-2	0.07 _{-0.07} ^{+0.00}	0.06 _{-0.06} ^{+0.00}	0.07 _{-0.07} ^{+0.00}	8E-01	3E-02
2A	5 ₋₂ ⁺³	0	2 ₋₂ ⁺⁰	5	2 ₋₂ ⁺⁰	5	0.00 _{-0.00} ^{+0.00}	-2	0.14 _{-0.06} ^{+0.09}	0.07 _{-0.07} ^{+0.00}	0.07 _{-0.07} ^{+0.00}	8E-01	4E-02
3	2 ₋₂ ⁺⁰	5	2 ₋₂ ⁺⁰	5	2 ₋₂ ⁺⁰	1	0.00 _{-0.00} ^{+0.00}	-2	0.07 _{-0.07} ^{+0.00}	0.07 _{-0.07} ^{+0.00}	0.06 _{-0.06} ^{+0.00}	-2E-01	1E+00
4A	5 ₋₂ ⁺³	0	2 ₋₂ ⁺⁰	5	2 ₋₂ ⁺⁰	5	0.00 _{-0.00} ^{+0.00}	-2	0.16 _{-0.06} ^{+0.10}	0.07 _{-0.07} ^{+0.00}	0.07 _{-0.07} ^{+0.00}	8E-01	2E-02
5A	160 ₋₁₂ ⁺¹³	0	88 ₋₉ ⁺¹⁰	0	71 ₋₈ ⁺⁹	0	-0.11 _{-0.08} ^{+0.08}	0	4.46 _{-0.35} ^{+0.38}	2.47 _{-0.26} ^{+0.29}	1.99 _{-0.23} ^{+0.26}	7E+00	0E+00
6A	102 ₋₁₀ ⁺¹¹	0	82 ₋₉ ⁺¹⁰	0	19 ₋₄ ⁺⁵	0	-0.62 _{-0.08} ^{+0.09}	0	2.85 _{-0.28} ^{+0.31}	2.31 _{-0.25} ^{+0.28}	0.54 _{-0.12} ^{+0.15}	3E+00	3E-22
7A	4 ₋₁ ⁺³	0	2 ₋₂ ⁺⁰	5	2 ₋₂ ⁺⁰	5	0.00 _{-0.00} ^{+0.00}	-2	0.12 _{-0.05} ^{+0.09}	0.07 _{-0.07} ^{+0.00}	0.07 _{-0.07} ^{+0.00}	6E-01	5E-02
8	32 ₋₅ ⁺⁶	0	23 ₋₄ ⁺⁶	0	8 ₋₂ ⁺⁴	0	-0.46 _{-0.16} ^{+0.19}	0	0.91 _{-0.16} ^{+0.19}	0.67 _{-0.14} ^{+0.17}	0.24 _{-0.08} ^{+0.11}	2E+00	6E-12
9A	42 ₋₆ ⁺⁷	0	34 ₋₅ ⁺⁷	0	7 ₋₂ ⁺³	0	-0.64 _{-0.12} ^{+0.15}	0	1.18 _{-0.18} ^{+0.21}	0.97 _{-0.16} ^{+0.19}	0.21 _{-0.08} ^{+0.11}	2E+00	5E-09
10	2 ₋₂ ⁺⁰	5	2 ₋₂ ⁺⁰	5	2 ₋₂ ⁺⁰	1	0.00 _{-0.00} ^{+0.00}	-2	0.07 _{-0.07} ^{+0.00}	0.07 _{-0.07} ^{+0.00}	0.06 _{-0.06} ^{+0.00}	-9E-02	1E+00
11	2 ₋₂ ⁺⁰	5	2 ₋₂ ⁺⁰	5	2 ₋₂ ⁺⁰	5	0.00 _{-0.00} ^{+0.00}	-2	0.07 _{-0.07} ^{+0.00}	0.07 _{-0.07} ^{+0.00}	0.07 _{-0.07} ^{+0.00}	2E-01	4E-01
12A	6 ₋₃ ⁺³	0	4 ₋₂ ⁺³	0	2 ₋₂ ⁺⁰	5	-0.35 _{-0.65} ^{+0.00}	1	0.19 _{-0.07} ^{+0.10}	0.14 _{-0.06} ^{+0.09}	0.07 _{-0.07} ^{+0.00}	7E-01	2E-02
13D	7 ₋₃ ⁺³	0	4 ₋₂ ⁺³	0	2 ₋₂ ⁺⁰	5	-0.34 _{-0.66} ^{+0.00}	1	0.22 _{-0.08} ^{+0.11}	0.14 _{-0.06} ^{+0.08}	0.07 _{-0.07} ^{+0.00}	1E+00	5E-04
14	2 ₋₂ ⁺⁰	5	2 ₋₂ ⁺⁰	1	2 ₋₂ ⁺⁰	5	0.00 _{-0.00} ^{+0.00}	-2	0.07 _{-0.07} ^{+0.00}	0.06 _{-0.06} ^{+0.00}	0.07 _{-0.07} ^{+0.00}	7E-01	6E-02
15B	9 ₋₃ ⁺⁴	0	8 ₋₂ ⁺⁴	0	2 ₋₂ ⁺⁰	5	-0.58 _{-0.42} ^{+0.00}	1	0.27 _{-0.09} ^{+0.12}	0.25 _{-0.08} ^{+0.11}	0.07 _{-0.07} ^{+0.00}	4E-01	1E-01
16B	83 ₋₉ ⁺¹⁰	0	81 ₋₉ ⁺¹⁰	0	2 ₋₂ ⁺⁰	5	-0.94 _{-0.06} ^{+0.00}	1	2.34 _{-0.25} ^{+0.28}	2.28 _{-0.25} ^{+0.28}	0.07 _{-0.07} ^{+0.00}	7E-01	8E-03
17B	12 ₋₃ ⁺⁴	0	9 ₋₃ ⁺⁴	0	2 ₋₂ ⁺⁰	5	-0.61 _{-0.39} ^{+0.00}	1	0.36 _{-0.10} ^{+0.13}	0.28 _{-0.09} ^{+0.12}	0.07 _{-0.07} ^{+0.00}	1E+00	3E-04
18	2 ₋₂ ⁺⁰	5	2 ₋₂ ⁺⁰	5	2 ₋₂ ⁺⁰	1	0.00 _{-0.00} ^{+0.00}	-2	0.07 _{-0.07} ^{+0.00}	0.07 _{-0.07} ^{+0.00}	0.06 _{-0.06} ^{+0.00}	-8E-02	1E+00
19	2 ₋₂ ⁺⁰	5	2 ₋₂ ⁺⁰	5	2 ₋₂ ⁺⁰	5	0.00 _{-0.00} ^{+0.00}	-2	0.07 _{-0.07} ^{+0.00}	0.07 _{-0.07} ^{+0.00}	0.07 _{-0.07} ^{+0.00}	2E-01	4E-01
20	2 ₋₂ ⁺⁰	5	2 ₋₂ ⁺⁰	5	2 ₋₂ ⁺⁰	1	0.00 _{-0.00} ^{+0.00}	-2	0.07 _{-0.07} ^{+0.00}	0.07 _{-0.07} ^{+0.00}	0.06 _{-0.06} ^{+0.00}	-2E-01	1E+00
21D	21 ₋₄ ⁺⁵	0	18 ₋₄ ⁺⁵	0	2 ₋₂ ⁺⁰	5	-0.78 _{-0.22} ^{+0.00}	1	0.61 _{-0.13} ^{+0.16}	0.53 _{-0.12} ^{+0.15}	0.07 _{-0.07} ^{+0.00}	1E+00	3E-04
22	21 ₋₄ ⁺⁵	0	4 ₋₂ ⁺³	0	16 ₋₄ ⁺⁵	0	0.55 _{-0.23} ^{+0.19}	0	0.60 _{-0.13} ^{+0.16}	0.14 _{-0.06} ^{+0.09}	0.47 _{-0.11} ^{+0.14}	3E+00	1E-24
23	78 ₋₈ ⁺⁹	0	59 ₋₇ ⁺⁸	0	18 ₋₄ ⁺⁵	0	-0.53 _{-0.10} ^{+0.11}	0	2.19 _{-0.25} ^{+0.28}	1.67 _{-0.21} ^{+0.24}	0.52 _{-0.12} ^{+0.15}	3E+00	8E-25
24	77 ₋₈ ⁺⁹	0	65 ₋₈ ⁺⁹	0	11 ₋₃ ⁺⁴	0	-0.70 _{-0.08} ^{+0.10}	0	2.17 _{-0.25} ^{+0.27}	1.84 _{-0.23} ^{+0.26}	0.33 _{-0.09} ^{+0.13}	3E+00	8E-18
25	2 ₋₂ ⁺⁰	5	2 ₋₂ ⁺⁰	1	2 ₋₂ ⁺⁰	5	0.00 _{-0.00} ^{+0.00}	-2	0.07 _{-0.07} ^{+0.00}	0.06 _{-0.06} ^{+0.00}	0.07 _{-0.07} ^{+0.00}	7E-01	4E-03
26	19 ₋₄ ⁺⁵	0	2 ₋₂ ⁺⁰	5	16 ₋₄ ⁺⁵	0	0.73 _{-0.00} ^{+0.27}	-1	0.55 _{-0.12} ^{+0.15}	0.07 _{-0.07} ^{+0.00}	0.45 _{-0.11} ^{+0.14}	3E+00	2E-09
27	2 ₋₂ ⁺⁰	5	2 ₋₂ ⁺⁰	5	2 ₋₂ ⁺⁰	1	0.00 _{-0.00} ^{+0.00}	-2	0.07 _{-0.07} ^{+0.00}	0.07 _{-0.07} ^{+0.00}	0.06 _{-0.06} ^{+0.00}	-4E-01	1E+00
28	85 ₋₉ ⁺¹⁰	0	48 ₋₆ ⁺⁸	0	37 ₋₆ ⁺⁷	0	-0.12 _{-0.11} ^{+0.12}	0	2.39 _{-0.26} ^{+0.29}	1.34 _{-0.19} ^{+0.22}	1.05 _{-0.17} ^{+0.20}	5E+00	7E-23
29	4 ₋₂ ⁺³	0	2 ₋₂ ⁺⁰	5	2 ₋₂ ⁺⁰	5	0.00 _{-0.00} ^{+0.00}	-2	0.14 _{-0.06} ^{+0.09}	0.07 _{-0.07} ^{+0.00}	0.07 _{-0.07} ^{+0.00}	7E-01	4E-03
30	8 ₋₂ ⁺⁴	0	5 ₋₂ ⁺³	0	2 ₋₂ ⁺⁰	5	-0.42 _{-0.58} ^{+0.00}	1	0.23 _{-0.08} ^{+0.11}	0.16 _{-0.07} ^{+0.10}	0.07 _{-0.07} ^{+0.00}	9E-01	1E-02
31	2 ₋₂ ⁺⁰	5	2 ₋₂ ⁺⁰	1	2 ₋₂ ⁺⁰	5	0.00 _{-0.00} ^{+0.00}	-2	0.07 _{-0.07} ^{+0.00}	0.06 _{-0.06} ^{+0.00}	0.07 _{-0.07} ^{+0.00}	7E-01	7E-03
32	6 ₋₃ ⁺³	0	2 ₋₂ ⁺⁰	5	2 ₋₂ ⁺⁰	5	0.00 _{-0.00} ^{+0.00}	-2	0.17 _{-0.07} ^{+0.10}	0.07 _{-0.07} ^{+0.00}	0.07 _{-0.07} ^{+0.00}	9E-01	3E-02
33	2 ₋₂ ⁺⁰	5	2 ₋₂ ⁺⁰	5	2 ₋₂ ⁺⁰	5	0.00 _{-0.00} ^{+0.00}	-2	0.07 _{-0.07} ^{+0.00}	0.07 _{-0.07} ^{+0.00}	0.07 _{-0.07} ^{+0.00}	7E-01	1E-02
34	12 ₋₃ ⁺⁴	0	2 ₋₂ ⁺⁰	5	9 ₋₃ ⁺⁴	0	0.60 _{-0.00} ^{+0.40}	-1	0.35 _{-0.10} ^{+0.13}	0.07 _{-0.07} ^{+0.00}	0.27 _{-0.09} ^{+0.12}	2E+00	9E-14
35	2 ₋₂ ⁺⁰	5	2 ₋₂ ⁺⁰	5	2 ₋₂ ⁺⁰	5	0.00 _{-0.00} ^{+0.00}	-2	0.07 _{-0.07} ^{+0.00}	0.07 _{-0.07} ^{+0.00}	0.07 _{-0.07} ^{+0.00}	6E-01	6E-02
36	8 ₋₂ ⁺⁴	0	2 ₋₂ ⁺⁰	5	6 ₋₃ ⁺³	0	0.45 _{-0.00} ^{+0.55}	-1	0.23 _{-0.08} ^{+0.11}	0.07 _{-0.07} ^{+0.00}	0.18 _{-0.07} ^{+0.10}	2E+00	2E-06
37	4 ₋₂ ⁺³	0	2 ₋₂ ⁺⁰	5	2 ₋₂ ⁺⁰	5	0.00 _{-0.00} ^{+0.00}	-2	0.12 _{-0.06} ^{+0.09}	0.07 _{-0.07} ^{+0.00}	0.07 _{-0.07} ^{+0.00}	8E-01	2E-02
38	18 ₋₄ ⁺⁵	0	15 ₋₃ ⁺⁵	0	2 ₋₂ ⁺⁰	5	-0.72 _{-0.28} ^{+0.00}	1	0.50 _{-0.12} ^{+0.15}	0.43 _{-0.11} ^{+0.14}	0.07 _{-0.07} ^{+0.00}	6E-01	2E-01
39	12 ₋₃ ⁺⁴	0	2 ₋₂ ⁺⁰	1	12 ₋₃ ⁺⁴	0	0.69 _{-0.00} ^{+0.31}	-1	0.35 _{-0.10} ^{+0.13}	0.06 _{-0.06} ^{+0.00}	0.36 _{-0.10} ^{+0.13}	3E+00	5E-19
40C	9 ₋₃ ⁺⁴	0	6 ₋₂ ⁺³	0	2 ₋₂ ⁺⁰	5	-0.47 _{-0.53} ^{+0.00}	1	0.26 _{-0.08} ^{+0.12}	0.19 _{-0.07} ^{+0.10}	0.07 _{-0.07} ^{+0.00}	9E-01	1E-02
41	19 ₋₄ ⁺⁵	0	14 ₋₃ ⁺⁵	0	4 ₋₂ ⁺³	0	-0.52 _{-0.21} ^{+0.25}	0	0.55 _{-0.12} ^{+0.15}	0.41 _{-0.11} ^{+0.14}	0.13 _{-0.06} ^{+0.09}	1E+00	1E-05
42C	27 ₋₅ ⁺⁶	0	24 ₋₄ ⁺⁶	0	2 ₋₂ ⁺⁰	5	-0.82 _{-0.18} ^{+0.00}	1	0.78 _{-0.15} ^{+0.14}	0.68 _{-0.14} ^{+0.17}	0.07 _{-0.07} ^{+0.00}	1E+00	3E-03

TABLE 20:

Counts, count rates and AE detection significance and no-source probabilities for X-ray point sources in HCG 7 (online only).

43	2^{+0}_{-2}	5	2^{+0}_{-2}	5	2^{+0}_{-2}	5	$0.00^{+0.00}_{-0.00}$	-2	$0.07^{+0.00}_{-0.07}$	$0.07^{+0.00}_{-0.07}$	$0.07^{+0.00}_{-0.07}$	5E-01	2E-01
44C	12^{+4}_{-3}	0	12^{+4}_{-3}	0	2^{+0}_{-2}	5	$-0.68^{+0.00}_{-0.32}$	1	$0.36^{+0.13}_{-0.10}$	$0.35^{+0.13}_{-0.10}$	$0.07^{+0.00}_{-0.07}$	2E-01	5E-01
45	2^{+0}_{-2}	5	2^{+0}_{-2}	1	2^{+0}_{-2}	5	$0.00^{+0.00}_{-0.00}$	-2	$0.07^{+0.00}_{-0.07}$	$0.06^{+0.00}_{-0.06}$	$0.07^{+0.00}_{-0.07}$	9E-01	5E-03
46C	7^{+3}_{-2}	0	7^{+3}_{-2}	0	2^{+0}_{-2}	1	$-0.53^{+0.00}_{-0.47}$	1	$0.20^{+0.11}_{-0.07}$	$0.21^{+0.11}_{-0.07}$	$0.06^{+0.00}_{-0.06}$	-3E-01	1E+00
47	2^{+0}_{-2}	5	2^{+0}_{-2}	5	2^{+0}_{-2}	1	$0.00^{+0.00}_{-0.00}$	-2	$0.07^{+0.00}_{-0.07}$	$0.07^{+0.00}_{-0.07}$	$0.06^{+0.00}_{-0.06}$	-3E-01	1E+00
48C	28^{+6}_{-5}	0	19^{+5}_{-4}	0	9^{+4}_{-3}	0	$-0.36^{+0.21}_{-0.19}$	0	$0.80^{+0.18}_{-0.15}$	$0.54^{+0.15}_{-0.12}$	$0.26^{+0.12}_{-0.08}$	2E+00	4E-08
49	74^{+9}_{-8}	0	54^{+8}_{-7}	0	20^{+5}_{-4}	0	$-0.46^{+0.12}_{-0.11}$	0	$2.09^{+0.27}_{-0.24}$	$1.53^{+0.24}_{-0.21}$	$0.56^{+0.16}_{-0.12}$	3E+00	1E-12
50	2^{+0}_{-2}	5	2^{+0}_{-2}	5	2^{+0}_{-2}	5	$0.00^{+0.00}_{-0.00}$	-2	$0.07^{+0.00}_{-0.07}$	$0.07^{+0.00}_{-0.07}$	$0.07^{+0.00}_{-0.07}$	9E-01	1E-02
51C	465^{+22}_{-21}	0	371^{+20}_{-19}	0	93^{+10}_{-9}	0	$-0.60^{+0.04}_{-0.04}$	0	$12.96^{+0.63}_{-0.60}$	$10.35^{+0.57}_{-0.54}$	$2.61^{+0.30}_{-0.27}$	9E+00	0E+00
52	13^{+4}_{-3}	0	2^{+0}_{-2}	5	11^{+4}_{-3}	0	$0.65^{+0.35}_{-0.00}$	-1	$0.37^{+0.13}_{-0.10}$	$0.07^{+0.00}_{-0.07}$	$0.32^{+0.13}_{-0.09}$	2E+00	6E-07
53	3^{+3}_{-1}	0	2^{+0}_{-2}	5	2^{+0}_{-2}	5	$0.00^{+0.00}_{-0.00}$	-2	$0.11^{+0.09}_{-0.05}$	$0.07^{+0.00}_{-0.07}$	$0.07^{+0.00}_{-0.07}$	8E-01	4E-02
54	2^{+0}_{-2}	5	2^{+0}_{-2}	1	2^{+0}_{-2}	5	$0.00^{+0.00}_{-0.00}$	-2	$0.07^{+0.00}_{-0.07}$	$0.06^{+0.00}_{-0.06}$	$0.07^{+0.00}_{-0.07}$	1E+00	4E-03
55	2^{+0}_{-2}	5	2^{+0}_{-2}	5	2^{+0}_{-2}	1	$0.00^{+0.00}_{-0.00}$	-2	$0.07^{+0.00}_{-0.07}$	$0.07^{+0.00}_{-0.07}$	$0.06^{+0.00}_{-0.06}$	-2E-01	1E+00
56	2^{+0}_{-2}	1	2^{+0}_{-2}	5	2^{+0}_{-2}	1	$0.00^{+0.00}_{-0.00}$	-2	$0.07^{+0.00}_{-0.07}$	$0.07^{+0.00}_{-0.07}$	$0.07^{+0.00}_{-0.07}$	-1E+00	1E+00
57	3^{+3}_{-1}	0	2^{+0}_{-2}	1	4^{+3}_{-2}	0	$0.30^{+0.70}_{-0.00}$	-1	$0.11^{+0.09}_{-0.05}$	$0.06^{+0.00}_{-0.06}$	$0.12^{+0.09}_{-0.06}$	1E+00	8E-04
58	9^{+4}_{-3}	0	5^{+3}_{-2}	0	4^{+3}_{-2}	0	$-0.14^{+0.38}_{-0.36}$	0	$0.28^{+0.12}_{-0.09}$	$0.16^{+0.10}_{-0.06}$	$0.12^{+0.09}_{-0.05}$	1E+00	1E-03
59	61^{+8}_{-7}	0	43^{+7}_{-6}	0	17^{+5}_{-4}	0	$-0.43^{+0.12}_{-0.12}$	0	$1.71^{+0.25}_{-0.22}$	$1.22^{+0.18}_{-0.18}$	$0.49^{+0.15}_{-0.12}$	3E+00	5E-22
60	4^{+3}_{-1}	0	2^{+0}_{-2}	5	2^{+0}_{-2}	5	$0.00^{+0.00}_{-0.00}$	-2	$0.12^{+0.05}_{-0.05}$	$0.07^{+0.00}_{-0.07}$	$0.07^{+0.00}_{-0.07}$	5E-01	1E-01
61	14^{+5}_{-3}	0	8^{+4}_{-2}	0	6^{+3}_{-2}	0	$-0.17^{+0.30}_{-0.29}$	0	$0.41^{+0.14}_{-0.11}$	$0.24^{+0.11}_{-0.08}$	$0.17^{+0.10}_{-0.07}$	1E+00	3E-03

TABLE 21:
Counts, count rates and AE detection significance and no-source probabilities for X-ray point sources in HCG 16 (online only).

ID (1)	c(FB) (2)	lim _F (3)	c(SB) (4)	lim _S (5)	c(HB) (6)	lim _S (7)	HR (8)	lim _{HR} (9)	cr(FB) (10)	cr(SB) (11)	cr(HB) (12)	AE(sig) (13)	AE(<i>P</i>) (14)
1	15^{+5}_{-3}	0	6^{+3}_{-2}	0	8^{+4}_{-2}	0	$0.12^{+0.29}_{-0.30}$	0	$1.22^{+0.40}_{-0.31}$	$0.54^{+0.30}_{-0.20}$	$0.68^{+0.32}_{-0.23}$	2E+00	3E-09
2	8^{+4}_{-2}	0	3^{+3}_{-1}	0	4^{+3}_{-2}	0	$0.11^{+0.40}_{-0.42}$	0	$0.67^{+0.32}_{-0.23}$	$0.30^{+0.25}_{-0.15}$	$0.37^{+0.27}_{-0.17}$	1E+00	4E-05
3	2^{+0}_{-2}	5	2^{+0}_{-2}	1	2^{+0}_{-2}	5	$0.00^{+0.00}_{-0.00}$	-2	$0.19^{+0.00}_{-0.19}$	$0.18^{+0.00}_{-0.18}$	$0.20^{+0.00}_{-0.20}$	7E-01	3E-02
4B	189^{+14}_{-13}	0	39^{+7}_{-6}	0	150^{+13}_{-12}	0	$0.58^{+0.06}_{-0.07}$	0	$15.11^{+1.18}_{-1.10}$	$3.17^{+0.59}_{-0.50}$	$11.95^{+1.06}_{-0.97}$	1E+01	0E+00
5	10^{+4}_{-3}	0	7^{+3}_{-2}	0	2^{+0}_{-2}	5	$-0.47^{+0.00}_{-0.53}$	1	$0.85^{+0.35}_{-0.26}$	$0.62^{+0.31}_{-0.22}$	$0.22^{+0.00}_{-0.22}$	1E+00	1E-03
6	9^{+4}_{-3}	0	7^{+3}_{-2}	0	2^{+0}_{-2}	5	$-0.51^{+0.00}_{-0.49}$	1	$0.79^{+0.34}_{-0.25}$	$0.60^{+0.31}_{-0.21}$	$0.20^{+0.00}_{-0.20}$	8E-01	3E-02
7	3^{+3}_{-1}	0	3^{+0}_{-3}	5	2^{+0}_{-2}	5	$0.00^{+0.00}_{-0.00}$	-2	$0.30^{+0.05}_{-0.15}$	$0.29^{+0.00}_{-0.29}$	$0.20^{+0.00}_{-0.20}$	4E-01	1E-01
8	2^{+0}_{-2}	5	3^{+0}_{-3}	5	2^{+0}_{-2}	1	$0.00^{+0.00}_{-0.00}$	-2	$0.22^{+0.00}_{-0.22}$	$0.26^{+0.00}_{-0.26}$	$0.18^{+0.00}_{-0.18}$	-5E-02	1E+00
9A	134^{+12}_{-11}	0	92^{+10}_{-9}	0	42^{+7}_{-6}	0	$-0.37^{+0.09}_{-0.08}$	0	$10.73^{+1.01}_{-0.92}$	$7.35^{+0.85}_{-0.76}$	$3.38^{+0.60}_{-0.52}$	6E+00	0E+00
10	3^{+3}_{-1}	0	2^{+0}_{-2}	1	4^{+3}_{-2}	0	$0.30^{+0.70}_{-0.00}$	-1	$0.30^{+0.25}_{-0.15}$	$0.18^{+0.00}_{-0.18}$	$0.34^{+0.26}_{-0.16}$	1E+00	1E-03
11	3^{+0}_{-1}	5	4^{+0}_{-4}	5	2^{+0}_{-2}	5	$0.00^{+0.00}_{-0.00}$	-2	$0.29^{+0.00}_{-0.29}$	$0.36^{+0.00}_{-0.36}$	$0.22^{+0.00}_{-0.22}$	4E-01	6E-02
12	3^{+3}_{-1}	0	4^{+3}_{-1}	0	2^{+0}_{-2}	1	$-0.26^{+0.00}_{-0.74}$	1	$0.31^{+0.25}_{-0.15}$	$0.32^{+0.15}_{-0.15}$	$0.18^{+0.00}_{-0.18}$	-4E-02	1E+00
13	2^{+0}_{-2}	5	3^{+0}_{-3}	5	2^{+0}_{-2}	1	$0.00^{+0.00}_{-0.00}$	-2	$0.22^{+0.00}_{-0.22}$	$0.28^{+0.00}_{-0.28}$	$0.18^{+0.00}_{-0.18}$	-5E-02	1E+00
14	3^{+3}_{-3}	5	3^{+0}_{-3}	5	2^{+0}_{-2}	5	$0.00^{+0.00}_{-0.00}$	-2	$0.25^{+0.00}_{-0.25}$	$0.26^{+0.00}_{-0.26}$	$0.22^{+0.00}_{-0.22}$	4E-01	6E-02
15A	50^{+8}_{-7}	0	38^{+7}_{-6}	0	11^{+4}_{-3}	0	$-0.54^{+0.14}_{-0.12}$	0	$3.99^{+0.63}_{-0.56}$	$3.07^{+0.58}_{-0.49}$	$0.92^{+0.36}_{-0.27}$	3E+00	1E-13
16	3^{+0}_{-3}	5	2^{+0}_{-2}	1	4^{+0}_{-4}	5	$0.00^{+0.00}_{-0.00}$	-2	$0.25^{+0.00}_{-0.25}$	$0.18^{+0.00}_{-0.18}$	$0.36^{+0.00}_{-0.36}$	7E-01	5E-04
17	3^{+3}_{-3}	5	4^{+0}_{-4}	5	2^{+0}_{-2}	1	$0.00^{+0.00}_{-0.00}$	-2	$0.25^{+0.00}_{-0.25}$	$0.36^{+0.00}_{-0.36}$	$0.18^{+0.00}_{-0.18}$	-2E-02	1E+00
18	5^{+3}_{-2}	0	5^{+0}_{-5}	5	3^{+0}_{-3}	5	$0.00^{+0.00}_{-0.00}$	-2	$0.47^{+0.29}_{-0.19}$	$0.46^{+0.00}_{-0.46}$	$0.29^{+0.00}_{-0.29}$	1E+00	1E-04
19	8^{+4}_{-2}	0	9^{+4}_{-2}	0	2^{+0}_{-2}	1	$-0.59^{+0.00}_{-0.41}$	1	$0.71^{+0.33}_{-0.23}$	$0.71^{+0.33}_{-0.23}$	$0.18^{+0.00}_{-0.18}$	-6E-03	1E+00
20	22^{+5}_{-4}	0	20^{+5}_{-4}	0	3^{+0}_{-3}	5	$-0.70^{+0.00}_{-0.30}$	1	$1.82^{+0.47}_{-0.38}$	$1.59^{+0.44}_{-0.35}$	$0.28^{+0.00}_{-0.28}$	1E+00	2E-04
21	52^{+8}_{-7}	0	2^{+0}_{-2}	5	51^{+8}_{-7}	0	$0.90^{+0.10}_{-0.00}$	-1	$4.21^{+0.66}_{-0.58}$	$0.23^{+0.00}_{-0.23}$	$4.13^{+0.66}_{-0.57}$	6E+00	0E+00
22	3^{+0}_{-3}	5	2^{+0}_{-2}	1	4^{+0}_{-4}	5	$0.00^{+0.00}_{-0.00}$	-2	$0.24^{+0.00}_{-0.24}$	$0.18^{+0.00}_{-0.18}$	$0.36^{+0.00}_{-0.36}$	7E-01	5E-04
23	2^{+0}_{-2}	5	2^{+0}_{-2}	1	3^{+0}_{-3}	5	$0.00^{+0.00}_{-0.00}$	-2	$0.21^{+0.00}_{-0.21}$	$0.18^{+0.00}_{-0.18}$	$0.26^{+0.00}_{-0.26}$	4E-01	3E-02
24	2^{+0}_{-2}	5	3^{+0}_{-3}	5	2^{+0}_{-2}	5	$0.00^{+0.00}_{-0.00}$	-2	$0.23^{+0.00}_{-0.23}$	$0.24^{+0.00}_{-0.24}$	$0.21^{+0.00}_{-0.21}$	4E-01	8E-02
25	2^{+0}_{-2}	5	2^{+0}_{-2}	1	2^{+0}_{-2}	5	$0.00^{+0.00}_{-0.00}$	-2	$0.22^{+0.00}_{-0.22}$	$0.18^{+0.00}_{-0.18}$	$0.23^{+0.00}_{-0.23}$	7E-01	6E-03
26	8^{+4}_{-2}	0	2^{+0}_{-2}	5	7^{+3}_{-2}	0	$0.50^{+0.50}_{-0.00}$	-1	$0.70^{+0.32}_{-0.23}$	$0.21^{+0.00}_{-0.21}$	$0.62^{+0.31}_{-0.22}$	2E+00	2E-10
27	14^{+5}_{-3}	0	5^{+3}_{-2}	0	9^{+4}_{-2}	0	$0.20^{+0.28}_{-0.30}$	0	$1.19^{+0.39}_{-0.30}$	$0.47^{+0.29}_{-0.19}$	$0.71^{+0.33}_{-0.23}$	2E+00	3E-15
28	3^{+0}_{-3}	5	2^{+0}_{-2}	1	3^{+0}_{-3}	5	$0.00^{+0.00}_{-0.00}$	-2	$0.28^{+0.00}_{-0.28}$	$0.18^{+0.00}_{-0.18}$	$0.28^{+0.00}_{-0.28}$	7E-01	1E-03
29	3^{+0}_{-3}	5	2^{+0}_{-2}	1	3^{+0}_{-3}	5	$0.00^{+0.00}_{-0.00}$	-2	$0.26^{+0.00}_{-0.26}$	$0.18^{+0.00}_{-0.18}$	$0.31^{+0.00}_{-0.31}$	7E-01	6E-04
30	3^{+0}_{-3}	5	2^{+0}_{-2}	1	3^{+0}_{-3}	5	$0.00^{+0.00}_{-0.00}$	-2	$0.25^{+0.00}_{-0.25}$	$0.18^{+0.00}_{-0.18}$	$0.31^{+0.00}_{-0.31}$	7E-01	7E-04
31	3^{+0}_{-3}	5	3^{+0}_{-3}	5	3^{+0}_{-3}	5	$0.00^{+0.00}_{-0.00}$	-2	$0.31^{+0.00}_{-0.31}$	$0.31^{+0.00}_{-0.31}$	$0.24^{+0.00}_{-0.24}$	4E-01	3E-02
32	32^{+6}_{-5}	0	21^{+5}_{-4}	0	10^{+4}_{-3}	0	$-0.34^{+0.19}_{-0.18}$	0	$2.60^{+0.54}_{-0.45}$	$1.75^{+0.46}_{-0.37}$	$0.86^{+0.35}_{-0.26}$	2E+00	6E-14
33	2^{+0}_{-2}	5	2^{+0}_{-2}	1	3^{+0}_{-3}	5	$0.00^{+0.00}_{-0.00}$	-2	$0.23^{+0.00}_{-0.23}$	$0.18^{+0.00}_{-0.18}$	$0.25^{+0.00}_{-0.25}$	7E-01	3E-03
34	3^{+0}_{-3}	5	3^{+0}_{-3}	5	2^{+0}_{-2}	5	$0.00^{+0.00}_{-0.00}$	-2	$0.25^{+0.00}_{-0.25}$	$0.24^{+0.00}_{-0.24}$	$0.23^{+0.00}_{-0.23}$	4E-01	5E-02
35	2^{+0}_{-2}	5	2^{+0}_{-2}	1	3^{+0}_{-3}	5	$0.00^{+0.00}_{-0.00}$	-2	$0.23^{+0.00}_{-0.23}$	$0.18^{+0.00}_{-0.18}$	$0.24^{+0.00}_{-0.24}$	4E-01	3E-02
36	2^{+0}_{-2}	5	2^{+0}_{-2}	5	3^{+0}_{-3}	5	$0.00^{+0.00}_{-0.00}$	-2	$0.19^{+0.00}_{-0.19}$	$0.19^{+0.00}_{-0.19}$	$0.24^{+0.00}_{-0.24}$	7E-01	5E-03
37	2^{+0}_{-2}	5	2^{+0}_{-2}	1	2^{+0}_{-2}	5	$0.00^{+0.00}_{-0.00}$	-2	$0.21^{+0.00}_{-0.21}$	$0.18^{+0.00}_{-0.18}$	$0.23^{+0.00}_{-0.23}$	1E+00	9E-04
38	2^{+0}_{-2}	5	2^{+0}_{-2}	5	2^{+0}_{-2}	1	$0.00^{+0.00}_{-0.00}$	-2	$0.19^{+0.00}_{-0.19}$	$0.19^{+0.00}_{-0.19}$	$0.18^{+0.00}_{-0.18}$	-8E-02	1E+00
39	2^{+0}_{-2}	1	2^{+0}_{-2}	1	2^{+0}_{-2}	1	$0.00^{+0.00}_{-0.00}$	-2	$0.18^{+0.00}_{-0.18}$	$0.19^{+0.00}_{-0.19}$	$0.18^{+0.00}_{-0.18}$	-1E-01	1E+00
40	4^{+3}_{-1}	0	4^{+0}_{-4}	5	4^{+0}_{-4}	5	$0.00^{+0.00}_{-0.00}$	-2	$0.32^{+0.25}_{-0.15}$	$0.36^{+0.00}_{-0.36}$	$0.36^{+0.00}_{-0.36}$	7E-01	3E-04
41	2^{+0}_{-2}	5	2^{+0}_{-2}	5	2^{+0}_{-2}	1	$0.00^{+0.00}_{-0.00}$	-2	$0.19^{+0.00}_{-0.19}$	$0.19^{+0.00}_{-0.19}$	$0.18^{+0.00}_{-0.18}$	-5E-02	1E+00
42	2^{+0}_{-2}	5	3^{+0}_{-3}	5	2^{+0}_{-2}	1	$0.00^{+0.00}_{-0.00}$	-2	$0.23^{+0.00}_{-0.23}$	$0.31^{+0.00}_{-0.31}$	$0.18^{+0.00}_{-0.18}$	-4E-02	1E+00

TABLE 21:

Counts, count rates and AE detection significance and no-source probabilities for X-ray point sources in HCG 16 (online only).

43C	9_{-3}^{+4}	0	6_{-2}^{+3}	0	2_{-2}^{+0}	5	$-0.40_{-0.60}^{+0.00}$	1	$0.74_{-0.24}^{+0.33}$	$0.52_{-0.20}^{+0.29}$	$0.22_{-0.22}^{+0.00}$	1E+00	2E-03
44C	24_{-4}^{+6}	0	20_{-4}^{+5}	0	3_{-1}^{+3}	0	$-0.69_{-0.15}^{+0.21}$	0	$1.92_{-0.39}^{+0.48}$	$1.62_{-0.36}^{+0.45}$	$0.30_{-0.15}^{+0.25}$	1E+00	4E-04
45	2_{-2}^{+0}	5	2_{-2}^{+0}	5	2_{-2}^{+0}	1	$0.00_{-0.00}^{+0.00}$	-2	$0.19_{-0.19}^{+0.00}$	$0.19_{-0.19}^{+0.00}$	$0.18_{-0.18}^{+0.00}$	-1E-01	1E+00
46C	5_{-2}^{+3}	0	6_{-2}^{+3}	0	2_{-2}^{+0}	1	$-0.44_{-0.56}^{+0.00}$	1	$0.44_{-0.18}^{+0.28}$	$0.47_{-0.19}^{+0.29}$	$0.18_{-0.18}^{+0.00}$	-3E-01	1E+00
47	2_{-2}^{+0}	5	2_{-2}^{+0}	5	2_{-2}^{+0}	1	$0.00_{-0.00}^{+0.00}$	-2	$0.19_{-0.19}^{+0.00}$	$0.19_{-0.19}^{+0.00}$	$0.18_{-0.18}^{+0.00}$	-4E-02	1E+00
48C	11_{-3}^{+4}	0	9_{-2}^{+4}	0	2_{-2}^{+0}	5	$-0.54_{-0.46}^{+0.00}$	1	$0.94_{-0.27}^{+0.36}$	$0.72_{-0.23}^{+0.33}$	$0.21_{-0.21}^{+0.00}$	9E-01	3E-03
49	4_{-4}^{+0}	5	2_{-2}^{+0}	1	4_{-4}^{+0}	5	$0.00_{-0.00}^{+0.00}$	-2	$0.36_{-0.36}^{+0.00}$	$0.18_{-0.18}^{+0.00}$	$0.36_{-0.36}^{+0.00}$	7E-01	3E-04
50C	5_{-2}^{+3}	0	5_{-2}^{+3}	0	2_{-2}^{+0}	1	$-0.43_{-0.57}^{+0.00}$	1	$0.45_{-0.18}^{+0.28}$	$0.47_{-0.19}^{+0.28}$	$0.18_{-0.18}^{+0.00}$	-1E-01	1E+00
51	29_{-5}^{+6}	0	25_{-5}^{+6}	0	4_{-1}^{+3}	0	$-0.73_{-0.13}^{+0.18}$	0	$2.31_{-0.43}^{+0.51}$	$1.99_{-0.39}^{+0.48}$	$0.32_{-0.15}^{+0.25}$	1E+00	1E-07
52	2_{-2}^{+0}	5	2_{-2}^{+0}	1	2_{-2}^{+0}	5	$0.00_{-0.00}^{+0.00}$	-2	$0.22_{-0.22}^{+0.00}$	$0.18_{-0.18}^{+0.00}$	$0.23_{-0.23}^{+0.00}$	4E-01	4E-02
53C	13_{-3}^{+4}	0	5_{-2}^{+3}	0	7_{-2}^{+3}	0	$0.14_{-0.32}^{+0.31}$	0	$1.08_{-0.29}^{+0.38}$	$0.46_{-0.19}^{+0.28}$	$0.62_{-0.22}^{+0.31}$	2E+00	2E-09
54	3_{-3}^{+0}	5	3_{-3}^{+0}	5	2_{-2}^{+0}	1	$0.00_{-0.00}^{+0.00}$	-2	$0.25_{-0.25}^{+0.00}$	$0.28_{-0.28}^{+0.00}$	$0.18_{-0.18}^{+0.00}$	-1E-02	1E+00
55	29_{-5}^{+6}	0	22_{-4}^{+5}	0	6_{-2}^{+3}	0	$-0.54_{-0.16}^{+0.19}$	0	$2.36_{-0.43}^{+0.52}$	$1.82_{-0.38}^{+0.47}$	$0.54_{-0.20}^{+0.30}$	2E+00	2E-08
56	3_{-3}^{+0}	5	2_{-2}^{+0}	1	4_{-4}^{+0}	5	$0.00_{-0.00}^{+0.00}$	-2	$0.28_{-0.28}^{+0.00}$	$0.18_{-0.18}^{+0.00}$	$0.36_{-0.36}^{+0.00}$	7E-01	3E-04
57D	37_{-6}^{+7}	0	33_{-5}^{+6}	0	3_{-1}^{+3}	0	$-0.79_{-0.10}^{+0.15}$	0	$2.94_{-0.48}^{+0.57}$	$2.63_{-0.46}^{+0.54}$	$0.31_{-0.15}^{+0.25}$	1E+00	2E-05
58	3_{-3}^{+0}	5	3_{-3}^{+0}	5	2_{-2}^{+0}	1	$0.00_{-0.00}^{+0.00}$	-2	$0.25_{-0.25}^{+0.00}$	$0.31_{-0.31}^{+0.00}$	$0.18_{-0.18}^{+0.00}$	-2E-02	1E+00
59	3_{-3}^{+0}	5	3_{-3}^{+0}	5	2_{-2}^{+0}	1	$0.00_{-0.00}^{+0.00}$	-2	$0.25_{-0.25}^{+0.00}$	$0.26_{-0.26}^{+0.00}$	$0.18_{-0.18}^{+0.00}$	-7E-03	1E+00
60	62_{-7}^{+9}	0	43_{-6}^{+7}	0	19_{-4}^{+5}	0	$-0.37_{-0.12}^{+0.13}$	0	$5.00_{-0.63}^{+0.71}$	$3.42_{-0.52}^{+0.61}$	$1.58_{-0.35}^{+0.44}$	4E+00	2E-32
61	23_{-4}^{+6}	0	20_{-4}^{+5}	0	5_{-5}^{+0}	5	$-0.62_{-0.38}^{+0.00}$	1	$1.90_{-0.39}^{+0.47}$	$1.66_{-0.36}^{+0.45}$	$0.39_{-0.39}^{+0.00}$	1E+00	2E-05

TABLE 22:

Counts, count rates and AE detection significance and no-source probabilities for X-ray point sources in HCG 22 (online only).

ID (1)	c(FB) (2)	lim _F (3)	c(SB) (4)	lim _S (5)	c(HB) (6)	lim _S (7)	HR (8)	lim _{HR} (9)	cr(FB) (10)	cr(SB) (11)	cr(HB) (12)	AE(sig) (13)	AE(<i>P</i>) (14)
1	2 ⁺⁰ ₋₂	5	2 ⁺⁰ ₋₂	5	2 ⁺⁰ ₋₂	5	0.00 ^{+0.00} _{-0.00}	-2	0.07 ^{+0.00} _{-0.07}	0.07 ^{+0.00} _{-0.07}	0.07 ^{+0.00} _{-0.07}	1E-01	5E-01
2	10 ⁺⁴ ₋₃	0	7 ⁺³ ₋₂	0	2 ⁺⁰ ₋₂	5	-0.51 ^{+0.00} _{-0.49}	1	0.32 ^{+0.14} _{-0.10}	0.23 ^{+0.12} _{-0.08}	0.08 ^{+0.00} _{-0.08}	9E-01	3E-02
3	2 ⁺⁰ ₋₂	5	2 ⁺⁰ ₋₂	5	2 ⁺⁰ ₋₂	5	0.00 ^{+0.00} _{-0.00}	-2	0.07 ^{+0.00} _{-0.07}	0.08 ^{+0.00} _{-0.08}	0.07 ^{+0.00} _{-0.07}	5E-01	2E-01
4	24 ⁺⁶ ₋₄	0	20 ⁺⁵ ₋₄	0	4 ⁺³ ₋₂	0	-0.64 ^{+0.21} _{-0.16}	0	0.78 ^{+0.19} _{-0.16}	0.64 ^{+0.18} _{-0.14}	0.14 ^{+0.10} _{-0.06}	1E+00	3E-02
5	11 ⁺⁴ ₋₃	0	7 ⁺³ ₋₂	0	4 ⁺³ ₋₁	0	-0.29 ^{+0.35} _{-0.32}	0	0.36 ^{+0.14} _{-0.11}	0.23 ^{+0.12} _{-0.08}	0.13 ^{+0.10} _{-0.06}	1E+00	1E-02
6	2 ⁺⁰ ₋₂	5	2 ⁺⁰ ₋₂	5	2 ⁺⁰ ₋₂	5	0.00 ^{+0.00} _{-0.00}	-2	0.08 ^{+0.00} _{-0.08}	0.07 ^{+0.00} _{-0.07}	0.08 ^{+0.00} _{-0.08}	8E-01	6E-02
7	3 ⁺³ ₋₁	0	2 ⁺⁰ ₋₂	1	4 ⁺³ ₋₁	0	0.28 ^{+0.72} _{-0.00}	-1	0.12 ^{+0.10} _{-0.06}	0.07 ^{+0.00} _{-0.07}	0.13 ^{+0.10} _{-0.06}	1E+00	2E-03
8	2 ⁺⁰ ₋₂	5	2 ⁺⁰ ₋₂	5	2 ⁺⁰ ₋₂	5	0.00 ^{+0.00} _{-0.00}	-2	0.07 ^{+0.00} _{-0.07}	0.07 ^{+0.00} _{-0.07}	0.07 ^{+0.00} _{-0.07}	2E-01	4E-01
9	4 ⁺³ ₋₂	0	4 ⁺³ ₋₂	0	2 ⁺⁰ ₋₂	5	-0.33 ^{+0.00} _{-0.67}	1	0.15 ^{+0.11} _{-0.07}	0.15 ^{+0.10} _{-0.07}	0.07 ^{+0.00} _{-0.07}	9E-02	6E-01
10	9 ⁺⁴ ₋₂	0	2 ⁺⁰ ₋₂	5	5 ⁺³ ₋₂	0	0.41 ^{+0.59} _{-0.00}	-1	0.28 ^{+0.13} _{-0.09}	0.08 ^{+0.00} _{-0.08}	0.18 ^{+0.11} _{-0.07}	1E+00	2E-03
11	4 ⁺³ ₋₁	0	2 ⁺⁰ ₋₂	1	4 ⁺³ ₋₂	0	0.30 ^{+0.00} _{-0.00}	-1	0.13 ^{+0.10} _{-0.06}	0.07 ^{+0.00} _{-0.07}	0.14 ^{+0.10} _{-0.06}	1E+00	9E-04
12	24 ⁺⁶ ₋₄	0	18 ⁺⁵ ₋₄	0	5 ⁺³ ₋₂	0	-0.55 ^{+0.22} _{-0.18}	0	0.76 ^{+0.19} _{-0.13}	0.59 ^{+0.17} _{-0.14}	0.17 ^{+0.11} _{-0.07}	2E+00	4E-05
13	7 ⁺³ ₋₂	0	3 ⁺³ ₋₁	0	2 ⁺⁰ ₋₂	5	-0.18 ^{+0.00} _{-0.82}	1	0.23 ^{+0.08} _{-0.10}	0.12 ^{+0.06} _{-0.06}	0.08 ^{+0.00} _{-0.08}	1E+00	1E-03
14	24 ⁺⁶ ₋₄	0	20 ⁺⁵ ₋₄	0	3 ⁺³ ₋₁	0	-0.69 ^{+0.20} _{-0.15}	0	0.77 ^{+0.19} _{-0.15}	0.65 ^{+0.18} _{-0.14}	0.12 ^{+0.10} _{-0.06}	1E+00	1E-02
15	2 ⁺⁰ ₋₂	1	2 ⁺⁰ ₋₂	1	2 ⁺⁰ ₋₂	5	0.00 ^{+0.00} _{-0.00}	-2	0.07 ^{+0.00} _{-0.07}	0.07 ^{+0.00} _{-0.07}	0.07 ^{+0.00} _{-0.07}	2E-01	5E-01
16	2 ⁺⁰ ₋₂	5	2 ⁺⁰ ₋₂	5	2 ⁺⁰ ₋₂	5	0.00 ^{+0.00} _{-0.00}	-2	0.07 ^{+0.00} _{-0.07}	0.07 ^{+0.00} _{-0.07}	0.07 ^{+0.00} _{-0.07}	3E-01	4E-01
17C	6 ⁺³ ₋₂	0	4 ⁺³ ₋₂	0	2 ⁺⁰ ₋₂	5	-0.32 ^{+0.00} _{-0.68}	1	0.19 ^{+0.08} _{-0.11}	0.15 ^{+0.11} _{-0.07}	0.08 ^{+0.00} _{-0.08}	5E-01	1E-01
18	17 ⁺⁵ ₋₄	0	12 ⁺⁴ ₋₃	0	4 ⁺³ ₋₂	0	-0.47 ^{+0.27} _{-0.23}	0	0.54 ^{+0.16} _{-0.13}	0.40 ^{+0.15} _{-0.11}	0.14 ^{+0.10} _{-0.06}	1E+00	5E-03
19	2 ⁺⁰ ₋₂	5	2 ⁺⁰ ₋₂	1	2 ⁺⁰ ₋₂	5	0.00 ^{+0.00} _{-0.00}	-2	0.08 ^{+0.00} _{-0.08}	0.07 ^{+0.00} _{-0.07}	0.08 ^{+0.00} _{-0.08}	1E+00	2E-03
20	7 ⁺³ ₋₂	0	2 ⁺⁰ ₋₂	5	6 ⁺³ ₋₂	0	0.44 ^{+0.56} _{-0.00}	-1	0.22 ^{+0.12} _{-0.08}	0.07 ^{+0.00} _{-0.07}	0.19 ^{+0.11} _{-0.08}	2E+00	1E-03
21C	36 ⁺⁷ ₋₆	0	27 ⁺⁶ ₋₅	0	8 ⁺⁴ ₋₂	0	-0.52 ^{+0.17} _{-0.15}	0	1.15 ^{+0.22} _{-0.19}	0.88 ^{+0.20} _{-0.17}	0.28 ^{+0.13} _{-0.09}	2E+00	1E-11
22B	7 ⁺³ ₋₂	0	4 ⁺³ ₋₂	0	2 ⁺⁰ ₋₂	5	-0.28 ^{+0.05} _{-0.72}	1	0.24 ^{+0.12} _{-0.08}	0.15 ^{+0.11} _{-0.07}	0.08 ^{+0.00} _{-0.08}	9E-01	4E-03
23	8 ⁺⁴ ₋₂	0	3 ⁺³ ₋₁	0	4 ⁺³ ₋₂	0	0.10 ^{+0.40} _{-0.41}	0	0.27 ^{+0.13} _{-0.09}	0.12 ^{+0.10} _{-0.06}	0.15 ^{+0.11} _{-0.07}	1E+00	1E-05
24	2 ⁺⁰ ₋₂	5	2 ⁺⁰ ₋₂	5	2 ⁺⁰ ₋₂	1	0.00 ^{+0.00} _{-0.00}	-2	0.08 ^{+0.00} _{-0.08}	0.08 ^{+0.00} _{-0.08}	0.07 ^{+0.00} _{-0.07}	-1E-01	1E+00
25	2 ⁺⁰ ₋₂	5	3 ⁺⁰ ₋₃	5	2 ⁺⁰ ₋₂	5	0.00 ^{+0.00} _{-0.00}	-2	0.09 ^{+0.00} _{-0.09}	0.10 ^{+0.00} _{-0.10}	0.08 ^{+0.00} _{-0.08}	4E-01	1E-01
26	2 ⁺⁰ ₋₂	5	3 ⁺⁰ ₋₃	5	2 ⁺⁰ ₋₂	1	0.00 ^{+0.00} _{-0.00}	-2	0.08 ^{+0.00} _{-0.08}	0.09 ^{+0.00} _{-0.09}	0.07 ^{+0.00} _{-0.07}	-1E-01	1E+00
27	2 ⁺⁰ ₋₂	5	3 ⁺⁰ ₋₃	5	2 ⁺⁰ ₋₂	5	0.00 ^{+0.00} _{-0.00}	-2	0.08 ^{+0.00} _{-0.08}	0.10 ^{+0.00} _{-0.10}	0.08 ^{+0.00} _{-0.08}	3E-01	2E-01
28	2 ⁺⁰ ₋₂	5	3 ⁺⁰ ₋₃	5	2 ⁺⁰ ₋₂	1	0.00 ^{+0.00} _{-0.00}	-2	0.09 ^{+0.00} _{-0.09}	0.10 ^{+0.00} _{-0.10}	0.07 ^{+0.00} _{-0.07}	-4E-02	1E+00
29	2 ⁺⁰ ₋₂	5	2 ⁺⁰ ₋₂	1	3 ⁺⁰ ₋₃	5	0.00 ^{+0.00} _{-0.00}	-2	0.08 ^{+0.00} _{-0.08}	0.07 ^{+0.00} _{-0.07}	0.09 ^{+0.00} _{-0.09}	1E+00	7E-04
30	5 ⁺³ ₋₂	0	2 ⁺⁰ ₋₂	5	4 ⁺³ ₋₂	0	0.31 ^{+0.69} _{-0.00}	-1	0.16 ^{+0.11} _{-0.07}	0.07 ^{+0.00} _{-0.07}	0.14 ^{+0.10} _{-0.06}	1E+00	5E-03
31	10 ⁺⁴ ₋₃	0	10 ⁺⁴ ₋₃	0	2 ⁺⁰ ₋₂	5	-0.60 ^{+0.00} _{-0.40}	1	0.34 ^{+0.14} _{-0.10}	0.31 ^{+0.13} _{-0.10}	0.08 ^{+0.00} _{-0.08}	4E-01	1E-01
32	4 ⁺³ ₋₂	0	2 ⁺⁰ ₋₂	5	2 ⁺⁰ ₋₂	5	0.00 ^{+0.00} _{-0.00}	-2	0.13 ^{+0.10} _{-0.06}	0.08 ^{+0.00} _{-0.08}	0.08 ^{+0.00} _{-0.08}	1E+00	5E-03
33	8 ⁺⁴ ₋₂	0	7 ⁺³ ₋₂	0	2 ⁺⁰ ₋₂	5	-0.52 ^{+0.00} _{-0.48}	1	0.28 ^{+0.13} _{-0.09}	0.25 ^{+0.12} _{-0.09}	0.08 ^{+0.00} _{-0.08}	4E-01	2E-01
34	2 ⁺⁰ ₋₂	5	2 ⁺⁰ ₋₂	5	2 ⁺⁰ ₋₂	1	0.00 ^{+0.00} _{-0.00}	-2	0.08 ^{+0.00} _{-0.08}	0.08 ^{+0.00} _{-0.08}	0.07 ^{+0.00} _{-0.07}	-9E-02	1E+00
35	2 ⁺⁰ ₋₂	5	2 ⁺⁰ ₋₂	5	2 ⁺⁰ ₋₂	5	0.00 ^{+0.00} _{-0.00}	-2	0.08 ^{+0.00} _{-0.08}	0.08 ^{+0.00} _{-0.08}	0.08 ^{+0.00} _{-0.08}	7E-01	3E-02
36	16 ⁺⁵ ₋₄	0	15 ⁺⁵ ₋₃	0	2 ⁺⁰ ₋₂	5	-0.74 ^{+0.00} _{-0.26}	1	0.52 ^{+0.16} _{-0.13}	0.50 ^{+0.16} _{-0.12}	0.08 ^{+0.00} _{-0.08}	3E-01	3E-01
37	2 ⁺⁰ ₋₂	5	2 ⁺⁰ ₋₂	5	2 ⁺⁰ ₋₂	1	0.00 ^{+0.00} _{-0.00}	-2	0.08 ^{+0.00} _{-0.08}	0.08 ^{+0.00} _{-0.08}	0.07 ^{+0.00} _{-0.07}	-8E-02	1E+00
38	2 ⁺⁰ ₋₂	5	2 ⁺⁰ ₋₂	5	2 ⁺⁰ ₋₂	5	0.00 ^{+0.00} _{-0.00}	-2	0.07 ^{+0.00} _{-0.07}	0.07 ^{+0.00} _{-0.07}	0.08 ^{+0.00} _{-0.08}	3E-01	2E-01
39	6 ⁺³ ₋₂	0	4 ⁺³ ₋₂	0	2 ⁺⁰ ₋₂	5	-0.27 ^{+0.00} _{-0.73}	1	0.21 ^{+0.12} _{-0.08}	0.15 ^{+0.11} _{-0.07}	0.09 ^{+0.00} _{-0.09}	7E-01	7E-03
40	2 ⁺⁰ ₋₂	5	2 ⁺⁰ ₋₂	5	2 ⁺⁰ ₋₂	5	0.00 ^{+0.00} _{-0.00}	-2	0.08 ^{+0.00} _{-0.08}	0.08 ^{+0.00} _{-0.08}	0.08 ^{+0.00} _{-0.08}	3E-01	2E-01
41	2 ⁺⁰ ₋₂	5	2 ⁺⁰ ₋₂	1	2 ⁺⁰ ₋₂	5	0.00 ^{+0.00} _{-0.00}	-2	0.08 ^{+0.00} _{-0.08}	0.07 ^{+0.00} _{-0.07}	0.08 ^{+0.00} _{-0.08}	9E-01	1E-02
42	3 ⁺³ ₋₁	0	3 ⁺³ ₋₁	0	2 ⁺⁰ ₋₂	5	-0.22 _{-0.78}	1	0.12 _{-0.06}	0.12 _{-0.06}	0.07 _{-0.07}	3E-02	6E-01

TABLE 22:

Counts, count rates and AE detection significance and no-source probabilities for X-ray point sources in HCG 22 (online only).

43	3 ⁺³	0	4 ⁺⁰	5	2 ⁺⁰	5	0.00 ^{+0.00}	-2	0.12 ^{+0.10}	0.13 ^{+0.00}	0.08 ^{+0.00}	4E-01	1E-01
44	6 ⁺³	0	7 ⁺³	0	2 ⁺⁰	1	-0.50 ^{+0.00}	1	0.22 ^{+0.12}	0.22 ^{+0.12}	0.07 ^{+0.00}	-7E-02	1E+00
45	2 ⁺⁰	5	2 ⁺⁰	1	2 ⁺⁰	5	0.00 ^{+0.00}	-2	0.08 ^{+0.00}	0.07 ^{+0.00}	0.08 ^{+0.00}	1E+00	3E-03
46	2 ⁺⁰	5	3 ⁺⁰	5	2 ⁺⁰	1	0.00 ^{+0.00}	-2	0.09 ^{+0.00}	0.11 ^{+0.00}	0.07 ^{+0.00}	-8E-02	1E+00
47	2 ⁺⁰	5	3 ⁺⁰	5	2 ⁺⁰	1	0.00 ^{+0.00}	-2	0.09 ^{+0.00}	0.11 ^{+0.00}	0.07 ^{+0.00}	-6E-02	1E+00
48	2 ⁺⁰	5	2 ⁺⁰	5	2 ⁺⁰	5	0.00 ^{+0.00}	-2	0.09 ^{+0.00}	0.09 ^{+0.00}	0.08 ^{+0.00}	4E-01	1E-01
49	10 ⁺⁴	0	9 ⁺⁴	0	2 ⁺⁰	5	-0.61 ^{+0.00}	1	0.32 ^{+0.13}	0.30 ^{+0.13}	0.07 ^{+0.00}	1E-01	5E-01
50	2 ⁺⁰	5	2 ⁺⁰	5	2 ⁺⁰	1	0.00 ^{+0.00}	-2	0.08 ^{+0.00}	0.09 ^{+0.00}	0.07 ^{+0.00}	-1E-01	1E+00
51	2 ⁺⁰	5	2 ⁺⁰	5	2 ⁺⁰	1	0.00 ^{+0.00}	-2	0.08 ^{+0.00}	0.08 ^{+0.00}	0.07 ^{+0.00}	-1E-01	1E+00
52	2 ⁺⁰	5	2 ⁺⁰	1	2 ⁺⁰	5	0.00 ^{+0.00}	-2	0.08 ^{+0.00}	0.07 ^{+0.00}	0.09 ^{+0.00}	7E-01	1E-02
53	5 ⁺³	0	6 ⁺³	0	2 ⁺⁰	1	-0.44 ^{+0.00}	1	0.19 ^{+0.11}	0.19 ^{+0.11}	0.07 ^{+0.00}	-6E-02	1E+00
54	4 ⁺³	0	4 ⁺³	0	2 ⁺⁰	1	-0.35 ^{+0.00}	1	0.15 ^{+0.10}	0.15 ^{+0.11}	0.07 ^{+0.00}	-1E-01	1E+00
55	2 ⁺⁰	5	3 ⁺⁰	5	2 ⁺⁰	5	0.00 ^{+0.00}	-2	0.08 ^{+0.00}	0.10 ^{+0.10}	0.08 ^{+0.00}	3E-01	3E-01
56A	4 ⁺³	0	3 ⁻¹	0	2 ⁺⁰	5	-0.22 ^{+0.00}	1	0.15 ^{+0.11}	0.12 ^{+0.06}	0.08 ^{+0.00}	4E-01	1E-01
57	2 ⁺⁰	5	2 ⁺⁰	5	2 ⁺⁰	5	0.00 ^{+0.00}	-2	0.08 ^{+0.00}	0.09 ^{+0.00}	0.08 ^{+0.00}	4E-01	2E-01
58	2 ⁺⁰	5	2 ⁺⁰	1	2 ⁺⁰	5	0.00 ^{+0.00}	-2	0.09 ^{+0.00}	0.07 ^{+0.00}	0.09 ^{+0.00}	7E-01	6E-03
59	2 ⁻²	5	3 ⁺³	5	2 ⁺⁰	1	0.00 ^{+0.00}	-2	0.09 ^{+0.00}	0.11 ^{+0.00}	0.07 ^{+0.00}	-4E-02	1E+00
60A	3 ⁺³	0	2 ⁺⁰	5	2 ⁺⁰	5	0.00 ^{+0.00}	-2	0.12 ^{+0.10}	0.09 ^{+0.00}	0.09 ^{+0.00}	7E-01	7E-03
61A	3 ⁺³	0	3 ⁻³	5	2 ⁺⁰	5	0.00 ^{+0.00}	-2	0.12 ^{+0.10}	0.11 ^{+0.00}	0.08 ^{+0.00}	4E-01	1E-01
62	2 ⁺⁰	5	2 ⁺⁰	5	2 ⁺⁰	1	0.00 ^{+0.00}	-2	0.08 ^{+0.00}	0.09 ^{+0.00}	0.07 ^{+0.00}	-1E-01	1E+00
63A	22 ⁺⁵	0	3 ⁺³	0	18 ⁺³	0	0.66 ^{+0.16}	0	0.72 ^{+0.18}	0.12 ^{+0.10}	0.59 ^{+0.17}	3E+00	3E-29
64A	4 ⁺³	0	3 ⁺⁰	5	2 ⁺⁰	5	0.00 ^{+0.00}	-2	0.15 ^{+0.10}	0.09 ^{+0.00}	0.08 ^{+0.00}	9E-01	3E-03
65	18 ⁺⁵	0	14 ⁺⁴	0	5 ⁺³	0	-0.48 ^{+0.26}	0	0.60 ^{+0.17}	0.44 ^{+0.15}	0.16 ^{+0.11}	1E+00	2E-08
66A	4 ⁺³	0	3 ⁺³	0	2 ⁺⁰	5	-0.18 ^{+0.00}	1	0.15 ^{+0.11}	0.12 ^{+0.10}	0.08 ^{+0.00}	4E-01	8E-02
67A	15 ⁺⁵	0	8 ⁺⁴	0	6 ⁺³	0	-0.12 ^{+0.29}	0	0.50 ^{+0.16}	0.28 ^{+0.13}	0.22 ^{+0.12}	2E+00	2E-11
68	2 ⁺⁰	5	3 ⁺⁰	5	2 ⁺⁰	1	0.00 ^{+0.00}	-2	0.08 ^{+0.00}	0.10 ^{+0.00}	0.07 ^{+0.00}	-7E-02	1E+00
69	3 ⁺⁰	5	3 ⁺⁰	5	2 ⁺⁰	5	0.00 ^{+0.00}	-2	0.10 ^{+0.00}	0.10 ^{+0.00}	0.08 ^{+0.00}	4E-01	9E-02
70	21 ⁺⁵	0	11 ⁺⁴	0	9 ⁺⁴	0	-0.09 ^{+0.24}	0	0.69 ^{+0.18}	0.37 ^{+0.14}	0.31 ^{+0.13}	2E+00	1E-16
71	2 ⁺⁰	5	3 ⁺⁰	5	2 ⁺⁰	5	0.00 ^{+0.00}	-2	0.09 ^{+0.00}	0.09 ^{+0.00}	0.08 ^{+0.00}	4E-01	1E-01
72A	5 ⁺³	0	4 ⁺³	0	2 ⁺⁰	5	-0.32 ^{+0.00}	1	0.17 ^{+0.11}	0.15 ^{+0.11}	0.08 ^{+0.00}	3E-01	2E-01
73	2 ⁺⁰	5	2 ⁺⁰	5	2 ⁺⁰	5	0.00 ^{+0.00}	-2	0.09 ^{+0.00}	0.09 ^{+0.00}	0.08 ^{+0.00}	4E-01	1E-01
74A	8 ⁺⁴	0	7 ⁺³	0	2 ⁺⁰	5	-0.52 ^{+0.00}	1	0.27 ^{+0.13}	0.25 ^{+0.12}	0.08 ^{+0.00}	4E-01	2E-01
75	2 ⁺⁰	5	2 ⁺⁰	1	2 ⁺⁰	5	0.00 ^{+0.00}	-2	0.08 ^{+0.00}	0.07 ^{+0.00}	0.09 ^{+0.00}	7E-01	1E-02
76A	7 ⁺³	0	4 ⁺³	0	2 ⁺⁰	5	-0.23 ^{+0.00}	1	0.23 ^{+0.12}	0.15 ^{+0.10}	0.09 ^{+0.00}	1E+00	9E-04
77A	9 ⁺⁴	0	7 ⁺³	0	2 ⁺⁰	5	-0.50 ^{+0.00}	1	0.30 ^{+0.13}	0.24 ^{+0.12}	0.08 ^{+0.00}	7E-01	3E-02
78A	21 ⁺⁵	0	18 ⁺⁵	0	2 ⁺⁰	5	-0.73 ^{+0.00}	1	0.68 ^{+0.18}	0.59 ^{+0.17}	0.09 ^{+0.00}	1E+00	9E-04
79A	2 ⁺⁰	5	3 ⁺³	0	2 ⁺⁰	1	0.00 ^{+0.00}	-2	0.08 ^{+0.00}	0.11 ^{+0.10}	0.07 ^{+0.00}	-1E-01	1E+00
80	2 ⁺⁰	5	3 ⁺⁰	5	2 ⁺⁰	1	0.00 ^{+0.00}	-2	0.08 ^{+0.00}	0.11 ^{+0.06}	0.07 ^{+0.00}	-8E-02	1E+00
81A	5 ⁺³	0	2 ⁺⁰	5	3 ⁺³	0	0.18 ^{+0.82}	-1	0.18 ^{+0.11}	0.08 ^{+0.00}	0.12 ^{+0.10}	1E+00	6E-05
82	3 ⁺⁰	5	3 ⁺⁰	5	2 ⁺⁰	5	0.00 ^{+0.00}	-2	0.10 ^{+0.00}	0.12 ^{+0.00}	0.08 ^{+0.00}	4E-01	1E-01
83A	4 ⁺³	0	3 ⁺⁰	5	2 ⁺⁰	5	0.00 ^{+0.00}	-2	0.15 ^{+0.10}	0.10 ^{+0.00}	0.08 ^{+0.00}	7E-01	2E-02
84A	5 ⁺³	0	2 ⁺⁰	5	2 ⁺⁰	5	0.00 ^{+0.00}	-2	0.18 ^{+0.11}	0.09 ^{+0.00}	0.09 ^{+0.00}	1E+00	2E-03
85	3 ⁺⁰	5	2 ⁺⁰	1	4 ⁺⁰	5	0.00 ^{+0.00}	-2	0.11 ^{+0.00}	0.07 ^{+0.00}	0.14 ^{+0.00}	1E+00	4E-05
86A	3 ⁺³	0	3 ⁺³	0	2 ⁺⁰	1	-0.25 ^{+0.00}	1	0.11 ^{+0.10}	0.12 ^{+0.10}	0.07 ^{+0.00}	-1E-01	1E+00
87A	4 ⁺³	0	3 ⁻¹	0	2 ⁺⁰	5	-0.21 ^{-0.79}	1	0.15 ^{-0.07}	0.12 ^{-0.06}	0.08 ^{-0.08}	4E-01	1E-01

TABLE 22:

Counts, count rates and AE detection significance and no-source probabilities for X-ray point sources in HCG 22 (online only).

88	2^{+0}_{-2}	5	3^{+0}_{-3}	5	2^{+0}_{-2}	1	$0.00^{+0.00}_{-0.00}$	-2	$0.08^{+0.00}_{-0.08}$	$0.10^{+0.00}_{-0.10}$	$0.07^{+0.00}_{-0.07}$	-9E-02	1E+00
89	2^{+0}_{-2}	5	4^{+0}_{-4}	5	2^{+0}_{-2}	1	$0.00^{+0.00}_{-0.00}$	-2	$0.09^{+0.00}_{-0.09}$	$0.14^{+0.00}_{-0.14}$	$0.07^{+0.00}_{-0.07}$	-8E-02	1E+00
90	5^{+3}_{-2}	0	4^{+3}_{-1}	0	2^{+0}_{-2}	5	$-0.18^{+0.00}_{-0.82}$	1	$0.18^{+0.11}_{-0.07}$	$0.13^{+0.10}_{-0.06}$	$0.09^{+0.00}_{-0.09}$	7E-01	1E-02
91	5^{+3}_{-2}	0	4^{+3}_{-2}	0	2^{+0}_{-2}	5	$-0.32^{+0.00}_{-0.68}$	1	$0.18^{+0.11}_{-0.07}$	$0.16^{+0.11}_{-0.07}$	$0.08^{+0.00}_{-0.08}$	4E-01	1E-01
92A	3^{+3}_{-1}	0	3^{+3}_{-1}	0	2^{+0}_{-2}	1	$-0.26^{+0.00}_{-0.74}$	1	$0.12^{+0.10}_{-0.06}$	$0.12^{+0.10}_{-0.06}$	$0.07^{+0.00}_{-0.07}$	-6E-02	1E+00
93A	8^{+4}_{-2}	0	6^{+3}_{-2}	0	3^{+0}_{-3}	5	$-0.24^{+0.00}_{-0.76}$	1	$0.28^{+0.13}_{-0.09}$	$0.19^{+0.11}_{-0.07}$	$0.12^{+0.00}_{-0.12}$	1E+00	1E-04
94	9^{+4}_{-3}	0	2^{+0}_{-2}	5	8^{+4}_{-2}	0	$0.51^{+0.49}_{-0.00}$	-1	$0.31^{+0.13}_{-0.10}$	$0.09^{+0.00}_{-0.09}$	$0.28^{+0.13}_{-0.09}$	2E+00	5E-12
95	6^{+3}_{-2}	0	2^{+0}_{-2}	5	4^{+3}_{-2}	0	$0.28^{+0.72}_{-0.00}$	-1	$0.20^{+0.12}_{-0.08}$	$0.08^{+0.00}_{-0.08}$	$0.14^{+0.10}_{-0.06}$	1E+00	1E-04
96A	6^{+3}_{-2}	0	3^{+3}_{-1}	0	2^{+0}_{-2}	5	$-0.16^{+0.00}_{-0.84}$	1	$0.21^{+0.12}_{-0.08}$	$0.12^{+0.10}_{-0.06}$	$0.09^{+0.00}_{-0.09}$	1E+00	1E-03
97A	8^{+4}_{-2}	0	3^{+0}_{-3}	5	5^{+3}_{-2}	0	$0.29^{+0.71}_{-0.00}$	-1	$0.27^{+0.13}_{-0.09}$	$0.10^{+0.00}_{-0.10}$	$0.18^{+0.11}_{-0.07}$	2E+00	2E-07
98	2^{+0}_{-2}	5	2^{+0}_{-2}	5	2^{+0}_{-2}	1	$0.00^{+0.00}_{-0.00}$	-2	$0.08^{+0.00}_{-0.08}$	$0.09^{+0.00}_{-0.09}$	$0.07^{+0.00}_{-0.07}$	-9E-02	1E+00
99	2^{+0}_{-2}	5	2^{+0}_{-2}	1	2^{+0}_{-2}	5	$0.00^{+0.00}_{-0.00}$	-2	$0.08^{+0.00}_{-0.08}$	$0.07^{+0.00}_{-0.07}$	$0.08^{+0.00}_{-0.08}$	9E-01	9E-03
100	3^{+3}_{-1}	0	4^{+3}_{-1}	0	2^{+0}_{-2}	1	$-0.27^{+0.00}_{-0.73}$	1	$0.12^{+0.10}_{-0.06}$	$0.13^{+0.10}_{-0.06}$	$0.07^{+0.00}_{-0.07}$	-6E-02	1E+00
101	9^{+4}_{-3}	0	3^{+0}_{-3}	5	6^{+3}_{-2}	0	$0.39^{+0.61}_{-0.00}$	-1	$0.30^{+0.13}_{-0.10}$	$0.09^{+0.00}_{-0.09}$	$0.21^{+0.12}_{-0.08}$	2E+00	2E-08
102	2^{+0}_{-2}	5	3^{+0}_{-3}	5	2^{+0}_{-2}	5	$0.00^{+0.00}_{-0.00}$	-2	$0.09^{+0.00}_{-0.09}$	$0.10^{+0.00}_{-0.10}$	$0.08^{+0.00}_{-0.08}$	4E-01	2E-01
103	2^{+0}_{-2}	5	3^{+3}_{-1}	0	2^{+0}_{-2}	1	$0.00^{+0.00}_{-0.00}$	-2	$0.08^{+0.00}_{-0.08}$	$0.12^{+0.10}_{-0.06}$	$0.07^{+0.00}_{-0.07}$	-3E-01	1E+00

TABLE 23:
Counts, count rates and AE detection significance and no-source probabilities for X-ray point sources in HCG 31 (online only).

ID (1)	c(FB) (2)	lim _F (3)	c(SB) (4)	lim _S (5)	c(HB) (6)	lim _S (7)	HR (8)	lim _{HR} (9)	cr(FB) (10)	cr(SB) (11)	cr(HB) (12)	AE(sig) (13)	AE(<i>P</i>) (14)
1	21 ⁺⁵ ₋₄	0	15 ⁺⁵ ₋₃	0	5 ⁺³ ₋₂	0	-0.48 ^{+0.24} _{-0.20}	0	0.60 ^{+0.16} _{-0.13}	0.45 ^{+0.14} _{-0.11}	0.16 ^{+0.10} _{-0.06}	1E+00	2E-02
2	9 ⁺⁴ ₋₃	0	4 ⁺³ ₋₂	0	4 ⁺³ ₋₂	0	-0.02 ^{+0.39} _{-0.38}	0	0.27 ^{+0.12} _{-0.09}	0.14 ^{+0.09} _{-0.06}	0.13 ^{+0.09} _{-0.06}	1E+00	3E-02
3	10 ⁺⁴ ₋₃	0	5 ⁺³ ₋₂	0	4 ⁺³ ₋₂	0	-0.13 ^{+0.38} _{-0.36}	0	0.29 ^{+0.12} _{-0.09}	0.16 ^{+0.10} _{-0.07}	0.12 ^{+0.09} _{-0.06}	1E+00	4E-04
4	2 ⁺⁰ ₋₂	5	3 ⁺³ ₋₁	0	2 ⁺⁰ ₋₂	1	0.00 ^{+0.00} _{-0.00}	-2	0.07 ^{+0.00} _{-0.07}	0.10 ^{+0.09} _{-0.05}	0.07 ^{+0.00} _{-0.07}	-4E-01	8E-01
5	6 ⁺³ ₋₂	0	2 ⁺⁰ ₋₂	5	5 ⁺³ ₋₂	0	0.39 ^{+0.61} _{-0.00}	-1	0.18 ^{+0.10} _{-0.07}	0.07 ^{+0.00} _{-0.07}	0.15 ^{+0.10} _{-0.06}	1E+00	2E-02
6	7 ⁺³ ₋₂	0	5 ⁺³ ₋₂	0	2 ⁺⁰ ₋₂	5	-0.43 ^{+0.00} _{-0.57}	1	0.20 ^{+0.11} _{-0.07}	0.17 ^{+0.10} _{-0.07}	0.07 ^{+0.00} _{-0.07}	4E-01	3E-01
7	4 ⁺³ ₋₁	0	2 ⁺⁰ ₋₂	5	2 ⁺⁰ ₋₂	5	0.00 ^{+0.00} _{-0.00}	-2	0.12 ^{+0.09} _{-0.05}	0.07 ^{+0.00} _{-0.07}	0.07 ^{+0.00} _{-0.07}	3E-01	4E-01
8	2 ⁺⁰ ₋₂	5	2 ⁺⁰ ₋₂	1	2 ⁺⁰ ₋₂	5	0.00 ^{+0.00} _{-0.00}	-2	0.07 ^{+0.00} _{-0.07}	0.06 ^{+0.00} _{-0.06}	0.07 ^{+0.00} _{-0.07}	3E-01	3E-01
9	32 ⁺⁶ ₋₅	0	22 ⁺⁵ ₋₄	0	10 ⁺⁴ ₋₃	0	-0.38 ^{+0.19} _{-0.17}	0	0.92 ^{+0.19} _{-0.16}	0.64 ^{+0.16} _{-0.13}	0.29 ^{+0.12} _{-0.09}	2E+00	4E-09
10	11 ⁺⁴ ₋₃	0	11 ⁺⁴ ₋₃	0	2 ⁺⁰ ₋₂	5	-0.66 ^{+0.00} _{-0.34}	1	0.33 ^{+0.13} _{-0.09}	0.32 ^{+0.13} _{-0.09}	0.07 ^{+0.00} _{-0.07}	7E-02	6E-01
11	17 ⁺⁵ ₋₄	0	12 ⁺⁴ ₋₃	0	5 ⁺³ ₋₂	0	-0.41 ^{+0.37} _{-0.23}	0	0.50 ^{+0.15} _{-0.12}	0.35 ^{+0.13} _{-0.10}	0.15 ^{+0.10} _{-0.06}	1E+00	2E-04
12	5 ⁺³ ₋₂	0	2 ⁺⁰ ₋₂	5	4 ⁺³ ₋₁	0	0.25 ^{+0.75} _{-0.00}	-1	0.16 ^{+0.10} _{-0.06}	0.07 ^{+0.00} _{-0.07}	0.11 ^{+0.09} _{-0.05}	1E+00	4E-02
13	2 ⁺⁰ ₋₂	5	2 ⁺⁰ ₋₂	5	2 ⁺⁰ ₋₂	1	0.00 ^{+0.00} _{-0.00}	-2	0.07 ^{+0.00} _{-0.07}	0.08 ^{+0.00} _{-0.08}	0.06 ^{+0.00} _{-0.06}	-3E-01	1E+00
14	105 ⁺¹¹ ₋₁₀	0	83 ⁺¹⁰ ₋₉	0	22 ⁺⁵ ₋₄	0	-0.58 ^{+0.09} _{-0.08}	0	2.97 ^{+0.32} _{-0.29}	2.35 ^{+0.29} _{-0.26}	0.62 ^{+0.16} _{-0.13}	4E+00	5E-23
15	2 ⁺⁰ ₋₂	5	2 ⁺⁰ ₋₂	5	2 ⁺⁰ ₋₂	5	0.00 ^{+0.00} _{-0.00}	-2	0.07 ^{+0.00} _{-0.07}	0.07 ^{+0.00} _{-0.07}	0.07 ^{+0.00} _{-0.07}	9E-01	1E-02
16	6 ⁺³ ₋₂	0	3 ⁺³ ₋₁	0	2 ⁺⁰ ₋₂	5	-0.21 ^{+0.00} _{-0.79}	1	0.18 ^{+0.10} _{-0.07}	0.11 ^{+0.09} _{-0.05}	0.07 ^{+0.00} _{-0.07}	9E-01	1E-02
17	17 ⁺⁵ ₋₄	0	16 ⁺⁵ ₋₄	0	2 ⁺⁰ ₋₂	5	-0.74 ^{+0.00} _{-0.26}	1	0.50 ^{+0.15} _{-0.12}	0.47 ^{+0.15} _{-0.11}	0.07 ^{+0.00} _{-0.07}	4E-01	2E-01
18	3 ⁺³ ₋₁	0	3 ⁺³ ₋₁	0	2 ⁺⁰ ₋₂	1	-0.26 ^{+0.00} _{-0.74}	1	0.10 ^{+0.09} _{-0.05}	0.11 ^{+0.09} _{-0.05}	0.06 ^{+0.00} _{-0.06}	-2E-01	1E+00
19	18 ⁺⁵ ₋₄	0	13 ⁺⁴ ₋₃	0	5 ⁺³ ₋₂	0	-0.42 ^{+0.26} _{-0.23}	0	0.53 ^{+0.15} _{-0.12}	0.37 ^{+0.13} _{-0.10}	0.15 ^{+0.10} _{-0.06}	1E+00	1E-02
20	24 ⁺⁶ ₋₄	0	19 ⁺⁵ ₋₄	0	4 ⁺³ ₋₂	0	-0.63 ^{+0.21} _{-0.16}	0	0.69 ^{+0.17} _{-0.14}	0.56 ^{+0.16} _{-0.12}	0.13 ^{+0.09} _{-0.06}	1E+00	2E-02
21	35 ⁺⁷ ₋₅	0	25 ⁺⁶ ₋₅	0	9 ⁺⁴ ₋₃	0	-0.47 ^{+0.18} _{-0.16}	0	0.99 ^{+0.20} _{-0.17}	0.73 ^{+0.17} _{-0.14}	0.26 ^{+0.12} _{-0.08}	2E+00	4E-09
22	9 ⁺⁴ ₋₃	0	4 ⁺³ ₋₂	0	5 ⁺³ ₋₂	0	0.04 ^{+0.38} _{-0.39}	0	0.27 ^{+0.12} _{-0.09}	0.13 ^{+0.09} _{-0.06}	0.14 ^{+0.10} _{-0.06}	1E+00	1E-02
23	9 ⁺⁴ ₋₃	0	9 ⁺⁴ ₋₃	0	2 ⁺⁰ ₋₂	1	-0.61 ^{+0.00} _{-0.39}	1	0.26 ^{+0.12} _{-0.08}	0.27 ^{+0.12} _{-0.08}	0.07 ^{+0.00} _{-0.07}	-1E-01	7E-01
24	42 ⁺⁷ ₋₆	0	33 ⁺⁶ ₋₅	0	8 ⁺⁴ ₋₂	0	-0.59 ^{+0.15} _{-0.13}	0	1.20 ^{+0.21} _{-0.18}	0.95 ^{+0.19} _{-0.16}	0.25 ^{+0.11} _{-0.08}	2E+00	4E-11
25	2 ⁺⁰ ₋₂	5	2 ⁺⁰ ₋₂	5	2 ⁺⁰ ₋₂	5	0.00 ^{+0.00} _{-0.00}	-2	0.07 ^{+0.00} _{-0.07}	0.07 ^{+0.00} _{-0.07}	0.07 ^{+0.00} _{-0.07}	9E-01	2E-02
26	5 ⁺³ ₋₂	0	3 ⁺⁰ ₋₃	5	2 ⁺⁰ ₋₂	5	0.00 ^{+0.00} _{-0.00}	-2	0.16 ^{+0.10} _{-0.06}	0.09 ^{+0.00} _{-0.09}	0.07 ^{+0.00} _{-0.07}	9E-01	4E-03
27	4 ⁺³ ₋₁	0	2 ⁺⁰ ₋₂	5	3 ⁺³ ₋₁	0	0.22 ^{+0.78} _{-0.00}	-1	0.11 ^{+0.09} _{-0.05}	0.07 ^{+0.00} _{-0.07}	0.10 ^{+0.09} _{-0.05}	1E+00	1E-02
28	2 ⁺⁰ ₋₂	5	2 ⁺⁰ ₋₂	1	2 ⁺⁰ ₋₂	5	0.00 ^{+0.00} _{-0.00}	-2	0.07 ^{+0.00} _{-0.07}	0.06 ^{+0.00} _{-0.06}	0.07 ^{+0.00} _{-0.07}	8E-01	2E-02
29B	8 ⁺⁴ ₋₂	0	3 ⁺³ ₋₁	0	4 ⁺³ ₋₂	0	0.12 ^{+0.40} _{-0.41}	0	0.24 ^{+0.11} _{-0.08}	0.11 ^{+0.09} _{-0.05}	0.13 ^{+0.09} _{-0.06}	1E+00	9E-06
30B	8 ⁺⁴ ₋₂	0	6 ⁺³ ₋₂	0	2 ⁺⁰ ₋₂	5	-0.45 ^{+0.00} _{-0.55}	1	0.24 ^{+0.11} _{-0.08}	0.19 ^{+0.11} _{-0.07}	0.07 ^{+0.00} _{-0.07}	7E-01	2E-02
31	17 ⁺⁵ ₋₄	0	5 ⁺³ ₋₂	0	11 ⁺⁴ ₋₃	0	0.32 ^{+0.25} _{-0.28}	0	0.49 ^{+0.15} _{-0.12}	0.17 ^{+0.10} _{-0.07}	0.32 ^{+0.13} _{-0.09}	3E+00	3E-12
32	2 ⁺⁰ ₋₂	5	3 ⁺⁰ ₋₃	5	2 ⁺⁰ ₋₂	1	0.00 ^{+0.00} _{-0.00}	-2	0.07 ^{+0.00} _{-0.07}	0.09 ^{+0.00} _{-0.06}	0.06 ^{+0.00} _{-0.06}	-2E-01	1E+00
33B	106 ⁺¹¹ ₋₁₀	0	65 ⁺⁹ ₋₈	0	40 ⁺⁷ ₋₆	0	-0.24 ^{+0.10} _{-0.10}	0	3.00 ^{+0.32} _{-0.29}	1.85 ^{+0.26} _{-0.23}	1.15 ^{+0.21} _{-0.18}	5E+00	0E+00
34	33 ⁺⁶ ₋₅	0	5 ⁺³ ₋₂	0	27 ⁺⁶ ₋₅	0	0.65 ^{+0.14} _{-0.17}	0	0.95 ^{+0.19} _{-0.16}	0.16 ^{+0.07} _{-0.07}	0.78 ^{+0.15} _{-0.10}	4E+00	3E-42
35	2 ⁺⁰ ₋₂	5	2 ⁺⁰ ₋₂	5	2 ⁺⁰ ₋₂	5	0.00 ^{+0.00} _{-0.00}	-2	0.07 ^{+0.00} _{-0.07}	0.07 ^{+0.00} _{-0.07}	0.08 ^{+0.00} _{-0.08}	7E-01	1E-02
36	14 ⁺⁴ ₋₃	0	3 ⁺³ ₋₁	0	10 ⁺⁴ ₋₃	0	0.47 ^{+0.25} _{-0.30}	0	0.41 ^{+0.14} _{-0.11}	0.11 ^{+0.09} _{-0.05}	0.30 ^{+0.12} _{-0.09}	2E+00	1E-13
37ACE	136 ⁺¹² ₋₁₁	0	87 ⁺¹⁰ ₋₉	0	48 ⁺⁸ ₋₇	0	-0.29 ^{+0.09} _{-0.09}	0	3.84 ^{+0.36} _{-0.33}	2.47 ^{+0.26} _{-0.26}	1.37 ^{+0.23} _{-0.20}	6E+00	0E+00
38ACE	128 ⁺¹² ₋₁₁	0	78 ⁺⁹ ₋₈	0	50 ⁺⁸ ₋₇	0	-0.21 ^{+0.09} _{-0.09}	0	3.61 ^{+0.35} _{-0.32}	2.19 ^{+0.28} _{-0.25}	1.42 ^{+0.23} _{-0.20}	6E+00	0E+00
39ACE	47 ⁺⁸ ₋₆	0	35 ⁺⁷ ₋₅	0	12 ⁺⁴ ₋₃	0	-0.47 ^{+0.15} _{-0.13}	0	1.34 ^{+0.22} _{-0.19}	0.99 ^{+0.20} _{-0.17}	0.36 ^{+0.13} _{-0.10}	3E+00	9E-16
40ACE	73 ⁺⁹ ₋₈	0	48 ⁺⁸ ₋₆	0	25 ⁺⁶ ₋₅	0	-0.32 ^{+0.12} _{-0.12}	0	2.07 ^{+0.27} _{-0.24}	1.36 ^{+0.23} _{-0.19}	0.71 ^{+0.17} _{-0.14}	4E+00	2E-27
41Q	4 ⁺³ ₋₂	0	3 ⁺³ ₋₁	0	2 ⁺⁰ ₋₂	5	-0.23 ^{+0.00} _{-0.77}	1	0.13 ^{+0.09} _{-0.06}	0.11 ^{+0.09} _{-0.05}	0.07 ^{+0.00} _{-0.07}	4E-01	2E-01
42ACE	13 ⁺⁴ ₋₃	0	7 ⁺³ ₋₂	0	5 ⁺³ ₋₂	0	-0.10 ^{+0.33} _{-0.32}	0	0.37 ^{+0.13} _{-0.10}	0.20 ^{+0.11} _{-0.07}	0.16 ^{+0.10} _{-0.07}	2E+00	1E-07

TABLE 23:

Counts, count rates and AE detection significance and no-source probabilities for X-ray point sources in HCG 31 (online only).

43ACE	78^{+9}_{-8}	0	56^{+8}_{-7}	0	21^{+5}_{-4}	0	$-0.44^{+0.11}_{-0.11}$	0	$2.21^{+0.28}_{-0.25}$	$1.60^{+0.24}_{-0.21}$	$0.62^{+0.16}_{-0.13}$	4E+00	2E-35
44	3^{+3}_{-1}	0	3^{+0}_{-3}	5	2^{+0}_{-2}	5	$0.00^{+0.00}_{-0.00}$	-2	$0.10^{+0.09}_{-0.05}$	$0.09^{+0.00}_{-0.09}$	$0.07^{+0.00}_{-0.07}$	3E-01	3E-01
45	120^{+12}_{-10}	0	86^{+10}_{-9}	0	34^{+6}_{-5}	0	$-0.43^{+0.09}_{-0.09}$	0	$3.38^{+0.34}_{-0.31}$	$2.42^{+0.29}_{-0.26}$	$0.96^{+0.19}_{-0.16}$	5E+00	1E-23
46ACE	60^{+8}_{-7}	0	49^{+8}_{-7}	0	10^{+4}_{-3}	0	$-0.64^{+0.12}_{-0.10}$	0	$1.70^{+0.25}_{-0.22}$	$1.40^{+0.23}_{-0.20}$	$0.31^{+0.12}_{-0.09}$	2E+00	6E-16
47	2^{+0}_{-2}	5	2^{+0}_{-2}	1	2^{+0}_{-2}	5	$0.00^{+0.00}_{-0.00}$	-2	$0.07^{+0.00}_{-0.07}$	$0.06^{+0.00}_{-0.06}$	$0.07^{+0.00}_{-0.07}$	9E-01	4E-03
48	2^{+0}_{-2}	5	2^{+0}_{-2}	1	3^{+3}_{-1}	0	$0.00^{+0.00}_{-0.00}$	-2	$0.07^{+0.00}_{-0.07}$	$0.06^{+0.00}_{-0.06}$	$0.10^{+0.09}_{-0.05}$	1E+00	3E-04
49	2^{+0}_{-2}	5	2^{+0}_{-2}	1	2^{+0}_{-2}	5	$0.00^{+0.00}_{-0.00}$	-2	$0.07^{+0.00}_{-0.07}$	$0.06^{+0.00}_{-0.06}$	$0.07^{+0.00}_{-0.07}$	4E-01	9E-02
50	2^{+0}_{-2}	5	2^{+0}_{-2}	5	2^{+0}_{-2}	1	$0.00^{+0.00}_{-0.00}$	-2	$0.07^{+0.00}_{-0.07}$	$0.07^{+0.00}_{-0.07}$	$0.06^{+0.00}_{-0.06}$	-9E-02	1E+00
51ACE	53^{+8}_{-7}	0	43^{+7}_{-6}	0	9^{+4}_{-3}	0	$-0.63^{+0.13}_{-0.11}$	0	$1.51^{+0.24}_{-0.21}$	$1.23^{+0.22}_{-0.19}$	$0.28^{+0.12}_{-0.09}$	2E+00	6E-15
52	2^{+0}_{-2}	5	2^{+0}_{-2}	5	2^{+0}_{-2}	5	$0.00^{+0.00}_{-0.00}$	-2	$0.07^{+0.00}_{-0.07}$	$0.08^{+0.00}_{-0.08}$	$0.07^{+0.00}_{-0.07}$	2E-01	4E-01
53	3^{+0}_{-3}	5	4^{+0}_{-4}	5	2^{+0}_{-2}	1	$0.00^{+0.00}_{-0.00}$	-2	$0.09^{+0.00}_{-0.09}$	$0.12^{+0.00}_{-0.12}$	$0.06^{+0.00}_{-0.06}$	-5E-02	1E+00
54ACE	42^{+7}_{-6}	0	21^{+5}_{-4}	0	20^{+5}_{-4}	0	$-0.02^{+0.17}_{-0.17}$	0	$1.20^{+0.21}_{-0.18}$	$0.62^{+0.16}_{-0.13}$	$0.59^{+0.16}_{-0.13}$	4E+00	1E-33
55	2^{+0}_{-2}	5	2^{+0}_{-2}	5	2^{+0}_{-2}	5	$0.00^{+0.00}_{-0.00}$	-2	$0.07^{+0.00}_{-0.07}$	$0.07^{+0.00}_{-0.07}$	$0.07^{+0.00}_{-0.07}$	5E-01	3E-01
56	3^{+1}_{-1}	0	4^{+3}_{-1}	0	2^{+0}_{-2}	1	$-0.27^{+0.00}_{-0.73}$	1	$0.11^{+0.09}_{-0.05}$	$0.11^{+0.09}_{-0.05}$	$0.06^{+0.00}_{-0.06}$	-7E-02	1E+00
57	2^{+0}_{-2}	5	2^{+0}_{-2}	5	2^{+0}_{-2}	1	$0.00^{+0.00}_{-0.00}$	-2	$0.07^{+0.00}_{-0.07}$	$0.08^{+0.00}_{-0.08}$	$0.06^{+0.00}_{-0.06}$	-1E-01	1E+00
58	5^{+3}_{-2}	0	5^{+3}_{-2}	0	2^{+0}_{-2}	5	$-0.32^{+0.00}_{-0.68}$	1	$0.16^{+0.10}_{-0.07}$	$0.14^{+0.10}_{-0.06}$	$0.07^{+0.00}_{-0.07}$	4E-01	1E-01
59	3^{+3}_{-1}	0	3^{+3}_{-1}	0	2^{+0}_{-2}	1	$-0.26^{+0.00}_{-0.74}$	1	$0.11^{+0.09}_{-0.05}$	$0.11^{+0.09}_{-0.05}$	$0.06^{+0.00}_{-0.06}$	-4E-02	1E+00
60	3^{+1}_{-1}	0	4^{+0}_{-4}	5	2^{+0}_{-2}	5	$0.00^{+0.00}_{-0.00}$	-2	$0.11^{+0.05}_{-0.05}$	$0.11^{+0.05}_{-0.11}$	$0.08^{+0.00}_{-0.08}$	4E-01	6E-02
61G	73^{+9}_{-8}	0	55^{+8}_{-7}	0	17^{+5}_{-4}	0	$-0.52^{+0.12}_{-0.10}$	0	$2.06^{+0.27}_{-0.24}$	$1.56^{+0.24}_{-0.21}$	$0.50^{+0.15}_{-0.12}$	3E+00	1E-25
62G	15^{+5}_{-3}	0	14^{+4}_{-3}	0	2^{+0}_{-2}	5	$-0.70^{+0.00}_{-0.30}$	1	$0.43^{+0.14}_{-0.11}$	$0.40^{+0.14}_{-0.11}$	$0.07^{+0.00}_{-0.07}$	4E-01	1E-01
63G	72^{+9}_{-8}	0	51^{+8}_{-7}	0	20^{+5}_{-4}	0	$-0.43^{+0.12}_{-0.11}$	0	$2.04^{+0.27}_{-0.24}$	$1.46^{+0.23}_{-0.20}$	$0.58^{+0.16}_{-0.13}$	4E+00	5E-28
64G	71^{+9}_{-8}	0	50^{+8}_{-7}	0	20^{+5}_{-4}	0	$-0.42^{+0.12}_{-0.11}$	0	$2.01^{+0.27}_{-0.24}$	$1.43^{+0.23}_{-0.20}$	$0.58^{+0.16}_{-0.13}$	4E+00	1E-30
65	12^{+4}_{-3}	0	8^{+4}_{-2}	0	3^{+3}_{-1}	0	$-0.40^{+0.33}_{-0.28}$	0	$0.36^{+0.13}_{-0.10}$	$0.25^{+0.12}_{-0.08}$	$0.11^{+0.09}_{-0.05}$	1E+00	8E-05
66	2^{+0}_{-2}	5	2^{+0}_{-2}	1	3^{+0}_{-3}	5	$0.00^{+0.00}_{-0.00}$	-2	$0.08^{+0.00}_{-0.08}$	$0.06^{+0.00}_{-0.06}$	$0.09^{+0.00}_{-0.09}$	1E+00	6E-04
67	16^{+5}_{-4}	0	7^{+3}_{-2}	0	9^{+4}_{-3}	0	$0.17^{+0.27}_{-0.28}$	0	$0.47^{+0.15}_{-0.11}$	$0.20^{+0.11}_{-0.07}$	$0.28^{+0.12}_{-0.09}$	2E+00	1E-14
68G	9^{+4}_{-3}	0	8^{+4}_{-2}	0	2^{+0}_{-2}	5	$-0.56^{+0.00}_{-0.44}$	1	$0.26^{+0.12}_{-0.08}$	$0.24^{+0.11}_{-0.08}$	$0.07^{+0.00}_{-0.07}$	3E-01	2E-01
69	2^{+0}_{-2}	5	2^{+0}_{-2}	1	2^{+0}_{-2}	5	$0.00^{+0.00}_{-0.00}$	-2	$0.07^{+0.00}_{-0.07}$	$0.06^{+0.00}_{-0.06}$	$0.07^{+0.00}_{-0.07}$	7E-01	7E-02
70	13^{+4}_{-3}	0	3^{+0}_{-3}	5	11^{+4}_{-3}	0	$0.54^{+0.46}_{-0.00}$	-1	$0.39^{+0.14}_{-0.10}$	$0.10^{+0.06}_{-0.10}$	$0.33^{+0.13}_{-0.10}$	3E+00	2E-17
71	3^{+0}_{-3}	5	2^{+0}_{-2}	5	3^{+0}_{-3}	5	$0.00^{+0.00}_{-0.00}$	-2	$0.09^{+0.00}_{-0.09}$	$0.08^{+0.00}_{-0.08}$	$0.08^{+0.00}_{-0.08}$	7E-01	5E-03
72	14^{+4}_{-3}	0	10^{+4}_{-3}	0	4^{+3}_{-1}	0	$-0.43^{+0.31}_{-0.26}$	0	$0.39^{+0.14}_{-0.10}$	$0.28^{+0.12}_{-0.09}$	$0.11^{+0.09}_{-0.05}$	1E+00	1E-08
73	2^{+0}_{-2}	5	2^{+0}_{-2}	1	2^{+0}_{-2}	5	$0.00^{+0.00}_{-0.00}$	-2	$0.07^{+0.00}_{-0.07}$	$0.06^{+0.00}_{-0.06}$	$0.07^{+0.00}_{-0.07}$	1E+00	1E-02
74	19^{+5}_{-4}	0	9^{+4}_{-3}	0	9^{+4}_{-3}	0	$-0.01^{+0.26}_{-0.26}$	0	$0.55^{+0.16}_{-0.12}$	$0.28^{+0.12}_{-0.09}$	$0.28^{+0.12}_{-0.10}$	2E+00	4E-13
75	6^{+3}_{-2}	0	6^{+3}_{-2}	0	2^{+0}_{-2}	1	$-0.49^{+0.00}_{-0.51}$	1	$0.17^{+0.10}_{-0.07}$	$0.19^{+0.10}_{-0.07}$	$0.06^{+0.00}_{-0.06}$	-4E-01	1E+00
76	2^{+0}_{-2}	5	2^{+0}_{-2}	1	2^{+0}_{-2}	5	$0.00^{+0.00}_{-0.00}$	-2	$0.07^{+0.00}_{-0.07}$	$0.06^{+0.00}_{-0.06}$	$0.08^{+0.00}_{-0.08}$	7E-01	7E-03
77	3^{+3}_{-1}	0	3^{+3}_{-1}	0	2^{+0}_{-2}	1	$-0.26^{+0.00}_{-0.74}$	1	$0.11^{+0.09}_{-0.05}$	$0.11^{+0.09}_{-0.05}$	$0.06^{+0.00}_{-0.06}$	-5E-02	1E+00
78	9^{+4}_{-1}	0	4^{+3}_{-1}	0	4^{+3}_{-1}	0	$-0.02^{+0.38}_{-0.38}$	0	$0.27^{+0.12}_{-0.09}$	$0.14^{+0.09}_{-0.06}$	$0.13^{+0.09}_{-0.06}$	1E+00	3E-05
79	5^{+3}_{-2}	0	3^{+5}_{-3}	5	2^{+0}_{-2}	5	$0.00^{+0.00}_{-0.00}$	-2	$0.15^{+0.10}_{-0.06}$	$0.09^{+0.00}_{-0.09}$	$0.07^{+0.00}_{-0.07}$	9E-01	9E-03

TABLE 24:

Counts, count rates and AE detection significance and no-source probabilities for X-ray point sources in HCG 42 (online only).

ID (1)	c(FB) (2)	lim _F (3)	c(SB) (4)	lim _S (5)	c(HB) (6)	lim _S (7)	HR (8)	lim _{HR} (9)	cr(FB) (10)	cr(SB) (11)	cr(HB) (12)	AE(sig) (13)	AE(P) (14)
1	10_{-3}^{+4}	0	6_{-2}^{+3}	0	3_{-1}^{+3}	0	$-0.26_{-0.34}^{+0.38}$	0	$0.32_{-0.10}^{+0.14}$	$0.20_{-0.08}^{+0.12}$	$0.12_{-0.06}^{+0.10}$	1E+00	3E-02
2	2_{-2}^{+0}	5	2_{-2}^{+0}	5	2_{-2}^{+0}	5	$0.00_{-0.00}^{+0.00}$	-2	$0.08_{-0.08}^{+0.00}$	$0.09_{-0.09}^{+0.00}$	$0.08_{-0.08}^{+0.00}$	3E-01	3E-01
3C	5_{-2}^{+3}	0	5_{-2}^{+3}	0	2_{-2}^{+0}	1	$-0.40_{-0.60}^{+0.00}$	1	$0.17_{-0.07}^{+0.11}$	$0.17_{-0.07}^{+0.11}$	$0.07_{-0.07}^{+0.00}$	-6E-03	6E-01
4	2_{-2}^{+0}	5	2_{-2}^{+0}	1	2_{-2}^{+0}	5	$0.00_{-0.00}^{+0.00}$	-2	$0.07_{-0.07}^{+0.00}$	$0.07_{-0.07}^{+0.00}$	$0.08_{-0.08}^{+0.00}$	6E-01	2E-01
5	2_{-2}^{+0}	5	2_{-2}^{+0}	5	2_{-2}^{+0}	1	$0.00_{-0.00}^{+0.00}$	-2	$0.08_{-0.08}^{+0.00}$	$0.08_{-0.08}^{+0.00}$	$0.07_{-0.07}^{+0.00}$	-2E-01	1E+00
6C	19_{-4}^{+5}	0	17_{-4}^{+5}	0	2_{-2}^{+0}	5	$-0.76_{-0.24}^{+0.00}$	1	$0.60_{-0.14}^{+0.17}$	$0.54_{-0.13}^{+0.17}$	$0.08_{-0.08}^{+0.00}$	6E-01	1E-01
7	5_{-2}^{+3}	0	2_{-2}^{+0}	5	2_{-2}^{+0}	5	$0.00_{-0.00}^{+0.00}$	-2	$0.17_{-0.07}^{+0.11}$	$0.08_{-0.08}^{+0.00}$	$0.08_{-0.08}^{+0.00}$	1E+00	1E-03
8C	6_{-2}^{+3}	0	7_{-2}^{+3}	0	2_{-2}^{+0}	1	$-0.50_{-0.50}^{+0.00}$	1	$0.19_{-0.07}^{+0.11}$	$0.22_{-0.08}^{+0.12}$	$0.07_{-0.07}^{+0.00}$	-5E-01	1E+00
9	2_{-2}^{+0}	5	2_{-2}^{+0}	5	2_{-2}^{+0}	1	$0.00_{-0.00}^{+0.00}$	-2	$0.07_{-0.07}^{+0.00}$	$0.07_{-0.07}^{+0.00}$	$0.07_{-0.07}^{+0.00}$	-1E-01	7E-01
10A	3_{-1}^{+3}	0	2_{-2}^{+0}	5	2_{-2}^{+0}	5	$0.00_{-0.00}^{+0.00}$	-2	$0.12_{-0.06}^{+0.10}$	$0.08_{-0.08}^{+0.00}$	$0.08_{-0.08}^{+0.00}$	3E-01	2E-01
11	6_{-2}^{+3}	0	2_{-2}^{+0}	5	5_{-2}^{+3}	0	$0.39_{-0.00}^{+0.61}$	-1	$0.21_{-0.08}^{+0.12}$	$0.08_{-0.08}^{+0.00}$	$0.18_{-0.07}^{+0.11}$	2E+00	2E-07
12	2_{-2}^{+0}	5	2_{-2}^{+0}	5	2_{-2}^{+0}	1	$0.00_{-0.00}^{+0.00}$	-2	$0.08_{-0.08}^{+0.00}$	$0.08_{-0.08}^{+0.00}$	$0.07_{-0.07}^{+0.00}$	-9E-02	1E+00
13D	6_{-2}^{+3}	0	5_{-2}^{+3}	0	2_{-2}^{+0}	5	$-0.40_{-0.60}^{+0.00}$	1	$0.21_{-0.12}^{+0.18}$	$0.18_{-0.07}^{+0.11}$	$0.08_{-0.08}^{+0.00}$	4E-01	2E-01
14	20_{-4}^{+5}	0	12_{-3}^{+4}	0	7_{-2}^{+3}	0	$-0.25_{-0.24}^{+0.25}$	0	$0.65_{-0.14}^{+0.18}$	$0.41_{-0.15}^{+0.15}$	$0.25_{-0.09}^{+0.25}$	2E+00	8E-10
15C	232_{-15}^{+16}	0	185_{-13}^{+14}	0	47_{-6}^{+8}	0	$-0.59_{-0.05}^{+0.06}$	0	$7.35_{-0.48}^{+0.51}$	$5.84_{-0.43}^{+0.46}$	$1.51_{-0.22}^{+0.25}$	6E+00	0E+00
16D	7_{-2}^{+3}	0	3_{-1}^{+3}	0	3_{-1}^{+3}	0	$0.01_{-0.43}^{+0.43}$	0	$0.24_{-0.09}^{+0.12}$	$0.12_{-0.06}^{+0.10}$	$0.12_{-0.06}^{+0.10}$	1E+00	1E-05
17	103_{-10}^{+11}	0	70_{-8}^{+9}	0	32_{-5}^{+6}	0	$-0.37_{-0.10}^{+0.10}$	0	$3.27_{-0.32}^{+0.35}$	$2.24_{-0.27}^{+0.30}$	$1.03_{-0.18}^{+0.21}$	5E+00	4E-34
18A	178_{-13}^{+14}	0	170_{-13}^{+14}	0	7_{-2}^{+3}	0	$-0.91_{-0.03}^{+0.04}$	0	$5.64_{-0.42}^{+0.45}$	$5.39_{-0.41}^{+0.44}$	$0.25_{-0.09}^{+0.12}$	2E+00	5E-06
19	2_{-2}^{+0}	5	3_{-3}^{+0}	5	2_{-2}^{+0}	1	$0.00_{-0.00}^{+0.00}$	-2	$0.08_{-0.08}^{+0.00}$	$0.09_{-0.09}^{+0.00}$	$0.07_{-0.07}^{+0.00}$	-1E-01	1E+00
20	4_{-2}^{+3}	0	5_{-2}^{+3}	0	2_{-2}^{+0}	1	$-0.43_{-0.57}^{+0.00}$	1	$0.14_{-0.06}^{+0.10}$	$0.18_{-0.07}^{+0.11}$	$0.07_{-0.07}^{+0.00}$	-8E-01	1E+00
21	23_{-4}^{+5}	0	16_{-4}^{+5}	0	6_{-2}^{+3}	0	$-0.42_{-0.20}^{+0.23}$	0	$0.75_{-0.15}^{+0.19}$	$0.53_{-0.13}^{+0.16}$	$0.22_{-0.08}^{+0.12}$	2E+00	5E-09
22	2_{-2}^{+0}	5	2_{-2}^{+0}	5	2_{-2}^{+0}	1	$0.00_{-0.00}^{+0.00}$	-2	$0.08_{-0.08}^{+0.00}$	$0.08_{-0.08}^{+0.00}$	$0.07_{-0.07}^{+0.00}$	-7E-02	1E+00
23	3_{-1}^{+3}	0	2_{-2}^{+0}	1	3_{-1}^{+3}	0	$0.26_{-0.00}^{+0.74}$	-1	$0.12_{-0.06}^{+0.10}$	$0.07_{-0.07}^{+0.00}$	$0.12_{-0.06}^{+0.10}$	1E+00	9E-06
24	3_{-3}^{+0}	5	2_{-2}^{+0}	5	3_{-3}^{+0}	5	$0.00_{-0.00}^{+0.00}$	-2	$0.10_{-0.10}^{+0.00}$	$0.08_{-0.08}^{+0.00}$	$0.11_{-0.11}^{+0.00}$	7E-01	2E-03
25	2_{-2}^{+0}	5	3_{-3}^{+0}	5	2_{-2}^{+0}	1	$0.00_{-0.00}^{+0.00}$	-2	$0.08_{-0.08}^{+0.00}$	$0.09_{-0.09}^{+0.00}$	$0.07_{-0.07}^{+0.00}$	-6E-02	1E+00
26	4_{-2}^{+3}	0	5_{-2}^{+3}	0	2_{-2}^{+0}	1	$-0.41_{-0.59}^{+0.00}$	1	$0.15_{-0.07}^{+0.10}$	$0.17_{-0.07}^{+0.11}$	$0.07_{-0.07}^{+0.00}$	-4E-01	8E-01
27	2_{-2}^{+0}	5	2_{-2}^{+0}	5	2_{-2}^{+0}	5	$0.00_{-0.00}^{+0.00}$	-2	$0.07_{-0.07}^{+0.00}$	$0.07_{-0.07}^{+0.00}$	$0.08_{-0.08}^{+0.00}$	9E-01	5E-02
28	49_{-7}^{+8}	0	34_{-5}^{+7}	0	15_{-3}^{+5}	0	$-0.40_{-0.14}^{+0.15}$	0	$1.57_{-0.22}^{+0.26}$	$1.10_{-0.19}^{+0.22}$	$0.47_{-0.12}^{+0.16}$	3E+00	8E-27
29	4_{-2}^{+3}	0	4_{-2}^{+3}	0	2_{-2}^{+0}	1	$-0.36_{-0.64}^{+0.00}$	1	$0.15_{-0.07}^{+0.11}$	$0.16_{-0.11}^{+0.11}$	$0.07_{-0.07}^{+0.00}$	-4E-02	1E+00
30	5_{-2}^{+3}	0	2_{-2}^{+0}	5	3_{-1}^{+3}	0	$0.19_{-0.00}^{+0.81}$	-1	$0.18_{-0.07}^{+0.11}$	$0.08_{-0.08}^{+0.00}$	$0.12_{-0.06}^{+0.10}$	1E+00	3E-05
31	6_{-2}^{+3}	0	3_{-1}^{+3}	0	2_{-2}^{+0}	5	$-0.17_{-0.83}^{+0.00}$	1	$0.20_{-0.10}^{+0.12}$	$0.11_{-0.10}^{+0.10}$	$0.08_{-0.08}^{+0.00}$	9E-01	8E-03
32	28_{-5}^{+6}	0	27_{-5}^{+6}	0	2_{-2}^{+0}	5	$-0.84_{-0.16}^{+0.00}$	1	$0.91_{-0.17}^{+0.20}$	$0.86_{-0.20}^{+0.20}$	$0.08_{-0.08}^{+0.00}$	5E-01	2E-01
33	5_{-2}^{+3}	0	3_{-1}^{+3}	0	2_{-2}^{+0}	5	$-0.15_{-0.00}^{+0.85}$	1	$0.18_{-0.07}^{+0.11}$	$0.12_{-0.10}^{+0.10}$	$0.09_{-0.09}^{+0.00}$	7E-01	6E-03
34	2_{-2}^{+0}	5	2_{-2}^{+0}	5	2_{-2}^{+0}	5	$0.00_{-0.00}^{+0.00}$	-2	$0.08_{-0.08}^{+0.00}$	$0.08_{-0.08}^{+0.00}$	$0.08_{-0.08}^{+0.00}$	3E-01	2E-01
35	3_{-1}^{+3}	0	5_{-5}^{+0}	5	2_{-2}^{+0}	5	$0.00_{-0.00}^{+0.00}$	-2	$0.12_{-0.06}^{+0.10}$	$0.16_{-0.16}^{+0.00}$	$0.08_{-0.08}^{+0.00}$	4E-01	9E-02
36	42_{-6}^{+7}	0	32_{-5}^{+6}	0	9_{-3}^{+4}	0	$-0.54_{-0.14}^{+0.16}$	0	$1.35_{-0.21}^{+0.24}$	$1.04_{-0.18}^{+0.21}$	$0.31_{-0.10}^{+0.13}$	2E+00	3E-14
37	3_{-1}^{+3}	0	3_{-3}^{+0}	5	3_{-3}^{+0}	5	$0.00_{-0.00}^{+0.00}$	-2	$0.12_{-0.06}^{+0.10}$	$0.11_{-0.11}^{+0.00}$	$0.10_{-0.10}^{+0.00}$	4E-01	3E-02
38	7_{-2}^{+3}	0	6_{-2}^{+3}	0	3_{-3}^{+0}	5	$-0.26_{-0.74}^{+0.00}$	1	$0.25_{-0.09}^{+0.12}$	$0.19_{-0.07}^{+0.11}$	$0.11_{-0.11}^{+0.00}$	7E-01	2E-03
39	3_{-1}^{+3}	0	3_{-3}^{+0}	5	5_{-5}^{+0}	5	$0.00_{-0.00}^{+0.00}$	-2	$0.12_{-0.06}^{+0.10}$	$0.09_{-0.09}^{+0.00}$	$0.17_{-0.16}^{+0.00}$	8E-01	1E-04
40	4_{-2}^{+3}	0	2_{-2}^{+0}	5	3_{-1}^{+3}	0	$0.18_{-0.00}^{+0.82}$	-1	$0.15_{-0.07}^{+0.11}$	$0.09_{-0.09}^{+0.00}$	$0.12_{-0.06}^{+0.10}$	1E+00	9E-06
41	5_{-2}^{+3}	0	2_{-2}^{+0}	5	2_{-2}^{+0}	5	$0.00_{-0.00}^{+0.00}$	-2	$0.17_{-0.07}^{+0.11}$	$0.08_{-0.08}^{+0.00}$	$0.08_{-0.08}^{+0.00}$	7E-01	3E-02
42	7_{-2}^{+3}	0	4_{-2}^{+3}	0	3_{-3}^{+0}	5	$-0.17_{-0.83}^{+0.00}$	1	$0.25_{-0.09}^{+0.12}$	$0.16_{-0.07}^{+0.11}$	$0.11_{-0.11}^{+0.00}$	1E+00	2E-04

TABLE 24:
Counts, count rates and AE detection significance and no-source probabilities for X-ray point sources in HCG 42 (online only).

43	2_{-2}^{+0}	5	2_{-2}^{+0}	1	2_{-2}^{+0}	5	$0.00^{+0.00}_{-0.00}$	-2	$0.08^{+0.00}_{-0.08}$	$0.07^{+0.00}_{-0.07}$	$0.08^{+0.00}_{-0.08}$	4E-01	9E-02
44	3_{-3}^{+0}	5	3_{-3}^{+0}	5	2_{-2}^{+0}	5	$0.00^{+0.00}_{-0.00}$	-2	$0.10^{+0.00}_{-0.10}$	$0.10^{+0.00}_{-0.10}$	$0.08^{+0.00}_{-0.08}$	4E-01	8E-02
45	13_{-3}^{+4}	0	12_{-3}^{+4}	0	2_{-2}^{+0}	5	$-0.67^{+0.00}_{-0.33}$	1	$0.44^{+0.15}_{-0.12}$	$0.39^{+0.15}_{-0.11}$	$0.08^{+0.00}_{-0.08}$	6E-01	1E-01
46	27_{-5}^{+6}	0	15_{-3}^{+5}	0	11_{-3}^{+4}	0	$-0.14^{+0.21}_{-0.21}$	0	$0.88^{+0.20}_{-0.17}$	$0.50^{+0.16}_{-0.12}$	$0.38^{+0.14}_{-0.11}$	3E+00	5E-20
47	21_{-4}^{+5}	0	17_{-4}^{+5}	0	4_{-2}^{+3}	0	$-0.59^{+0.23}_{-0.18}$	0	$0.67^{+0.18}_{-0.14}$	$0.54^{+0.16}_{-0.13}$	$0.14^{+0.10}_{-0.06}$	1E+00	8E-03
48	3_{-1}^{+3}	0	3_{-3}^{+0}	5	3_{-3}^{+0}	5	$0.00^{+0.00}_{-0.00}$	-2	$0.12^{+0.10}_{-0.06}$	$0.12^{+0.00}_{-0.12}$	$0.10^{+0.00}_{-0.10}$	7E-01	3E-03
49	2_{-2}^{+0}	5	2_{-2}^{+0}	1	3_{-3}^{+0}	5	$0.00^{+0.00}_{-0.00}$	-2	$0.08^{+0.00}_{-0.08}$	$0.07^{+0.00}_{-0.07}$	$0.10^{+0.00}_{-0.10}$	4E-01	3E-02
50	113_{-10}^{+11}	0	68_{-8}^{+9}	0	44_{-6}^{+7}	0	$-0.21^{+0.10}_{-0.10}$	0	$3.59^{+0.37}_{-0.34}$	$2.17^{+0.29}_{-0.26}$	$1.41^{+0.24}_{-0.21}$	6E+00	0E+00
51	2_{-2}^{+0}	5	2_{-2}^{+0}	5	2_{-2}^{+0}	5	$0.00^{+0.00}_{-0.00}$	-2	$0.08^{+0.00}_{-0.08}$	$0.08^{+0.00}_{-0.08}$	$0.08^{+0.00}_{-0.08}$	3E-01	2E-01
52B	5_{-2}^{+3}	0	4_{-2}^{+3}	0	2_{-2}^{+0}	5	$-0.32^{+0.00}_{-0.68}$	1	$0.18^{+0.11}_{-0.07}$	$0.15^{+0.11}_{-0.07}$	$0.08^{+0.00}_{-0.08}$	4E-01	1E-01
53	165_{-12}^{+13}	0	123_{-11}^{+12}	0	41_{-6}^{+7}	0	$-0.49^{+0.07}_{-0.07}$	0	$5.23^{+0.44}_{-0.41}$	$3.91^{+0.38}_{-0.35}$	$1.32^{+0.24}_{-0.20}$	6E+00	0E+00
54	6_{-2}^{+3}	0	5_{-2}^{+3}	0	2_{-2}^{+0}	5	$-0.40^{+0.00}_{-0.60}$	1	$0.21^{+0.12}_{-0.08}$	$0.18^{+0.11}_{-0.07}$	$0.08^{+0.00}_{-0.08}$	3E-01	2E-01
55B	8_{-2}^{+4}	0	4_{-2}^{+3}	0	3_{-1}^{+3}	0	$-0.10^{+0.42}_{-0.40}$	0	$0.27^{+0.13}_{-0.09}$	$0.15^{+0.11}_{-0.07}$	$0.12^{+0.10}_{-0.06}$	1E+00	8E-05
56	11_{-3}^{+4}	0	7_{-2}^{+3}	0	3_{-1}^{+3}	0	$-0.34^{+0.35}_{-0.30}$	0	$0.37^{+0.14}_{-0.11}$	$0.25^{+0.12}_{-0.09}$	$0.12^{+0.10}_{-0.06}$	1E+00	6E-06
57B	5_{-2}^{+3}	0	4_{-2}^{+3}	0	2_{-2}^{+0}	5	$-0.31^{+0.00}_{-0.69}$	1	$0.18^{+0.11}_{-0.07}$	$0.15^{+0.11}_{-0.07}$	$0.08^{+0.00}_{-0.08}$	4E-01	1E-01
58	6_{-2}^{+3}	0	4_{-2}^{+3}	0	2_{-2}^{+0}	5	$-0.27^{+0.00}_{-0.73}$	1	$0.20^{+0.12}_{-0.08}$	$0.13^{+0.10}_{-0.06}$	$0.08^{+0.00}_{-0.08}$	8E-01	4E-02
59	94_{-9}^{+10}	0	69_{-8}^{+9}	0	24_{-6}^{+6}	0	$-0.47^{+0.10}_{-0.09}$	0	$2.99^{+0.34}_{-0.31}$	$2.20^{+0.30}_{-0.26}$	$0.79^{+0.08}_{-0.16}$	4E+00	4E-40
60	11_{-3}^{+4}	0	8_{-2}^{+4}	0	2_{-2}^{+0}	5	$-0.55^{+0.00}_{-0.45}$	1	$0.35^{+0.14}_{-0.10}$	$0.27^{+0.13}_{-0.09}$	$0.08^{+0.00}_{-0.08}$	9E-01	1E-02
61	7_{-2}^{+3}	0	2_{-2}^{+0}	5	6_{-2}^{+3}	0	$0.43^{+0.57}_{-0.00}$	-1	$0.24^{+0.12}_{-0.09}$	$0.08^{+0.00}_{-0.08}$	$0.21^{+0.12}_{-0.08}$	2E+00	1E-07
62	13_{-3}^{+4}	0	2_{-2}^{+0}	5	11_{-3}^{+4}	0	$0.61^{+0.39}_{-0.00}$	-1	$0.43^{+0.15}_{-0.12}$	$0.09^{+0.00}_{-0.09}$	$0.37^{+0.14}_{-0.11}$	3E+00	2E-17
63	4_{-2}^{+3}	0	2_{-2}^{+0}	5	3_{-3}^{+0}	5	$0.00^{+0.00}_{-0.00}$	-2	$0.15^{+0.10}_{-0.07}$	$0.08^{+0.00}_{-0.08}$	$0.09^{+0.00}_{-0.09}$	1E+00	7E-04
64	2_{-2}^{+0}	5	2_{-2}^{+0}	5	2_{-2}^{+0}	1	$0.00^{+0.00}_{-0.00}$	-2	$0.08^{+0.00}_{-0.08}$	$0.08^{+0.00}_{-0.08}$	$0.07^{+0.00}_{-0.07}$	-1E-01	1E+00
65	3_{-1}^{+3}	0	3_{-3}^{+0}	5	2_{-2}^{+0}	5	$0.00^{+0.00}_{-0.00}$	-2	$0.12^{+0.10}_{-0.06}$	$0.10^{+0.00}_{-0.10}$	$0.08^{+0.00}_{-0.08}$	3E-01	2E-01

TABLE 25:

Counts, count rates and AE detection significance and no-source probabilities for X-ray point sources in HCG 59 (online only).

ID (1)	c(FB) (2)	lim _F (3)	c(SB) (4)	lim _S (5)	c(HB) (6)	lim _S (7)	HR (8)	lim _{HR} (9)	cr(FB) (10)	cr(SB) (11)	cr(HB) (12)	AE(sig) (13)	AE(P) (14)
1	2 ₋₂ ⁺⁰	5	2 ₋₂ ⁺⁰	1	2 ₋₂ ⁺⁰	5	0.00 _{-0.00} ^{+0.00}	-2	0.06 _{-0.06} ^{+0.00}	0.06 _{-0.06} ^{+0.00}	0.07 _{-0.07} ^{+0.00}	9E-01	1E-02
2	2 ₋₂ ⁺⁰	5	2 ₋₂ ⁺⁰	5	2 ₋₂ ⁺⁰	5	0.00 _{-0.00} ^{+0.00}	-2	0.06 _{-0.06} ^{+0.00}	0.07 _{-0.07} ^{+0.00}	0.06 _{-0.06} ^{+0.00}	3E-01	3E-01
3	2 ₋₂ ⁺⁰	5	2 ₋₂ ⁺⁰	5	2 ₋₂ ⁺⁰	1	0.00 _{-0.00} ^{+0.00}	-2	0.07 _{-0.07} ^{+0.00}	0.07 _{-0.07} ^{+0.00}	0.06 _{-0.06} ^{+0.00}	-2E-01	1E+00
4	6 ₋₂ ⁺³	0	4 ₋₂ ⁺³	0	2 ₋₂ ⁺⁰	5	-0.31 _{-0.69} ^{+0.00}	1	0.17 _{-0.06} ^{+0.10}	0.13 _{-0.05} ^{+0.09}	0.07 _{-0.07} ^{+0.00}	7E-01	3E-02
5	3 ₋₃ ⁺⁰	5	2 ₋₂ ⁺⁰	1	3 ₋₃ ⁺⁰	5	0.00 _{-0.00} ^{+0.00}	-2	0.08 _{-0.08} ^{+0.00}	0.06 _{-0.06} ^{+0.00}	0.08 _{-0.08} ^{+0.00}	1E+00	3E-04
6	12 ₋₃ ⁺⁴	0	2 ₋₂ ⁺⁰	1	12 ₋₃ ⁺⁴	0	0.69 _{-0.00} ^{+0.31}	-1	0.33 _{-0.09} ^{+0.12}	0.06 _{-0.06} ^{+0.00}	0.33 _{-0.09} ^{+0.12}	3E+00	6E-17
7	6 ₋₂ ⁺³	0	2 ₋₂ ⁺⁰	5	2 ₋₂ ⁺⁰	5	0.00 _{-0.00} ^{+0.00}	-2	0.16 _{-0.06} ^{+0.09}	0.07 _{-0.07} ^{+0.00}	0.07 _{-0.07} ^{+0.00}	1E+00	3E-03
8	2 ₋₂ ⁺⁰	5	3 ₋₃ ⁺⁰	5	2 ₋₂ ⁺⁰	1	0.00 _{-0.00} ^{+0.00}	-2	0.07 _{-0.07} ^{+0.00}	0.10 _{-0.10} ^{+0.00}	0.06 _{-0.06} ^{+0.00}	-9E-02	1E+00
9	6 ₋₂ ⁺³	0	4 ₋₄ ⁺⁰	5	4 ₋₁ ⁺³	0	-0.05 _{-0.00} ^{+1.05}	-1	0.18 _{-0.07} ^{+0.10}	0.11 _{-0.11} ^{+0.00}	0.10 _{-0.05} ^{+0.08}	1E+00	1E-06
10	5 ₋₂ ⁺³	0	5 ₋₅ ⁺⁰	5	2 ₋₂ ⁺⁰	5	0.00 _{-0.00} ^{+0.00}	-2	0.15 _{-0.06} ^{+0.09}	0.13 _{-0.13} ^{+0.00}	0.07 _{-0.07} ^{+0.00}	9E-01	2E-03
11	2 ₋₂ ⁺⁰	5	3 ₋₃ ⁺⁰	5	2 ₋₂ ⁺⁰	1	0.00 _{-0.00} ^{+0.00}	-2	0.07 _{-0.07} ^{+0.00}	0.10 _{-0.10} ^{+0.00}	0.06 _{-0.06} ^{+0.00}	-1E-01	1E+00
12	4 ₋₂ ⁺⁰	0	2 ₋₂ ⁺⁰	5	4 ₋₁ ⁺⁰	0	0.26 _{-0.00} ^{+0.74}	-1	0.12 _{-0.05} ^{+0.09}	0.06 _{-0.06} ^{+0.00}	0.10 _{-0.05} ^{+0.05}	1E+00	4E-03
13	2 ₋₂ ⁺⁰	5	2 ₋₂ ⁺⁰	5	2 ₋₂ ⁺⁰	5	0.00 _{-0.00} ^{+0.00}	-2	0.07 _{-0.07} ^{+0.00}	0.07 _{-0.07} ^{+0.00}	0.06 _{-0.06} ^{+0.00}	3E-01	3E-01
14	2 ₋₂ ⁺⁰	5	2 ₋₂ ⁺⁰	5	2 ₋₂ ⁺⁰	1	0.00 _{-0.00} ^{+0.00}	-2	0.07 _{-0.07} ^{+0.00}	0.07 _{-0.07} ^{+0.00}	0.06 _{-0.06} ^{+0.00}	-7E-02	1E+00
15	2 ₋₂ ⁺⁰	5	2 ₋₂ ⁺⁰	5	2 ₋₂ ⁺⁰	5	0.00 _{-0.00} ^{+0.00}	-2	0.07 _{-0.07} ^{+0.00}	0.07 _{-0.07} ^{+0.00}	0.06 _{-0.06} ^{+0.00}	3E-01	3E-01
16	3 ₋₁ ⁺³	0	2 ₋₂ ⁺⁰	1	3 ₋₁ ⁺³	0	0.26 _{-0.00} ^{+0.74}	-1	0.10 _{-0.05} ^{+0.08}	0.06 _{-0.06} ^{+0.00}	0.10 _{-0.05} ^{+0.08}	1E+00	6E-06
17	2 ₋₂ ⁺⁰	5	2 ₋₂ ⁺⁰	5	2 ₋₂ ⁺⁰	5	0.00 _{-0.00} ^{+0.00}	-2	0.07 _{-0.07} ^{+0.00}	0.07 _{-0.07} ^{+0.00}	0.06 _{-0.06} ^{+0.00}	3E-01	2E-01
18	3 ₋₃ ⁺⁰	5	3 ₋₃ ⁺⁰	5	2 ₋₂ ⁺⁰	5	0.00 _{-0.00} ^{+0.00}	-2	0.10 _{-0.10} ^{+0.00}	0.10 _{-0.10} ^{+0.00}	0.07 _{-0.07} ^{+0.00}	4E-01	5E-02
19	4 ₋₂ ⁺³	0	2 ₋₂ ⁺⁰	5	2 ₋₂ ⁺⁰	5	0.00 _{-0.00} ^{+0.00}	-2	0.12 _{-0.05} ^{+0.09}	0.06 _{-0.06} ^{+0.00}	0.06 _{-0.06} ^{+0.00}	1E+00	2E-02
20	2 ₋₂ ⁺⁰	5	3 ₋₃ ⁺⁰	5	2 ₋₂ ⁺⁰	5	0.00 _{-0.00} ^{+0.00}	-2	0.07 _{-0.07} ^{+0.00}	0.08 _{-0.08} ^{+0.00}	0.06 _{-0.06} ^{+0.00}	3E-01	2E-01
21B	5 ₋₂ ⁺³	0	5 ₋₂ ⁺³	0	2 ₋₂ ⁺⁰	1	-0.44 _{-0.56} ^{+0.00}	1	0.15 _{-0.06} ^{+0.09}	0.15 _{-0.09} ^{+0.00}	0.06 _{-0.06} ^{+0.00}	-6E-02	1E+00
22B	4 ₋₂ ⁺³	0	2 ₋₂ ⁺⁰	5	2 ₋₂ ⁺⁰	5	0.00 _{-0.00} ^{+0.00}	-2	0.12 _{-0.05} ^{+0.09}	0.08 _{-0.08} ^{+0.00}	0.08 _{-0.08} ^{+0.00}	1E+00	9E-04
23B	5 ₋₂ ⁺³	0	5 ₋₂ ⁺³	0	2 ₋₂ ⁺⁰	1	-0.44 _{-0.56} ^{+0.00}	1	0.15 _{-0.06} ^{+0.09}	0.15 _{-0.09} ^{+0.00}	0.06 _{-0.06} ^{+0.00}	-4E-02	1E+00
24	2 ₋₂ ⁺⁰	5	3 ₋₃ ⁺⁰	5	2 ₋₂ ⁺⁰	5	0.00 _{-0.00} ^{+0.00}	-2	0.08 _{-0.08} ^{+0.00}	0.09 _{-0.09} ^{+0.00}	0.07 _{-0.07} ^{+0.00}	4E-01	1E-01
25	5 ₋₂ ⁺³	0	2 ₋₂ ⁺⁰	5	2 ₋₂ ⁺⁰	5	0.00 _{-0.00} ^{+0.00}	-2	0.15 _{-0.06} ^{+0.09}	0.07 _{-0.07} ^{+0.00}	0.06 _{-0.06} ^{+0.00}	8E-01	3E-02
26B	10 ₋₃ ⁺⁴	0	7 ₋₂ ⁺³	0	3 ₋₃ ⁺⁰	5	-0.44 _{-0.56} ^{+0.00}	1	0.28 _{-0.08} ^{+0.11}	0.21 _{-0.07} ^{+0.10}	0.08 _{-0.08} ^{+0.00}	1E+00	5E-04
27	2 ₋₂ ⁺⁰	5	2 ₋₂ ⁺⁰	1	2 ₋₂ ⁺⁰	5	0.00 _{-0.00} ^{+0.00}	-2	0.07 _{-0.07} ^{+0.00}	0.06 _{-0.06} ^{+0.00}	0.07 _{-0.07} ^{+0.00}	9E-01	5E-03
28	3 ₋₁ ⁺³	0	4 ₋₄ ⁺⁰	5	2 ₋₂ ⁺⁰	5	0.00 _{-0.00} ^{+0.00}	-2	0.10 _{-0.05} ^{+0.08}	0.10 _{-0.10} ^{+0.00}	0.07 _{-0.07} ^{+0.00}	4E-01	1E-01
29	2 ₋₂ ⁺⁰	5	2 ₋₂ ⁺⁰	5	2 ₋₂ ⁺⁰	1	0.00 _{-0.00} ^{+0.00}	-2	0.06 _{-0.06} ^{+0.00}	0.07 _{-0.07} ^{+0.00}	0.06 _{-0.06} ^{+0.00}	-1E-01	1E+00
30	2 ₋₂ ⁺⁰	5	3 ₋₃ ⁺⁰	5	2 ₋₂ ⁺⁰	1	0.00 _{-0.00} ^{+0.00}	-2	0.07 _{-0.07} ^{+0.00}	0.08 _{-0.08} ^{+0.00}	0.06 _{-0.06} ^{+0.00}	-4E-02	1E+00
31	2 ₋₂ ⁺⁰	5	2 ₋₂ ⁺⁰	5	2 ₋₂ ⁺⁰	1	0.00 _{-0.00} ^{+0.00}	-2	0.06 _{-0.06} ^{+0.00}	0.08 _{-0.08} ^{+0.00}	0.06 _{-0.06} ^{+0.00}	-2E-01	1E+00
32	3 ₋₁ ⁺³	0	2 ₋₂ ⁺⁰	5	3 ₋₃ ⁺⁰	5	0.00 _{-0.00} ^{+0.00}	-2	0.10 _{-0.05} ^{+0.08}	0.07 _{-0.07} ^{+0.00}	0.08 _{-0.08} ^{+0.00}	1E+00	5E-04
33	2 ₋₂ ⁺⁰	5	3 ₋₃ ⁺⁰	5	2 ₋₂ ⁺⁰	1	0.00 _{-0.00} ^{+0.00}	-2	0.07 _{-0.07} ^{+0.00}	0.09 _{-0.09} ^{+0.00}	0.06 _{-0.06} ^{+0.00}	-6E-02	1E+00
34	31 ₋₅ ⁺⁶	0	24 ₋₅ ⁺⁶	0	6 ₋₂ ⁺³	0	-0.57 _{-0.15} ^{+0.18}	0	0.83 _{-0.15} ^{+0.17}	0.65 _{-0.13} ^{+0.16}	0.18 _{-0.07} ^{+0.10}	2E+00	5E-09
35	7 ₋₂ ⁺³	0	2 ₋₂ ⁺⁰	5	5 ₋₂ ⁺³	0	0.36 _{-0.00} ^{+0.64}	-1	0.20 _{-0.07} ^{+0.12}	0.06 _{-0.06} ^{+0.00}	0.14 _{-0.06} ^{+0.09}	1E+00	1E-04
36	2 ₋₂ ⁺⁰	5	2 ₋₂ ⁺⁰	5	2 ₋₂ ⁺⁰	5	0.00 _{-0.00} ^{+0.00}	-2	0.07 _{-0.07} ^{+0.00}	0.07 _{-0.07} ^{+0.00}	0.06 _{-0.06} ^{+0.00}	3E-01	3E-01
37	3 ₋₁ ⁺³	0	4 ₋₄ ⁺⁰	5	2 ₋₂ ⁺⁰	5	0.00 _{-0.00} ^{+0.00}	-2	0.10 _{-0.05} ^{+0.08}	0.11 _{-0.11} ^{+0.00}	0.07 _{-0.07} ^{+0.00}	4E-01	1E-01
38	2 ₋₂ ⁺⁰	5	3 ₋₃ ⁺⁰	5	2 ₋₂ ⁺⁰	1	0.00 _{-0.00} ^{+0.00}	-2	0.07 _{-0.07} ^{+0.00}	0.10 _{-0.10} ^{+0.00}	0.06 _{-0.06} ^{+0.00}	-6E-02	1E+00
39	6 ₋₂ ⁺³	0	4 ₋₁ ⁺³	0	4 ₋₄ ⁺⁰	5	-0.00 _{-1.00} ^{+0.00}	1	0.18 _{-0.07} ^{+0.10}	0.10 _{-0.05} ^{+0.08}	0.10 _{-0.10} ^{+0.00}	1E+00	8E-05
40	2 ₋₂ ⁺⁰	5	3 ₋₃ ⁺⁰	5	2 ₋₂ ⁺⁰	1	0.00 _{-0.00} ^{+0.00}	-2	0.07 _{-0.07} ^{+0.00}	0.08 _{-0.08} ^{+0.00}	0.06 _{-0.06} ^{+0.00}	-6E-02	1E+00
41	2 ₋₂ ⁺⁰	5	3 ₋₃ ⁺⁰	5	2 ₋₂ ⁺⁰	1	0.00 _{-0.00} ^{+0.00}	-2	0.07 _{-0.07} ^{+0.00}	0.09 _{-0.09} ^{+0.00}	0.06 _{-0.06} ^{+0.00}	-6E-02	1E+00
42	2 ₋₂ ⁺⁰	5	3 ₋₃ ⁺⁰	5	2 ₋₂ ⁺⁰	5	0.00 _{-0.00} ^{+0.00}	-2	0.07 _{-0.07} ^{+0.00}	0.09 _{-0.09} ^{+0.00}	0.07 _{-0.07} ^{+0.00}	4E-01	1E-01

TABLE 25:

Counts, count rates and AE detection significance and no-source probabilities for X-ray point sources in HCG 59 (online only).

43	2^{+0}_{-2}	5	5^{+0}_{-5}	5	2^{+0}_{-2}	1	$0.00^{+0.00}_{-0.00}$	-2	$0.08^{+0.00}_{-0.08}$	$0.13^{+0.00}_{-0.13}$	$0.06^{+0.00}_{-0.06}$	-7E-02	1E+00
44	2^{+0}_{-2}	5	3^{+0}_{-3}	5	2^{+0}_{-2}	1	$0.00^{+0.00}_{-0.00}$	-2	$0.07^{+0.00}_{-0.07}$	$0.10^{+0.00}_{-0.10}$	$0.06^{+0.00}_{-0.06}$	-1E-01	1E+00
45	2^{+0}_{-2}	5	3^{+0}_{-3}	5	2^{+0}_{-2}	1	$0.00^{+0.00}_{-0.00}$	-2	$0.07^{+0.00}_{-0.07}$	$0.08^{+0.00}_{-0.08}$	$0.06^{+0.00}_{-0.06}$	-9E-02	1E+00
46	2^{+0}_{-2}	5	2^{+0}_{-2}	5	2^{+0}_{-2}	1	$0.00^{+0.00}_{-0.00}$	-2	$0.06^{+0.00}_{-0.06}$	$0.07^{+0.00}_{-0.07}$	$0.06^{+0.00}_{-0.06}$	-1E-01	1E+00
47	10^{+4}_{-3}	0	10^{+4}_{-3}	0	2^{+0}_{-2}	1	$-0.65^{+0.00}_{-0.35}$	1	$0.27^{+0.11}_{-0.08}$	$0.28^{+0.11}_{-0.08}$	$0.06^{+0.00}_{-0.06}$	-3E-01	1E+00
48	2^{+0}_{-2}	5	2^{+0}_{-2}	5	2^{+0}_{-2}	1	$0.00^{+0.00}_{-0.00}$	-2	$0.07^{+0.00}_{-0.07}$	$0.08^{+0.00}_{-0.08}$	$0.06^{+0.00}_{-0.06}$	-6E-02	1E+00
49	2^{+0}_{-2}	5	2^{+0}_{-2}	1	4^{+0}_{-4}	5	$0.00^{+0.00}_{-0.00}$	-2	$0.08^{+0.00}_{-0.08}$	$0.06^{+0.00}_{-0.06}$	$0.11^{+0.00}_{-0.11}$	1E+00	4E-05
50A	43^{+7}_{-6}	0	23^{+6}_{-4}	0	19^{+5}_{-4}	0	$-0.09^{+0.17}_{-0.16}$	0	$1.14^{+0.20}_{-0.17}$	$0.62^{+0.16}_{-0.13}$	$0.52^{+0.14}_{-0.11}$	4E+00	1E-29
51	3^{+0}_{-3}	5	3^{+0}_{-3}	5	2^{+0}_{-2}	5	$0.00^{+0.00}_{-0.00}$	-2	$0.08^{+0.00}_{-0.08}$	$0.08^{+0.00}_{-0.08}$	$0.08^{+0.00}_{-0.08}$	7E-01	6E-03
52	2^{+0}_{-2}	5	2^{+0}_{-2}	5	2^{+0}_{-2}	5	$0.00^{+0.00}_{-0.00}$	-2	$0.06^{+0.00}_{-0.06}$	$0.07^{+0.00}_{-0.07}$	$0.06^{+0.00}_{-0.06}$	3E-01	3E-01
53	9^{+4}_{-3}	0	2^{+0}_{-2}	5	7^{+3}_{-2}	0	$0.53^{+0.47}_{-0.00}$	-1	$0.24^{+0.08}_{-0.08}$	$0.06^{+0.00}_{-0.06}$	$0.21^{+0.10}_{-0.07}$	2E+00	3E-06
54	2^{+0}_{-2}	5	2^{+0}_{-2}	1	3^{+0}_{-3}	5	$0.00^{+0.00}_{-0.00}$	-2	$0.08^{+0.00}_{-0.08}$	$0.06^{+0.00}_{-0.06}$	$0.08^{+0.00}_{-0.08}$	7E-01	3E-03
55	2^{+0}_{-2}	5	2^{+0}_{-2}	5	2^{+0}_{-2}	1	$0.00^{+0.00}_{-0.00}$	-2	$0.06^{+0.00}_{-0.06}$	$0.06^{+0.00}_{-0.06}$	$0.06^{+0.00}_{-0.06}$	-2E-01	1E+00
56	3^{+3}_{-1}	0	4^{+3}_{-1}	0	2^{+0}_{-2}	1	$-0.26^{+0.00}_{-0.74}$	1	$0.10^{+0.08}_{-0.05}$	$0.10^{+0.08}_{-0.05}$	$0.06^{+0.00}_{-0.06}$	-8E-02	1E+00
57	3^{+0}_{-3}	5	2^{+0}_{-2}	5	3^{+0}_{-3}	5	$0.00^{+0.00}_{-0.00}$	-2	$0.08^{+0.00}_{-0.08}$	$0.07^{+0.00}_{-0.07}$	$0.08^{+0.00}_{-0.08}$	7E-01	3E-03
58	2^{+0}_{-2}	5	2^{+0}_{-2}	5	2^{+0}_{-2}	1	$0.00^{+0.00}_{-0.00}$	-2	$0.06^{+0.00}_{-0.06}$	$0.07^{+0.00}_{-0.07}$	$0.06^{+0.00}_{-0.06}$	-1E-01	1E+00
59	26^{+6}_{-5}	0	17^{+5}_{-4}	0	8^{+4}_{-2}	0	$-0.33^{+0.22}_{-0.20}$	0	$0.69^{+0.16}_{-0.13}$	$0.46^{+0.14}_{-0.16}$	$0.23^{+0.11}_{-0.09}$	2E+00	1E-04
60	14^{+4}_{-3}	0	6^{+3}_{-2}	0	7^{+3}_{-2}	0	$0.06^{+0.30}_{-0.31}$	0	$0.37^{+0.13}_{-0.10}$	$0.18^{+0.10}_{-0.07}$	$0.20^{+0.10}_{-0.07}$	2E+00	3E-08
61	2^{+0}_{-2}	5	2^{+0}_{-2}	5	2^{+0}_{-2}	1	$0.00^{+0.00}_{-0.00}$	-2	$0.06^{+0.00}_{-0.06}$	$0.07^{+0.00}_{-0.07}$	$0.06^{+0.00}_{-0.06}$	-1E-01	1E+00
62	2^{+0}_{-2}	5	2^{+0}_{-2}	5	2^{+0}_{-2}	1	$0.00^{+0.00}_{-0.00}$	-2	$0.06^{+0.00}_{-0.06}$	$0.06^{+0.00}_{-0.06}$	$0.06^{+0.00}_{-0.06}$	-7E-02	1E+00
63	2^{+0}_{-2}	5	2^{+0}_{-2}	5	2^{+0}_{-2}	1	$0.00^{+0.00}_{-0.00}$	-2	$0.06^{+0.00}_{-0.06}$	$0.07^{+0.00}_{-0.07}$	$0.06^{+0.00}_{-0.06}$	-2E-01	1E+00
64	2^{+0}_{-2}	5	3^{+0}_{-3}	5	2^{+0}_{-2}	1	$0.00^{+0.00}_{-0.00}$	-2	$0.07^{+0.00}_{-0.07}$	$0.09^{+0.00}_{-0.09}$	$0.06^{+0.00}_{-0.06}$	-1E-01	1E+00
65	2^{+0}_{-2}	5	2^{+0}_{-2}	5	2^{+0}_{-2}	1	$0.00^{+0.00}_{-0.00}$	-2	$0.06^{+0.00}_{-0.06}$	$0.06^{+0.00}_{-0.06}$	$0.06^{+0.00}_{-0.06}$	-6E-02	1E+00
66D	2^{+0}_{-2}	5	2^{+0}_{-2}	1	3^{+3}_{-1}	0	$0.00^{+0.00}_{-0.00}$	-2	$0.06^{+0.00}_{-0.06}$	$0.06^{+0.00}_{-0.06}$	$0.10^{+0.08}_{-0.05}$	1E+00	2E-04
67	2^{+0}_{-2}	5	2^{+0}_{-2}	5	2^{+0}_{-2}	1	$0.00^{+0.00}_{-0.00}$	-2	$0.07^{+0.00}_{-0.07}$	$0.07^{+0.00}_{-0.07}$	$0.06^{+0.00}_{-0.06}$	-8E-02	1E+00
68	2^{+0}_{-2}	5	3^{+0}_{-3}	5	2^{+0}_{-2}	5	$0.00^{+0.00}_{-0.00}$	-2	$0.07^{+0.00}_{-0.07}$	$0.08^{+0.00}_{-0.08}$	$0.07^{+0.00}_{-0.07}$	7E-01	1E-02
69	9^{+4}_{-3}	0	9^{+4}_{-3}	0	2^{+0}_{-2}	1	$-0.62^{+0.00}_{-0.38}$	1	$0.25^{+0.11}_{-0.08}$	$0.26^{+0.11}_{-0.08}$	$0.06^{+0.00}_{-0.06}$	-9E-02	1E+00
70C	19^{+5}_{-4}	0	8^{+4}_{-2}	0	10^{+4}_{-3}	0	$0.10^{+0.25}_{-0.26}$	0	$0.51^{+0.14}_{-0.11}$	$0.23^{+0.11}_{-0.08}$	$0.28^{+0.11}_{-0.08}$	2E+00	2E-15
71	2^{+0}_{-2}	5	2^{+0}_{-2}	5	2^{+0}_{-2}	1	$0.00^{+0.00}_{-0.00}$	-2	$0.06^{+0.00}_{-0.06}$	$0.07^{+0.00}_{-0.07}$	$0.06^{+0.00}_{-0.06}$	-1E-01	1E+00
72	14^{+4}_{-3}	0	10^{+4}_{-3}	0	4^{+3}_{-2}	0	$-0.40^{+0.30}_{-0.26}$	0	$0.38^{+0.13}_{-0.10}$	$0.27^{+0.11}_{-0.08}$	$0.12^{+0.09}_{-0.05}$	1E+00	3E-02
73	7^{+3}_{-2}	0	5^{+3}_{-2}	0	2^{+0}_{-2}	5	$-0.41^{+0.00}_{-0.59}$	1	$0.20^{+0.10}_{-0.07}$	$0.15^{+0.09}_{-0.06}$	$0.06^{+0.00}_{-0.06}$	6E-01	6E-02
74	2^{+0}_{-2}	5	2^{+0}_{-2}	5	2^{+0}_{-2}	5	$0.00^{+0.00}_{-0.00}$	-2	$0.06^{+0.00}_{-0.06}$	$0.08^{+0.00}_{-0.08}$	$0.06^{+0.00}_{-0.06}$	2E-01	4E-01
75	9^{+4}_{-3}	0	3^{+3}_{-1}	0	5^{+3}_{-2}	0	$0.19^{+0.36}_{-0.39}$	0	$0.25^{+0.11}_{-0.08}$	$0.10^{+0.08}_{-0.05}$	$0.15^{+0.09}_{-0.06}$	2E+00	3E-06
76	16^{+5}_{-4}	0	10^{+4}_{-3}	0	5^{+3}_{-2}	0	$-0.28^{+0.29}_{-0.26}$	0	$0.43^{+0.13}_{-0.10}$	$0.27^{+0.11}_{-0.08}$	$0.15^{+0.09}_{-0.06}$	1E+00	5E-03
77	67^{+9}_{-8}	0	50^{+8}_{-7}	0	16^{+5}_{-4}	0	$-0.50^{+0.12}_{-0.11}$	0	$1.75^{+0.24}_{-0.21}$	$1.31^{+0.21}_{-0.18}$	$0.44^{+0.14}_{-0.11}$	3E+00	4E-12
78	2^{+0}_{-2}	5	2^{+0}_{-2}	1	2^{+0}_{-2}	5	$0.00^{+0.00}_{-0.00}$	-2	$0.06^{+0.00}_{-0.06}$	$0.06^{+0.00}_{-0.06}$	$0.06^{+0.00}_{-0.06}$	5E-01	1E-01
79	6^{+3}_{-2}	0	3^{+3}_{-1}	0	2^{+0}_{-2}	5	$-0.20^{+0.00}_{-0.80}$	1	$0.17^{+0.10}_{-0.06}$	$0.10^{+0.08}_{-0.05}$	$0.07^{+0.00}_{-0.07}$	9E-01	6E-03
80	4^{+3}_{-2}	0	2^{+0}_{-2}	1	4^{+3}_{-2}	0	$0.34^{+0.66}_{-0.00}$	-1	$0.12^{+0.09}_{-0.05}$	$0.06^{+0.00}_{-0.06}$	$0.12^{+0.09}_{-0.05}$	1E+00	4E-05
81	41^{+7}_{-6}	0	34^{+7}_{-5}	0	6^{+3}_{-2}	0	$-0.68^{+0.15}_{-0.12}$	0	$1.08^{+0.20}_{-0.17}$	$0.91^{+0.18}_{-0.15}$	$0.17^{+0.10}_{-0.07}$	2E+00	1E-07
82	2^{+0}_{-2}	5	2^{+0}_{-2}	5	2^{+0}_{-2}	5	$0.00^{+0.00}_{-0.00}$	-2	$0.06^{+0.00}_{-0.06}$	$0.06^{+0.00}_{-0.06}$	$0.06^{+0.00}_{-0.06}$	5E-01	1E-01
83	7^{+3}_{-2}	0	3^{+0}_{-3}	5	4^{+3}_{-2}	0	$0.21^{+0.79}_{-0.00}$	-1	$0.19^{+0.10}_{-0.07}$	$0.08^{+0.00}_{-0.08}$	$0.12^{+0.09}_{-0.05}$	1E+00	2E-04
84	32^{+6}_{-5}	0	19^{+5}_{-4}	0	12^{+4}_{-3}	0	$-0.23^{+0.20}_{-0.19}$	0	$0.83^{+0.18}_{-0.15}$	$0.51^{+0.14}_{-0.11}$	$0.32^{+0.12}_{-0.09}$	3E+00	6E-12
85	6^{+3}_{-2}	0	4^{+3}_{-2}	0	2^{+0}_{-2}	5	$-0.33^{+0.00}_{-0.67}$	1	$0.16^{+0.10}_{-0.06}$	$0.13^{+0.09}_{-0.06}$	$0.06^{+0.00}_{-0.06}$	6E-01	1E-01
86	2^{+0}_{-2}	5	2^{+0}_{-2}	5	2^{+0}_{-2}	5	$0.00^{+0.00}_{-0.00}$	-2	$0.06^{+0.00}_{-0.06}$	$0.06^{+0.00}_{-0.06}$	$0.06^{+0.00}_{-0.06}$	8E-01	2E-02
87	18^{+5}_{-4}	0	12^{+4}_{-3}	0	6^{+3}_{-2}	0	$-0.34^{+0.26}_{-0.24}$	0	$0.49^{+0.14}_{-0.11}$	$0.33^{+0.12}_{-0.09}$	$0.16^{+0.09}_{-0.06}$	2E+00	2E-05

TABLE 25:

Counts, count rates and AE detection significance and no-source probabilities for X-ray point sources in HCG 59 (online only).

88	7^{+3}_{-2}	0	2^{+0}_{-2}	5	5^{+3}_{-2}	0	$0.37^{+0.63}_{-0.00}$	-1	$0.19^{+0.10}_{-0.07}$	$0.07^{+0.00}_{-0.07}$	$0.14^{+0.09}_{-0.06}$	2E+00	1E-05
89	2^{+0}_{-2}	5	2^{+0}_{-2}	1	2^{+0}_{-2}	5	$0.00^{+0.00}_{-0.00}$	-2	$0.06^{+0.00}_{-0.06}$	$0.06^{+0.00}_{-0.06}$	$0.06^{+0.00}_{-0.06}$	5E-01	2E-01
90	13^{+4}_{-3}	0	6^{+3}_{-2}	0	7^{+3}_{-2}	0	$0.02^{+0.31}_{-0.32}$	0	$0.35^{+0.12}_{-0.09}$	$0.17^{+0.10}_{-0.07}$	$0.18^{+0.10}_{-0.07}$	2E+00	2E-05
91	28^{+6}_{-5}	0	23^{+5}_{-4}	0	5^{+3}_{-2}	0	$-0.65^{+0.19}_{-0.15}$	0	$0.74^{+0.17}_{-0.14}$	$0.61^{+0.15}_{-0.12}$	$0.13^{+0.09}_{-0.06}$	1E+00	2E-02
92	2^{+0}_{-2}	5	2^{+0}_{-2}	5	2^{+0}_{-2}	1	$0.00^{+0.00}_{-0.00}$	-2	$0.06^{+0.00}_{-0.06}$	$0.06^{+0.00}_{-0.06}$	$0.06^{+0.00}_{-0.06}$	-3E-01	8E-01
93	130^{+12}_{-11}	0	95^{+10}_{-9}	0	34^{+7}_{-5}	0	$-0.46^{+0.09}_{-0.08}$	0	$3.39^{+0.32}_{-0.30}$	$2.48^{+0.28}_{-0.25}$	$0.91^{+0.18}_{-0.15}$	5E+00	2E-31
94	133^{+12}_{-11}	0	124^{+12}_{-11}	0	9^{+4}_{-2}	0	$-0.87^{+0.06}_{-0.04}$	0	$3.48^{+0.33}_{-0.30}$	$3.24^{+0.32}_{-0.29}$	$0.23^{+0.11}_{-0.08}$	2E+00	2E-07
95	24^{+6}_{-4}	0	18^{+5}_{-4}	0	6^{+3}_{-2}	0	$-0.48^{+0.22}_{-0.19}$	0	$0.65^{+0.16}_{-0.13}$	$0.48^{+0.14}_{-0.11}$	$0.17^{+0.10}_{-0.06}$	2E+00	3E-04
96	109^{+11}_{-10}	0	88^{+10}_{-9}	0	20^{+5}_{-4}	0	$-0.62^{+0.09}_{-0.08}$	0	$2.84^{+0.30}_{-0.27}$	$2.30^{+0.27}_{-0.24}$	$0.54^{+0.15}_{-0.12}$	4E+00	3E-18
97	2^{+0}_{-2}	5	2^{+0}_{-2}	5	2^{+0}_{-2}	5	$0.00^{+0.00}_{-0.00}$	-2	$0.06^{+0.00}_{-0.06}$	$0.06^{+0.00}_{-0.06}$	$0.06^{+0.00}_{-0.06}$	6E-01	2E-01
98	4^{+3}_{-2}	0	4^{+3}_{-2}	0	2^{+0}_{-2}	5	$-0.30^{+0.00}_{-0.70}$	1	$0.12^{+0.09}_{-0.05}$	$0.11^{+0.08}_{-0.05}$	$0.06^{+0.00}_{-0.06}$	2E-01	5E-01
99	2^{+0}_{-2}	5	2^{+0}_{-2}	5	2^{+0}_{-2}	5	$0.00^{+0.00}_{-0.00}$	-2	$0.06^{+0.00}_{-0.06}$	$0.06^{+0.00}_{-0.06}$	$0.06^{+0.00}_{-0.06}$	3E-01	3E-01
100	2^{+0}_{-2}	5	2^{+0}_{-2}	5	2^{+0}_{-2}	1	$0.00^{+0.00}_{-0.00}$	-2	$0.06^{+0.00}_{-0.06}$	$0.07^{+0.00}_{-0.07}$	$0.06^{+0.00}_{-0.06}$	-5E-02	7E-01
101	2^{+0}_{-2}	1	2^{+0}_{-2}	1	2^{+0}_{-2}	5	$0.00^{+0.00}_{-0.00}$	-2	$0.06^{+0.00}_{-0.06}$	$0.06^{+0.00}_{-0.06}$	$0.06^{+0.00}_{-0.06}$	2E-01	4E-01
102	5^{+3}_{-2}	0	4^{+3}_{-1}	0	2^{+0}_{-2}	5	$-0.28^{+0.00}_{-0.72}$	1	$0.13^{+0.09}_{-0.06}$	$0.11^{+0.08}_{-0.05}$	$0.06^{+0.00}_{-0.06}$	3E-01	4E-01
103	2^{+0}_{-2}	5	2^{+0}_{-2}	5	2^{+0}_{-2}	5	$0.00^{+0.00}_{-0.00}$	-2	$0.06^{+0.00}_{-0.06}$	$0.06^{+0.00}_{-0.06}$	$0.06^{+0.00}_{-0.06}$	4E-01	3E-01
104	64^{+9}_{-8}	0	19^{+5}_{-4}	0	45^{+6}_{-6}	0	$0.41^{+0.12}_{-0.13}$	0	$1.69^{+0.24}_{-0.21}$	$0.50^{+0.14}_{-0.11}$	$1.19^{+0.20}_{-0.18}$	6E+00	1E-43
105	5^{+3}_{-2}	0	2^{+0}_{-2}	5	2^{+0}_{-2}	5	$0.00^{+0.00}_{-0.00}$	-2	$0.13^{+0.09}_{-0.06}$	$0.06^{+0.00}_{-0.06}$	$0.06^{+0.00}_{-0.06}$	6E-01	2E-01
106	4^{+3}_{-2}	0	2^{+0}_{-2}	5	3^{+3}_{-1}	0	$0.24^{+0.76}_{-0.00}$	-1	$0.11^{+0.09}_{-0.05}$	$0.06^{+0.00}_{-0.06}$	$0.10^{+0.08}_{-0.05}$	1E+00	7E-03
107	2^{+0}_{-2}	5	2^{+0}_{-2}	5	2^{+0}_{-2}	5	$0.00^{+0.00}_{-0.00}$	-2	$0.06^{+0.00}_{-0.06}$	$0.07^{+0.00}_{-0.07}$	$0.06^{+0.00}_{-0.06}$	9E-02	6E-01
108	85^{+10}_{-9}	0	80^{+10}_{-9}	0	5^{+3}_{-2}	0	$-0.88^{+0.07}_{-0.05}$	0	$2.23^{+0.27}_{-0.24}$	$2.10^{+0.26}_{-0.23}$	$0.13^{+0.09}_{-0.06}$	1E+00	2E-02
109	18^{+5}_{-4}	0	14^{+4}_{-3}	0	4^{+3}_{-2}	0	$-0.51^{+0.26}_{-0.21}$	0	$0.48^{+0.14}_{-0.11}$	$0.37^{+0.13}_{-0.10}$	$0.12^{+0.09}_{-0.05}$	1E+00	1E-02
110	5^{+3}_{-2}	0	2^{+0}_{-2}	1	6^{+3}_{-2}	0	$0.48^{+0.52}_{-0.00}$	-1	$0.14^{+0.09}_{-0.06}$	$0.06^{+0.00}_{-0.06}$	$0.17^{+0.10}_{-0.06}$	1E+00	1E-02

TABLE 26:
Counts, count rates and AE detection significance and no-source probabilities for X-ray point sources in HCG 62 (online only).

ID (1)	c(FB) (2)	lim _F (3)	c(SB) (4)	lim _S (5)	c(HB) (6)	lim _S (7)	HR (8)	lim _{HR} (9)	cr(FB) (10)	cr(SB) (11)	cr(HB) (12)	AE(sig) (13)	AE(P) (14)
1	30 ₋₅ ⁺⁶	0	14 ₋₃ ⁺⁴	0	15 ₋₃ ⁺⁵	0	0.03 _{-0.20} ^{+0.20}	0	0.18 _{-0.03} ^{+0.04}	0.09 _{-0.02} ^{+0.03}	0.09 _{-0.02} ^{+0.03}	2E+00	2E-03
2	13 ₋₃ ⁺⁴	0	5 ₋₂ ⁺³	0	7 ₋₂ ⁺³	0	0.17 _{-0.33} ^{+0.31}	0	0.08 _{-0.02} ^{+0.03}	0.03 _{-0.01} ^{+0.02}	0.05 _{-0.02} ^{+0.02}	1E+00	2E-02
3	35 ₋₅ ⁺⁷	0	15 ₋₃ ⁺⁵	0	19 ₋₄ ⁺⁵	0	0.14 _{-0.19} ^{+0.18}	0	0.21 _{-0.04} ^{+0.04}	0.09 _{-0.02} ^{+0.03}	0.12 _{-0.03} ^{+0.03}	3E+00	1E-04
4	2 ₋₂ ⁺⁰	5	2 ₋₂ ⁺⁰	5	2 ₋₂ ⁺⁰	1	0.00 _{-0.00} ^{+0.00}	-2	0.01 _{-0.01} ^{+0.00}	0.02 _{-0.02} ^{+0.00}	0.01 _{-0.01} ^{+0.00}	-8E-02	7E-01
5	62 ₋₇ ⁺⁸	0	33 ₋₅ ⁺⁶	0	29 ₋₅ ⁺⁶	0	-0.06 _{-0.14} ^{+0.14}	0	0.37 _{-0.05} ^{+0.05}	0.20 _{-0.03} ^{+0.04}	0.17 _{-0.03} ^{+0.04}	4E+00	4E-08
6	35 ₋₅ ⁺⁷	0	22 ₋₄ ⁺⁵	0	13 ₋₃ ⁺⁴	0	-0.26 _{-0.18} ^{+0.19}	0	0.21 _{-0.04} ^{+0.04}	0.13 _{-0.03} ^{+0.03}	0.08 _{-0.02} ^{+0.03}	2E+00	1E-03
7	119 ₋₁₀ ⁺¹²	0	91 ₋₉ ⁺¹⁰	0	28 ₋₅ ⁺⁶	0	-0.52 _{-0.08} ^{+0.09}	0	0.72 _{-0.07} ^{+0.07}	0.55 _{-0.06} ^{+0.06}	0.17 _{-0.03} ^{+0.04}	4E+00	7E-10
8	68 ₋₈ ⁺⁹	0	53 ₋₇ ⁺⁸	0	15 ₋₃ ⁺⁵	0	-0.56 _{-0.10} ^{+0.12}	0	0.41 _{-0.05} ^{+0.06}	0.32 _{-0.04} ^{+0.05}	0.09 _{-0.02} ^{+0.03}	3E+00	5E-06
9	10 ₋₃ ⁺⁴	0	5 ₋₂ ⁺³	0	4 ₋₂ ⁺³	0	-0.10 _{-0.36} ^{+0.37}	0	0.06 _{-0.02} ^{+0.03}	0.03 _{-0.01} ^{+0.02}	0.03 _{-0.01} ^{+0.02}	1E+00	4E-03
10	20 ₋₄ ⁺⁵	0	14 ₋₃ ⁺⁴	0	6 ₋₂ ⁺³	0	-0.41 _{-0.22} ^{+0.25}	0	0.12 _{-0.03} ^{+0.03}	0.09 _{-0.02} ^{+0.03}	0.04 _{-0.01} ^{+0.02}	1E+00	1E-02
11	179 ₋₁₃ ⁺¹⁴	0	130 ₋₁₁ ⁺¹²	0	48 ₋₆ ⁺⁸	0	-0.46 _{-0.07} ^{+0.07}	0	1.07 _{-0.08} ^{+0.09}	0.78 _{-0.07} ^{+0.07}	0.29 _{-0.04} ^{+0.05}	5E+00	2E-15
12	34 ₋₅ ⁺⁶	0	26 ₋₅ ⁺⁶	0	7 ₋₂ ⁺³	0	-0.56 _{-0.15} ^{+0.18}	0	0.21 _{-0.03} ^{+0.04}	0.16 _{-0.03} ^{+0.04}	0.05 _{-0.02} ^{+0.02}	1E+00	4E-02
13	18 ₋₄ ⁺⁴	0	7 ₋₂ ⁺³	0	11 ₋₃ ⁺⁴	0	0.24 _{-0.27} ^{+0.25}	0	0.11 _{-0.03} ^{+0.03}	0.04 _{-0.02} ^{+0.03}	0.07 _{-0.02} ^{+0.03}	2E+00	2E-03
14	28 ₋₅ ⁺⁶	0	31 ₋₅ ⁺⁶	0	2 ₋₂ ⁺⁰	1	-0.85 _{-0.15} ^{+0.00}	1	0.17 _{-0.03} ^{+0.04}	0.19 _{-0.03} ^{+0.04}	0.02 _{-0.02} ^{+0.00}	-9E-01	9E-01
15	2 ₋₂ ⁺⁰	5	2 ₋₂ ⁺⁰	5	2 ₋₂ ⁺⁰	1	0.00 _{-0.00} ^{+0.00}	-2	0.01 _{-0.01} ^{+0.00}	0.02 _{-0.02} ^{+0.00}	0.01 _{-0.01} ^{+0.00}	-5E-01	8E-01
16	3 ₋₁ ⁺³	0	2 ₋₂ ⁺⁰	5	2 ₋₂ ⁺⁰	5	0.00 _{-0.00} ^{+0.00}	-2	0.02 _{-0.01} ^{+0.02}	0.02 _{-0.02} ^{+0.00}	0.01 _{-0.01} ^{+0.00}	1E-01	5E-01
17	4 ₋₂ ⁺³	0	2 ₋₂ ⁺⁰	5	2 ₋₂ ⁺⁰	5	0.00 _{-0.00} ^{+0.00}	-2	0.03 _{-0.01} ^{+0.02}	0.02 _{-0.02} ^{+0.00}	0.01 _{-0.01} ^{+0.00}	2E-01	4E-01
18	10 ₋₃ ⁺⁴	0	9 ₋₃ ⁺⁴	0	2 ₋₂ ⁺⁰	5	-0.58 _{-0.42} ^{+0.00}	1	0.06 _{-0.02} ^{+0.03}	0.06 _{-0.02} ^{+0.03}	0.01 _{-0.01} ^{+0.00}	2E-01	5E-01
19	19 ₋₄ ⁺⁵	0	4 ₋₂ ⁺³	0	14 ₋₃ ⁺⁵	0	0.53 _{-0.25} ^{+0.20}	0	0.12 _{-0.03} ^{+0.03}	0.03 _{-0.01} ^{+0.03}	0.09 _{-0.02} ^{+0.03}	3E+00	4E-06
20	20 ₋₄ ⁺⁵	0	13 ₋₃ ⁺⁴	0	7 ₋₂ ⁺³	0	-0.24 _{-0.23} ^{+0.25}	0	0.12 _{-0.03} ^{+0.03}	0.08 _{-0.02} ^{+0.03}	0.05 _{-0.02} ^{+0.02}	2E+00	2E-04
21	13 ₋₃ ⁺⁴	0	5 ₋₂ ⁺³	0	8 ₋₂ ⁺⁴	0	0.22 _{-0.30} ^{+0.30}	0	0.08 _{-0.02} ^{+0.03}	0.03 _{-0.01} ^{+0.02}	0.05 _{-0.02} ^{+0.02}	2E+00	5E-04
22	16 ₋₄ ⁺⁵	0	2 ₋₂ ⁺⁰	5	15 ₋₃ ⁺⁵	0	0.72 _{-0.00} ^{+0.00}	-1	0.10 _{-0.02} ^{+0.03}	0.01 _{-0.01} ^{+0.00}	0.09 _{-0.02} ^{+0.03}	3E+00	1E-08
23	2 ₋₂ ⁺⁰	5	2 ₋₂ ⁺⁰	5	2 ₋₂ ⁺⁰	5	0.00 _{-0.00} ^{+0.00}	-2	0.01 _{-0.01} ^{+0.00}	0.01 _{-0.01} ^{+0.00}	0.01 _{-0.01} ^{+0.00}	4E-01	3E-01
24	2 ₋₂ ⁺⁰	5	2 ₋₂ ⁺⁰	1	4 ₋₂ ⁺³	0	0.00 _{-0.00} ^{+0.00}	-2	0.01 _{-0.01} ^{+0.00}	0.01 _{-0.01} ^{+0.00}	0.03 _{-0.01} ^{+0.02}	1E+00	1E-03
25	28 ₋₅ ⁺⁶	0	9 ₋₃ ⁺⁴	0	19 ₋₄ ⁺⁵	0	0.34 _{-0.21} ^{+0.19}	0	0.17 _{-0.03} ^{+0.04}	0.06 _{-0.02} ^{+0.03}	0.11 _{-0.03} ^{+0.03}	3E+00	4E-10
26	9 ₋₃ ⁺⁴	0	2 ₋₂ ⁺⁰	5	7 ₋₂ ⁺³	0	0.52 _{-0.00} ^{+0.48}	-1	0.06 _{-0.02} ^{+0.03}	0.02 _{-0.02} ^{+0.00}	0.05 _{-0.02} ^{+0.02}	2E+00	7E-04
27	5 ₋₂ ⁺³	0	7 ₋₂ ⁺³	0	2 ₋₂ ⁺⁰	1	-0.53 _{-0.47} ^{+0.00}	1	0.03 _{-0.01} ^{+0.01}	0.05 _{-0.02} ^{+0.02}	0.01 _{-0.01} ^{+0.00}	-1E+00	1E+00
28	2 ₋₂ ⁺⁰	5	2 ₋₂ ⁺⁰	5	2 ₋₂ ⁺⁰	5	0.00 _{-0.00} ^{+0.00}	-2	0.01 _{-0.01} ^{+0.00}	0.01 _{-0.01} ^{+0.00}	0.01 _{-0.01} ^{+0.00}	1E-01	5E-01
29	16 ₋₄ ⁺⁵	0	13 ₋₃ ⁺⁴	0	2 ₋₂ ⁺⁰	5	-0.68 _{-0.32} ^{+0.00}	1	0.10 _{-0.02} ^{+0.03}	0.08 _{-0.02} ^{+0.03}	0.02 _{-0.02} ^{+0.00}	7E-01	2E-01
30	7 ₋₂ ⁺³	0	7 ₋₂ ⁺³	0	2 ₋₂ ⁺⁰	1	-0.49 _{-0.51} ^{+0.00}	1	0.04 _{-0.02} ^{+0.02}	0.04 _{-0.02} ^{+0.02}	0.01 _{-0.01} ^{+0.00}	-3E-02	7E-01
31	5 ₋₂ ⁺³	0	7 ₋₂ ⁺³	0	2 ₋₂ ⁺⁰	1	-0.51 _{-0.49} ^{+0.00}	1	0.03 _{-0.01} ^{+0.01}	0.04 _{-0.02} ^{+0.02}	0.01 _{-0.01} ^{+0.00}	-8E-01	1E+00
32	2 ₋₂ ⁺⁰	5	2 ₋₂ ⁺⁰	5	2 ₋₂ ⁺⁰	1	0.00 _{-0.00} ^{+0.00}	-2	0.01 _{-0.01} ^{+0.00}	0.01 _{-0.01} ^{+0.00}	0.01 _{-0.01} ^{+0.00}	-9E-02	7E-01
33	2 ₋₂ ⁺⁰	5	2 ₋₂ ⁺⁰	5	2 ₋₂ ⁺⁰	1	0.00 _{-0.09} ^{+0.00}	-2	0.01 _{-0.01} ^{+0.00}	0.01 _{-0.01} ^{+0.00}	0.01 _{-0.01} ^{+0.00}	-2E-01	1E+00
34	17 ₋₄ ⁺⁵	0	11 ₋₃ ⁺⁴	0	5 ₋₂ ⁺³	0	-0.36 _{-0.24} ^{+0.28}	0	0.10 _{-0.02} ^{+0.03}	0.07 _{-0.02} ^{+0.03}	0.03 _{-0.01} ^{+0.02}	1E+00	9E-04
35	33 ₋₅ ⁺⁶	0	28 ₋₅ ⁺⁶	0	4 ₋₂ ⁺³	0	-0.72 _{-0.12} ^{+0.17}	0	0.20 _{-0.03} ^{+0.04}	0.17 _{-0.03} ^{+0.04}	0.03 _{-0.01} ^{+0.02}	1E+00	1E-02
36	87 ₋₉ ⁺¹⁰	0	5 ₋₂ ⁺³	0	81 ₋₉ ⁺¹⁰	0	0.87 _{-0.07} ^{+0.05}	0	0.52 _{-0.06} ^{+0.06}	0.03 _{-0.01} ^{+0.02}	0.49 _{-0.05} ^{+0.06}	8E+00	0E+00
37	16 ₋₄ ⁺⁵	0	5 ₋₂ ⁺³	0	10 ₋₂ ⁺⁴	0	0.36 _{-0.29} ^{+0.25}	0	0.10 _{-0.02} ^{+0.03}	0.03 _{-0.01} ^{+0.02}	0.07 _{-0.02} ^{+0.03}	2E+00	4E-08
38	41 ₋₆ ⁺⁷	0	5 ₋₂ ⁺³	0	36 ₋₆ ⁺⁷	0	0.73 _{-0.14} ^{+0.11}	0	0.25 _{-0.04} ^{+0.05}	0.03 _{-0.01} ^{+0.02}	0.22 _{-0.04} ^{+0.04}	5E+00	1E-42
39	2 ₋₂ ⁺⁰	5	2 ₋₂ ⁺⁰	5	2 ₋₂ ⁺⁰	5	0.00 _{-0.00} ^{+0.00}	-2	0.01 _{-0.01} ^{+0.00}	0.01 _{-0.01} ^{+0.00}	0.01 _{-0.01} ^{+0.00}	9E-01	8E-03
40	14 ₋₃ ⁺⁴	0	10 ₋₃ ⁺⁴	0	2 ₋₂ ⁺⁰	5	-0.58 _{-0.42} ^{+0.00}	1	0.08 _{-0.02} ^{+0.03}	0.06 _{-0.02} ^{+0.03}	0.02 _{-0.02} ^{+0.00}	1E+00	3E-02
41	4 ₋₁ ⁺³	0	2 ₋₂ ⁺⁰	1	4 ₋₂ ⁺³	0	0.29 _{-0.00} ^{+0.71}	-1	0.02 _{-0.01} ^{+0.02}	0.01 _{-0.01} ^{+0.00}	0.03 _{-0.01} ^{+0.02}	1E+00	1E-03
42	3 ₋₁ ⁺³	0	2 ₋₂ ⁺⁰	1	5 ₋₂ ⁺³	0	0.38 _{-0.00} ^{+0.62}	-1	0.02 _{-0.01} ^{+0.02}	0.01 _{-0.01} ^{+0.00}	0.03 _{-0.01} ^{+0.02}	1E+00	3E-04

TABLE 26:

Counts, count rates and AE detection significance and no-source probabilities for X-ray point sources in HCG 62 (online only).

43	70 ⁺⁹ ₋₈	0	56 ⁺⁸ ₋₇	0	13 ⁺⁴ ₋₃	0	-0.61 ^{+0.11} _{-0.10}	0	0.42 ^{+0.06} _{-0.05}	0.34 ^{+0.05} _{-0.04}	0.08 ^{+0.03} _{-0.02}	3E+00	2E-11
44B	23 ⁺⁵ ₋₄	0	12 ⁺⁴ ₋₃	0	10 ⁺⁴ ₋₃	0	-0.08 ^{+0.23} _{-0.23}	0	0.14 ^{+0.04} _{-0.03}	0.08 ^{+0.03} _{-0.02}	0.07 ^{+0.03} _{-0.02}	2E+00	6E-08
45	2 ⁺⁰ ₋₂	5	2 ⁺⁰ ₋₂	5	2 ⁺⁰ ₋₂	1	0.00 ^{+0.00} _{-0.00}	-2	0.01 ^{+0.00} _{-0.01}	0.01 ^{+0.00} _{-0.01}	0.01 ^{+0.00} _{-0.01}	-8E-01	1E+00
46	1912 ⁺⁴⁴ ₋₄₃	0	1485 ⁺³⁹ ₋₃₈	0	426 ⁺²¹ ₋₂₀	0	-0.55 ^{+0.02} _{-0.02}	0	11.45 ^{+0.27} _{-0.26}	8.90 ^{+0.24} _{-0.23}	2.55 ^{+0.13} _{-0.12}	2E+01	0E+00
47	18 ⁺⁵ ₋₄	0	6 ⁺³ ₋₂	0	12 ⁺⁴ ₋₃	0	0.33 ^{+0.24} _{-0.27}	0	0.11 ^{+0.03} _{-0.03}	0.04 ^{+0.02} _{-0.01}	0.07 ^{+0.03} _{-0.02}	3E+00	3E-09
48	16 ⁺⁵ ₋₄	0	2 ⁺⁰ ₋₂	5	15 ⁺⁵ ₋₃	0	0.73 ^{+0.27} _{-0.00}	-1	0.10 ^{+0.03} _{-0.02}	0.01 ^{+0.00} _{-0.01}	0.09 ^{+0.03} _{-0.02}	3E+00	3E-17
49B	17 ⁺⁵ ₋₄	0	15 ⁺⁵ ₋₃	0	3 ⁺⁰ ₋₃	5	-0.66 ^{+0.00} _{-0.34}	1	0.10 ^{+0.03} _{-0.02}	0.09 ^{+0.03} _{-0.02}	0.02 ^{+0.00} _{-0.02}	6E-01	1E-01
50	442 ⁺²² ₋₂₁	0	357 ⁺¹⁹ ₋₁₈	0	85 ⁺¹⁰ ₋₉	0	-0.61 ^{+0.04} _{-0.04}	0	2.65 ^{+0.13} _{-0.13}	2.14 ^{+0.12} _{-0.11}	0.51 ^{+0.06} _{-0.06}	8E+00	0E+00
51	6 ⁺³ ₋₂	0	4 ⁺³ ₋₂	0	2 ⁺⁰ ₋₂	5	-0.29 ^{+0.00} _{-0.71}	1	0.04 ^{+0.02} _{-0.01}	0.03 ^{+0.02} _{-0.01}	0.02 ^{+0.00} _{-0.02}	5E-01	1E-01
52	7 ⁺³ ₋₂	0	2 ⁺⁰ ₋₂	5	4 ⁺³ ₋₂	0	0.25 ^{+0.75} _{-0.00}	-1	0.05 ^{+0.02} _{-0.02}	0.02 ^{+0.00} _{-0.02}	0.03 ^{+0.02} _{-0.01}	1E+00	3E-02
53	2 ⁺⁰ ₋₂	5	2 ⁺⁰ ₋₂	1	2 ⁺⁰ ₋₂	5	0.00 ^{+0.00} _{-0.00}	-2	0.01 ^{+0.00} _{-0.01}	0.01 ^{+0.00} _{-0.01}	0.01 ^{+0.00} _{-0.01}	1E+00	9E-03
54	10 ⁺⁴ ₋₃	0	9 ⁺⁴ ₋₃	0	2 ⁺⁰ ₋₂	5	-0.62 ^{+0.00} _{-0.38}	1	0.06 ^{+0.03} _{-0.02}	0.06 ^{+0.03} _{-0.02}	0.01 ^{+0.00} _{-0.01}	1E-01	5E-01
55B	12 ⁺⁴ ₋₃	0	11 ⁺⁴ ₋₃	0	2 ⁺⁰ ₋₂	5	-0.61 ^{+0.00} _{-0.39}	1	0.08 ^{+0.02} _{-0.02}	0.07 ^{+0.03} _{-0.02}	0.02 ^{+0.00} _{-0.02}	6E-01	1E-01
56	60 ⁺⁸ ₋₇	0	50 ⁺⁸ ₋₇	0	9 ⁺⁴ ₋₃	0	-0.67 ^{+0.12} _{-0.10}	0	0.36 ^{+0.05} _{-0.05}	0.30 ^{+0.05} _{-0.04}	0.06 ^{+0.03} _{-0.02}	2E+00	5E-05
57B	68 ⁺⁹ ₋₈	0	48 ⁺⁸ ₋₇	0	20 ⁺⁵ ₋₄	0	-0.42 ^{+0.12} _{-0.12}	0	0.41 ^{+0.06} _{-0.05}	0.29 ^{+0.05} _{-0.04}	0.12 ^{+0.03} _{-0.03}	3E+00	7E-11
58	10 ⁺⁴ ₋₃	0	6 ⁺³ ₋₂	0	3 ⁺³ ₋₁	0	-0.28 ^{+0.37} _{-0.33}	0	0.06 ^{+0.03} _{-0.02}	0.04 ^{+0.02} _{-0.02}	0.02 ^{+0.02} _{-0.01}	1E+00	4E-05
59	117 ⁺¹¹ ₋₁₀	0	85 ⁺¹⁰ ₋₉	0	31 ⁺⁶ ₋₅	0	-0.46 ^{+0.09} _{-0.09}	0	0.70 ^{+0.07} _{-0.06}	0.51 ^{+0.06} _{-0.06}	0.19 ^{+0.04} _{-0.03}	5E+00	0E+00
60	18 ⁺⁵ ₋₄	0	7 ⁺³ ₋₂	0	10 ⁺⁴ ₋₃	0	0.14 ^{+0.26} _{-0.27}	0	0.11 ^{+0.03} _{-0.03}	0.05 ^{+0.02} _{-0.02}	0.06 ^{+0.02} _{-0.02}	2E+00	5E-11
61	23 ⁺⁵ ₋₄	0	16 ⁺⁵ ₋₄	0	6 ⁺³ ₋₂	0	-0.42 ^{+0.23} _{-0.20}	0	0.14 ^{+0.04} _{-0.03}	0.10 ^{+0.03} _{-0.02}	0.04 ^{+0.02} _{-0.02}	2E+00	6E-09
62	17 ⁺⁵ ₋₄	0	15 ⁺⁵ ₋₃	0	2 ⁺⁰ ₋₂	5	-0.72 ^{+0.00} _{-0.28}	1	0.10 ^{+0.03} _{-0.02}	0.09 ^{+0.03} _{-0.02}	0.02 ^{+0.00} _{-0.02}	6E-01	1E-01
63	268 ⁺¹⁷ ₋₁₆	0	205 ⁺¹⁵ ₋₁₄	0	63 ⁺⁹ ₋₇	0	-0.53 ^{+0.06} _{-0.05}	0	1.61 ^{+0.10} _{-0.10}	1.23 ^{+0.09} _{-0.09}	0.38 ^{+0.05} _{-0.05}	6E+00	3E-20
64	53 ⁺⁸ ₋₇	0	22 ⁺⁵ ₋₄	0	31 ⁺⁶ ₋₅	0	0.15 ^{+0.14} _{-0.15}	0	0.32 ^{+0.05} _{-0.04}	0.14 ^{+0.04} _{-0.03}	0.19 ^{+0.04} _{-0.03}	4E+00	9E-09
65	13 ⁺⁴ ₋₃	0	4 ⁺³ ₋₂	0	9 ⁺⁴ ₋₃	0	0.36 ^{+0.28} _{-0.32}	0	0.08 ^{+0.03} _{-0.02}	0.03 ^{+0.02} _{-0.01}	0.06 ^{+0.02} _{-0.02}	2E+00	3E-04
66	1013 ⁺³² ₋₃₁	0	1010 ⁺³² ₋₃₁	0	3 ⁺⁰ ₋₃	5	-0.99 ^{+0.00} _{-0.01}	1	6.07 ^{+0.20} _{-0.19}	6.05 ^{+0.20} _{-0.19}	0.02 ^{+0.00} _{-0.02}	9E-01	7E-02
67B	116 ⁺¹¹ ₋₁₀	0	105 ⁺¹¹ ₋₁₀	0	11 ⁺⁴ ₋₃	0	-0.80 ^{+0.07} _{-0.06}	0	0.70 ^{+0.07} _{-0.06}	0.63 ^{+0.07} _{-0.06}	0.07 ^{+0.03} _{-0.02}	2E+00	2E-06
68	4 ⁺³ ₋₂	0	2 ⁺⁰ ₋₂	1	5 ⁺³ ₋₂	0	0.38 ^{+0.62} _{-0.00}	-1	0.03 ^{+0.02} _{-0.01}	0.01 ^{+0.00} _{-0.01}	0.03 ^{+0.02} _{-0.01}	1E+00	2E-04
69	29 ⁺⁶ ₋₅	0	18 ⁺⁵ ₋₄	0	11 ⁺⁴ ₋₃	0	-0.22 ^{+0.21} _{-0.19}	0	0.18 ^{+0.04} _{-0.03}	0.11 ^{+0.03} _{-0.03}	0.07 ^{+0.03} _{-0.02}	2E+00	1E-05
70	2 ⁺⁰ ₋₂	1	2 ⁺⁰ ₋₂	1	2 ⁺⁰ ₋₂	5	0.00 ^{+0.00} _{-0.00}	-2	0.01 ^{+0.01} _{-0.01}	0.01 ^{+0.00} _{-0.01}	0.02 ^{+0.00} _{-0.02}	8E-01	8E-02
71	3 ⁺³ ₋₁	0	3 ⁺³ ₋₁	0	2 ⁺⁰ ₋₂	1	-0.24 ^{+0.00} _{-0.76}	1	0.02 ^{+0.02} _{-0.01}	0.02 ^{+0.02} _{-0.01}	0.01 ^{+0.00} _{-0.01}	-7E-02	1E+00
72A	16 ⁺⁵ ₋₄	0	4 ⁺³ ₋₂	0	11 ⁺⁴ ₋₃	0	0.43 ^{+0.24} _{-0.28}	0	0.10 ^{+0.03} _{-0.02}	0.03 ^{+0.02} _{-0.01}	0.07 ^{+0.03} _{-0.02}	2E+00	5E-07
73	27 ⁺⁶ ₋₅	0	16 ⁺⁵ ₋₄	0	10 ⁺⁴ ₋₃	0	-0.22 ^{+0.22} _{-0.20}	0	0.16 ^{+0.04} _{-0.03}	0.10 ^{+0.03} _{-0.02}	0.06 ^{+0.03} _{-0.02}	2E+00	6E-03
74	231 ⁺¹⁶ ₋₁₅	0	175 ⁺¹⁴ ₋₁₃	0	56 ⁺⁸ ₋₇	0	-0.51 ^{+0.06} _{-0.06}	0	1.39 ^{+0.10} _{-0.09}	1.05 ^{+0.09} _{-0.08}	0.34 ^{+0.05} _{-0.04}	7E+00	0E+00
75B	15 ⁺⁵ ₋₃	0	9 ⁺⁴ ₋₃	0	6 ⁺³ ₋₂	0	-0.22 ^{+0.30} _{-0.28}	0	0.09 ^{+0.03} _{-0.02}	0.06 ^{+0.03} _{-0.02}	0.04 ^{+0.02} _{-0.01}	2E+00	4E-04
76	7 ⁺³ ₋₂	0	2 ⁺⁰ ₋₂	5	4 ⁺³ ₋₂	0	0.26 ^{+0.74} _{-0.00}	-1	0.04 ^{+0.02} _{-0.02}	0.01 ^{+0.01} _{-0.01}	0.03 ^{+0.02} _{-0.01}	1E+00	2E-03
77	5 ⁺³ ₋₂	0	2 ⁺⁰ ₋₂	1	9 ⁺⁴ ₋₃	0	0.60 ^{+0.40} _{-0.00}	-1	0.04 ^{+0.01} _{-0.01}	0.01 ^{+0.00} _{-0.01}	0.06 ^{+0.03} _{-0.02}	2E+00	3E-05
78A	153 ⁺¹³ ₋₁₂	0	97 ⁺¹⁰ ₋₉	0	56 ⁺⁸ ₋₇	0	-0.26 ^{+0.08} _{-0.08}	0	0.92 ^{+0.08} _{-0.07}	0.58 ^{+0.07} _{-0.06}	0.34 ^{+0.05} _{-0.04}	7E+00	2E-37
79	285 ⁺¹⁶ ₋₁₅	0	239 ⁺¹⁶ ₋₁₅	0	45 ⁺⁷ ₋₆	0	-0.68 ^{+0.05} _{-0.04}	0	1.71 ^{+0.11} _{-0.10}	1.43 ^{+0.10} _{-0.09}	0.27 ^{+0.05} _{-0.04}	6E+00	0E+00
80A	80 ⁺¹⁰ ₋₉	0	67 ⁺⁹ ₋₈	0	12 ⁺⁴ ₋₃	0	-0.68 ^{+0.10} _{-0.08}	0	0.48 ^{+0.06} _{-0.05}	0.41 ^{+0.06} _{-0.05}	0.08 ^{+0.03} _{-0.02}	3E+00	2E-07
81A	11 ⁺⁴ ₋₃	0	10 ⁺⁴ ₋₃	0	2 ⁺⁰ ₋₂	5	-0.63 ^{+0.00} _{-0.37}	1	0.07 ^{+0.03} _{-0.02}	0.07 ^{+0.03} _{-0.02}	0.01 ^{+0.00} _{-0.01}	5E-02	6E-01
82A	116 ⁺¹¹ ₋₁₀	0	104 ⁺¹¹ ₋₁₀	0	11 ⁺⁴ ₋₃	0	-0.80 ^{+0.07} _{-0.06}	0	0.69 ^{+0.07} _{-0.06}	0.63 ^{+0.07} _{-0.06}	0.07 ^{+0.03} _{-0.02}	2E+00	4E-06
83A	133 ⁺¹² ₋₁₁	0	119 ⁺¹² ₋₁₀	0	13 ⁺⁴ ₋₃	0	-0.79 ^{+0.07} _{-0.05}	0	0.80 ^{+0.08} _{-0.07}	0.72 ^{+0.07} _{-0.07}	0.08 ^{+0.03} _{-0.02}	3E+00	1E-06
84	10 ⁺⁴ ₋₃	0	7 ⁺³ ₋₂	0	2 ⁺⁰ ₋₂	5	-0.45 ^{+0.00} _{-0.55}	1	0.06 ^{+0.03} _{-0.02}	0.05 ^{+0.02} _{-0.02}	0.02 ^{+0.00} _{-0.02}	8E-01	3E-02
85A	72 ⁺⁹ ₋₈	0	72 ⁺⁹ ₋₈	0	2 ⁺⁰ ₋₂	1	-0.93 ^{+0.00} _{-0.07}	1	0.43 ^{+0.06} _{-0.05}	0.44 ^{+0.06} _{-0.05}	0.01 ^{+0.00} _{-0.01}	-1E-01	7E-01
86	4 ⁺³ ₋₂	0	4 ⁺³ ₋₂	0	2 ⁺⁰ ₋₂	1	-0.34 ^{+0.00} _{-0.66}	1	0.03 ^{+0.02} _{-0.01}	0.03 ^{+0.02} _{-0.01}	0.01 ^{+0.00} _{-0.01}	-8E-02	1E+00
87	4 ⁺³ ₋₂	0	4 ⁺³ ₋₂	0	2 ⁺⁰ ₋₂	1	-0.35 ^{+0.00} _{-0.65}	1	0.03 ^{+0.02} _{-0.01}	0.03 ^{+0.02} _{-0.01}	0.01 ^{+0.00} _{-0.01}	-3E-01	1E+00

TABLE 26:

Counts, count rates and AE detection significance and no-source probabilities for X-ray point sources in HCG 62 (online only).

88	287^{+18}_{-16}	0	189^{+14}_{-13}	0	97^{+10}_{-9}	0	$-0.32^{+0.06}_{-0.06}$	0	$1.72^{+0.11}_{-0.10}$	$1.14^{+0.09}_{-0.08}$	$0.58^{+0.07}_{-0.06}$	9E+00	0E+00
89	250^{+16}_{-15}	0	145^{+13}_{-12}	0	104^{+11}_{-10}	0	$-0.17^{+0.07}_{-0.06}$	0	$1.50^{+0.10}_{-0.09}$	$0.87^{+0.08}_{-0.07}$	$0.62^{+0.07}_{-0.06}$	9E+00	0E+00
90	20^{+5}_{-4}	0	16^{+5}_{-4}	0	2^{+0}_{-2}	5	$-0.71^{+0.00}_{-0.29}$	1	$0.12^{+0.03}_{-0.03}$	$0.10^{+0.03}_{-0.02}$	$0.02^{+0.00}_{-0.02}$	1E+00	1E-03
91	4^{+3}_{-2}	0	2^{+0}_{-2}	1	8^{+4}_{-2}	0	$0.56^{+0.44}_{-0.00}$	-1	$0.03^{+0.02}_{-0.01}$	$0.01^{+0.00}_{-0.01}$	$0.05^{+0.02}_{-0.02}$	2E+00	2E-05
92	10^{+4}_{-3}	0	6^{+3}_{-2}	0	4^{+3}_{-2}	0	$-0.15^{+0.37}_{-0.35}$	0	$0.06^{+0.03}_{-0.02}$	$0.04^{+0.02}_{-0.01}$	$0.03^{+0.02}_{-0.01}$	1E+00	3E-04
93	45^{+7}_{-6}	0	27^{+6}_{-5}	0	18^{+5}_{-4}	0	$-0.20^{+0.16}_{-0.16}$	0	$0.27^{+0.05}_{-0.04}$	$0.16^{+0.04}_{-0.03}$	$0.11^{+0.03}_{-0.03}$	3E+00	6E-13
94A	6^{+3}_{-2}	0	5^{+3}_{-2}	0	2^{+0}_{-2}	5	$-0.37^{+0.00}_{-0.63}$	1	$0.04^{+0.02}_{-0.01}$	$0.03^{+0.02}_{-0.01}$	$0.02^{+0.00}_{-0.02}$	2E-01	4E-01
95D	24^{+6}_{-4}	0	5^{+3}_{-2}	0	19^{+5}_{-4}	0	$0.54^{+0.18}_{-0.22}$	0	$0.15^{+0.04}_{-0.03}$	$0.03^{+0.02}_{-0.01}$	$0.11^{+0.03}_{-0.03}$	3E+00	5E-07
96	43^{+7}_{-6}	0	30^{+6}_{-5}	0	12^{+4}_{-3}	0	$-0.42^{+0.16}_{-0.15}$	0	$0.26^{+0.05}_{-0.04}$	$0.18^{+0.04}_{-0.03}$	$0.07^{+0.03}_{-0.02}$	3E+00	2E-07
97	4^{+3}_{-1}	0	2^{+0}_{-2}	5	2^{+0}_{-2}	5	$0.00^{+0.00}_{-0.00}$	-2	$0.02^{+0.02}_{-0.01}$	$0.01^{+0.00}_{-0.01}$	$0.01^{+0.00}_{-0.01}$	6E-01	8E-02
98A	11^{+4}_{-3}	0	9^{+4}_{-3}	0	2^{+0}_{-2}	5	$-0.54^{+0.00}_{-0.46}$	1	$0.07^{+0.03}_{-0.02}$	$0.05^{+0.02}_{-0.02}$	$0.02^{+0.00}_{-0.02}$	8E-01	9E-02
99	2^{+0}_{-2}	5	2^{+0}_{-2}	1	4^{+3}_{-2}	0	$0.00^{+0.00}_{-0.00}$	-2	$0.02^{+0.00}_{-0.02}$	$0.01^{+0.00}_{-0.01}$	$0.03^{+0.02}_{-0.01}$	1E+00	3E-03
100A	18^{+5}_{-4}	0	12^{+4}_{-3}	0	5^{+3}_{-2}	0	$-0.36^{+0.27}_{-0.24}$	0	$0.11^{+0.03}_{-0.03}$	$0.08^{+0.03}_{-0.02}$	$0.04^{+0.02}_{-0.01}$	2E+00	4E-04
101	5^{+3}_{-2}	0	6^{+3}_{-2}	0	2^{+0}_{-2}	1	$-0.46^{+0.00}_{-0.54}$	1	$0.03^{+0.02}_{-0.01}$	$0.04^{+0.02}_{-0.01}$	$0.01^{+0.00}_{-0.01}$	-4E-01	1E+00
102	13^{+4}_{-3}	0	2^{+0}_{-2}	5	10^{+4}_{-3}	0	$0.61^{+0.39}_{-0.00}$	-1	$0.08^{+0.03}_{-0.02}$	$0.02^{+0.00}_{-0.02}$	$0.06^{+0.03}_{-0.02}$	2E+00	5E-05
103A	3^{+3}_{-1}	0	5^{+3}_{-2}	0	2^{+0}_{-2}	1	$-0.38^{+0.00}_{-0.62}$	1	$0.02^{+0.02}_{-0.01}$	$0.03^{+0.02}_{-0.01}$	$0.01^{+0.00}_{-0.01}$	-7E-01	1E+00
104	2^{+0}_{-2}	5	3^{+3}_{-1}	0	2^{+0}_{-2}	1	$0.00^{+0.00}_{-0.00}$	-2	$0.01^{+0.00}_{-0.01}$	$0.02^{+0.02}_{-0.01}$	$0.01^{+0.00}_{-0.01}$	-9E-02	1E+00
105C	9^{+4}_{-3}	0	2^{+0}_{-2}	5	7^{+3}_{-2}	0	$0.49^{+0.31}_{-0.00}$	-1	$0.06^{+0.03}_{-0.02}$	$0.02^{+0.02}_{-0.02}$	$0.04^{+0.02}_{-0.02}$	2E+00	6E-06
106C	8^{+4}_{-2}	0	9^{+4}_{-3}	0	2^{+0}_{-2}	1	$-0.60^{+0.00}_{-0.40}$	1	$0.05^{+0.02}_{-0.02}$	$0.06^{+0.02}_{-0.02}$	$0.01^{+0.00}_{-0.01}$	-6E-01	1E+00
107C	16^{+5}_{-4}	0	10^{+4}_{-3}	0	5^{+3}_{-2}	0	$-0.33^{+0.29}_{-0.26}$	0	$0.10^{+0.03}_{-0.02}$	$0.06^{+0.03}_{-0.02}$	$0.03^{+0.02}_{-0.01}$	2E+00	1E-04
108	26^{+6}_{-5}	0	18^{+5}_{-4}	0	8^{+4}_{-3}	0	$-0.35^{+0.22}_{-0.20}$	0	$0.16^{+0.04}_{-0.03}$	$0.11^{+0.03}_{-0.03}$	$0.05^{+0.02}_{-0.02}$	1E+00	3E-02
109C	18^{+5}_{-4}	0	13^{+4}_{-3}	0	5^{+3}_{-2}	0	$-0.44^{+0.26}_{-0.23}$	0	$0.11^{+0.03}_{-0.03}$	$0.08^{+0.03}_{-0.02}$	$0.03^{+0.02}_{-0.01}$	1E+00	7E-04
110	3^{+3}_{-1}	0	2^{+0}_{-2}	5	2^{+0}_{-2}	5	$0.00^{+0.00}_{-0.00}$	-2	$0.02^{+0.02}_{-0.01}$	$0.01^{+0.00}_{-0.01}$	$0.02^{+0.00}_{-0.02}$	9E-01	1E-02
111	8^{+4}_{-2}	0	6^{+3}_{-2}	0	2^{+0}_{-2}	5	$-0.39^{+0.00}_{-0.61}$	1	$0.05^{+0.02}_{-0.02}$	$0.04^{+0.02}_{-0.01}$	$0.02^{+0.00}_{-0.02}$	9E-01	6E-03
112C	27^{+6}_{-5}	0	21^{+5}_{-4}	0	6^{+3}_{-2}	0	$-0.55^{+0.20}_{-0.17}$	0	$0.17^{+0.04}_{-0.03}$	$0.13^{+0.03}_{-0.03}$	$0.04^{+0.02}_{-0.01}$	2E+00	2E-05
113	7^{+3}_{-2}	0	2^{+0}_{-2}	5	4^{+3}_{-2}	0	$0.33^{+0.67}_{-0.00}$	-1	$0.05^{+0.02}_{-0.02}$	$0.01^{+0.00}_{-0.01}$	$0.03^{+0.02}_{-0.01}$	1E+00	9E-07
114C	50^{+8}_{-7}	0	46^{+7}_{-6}	0	4^{+3}_{-1}	0	$-0.84^{+0.11}_{-0.08}$	0	$0.30^{+0.05}_{-0.04}$	$0.28^{+0.05}_{-0.04}$	$0.02^{+0.02}_{-0.01}$	1E+00	4E-03
115C	33^{+6}_{-5}	0	25^{+6}_{-5}	0	7^{+3}_{-2}	0	$-0.54^{+0.18}_{-0.15}$	0	$0.20^{+0.04}_{-0.03}$	$0.15^{+0.04}_{-0.03}$	$0.05^{+0.02}_{-0.02}$	2E+00	3E-05
116C	26^{+6}_{-5}	0	16^{+5}_{-4}	0	10^{+4}_{-3}	0	$-0.24^{+0.22}_{-0.21}$	0	$0.16^{+0.04}_{-0.03}$	$0.10^{+0.03}_{-0.02}$	$0.06^{+0.03}_{-0.02}$	2E+00	1E-08
117	125^{+12}_{-11}	0	72^{+9}_{-8}	0	52^{+8}_{-7}	0	$-0.16^{+0.09}_{-0.09}$	0	$0.75^{+0.07}_{-0.07}$	$0.44^{+0.06}_{-0.05}$	$0.32^{+0.05}_{-0.04}$	5E+00	2E-14
118	3^{+3}_{-1}	0	2^{+0}_{-2}	5	2^{+0}_{-2}	5	$0.00^{+0.00}_{-0.00}$	-2	$0.02^{+0.02}_{-0.01}$	$0.01^{+0.00}_{-0.01}$	$0.01^{+0.00}_{-0.01}$	2E-01	4E-01
119	2^{+0}_{-2}	5	2^{+0}_{-2}	5	2^{+0}_{-2}	1	$0.00^{+0.00}_{-0.00}$	-2	$0.01^{+0.00}_{-0.01}$	$0.01^{+0.00}_{-0.01}$	$0.01^{+0.00}_{-0.01}$	-7E-02	1E+00
120	38^{+7}_{-6}	0	32^{+6}_{-5}	0	5^{+3}_{-2}	0	$-0.71^{+0.15}_{-0.12}$	0	$0.23^{+0.04}_{-0.04}$	$0.20^{+0.04}_{-0.03}$	$0.03^{+0.02}_{-0.01}$	1E+00	2E-03
121	215^{+15}_{-14}	0	167^{+14}_{-12}	0	48^{+8}_{-6}	0	$-0.55^{+0.06}_{-0.06}$	0	$1.29^{+0.09}_{-0.09}$	$1.00^{+0.08}_{-0.08}$	$0.29^{+0.05}_{-0.04}$	6E+00	0E+00
122	39^{+7}_{-6}	0	8^{+4}_{-2}	0	31^{+6}_{-5}	0	$0.60^{+0.13}_{-0.16}$	0	$0.24^{+0.04}_{-0.04}$	$0.05^{+0.02}_{-0.02}$	$0.19^{+0.04}_{-0.03}$	5E+00	9E-25
123	12^{+4}_{-3}	0	2^{+0}_{-2}	1	13^{+4}_{-3}	0	$0.71^{+0.29}_{-0.09}$	-1	$0.07^{+0.03}_{-0.02}$	$0.01^{+0.00}_{-0.01}$	$0.08^{+0.03}_{-0.02}$	3E+00	6E-14
124	59^{+7}_{-6}	0	41^{+7}_{-6}	0	18^{+5}_{-4}	0	$-0.39^{+0.14}_{-0.13}$	0	$0.35^{+0.05}_{-0.05}$	$0.25^{+0.04}_{-0.04}$	$0.11^{+0.03}_{-0.03}$	3E+00	5E-10
125C	11^{+4}_{-3}	0	2^{+0}_{-2}	5	10^{+4}_{-3}	0	$0.61^{+0.39}_{-0.00}$	-1	$0.07^{+0.03}_{-0.02}$	$0.01^{+0.00}_{-0.01}$	$0.06^{+0.03}_{-0.02}$	2E+00	6E-08
126	41^{+7}_{-6}	0	32^{+6}_{-5}	0	9^{+4}_{-3}	0	$-0.54^{+0.16}_{-0.14}$	0	$0.25^{+0.04}_{-0.04}$	$0.19^{+0.04}_{-0.03}$	$0.06^{+0.03}_{-0.02}$	2E+00	2E-02
127	88^{+10}_{-9}	0	2^{+0}_{-2}	5	85^{+10}_{-9}	0	$0.94^{+0.06}_{-0.06}$	-1	$0.53^{+0.06}_{-0.06}$	$0.01^{+0.00}_{-0.01}$	$0.51^{+0.06}_{-0.06}$	8E+00	0E+00
128	4^{+3}_{-1}	0	4^{+3}_{-2}	0	2^{+0}_{-2}	1	$-0.32^{+0.00}_{-0.68}$	1	$0.02^{+0.02}_{-0.01}$	$0.03^{+0.02}_{-0.01}$	$0.01^{+0.00}_{-0.01}$	-2E-01	1E+00
129	216^{+15}_{-14}	0	164^{+13}_{-12}	0	51^{+8}_{-7}	0	$-0.52^{+0.06}_{-0.06}$	0	$1.29^{+0.09}_{-0.09}$	$0.98^{+0.08}_{-0.08}$	$0.31^{+0.05}_{-0.04}$	6E+00	0E+00
130	243^{+16}_{-15}	0	165^{+13}_{-12}	0	77^{+9}_{-8}	0	$-0.36^{+0.06}_{-0.06}$	0	$1.46^{+0.10}_{-0.09}$	$0.99^{+0.08}_{-0.08}$	$0.47^{+0.06}_{-0.05}$	7E+00	9E-27
131	19^{+5}_{-4}	0	9^{+4}_{-3}	0	10^{+4}_{-3}	0	$0.08^{+0.25}_{-0.26}$	0	$0.12^{+0.03}_{-0.03}$	$0.05^{+0.02}_{-0.02}$	$0.06^{+0.03}_{-0.02}$	2E+00	3E-12
132	14^{+4}_{-3}	0	8^{+4}_{-2}	0	6^{+3}_{-2}	0	$-0.11^{+0.31}_{-0.30}$	0	$0.09^{+0.03}_{-0.02}$	$0.05^{+0.02}_{-0.02}$	$0.04^{+0.02}_{-0.01}$	2E+00	5E-06

TABLE 26:

Counts, count rates and AE detection significance and no-source probabilities for X-ray point sources in HCG 62 (online only).

133	3^{+3}_{-1}	0	4^{+3}_{-2}	0	2^{+0}_{-2}	1	$-0.33^{+0.00}_{-0.67}$	1	$0.02^{+0.02}_{-0.01}$	$0.03^{+0.02}_{-0.01}$	$0.01^{+0.00}_{-0.01}$	-5E-01	1E+00
134	23^{+5}_{-4}	0	18^{+5}_{-4}	0	5^{+3}_{-2}	0	$-0.52^{+0.22}_{-0.19}$	0	$0.14^{+0.04}_{-0.03}$	$0.11^{+0.03}_{-0.03}$	$0.03^{+0.02}_{-0.01}$	1E+00	9E-04
135	5^{+3}_{-2}	0	4^{+3}_{-1}	0	2^{+0}_{-2}	5	$-0.25^{+0.00}_{-0.75}$	1	$0.03^{+0.02}_{-0.01}$	$0.02^{+0.02}_{-0.01}$	$0.01^{+0.00}_{-0.01}$	6E-01	1E-01
136	7^{+3}_{-2}	0	4^{+3}_{-2}	0	2^{+0}_{-2}	5	$-0.32^{+0.00}_{-0.68}$	1	$0.05^{+0.02}_{-0.02}$	$0.03^{+0.02}_{-0.01}$	$0.01^{+0.00}_{-0.01}$	1E+00	5E-04
137	14^{+4}_{-3}	0	4^{+3}_{-2}	0	10^{+4}_{-3}	0	$0.41^{+0.26}_{-0.31}$	0	$0.09^{+0.03}_{-0.02}$	$0.03^{+0.02}_{-0.01}$	$0.06^{+0.03}_{-0.02}$	2E+00	9E-09
138	5^{+3}_{-2}	0	2^{+0}_{-2}	5	2^{+0}_{-2}	5	$0.00^{+0.00}_{-0.00}$	-2	$0.03^{+0.02}_{-0.01}$	$0.01^{+0.00}_{-0.01}$	$0.01^{+0.00}_{-0.01}$	8E-01	5E-02
139	12^{+4}_{-3}	0	7^{+3}_{-2}	0	5^{+3}_{-2}	0	$-0.10^{+0.33}_{-0.32}$	0	$0.08^{+0.03}_{-0.02}$	$0.04^{+0.02}_{-0.02}$	$0.03^{+0.02}_{-0.01}$	2E+00	4E-04
140	86^{+10}_{-9}	0	67^{+9}_{-8}	0	19^{+5}_{-4}	0	$-0.55^{+0.10}_{-0.09}$	0	$0.52^{+0.06}_{-0.06}$	$0.40^{+0.06}_{-0.05}$	$0.12^{+0.03}_{-0.03}$	3E+00	2E-05
141	80^{+10}_{-9}	0	63^{+9}_{-7}	0	17^{+5}_{-4}	0	$-0.57^{+0.11}_{-0.10}$	0	$0.48^{+0.06}_{-0.05}$	$0.38^{+0.05}_{-0.05}$	$0.10^{+0.03}_{-0.02}$	3E+00	1E-19
142	286^{+17}_{-16}	0	90^{+10}_{-9}	0	195^{+15}_{-14}	0	$0.37^{+0.06}_{-0.06}$	0	$1.72^{+0.11}_{-0.10}$	$0.54^{+0.06}_{-0.06}$	$1.17^{+0.09}_{-0.08}$	1E+01	0E+00
143	46^{+7}_{-6}	0	36^{+7}_{-6}	0	10^{+4}_{-3}	0	$-0.56^{+0.15}_{-0.13}$	0	$0.28^{+0.05}_{-0.04}$	$0.22^{+0.04}_{-0.04}$	$0.06^{+0.03}_{-0.02}$	2E+00	2E-06
144	2^{+0}_{-2}	5	2^{+0}_{-2}	1	2^{+0}_{-2}	5	$0.00^{+0.00}_{-0.00}$	-2	$0.01^{+0.00}_{-0.01}$	$0.01^{+0.00}_{-0.01}$	$0.01^{+0.00}_{-0.01}$	8E-01	5E-02
145	199^{+15}_{-14}	0	54^{+8}_{-7}	0	145^{+13}_{-12}	0	$0.46^{+0.06}_{-0.07}$	0	$1.20^{+0.09}_{-0.08}$	$0.32^{+0.05}_{-0.04}$	$0.87^{+0.08}_{-0.07}$	1E+01	0E+00
146	26^{+6}_{-5}	0	17^{+5}_{-4}	0	9^{+4}_{-2}	0	$-0.33^{+0.22}_{-0.20}$	0	$0.16^{+0.04}_{-0.03}$	$0.11^{+0.03}_{-0.02}$	$0.05^{+0.02}_{-0.02}$	2E+00	2E-02
147	8^{+4}_{-2}	0	2^{+0}_{-2}	5	7^{+3}_{-2}	0	$0.51^{+0.49}_{-0.00}$	-1	$0.05^{+0.02}_{-0.02}$	$0.01^{+0.00}_{-0.01}$	$0.05^{+0.02}_{-0.02}$	2E+00	3E-03
148	16^{+5}_{-4}	0	11^{+4}_{-3}	0	5^{+3}_{-2}	0	$-0.32^{+0.28}_{-0.26}$	0	$0.10^{+0.03}_{-0.02}$	$0.07^{+0.03}_{-0.02}$	$0.03^{+0.02}_{-0.01}$	2E+00	7E-04
149	9^{+4}_{-3}	0	8^{+4}_{-2}	0	2^{+0}_{-2}	5	$-0.58^{+0.00}_{-0.42}$	1	$0.05^{+0.02}_{-0.02}$	$0.05^{+0.02}_{-0.02}$	$0.01^{+0.00}_{-0.01}$	1E-01	5E-01
150	5^{+3}_{-2}	0	2^{+0}_{-2}	5	5^{+3}_{-2}	0	$0.41^{+0.39}_{-0.00}$	-1	$0.04^{+0.02}_{-0.01}$	$0.01^{+0.00}_{-0.01}$	$0.03^{+0.01}_{-0.01}$	2E+00	7E-04
151	162^{+13}_{-12}	0	133^{+12}_{-11}	0	29^{+6}_{-5}	0	$-0.63^{+0.07}_{-0.06}$	0	$0.98^{+0.08}_{-0.08}$	$0.80^{+0.08}_{-0.07}$	$0.18^{+0.04}_{-0.03}$	4E+00	1E-28
152	2^{+0}_{-2}	5	2^{+0}_{-2}	5	2^{+0}_{-2}	5	$0.00^{+0.00}_{-0.00}$	-2	$0.01^{+0.00}_{-0.01}$	$0.01^{+0.00}_{-0.01}$	$0.01^{+0.00}_{-0.01}$	5E-01	2E-01
153	10^{+4}_{-3}	0	2^{+0}_{-2}	5	9^{+4}_{-3}	0	$0.61^{+0.39}_{-0.00}$	-1	$0.06^{+0.03}_{-0.02}$	$0.01^{+0.00}_{-0.01}$	$0.06^{+0.03}_{-0.02}$	2E+00	1E-07
154	2^{+0}_{-2}	5	2^{+0}_{-2}	5	2^{+0}_{-2}	5	$0.00^{+0.00}_{-0.00}$	-2	$0.01^{+0.00}_{-0.01}$	$0.01^{+0.00}_{-0.01}$	$0.01^{+0.00}_{-0.01}$	3E-01	4E-01
155	16^{+5}_{-4}	0	9^{+4}_{-2}	0	7^{+3}_{-2}	0	$-0.11^{+0.29}_{-0.28}$	0	$0.10^{+0.03}_{-0.02}$	$0.05^{+0.02}_{-0.02}$	$0.04^{+0.02}_{-0.02}$	2E+00	1E-03
156	20^{+5}_{-4}	0	15^{+5}_{-3}	0	4^{+3}_{-2}	0	$-0.52^{+0.24}_{-0.20}$	0	$0.12^{+0.03}_{-0.03}$	$0.09^{+0.03}_{-0.02}$	$0.03^{+0.02}_{-0.01}$	1E+00	2E-02
157	2^{+0}_{-2}	5	2^{+0}_{-2}	5	2^{+0}_{-2}	5	$0.00^{+0.00}_{-0.00}$	-2	$0.01^{+0.00}_{-0.01}$	$0.01^{+0.00}_{-0.01}$	$0.01^{+0.00}_{-0.01}$	3E-01	2E-01
158	2^{+0}_{-2}	5	2^{+0}_{-2}	5	2^{+0}_{-2}	1	$0.00^{+0.00}_{-0.00}$	-2	$0.01^{+0.00}_{-0.01}$	$0.01^{+0.00}_{-0.01}$	$0.01^{+0.00}_{-0.01}$	-1E-01	1E+00
159	10^{+4}_{-3}	0	2^{+0}_{-2}	5	9^{+4}_{-3}	0	$0.60^{+0.40}_{-0.00}$	-1	$0.06^{+0.03}_{-0.02}$	$0.01^{+0.00}_{-0.01}$	$0.06^{+0.03}_{-0.02}$	2E+00	1E-05
160	13^{+4}_{-3}	0	2^{+0}_{-2}	5	11^{+4}_{-3}	0	$0.63^{+0.37}_{-0.00}$	-1	$0.08^{+0.03}_{-0.02}$	$0.01^{+0.00}_{-0.01}$	$0.07^{+0.03}_{-0.02}$	2E+00	6E-07
161	4^{+3}_{-2}	0	4^{+3}_{-2}	0	2^{+0}_{-2}	1	$-0.32^{+0.00}_{-0.68}$	1	$0.03^{+0.02}_{-0.01}$	$0.03^{+0.02}_{-0.01}$	$0.01^{+0.00}_{-0.01}$	-2E-01	1E+00
162	6^{+3}_{-2}	0	2^{+0}_{-2}	5	2^{+0}_{-2}	5	$0.00^{+0.00}_{-0.00}$	-2	$0.04^{+0.02}_{-0.01}$	$0.01^{+0.00}_{-0.01}$	$0.01^{+0.00}_{-0.01}$	1E+00	7E-03
163	14^{+4}_{-3}	0	14^{+4}_{-3}	0	2^{+0}_{-2}	5	$-0.72^{+0.00}_{-0.28}$	1	$0.09^{+0.03}_{-0.02}$	$0.09^{+0.03}_{-0.02}$	$0.01^{+0.00}_{-0.01}$	2E-01	4E-01
164	22^{+5}_{-4}	0	17^{+5}_{-4}	0	5^{+3}_{-2}	0	$-0.52^{+0.23}_{-0.19}$	0	$0.13^{+0.03}_{-0.03}$	$0.10^{+0.03}_{-0.02}$	$0.03^{+0.02}_{-0.01}$	2E+00	5E-05
165	17^{+5}_{-4}	0	14^{+4}_{-3}	0	2^{+0}_{-2}	5	$-0.71^{+0.00}_{-0.29}$	1	$0.10^{+0.02}_{-0.02}$	$0.09^{+0.03}_{-0.02}$	$0.01^{+0.00}_{-0.01}$	9E-01	4E-03

TABLE 27:
Counts, count rates and AE detection significance and no-source probabilities for X-ray point sources in HCG 90 (online only).

ID (1)	c(FB) (2)	lim _F (3)	c(SB) (4)	lim _S (5)	c(HB) (6)	lim _S (7)	HR (8)	lim _{HR} (9)	cr(FB) (10)	cr(SB) (11)	cr(HB) (12)	AE(sig) (13)	AE(<i>P</i>) (14)
1	29 ⁺⁶ ₋₅	0	21 ⁺⁵ ₋₄	0	7 ⁺³ ₋₂	0	-0.50 ^{+0.20} _{-0.17}	0	0.59 ^{+0.13} _{-0.11}	0.44 ^{+0.12} _{-0.09}	0.15 ^{+0.08} _{-0.05}	2E+00	6E-03
2	64 ⁺⁹ ₋₈	0	50 ⁺⁸ ₋₇	0	13 ⁺⁴ ₋₃	0	-0.56 ^{+0.12} _{-0.11}	0	1.29 ^{+0.18} _{-0.16}	1.01 ^{+0.16} _{-0.14}	0.28 ^{+0.10} _{-0.07}	3E+00	1E-09
3	49 ⁺⁸ ₋₇	0	12 ⁺⁴ ₋₃	0	36 ⁺⁷ ₋₆	0	0.48 ^{+0.13} _{-0.15}	0	0.99 ^{+0.16} _{-0.14}	0.26 ^{+0.09} _{-0.07}	0.74 ^{+0.14} _{-0.12}	5E+00	1E-26
4	98 ⁺¹¹ ₋₉	0	74 ⁺⁹ ₋₈	0	24 ⁺⁶ ₋₄	0	-0.50 ^{+0.10} _{-0.09}	0	1.99 ^{+0.22} _{-0.20}	1.50 ^{+0.19} _{-0.17}	0.50 ^{+0.12} _{-0.10}	4E+00	5E-19
5	26 ⁺⁶ ₋₅	0	18 ⁺⁵ ₋₄	0	7 ⁺³ ₋₂	0	-0.43 ^{+0.22} _{-0.19}	0	0.53 ^{+0.12} _{-0.10}	0.38 ^{+0.11} _{-0.09}	0.15 ^{+0.08} _{-0.05}	2E+00	1E-03
6	23 ⁺⁵ ₋₄	0	17 ⁺⁵ ₋₄	0	6 ⁺³ ₋₂	0	-0.45 ^{+0.23} _{-0.20}	0	0.48 ^{+0.12} _{-0.10}	0.35 ^{+0.11} _{-0.08}	0.13 ^{+0.07} _{-0.05}	2E+00	4E-03
7	33 ⁺⁶ ₋₅	0	24 ⁺⁶ ₋₄	0	9 ⁺⁴ ₋₂	0	-0.45 ^{+0.19} _{-0.16}	0	0.67 ^{+0.14} _{-0.12}	0.49 ^{+0.12} _{-0.10}	0.18 ^{+0.08} _{-0.06}	2E+00	1E-05
8	19 ⁺⁵ ₋₄	0	9 ⁺⁴ ₋₂	0	10 ⁺⁴ ₋₃	0	0.09 ^{+0.25} _{-0.26}	0	0.40 ^{+0.11} _{-0.09}	0.18 ^{+0.08} _{-0.06}	0.22 ^{+0.09} _{-0.07}	2E+00	9E-07
9	74 ⁺⁹ ₋₈	0	54 ⁺⁸ ₋₇	0	20 ⁺⁵ ₋₄	0	-0.44 ^{+0.12} _{-0.11}	0	1.51 ^{+0.20} _{-0.17}	1.09 ^{+0.17} _{-0.15}	0.42 ^{+0.11} _{-0.09}	3E+00	2E-11
10	145 ⁺¹³ ₋₁₂	0	97 ⁺¹⁰ ₋₉	0	47 ⁺⁸ ₋₆	0	-0.34 ^{+0.08} _{-0.08}	0	2.93 ^{+0.26} _{-0.24}	1.97 ^{+0.22} _{-0.20}	0.96 ^{+0.16} _{-0.14}	6E+00	0E+00
11	7 ⁺³ ₋₂	0	4 ⁺³ ₋₁	0	3 ⁺³ ₋₁	0	-0.05 ^{+0.43} _{-0.42}	0	0.16 ^{+0.08} _{-0.06}	0.08 ^{+0.04} _{-0.04}	0.07 ^{+0.06} _{-0.04}	1E+00	3E-02
12	2 ⁺⁰ ₋₂	5	2 ⁺² ₋₂	5	2 ⁺⁰ ₋₂	5	0.00 ^{+0.00} _{-0.00}	-2	0.05 ^{+0.05} _{-0.05}	0.05 ^{+0.05} _{-0.05}	0.05 ^{+0.00} _{-0.05}	3E-01	3E-01
13	10 ⁺⁴ ₋₃	0	8 ⁺² ₋₃	0	2 ⁺² ₋₂	5	-0.57 ^{+0.00} _{-0.43}	1	0.20 ^{+0.06} _{-0.06}	0.17 ^{+0.03} _{-0.06}	0.05 ^{+0.00} _{-0.05}	4E-01	3E-01
14	5 ⁺³ ₋₂	0	4 ⁺³ ₋₂	0	2 ⁺² ₋₂	5	-0.31 ^{+0.00} _{-0.69}	1	0.11 ^{+0.07} _{-0.05}	0.09 ^{+0.07} _{-0.04}	0.05 ^{+0.00} _{-0.05}	3E-01	3E-01
15	69 ⁺⁹ ₋₈	0	23 ⁺⁵ ₋₄	0	46 ⁺⁷ ₋₆	0	0.34 ^{+0.12} _{-0.13}	0	1.41 ^{+0.19} _{-0.17}	0.47 ^{+0.12} _{-0.10}	0.94 ^{+0.16} _{-0.14}	6E+00	1E-43
16	8 ⁺⁴ ₋₂	0	5 ⁺³ ₋₂	0	2 ⁺⁰ ₋₂	5	-0.38 ^{+0.00} _{-0.62}	1	0.18 ^{+0.08} _{-0.06}	0.11 ^{+0.07} _{-0.05}	0.05 ^{+0.00} _{-0.05}	1E+00	2E-02
17	3 ⁺³ ₋₁	0	2 ⁺² ₋₂	5	2 ⁺⁰ ₋₂	5	0.00 ^{+0.00} _{-0.00}	-2	0.07 ^{+0.06} _{-0.04}	0.05 ^{+0.00} _{-0.05}	0.05 ^{+0.00} _{-0.05}	7E-01	7E-02
18	91 ⁺¹⁰ ₋₉	0	65 ⁺⁹ ₋₈	0	25 ⁺⁶ ₋₅	0	-0.44 ^{+0.11} _{-0.10}	0	1.84 ^{+0.21} _{-0.19}	1.33 ^{+0.18} _{-0.16}	0.52 ^{+0.12} _{-0.10}	4E+00	3E-17
19	41 ⁺⁷ ₋₆	0	28 ⁺⁶ ₋₅	0	12 ⁺⁴ ₋₃	0	-0.39 ^{+0.17} _{-0.15}	0	0.83 ^{+0.15} _{-0.13}	0.57 ^{+0.13} _{-0.11}	0.25 ^{+0.09} _{-0.07}	2E+00	1E-06
20	4 ⁺³ ₋₂	0	2 ⁺⁰ ₋₂	5	2 ⁺⁰ ₋₂	5	0.00 ^{+0.00} _{-0.00}	-2	0.10 ^{+0.07} _{-0.04}	0.05 ^{+0.00} _{-0.05}	0.05 ^{+0.00} _{-0.05}	1E+00	8E-03
21	20 ⁺⁵ ₋₄	0	14 ⁺⁴ ₋₃	0	5 ⁺³ ₋₂	0	-0.46 ^{+0.25} _{-0.21}	0	0.40 ^{+0.11} _{-0.09}	0.30 ^{+0.10} _{-0.08}	0.11 ^{+0.07} _{-0.05}	1E+00	7E-05
22	195 ⁺¹⁵ ₋₁₄	0	149 ⁺¹³ ₋₁₂	0	46 ⁺⁷ ₋₆	0	-0.53 ^{+0.07} _{-0.06}	0	3.95 ^{+0.30} _{-0.28}	3.02 ^{+0.27} _{-0.25}	0.93 ^{+0.16} _{-0.14}	6E+00	0E+00
23	19 ⁺⁵ ₋₄	0	18 ⁺⁵ ₋₄	0	2 ⁺⁰ ₋₂	5	-0.77 ^{+0.00} _{-0.23}	1	0.40 ^{+0.11} _{-0.09}	0.37 ^{+0.11} _{-0.09}	0.05 ^{+0.00} _{-0.05}	5E-01	2E-01
24	20 ⁺⁵ ₋₄	0	12 ⁺⁴ ₋₃	0	7 ⁺³ ₋₂	0	-0.26 ^{+0.25} _{-0.24}	0	0.41 ^{+0.11} _{-0.09}	0.26 ^{+0.09} _{-0.07}	0.15 ^{+0.08} _{-0.05}	2E+00	1E-07
25	31 ⁺⁶ ₋₅	0	27 ⁺⁶ ₋₅	0	2 ⁺⁰ ₋₂	5	-0.84 ^{+0.00} _{-0.16}	1	0.63 ^{+0.13} _{-0.11}	0.55 ^{+0.13} _{-0.10}	0.05 ^{+0.00} _{-0.05}	1E+00	2E-02
26	8 ⁺⁴ ₋₂	0	5 ⁺³ ₋₂	0	2 ⁺⁰ ₋₂	5	-0.37 ^{+0.00} _{-0.63}	1	0.17 ^{+0.08} _{-0.06}	0.12 ^{+0.07} _{-0.05}	0.05 ^{+0.00} _{-0.05}	9E-01	3E-03
27	3 ⁺³ ₋₁	0	4 ⁺³ ₋₂	0	2 ⁺⁰ ₋₂	1	-0.30 ^{+0.00} _{-0.70}	1	0.07 ^{+0.06} _{-0.04}	0.09 ^{+0.07} _{-0.04}	0.05 ^{+0.00} _{-0.05}	-3E-01	8E-01
28	2 ⁺⁰ ₋₂	5	2 ⁺⁰ ₋₂	1	2 ⁺⁰ ₋₂	5	0.00 ^{+0.00} _{-0.00}	-2	0.05 ^{+0.05} _{-0.05}	0.05 ^{+0.00} _{-0.05}	0.05 ^{+0.00} _{-0.05}	9E-01	3E-03
29	8 ⁺⁴ ₋₂	0	6 ⁺³ ₋₂	0	2 ⁺⁰ ₋₂	5	-0.45 ^{+0.00} _{-0.55}	1	0.18 ^{+0.08} _{-0.06}	0.14 ^{+0.08} _{-0.05}	0.05 ^{+0.00} _{-0.05}	7E-01	2E-02
30	2 ⁺⁰ ₋₂	5	2 ⁺⁰ ₋₂	5	2 ⁺⁰ ₋₂	1	0.00 ^{+0.00} _{-0.00}	-2	0.05 ^{+0.05} _{-0.05}	0.05 ^{+0.00} _{-0.05}	0.05 ^{+0.00} _{-0.05}	-9E-02	1E+00
31	5 ⁺³ ₋₂	0	2 ⁺⁰ ₋₂	5	2 ⁺⁰ ₋₂	5	0.00 ^{+0.00} _{-0.00}	-2	0.11 ^{+0.07} _{-0.05}	0.05 ^{+0.00} _{-0.05}	0.05 ^{+0.00} _{-0.05}	9E-01	5E-03
32	2 ⁺⁰ ₋₂	5	2 ⁺⁰ ₋₂	1	2 ⁺⁰ ₋₂	5	0.00 ^{+0.00} _{-0.00}	-2	0.05 ^{+0.05} _{-0.05}	0.05 ^{+0.00} _{-0.05}	0.05 ^{+0.00} _{-0.05}	6E-01	6E-02
33	28 ⁺⁶ ₋₅	0	23 ⁺⁶ ₋₄	0	4 ⁺³ ₋₂	0	-0.68 ^{+0.19} _{-0.14}	0	0.58 ^{+0.13} _{-0.11}	0.48 ^{+0.12} _{-0.10}	0.09 ^{+0.07} _{-0.04}	1E+00	9E-05
34	2 ⁺⁰ ₋₂	5	3 ⁺⁰ ₋₃	5	2 ⁺⁰ ₋₂	1	0.00 ^{+0.00} _{-0.00}	-2	0.06 ^{+0.06} _{-0.06}	0.07 ^{+0.07} _{-0.07}	0.05 ^{+0.00} _{-0.05}	-4E-02	1E+00
35	2 ⁺⁰ ₋₂	5	3 ⁺⁰ ₋₃	5	2 ⁺⁰ ₋₂	1	0.00 ^{+0.00} _{-0.00}	-2	0.06 ^{+0.06} _{-0.06}	0.06 ^{+0.06} _{-0.06}	0.05 ^{+0.00} _{-0.05}	-6E-02	1E+00
36	2 ⁺⁰ ₋₂	5	2 ⁺⁰ ₋₂	1	3 ⁺⁰ ₋₃	5	0.00 ^{+0.00} _{-0.00}	-2	0.06 ^{+0.06} _{-0.06}	0.05 ^{+0.06} _{-0.05}	0.07 ^{+0.00} _{-0.07}	7E-01	3E-03
37	4 ⁺³ ₋₂	0	3 ⁺⁰ ₋₃	5	3 ⁺⁰ ₋₃	5	0.00 ^{+0.00} _{-0.00}	-2	0.10 ^{+0.07} _{-0.04}	0.07 ^{+0.06} _{-0.07}	0.07 ^{+0.00} _{-0.07}	1E+00	3E-04
38	2 ⁺⁰ ₋₂	5	2 ⁺⁰ ₋₂	1	3 ⁺³ ₋₁	0	0.00 ^{+0.00} _{-0.00}	-2	0.05 ^{+0.06} _{-0.05}	0.05 ^{+0.06} _{-0.05}	0.07 ^{+0.06} _{-0.04}	1E+00	5E-04
39	2 ⁺⁰ ₋₂	5	2 ⁺⁰ ₋₂	5	2 ⁺⁰ ₋₂	1	0.00 ^{+0.00} _{-0.00}	-2	0.05 ^{+0.06} _{-0.05}	0.06 ^{+0.06} _{-0.06}	0.05 ^{+0.00} _{-0.05}	-5E-02	1E+00
40	8 ⁺⁴ ₋₂	0	2 ⁺⁰ ₋₂	5	7 ⁺³ ₋₂	0	0.51 ^{+0.49} _{-0.00}	-1	0.17 ^{+0.08} _{-0.06}	0.05 ^{+0.00} _{-0.05}	0.15 ^{+0.08} _{-0.05}	2E+00	2E-07
41	3 ⁺³ ₋₁	0	2 ⁺⁰ ₋₂	5	3 ⁺⁰ ₋₃	5	0.00 ^{+0.00} _{-0.00}	-2	0.08 ^{+0.06} _{-0.04}	0.05 ^{+0.00} _{-0.05}	0.06 ^{+0.00} _{-0.06}	1E+00	3E-04
42	3 ⁺³ ₋₁	0	2 ⁺⁰ ₋₂	5	3 ⁺⁰ ₋₃	5	0.00 ^{+0.00} _{-0.00}	-2	0.08 ^{+0.06} _{-0.04}	0.05 ^{+0.00} _{-0.05}	0.07 ^{+0.00} _{-0.07}	1E+00	1E-04

TABLE 27:

Counts, count rates and AE detection significance and no-source probabilities for X-ray point sources in HCG 90 (online only).

43	7 ₋₂ ⁺³	0	2 ₋₂ ⁺⁰	1	7 ₋₂ ⁺³	0	0.55 _{-0.00} ^{+0.45}	-1	0.16 _{-0.06} ^{+0.08}	0.05 _{-0.05} ^{+0.00}	0.16 _{-0.06} ^{+0.08}	2E+00	1E-11
44	2 ₋₂ ⁺⁰	5	2 ₋₂ ⁺⁰	5	2 ₋₂ ⁺⁰	5	0.00 _{-0.00} ^{+0.00}	-2	0.05 _{-0.05} ^{+0.00}	0.05 _{-0.05} ^{+0.00}	0.05 _{-0.05} ^{+0.00}	7E-01	8E-02
45	2 ₋₂ ⁺⁰	5	2 ₋₂ ⁺⁰	5	2 ₋₂ ⁺⁰	1	0.00 _{-0.00} ^{+0.00}	-2	0.05 _{-0.05} ^{+0.00}	0.06 _{-0.06} ^{+0.00}	0.05 _{-0.05} ^{+0.00}	-1E-01	1E+00
46	4 ₋₂ ⁺³	0	3 ₋₁ ⁺³	0	2 ₋₂ ⁺⁰	5	-0.20 _{-0.80} ^{+0.00}	1	0.10 _{-0.04} ^{+0.07}	0.08 _{-0.04} ^{+0.06}	0.05 _{-0.05} ^{+0.00}	4E-01	1E-01
47	5 ₋₂ ⁺³	0	4 ₋₄ ⁺⁰	5	3 ₋₃ ⁺⁰	5	0.00 _{-0.00} ^{+0.00}	-2	0.12 _{-0.05} ^{+0.07}	0.09 _{-0.09} ^{+0.00}	0.06 _{-0.06} ^{+0.00}	1E+00	3E-04
48	6 ₋₂ ⁺³	0	5 ₋₂ ⁺³	0	2 ₋₂ ⁺⁰	5	-0.39 _{-0.61} ^{+0.00}	1	0.14 _{-0.05} ^{+0.08}	0.12 _{-0.05} ^{+0.07}	0.05 _{-0.05} ^{+0.00}	4E-01	1E-01
49	2 ₋₂ ⁺⁰	5	2 ₋₂ ⁺⁰	5	2 ₋₂ ⁺⁰	5	0.00 _{-0.00} ^{+0.00}	-2	0.05 _{-0.05} ^{+0.00}	0.05 _{-0.05} ^{+0.00}	0.05 _{-0.05} ^{+0.00}	4E-01	1E-01
50	24 ₋₄ ⁺⁶	0	17 ₋₄ ⁺⁵	0	6 ₋₂ ⁺³	0	-0.46 _{-0.19} ^{+0.22}	0	0.49 _{-0.10} ^{+0.12}	0.36 _{-0.08} ^{+0.11}	0.13 _{-0.05} ^{+0.07}	2E+00	7E-07
51	2 ₋₂ ⁺⁰	5	3 ₋₃ ⁺⁰	5	2 ₋₂ ⁺⁰	5	0.00 _{-0.00} ^{+0.00}	-2	0.06 _{-0.06} ^{+0.00}	0.07 _{-0.07} ^{+0.00}	0.05 _{-0.05} ^{+0.00}	4E-01	1E-01
52	4 ₋₂ ⁺³	0	2 ₋₂ ⁺⁰	5	3 ₋₁ ⁺³	0	0.18 _{-0.00} ^{+0.82}	-1	0.10 _{-0.04} ^{+0.07}	0.06 _{-0.06} ^{+0.00}	0.08 _{-0.04} ^{+0.06}	1E+00	4E-06
53	2 ₋₂ ⁺⁰	5	2 ₋₂ ⁺⁰	1	2 ₋₂ ⁺⁰	5	0.00 _{-0.00} ^{+0.00}	-2	0.05 _{-0.05} ^{+0.00}	0.05 _{-0.05} ^{+0.00}	0.05 _{-0.05} ^{+0.00}	7E-01	1E-02
54	4 ₋₂ ⁺³	0	2 ₋₂ ⁺⁰	5	3 ₋₃ ⁺⁰	5	0.00 _{-0.00} ^{+0.00}	-2	0.10 _{-0.04} ^{+0.07}	0.06 _{-0.06} ^{+0.00}	0.06 _{-0.06} ^{+0.00}	1E+00	6E-04
55	3 ₋₃ ⁺⁰	5	3 ₋₃ ⁺⁰	5	2 ₋₂ ⁺⁰	1	0.00 _{-0.00} ^{+0.00}	-2	0.06 _{-0.06} ^{+0.00}	0.07 _{-0.07} ^{+0.00}	0.05 _{-0.05} ^{+0.00}	-1E-02	1E+00
56	2 ₋₂ ⁺⁰	5	2 ₋₂ ⁺⁰	5	2 ₋₂ ⁺⁰	1	0.00 _{-0.00} ^{+0.00}	-2	0.05 _{-0.05} ^{+0.00}	0.05 _{-0.05} ^{+0.00}	0.05 _{-0.05} ^{+0.00}	-5E-01	1E+00
57	3 ₋₁ ⁺³	0	3 ₋₃ ⁺⁰	5	2 ₋₂ ⁺⁰	5	0.00 _{-0.00} ^{+0.00}	-2	0.08 _{-0.04} ^{+0.06}	0.07 _{-0.07} ^{+0.00}	0.05 _{-0.05} ^{+0.00}	4E-01	8E-02
58	9 ₋₃ ⁺⁴	0	5 ₋₂ ⁺³	0	3 ₋₁ ⁺³	0	-0.20 _{-0.36} ^{+0.38}	0	0.20 _{-0.06} ^{+0.09}	0.12 _{-0.05} ^{+0.07}	0.08 _{-0.04} ^{+0.06}	1E+00	4E-06
59	3 ₋₁ ⁺³	0	2 ₋₂ ⁺⁰	5	3 ₋₁ ⁺⁰	5	0.00 _{-0.00} ^{+0.00}	-2	0.08 _{-0.04} ^{+0.06}	0.06 _{-0.06} ^{+0.00}	0.07 _{-0.07} ^{+0.00}	7E-01	2E-03
60	2 ₋₂ ⁺⁰	5	2 ₋₂ ⁺⁰	1	3 ₋₃ ⁺⁰	5	0.00 _{-0.00} ^{+0.00}	-2	0.06 _{-0.06} ^{+0.00}	0.05 _{-0.05} ^{+0.00}	0.07 _{-0.07} ^{+0.00}	7E-01	2E-03
61	2 ₋₂ ⁺⁰	5	2 ₋₂ ⁺⁰	1	3 ₋₃ ⁺⁰	5	0.00 _{-0.00} ^{+0.00}	-2	0.06 _{-0.06} ^{+0.00}	0.05 _{-0.05} ^{+0.00}	0.06 _{-0.06} ^{+0.00}	7E-01	3E-03
62	23 ₋₄ ⁺⁶	0	14 ₋₃ ⁺⁴	0	9 ₋₃ ⁺⁴	0	-0.23 _{-0.22} ^{+0.23}	0	0.48 _{-0.10} ^{+0.12}	0.30 _{-0.08} ^{+0.10}	0.18 _{-0.06} ^{+0.08}	2E+00	6E-08
63	3 ₋₁ ⁺³	0	2 ₋₂ ⁺⁰	5	4 ₋₄ ⁺⁰	5	0.00 _{-0.00} ^{+0.00}	-2	0.08 _{-0.04} ^{+0.06}	0.06 _{-0.06} ^{+0.00}	0.09 _{-0.09} ^{+0.00}	7E-01	5E-04
64	4 ₋₂ ⁺³	0	2 ₋₂ ⁺⁰	1	4 ₋₂ ⁺³	0	0.35 _{-0.00} ^{+0.65}	-1	0.09 _{-0.04} ^{+0.07}	0.05 _{-0.05} ^{+0.00}	0.10 _{-0.04} ^{+0.00}	1E+00	4E-06
65	2 ₋₂ ⁺⁰	5	2 ₋₂ ⁺⁰	5	2 ₋₂ ⁺⁰	1	0.00 _{-0.00} ^{+0.00}	-2	0.05 _{-0.05} ^{+0.00}	0.06 _{-0.06} ^{+0.00}	0.05 _{-0.05} ^{+0.00}	-9E-02	1E+00
66	3 ₋₁ ⁺³	0	2 ₋₂ ⁺⁰	1	3 ₋₁ ⁺³	0	0.26 _{-0.00} ^{+0.74}	-1	0.08 _{-0.04} ^{+0.06}	0.05 _{-0.05} ^{+0.00}	0.08 _{-0.04} ^{+0.06}	1E+00	4E-06
67	55 ₋₇ ⁺⁸	0	38 ₋₆ ⁺⁷	0	16 ₋₄ ⁺⁵	0	-0.41 _{-0.13} ^{+0.14}	0	1.11 _{-0.15} ^{+0.17}	0.78 _{-0.13} ^{+0.15}	0.33 _{-0.08} ^{+0.10}	3E+00	2E-18
68	29 ₋₅ ⁺⁶	0	18 ₋₄ ⁺⁵	0	11 ₋₃ ⁺⁴	0	-0.26 _{-0.19} ^{+0.21}	0	0.60 _{-0.11} ^{+0.13}	0.38 _{-0.09} ^{+0.11}	0.22 _{-0.07} ^{+0.09}	2E+00	1E-09
69	2 ₋₂ ⁺⁰	5	2 ₋₂ ⁺⁰	5	2 ₋₂ ⁺⁰	1	0.00 _{-0.00} ^{+0.00}	-2	0.05 _{-0.05} ^{+0.00}	0.05 _{-0.05} ^{+0.00}	0.05 _{-0.05} ^{+0.00}	-5E-02	1E+00
70	3 ₋₁ ⁺³	0	5 ₋₅ ⁺⁰	5	2 ₋₂ ⁺⁰	5	0.00 _{-0.00} ^{+0.00}	-2	0.08 _{-0.04} ^{+0.06}	0.10 _{-0.10} ^{+0.00}	0.05 _{-0.05} ^{+0.00}	4E-01	9E-02
71	9 ₋₃ ⁺⁴	0	8 ₋₂ ⁺⁴	0	2 ₋₂ ⁺⁰	5	-0.56 _{-0.44} ^{+0.00}	1	0.20 _{-0.06} ^{+0.09}	0.18 _{-0.06} ^{+0.08}	0.05 _{-0.05} ^{+0.00}	4E-01	1E-01
72	2 ₋₂ ⁺⁰	1	2 ₋₂ ⁺⁰	5	2 ₋₂ ⁺⁰	1	0.00 _{-0.00} ^{+0.00}	-2	0.05 _{-0.05} ^{+0.00}	0.05 _{-0.05} ^{+0.00}	0.05 _{-0.05} ^{+0.00}	-1E+00	1E+00
73	5 ₋₂ ⁺³	0	3 ₋₁ ⁺³	0	2 ₋₂ ⁺⁰	5	-0.19 _{-0.81} ^{+0.00}	1	0.12 _{-0.05} ^{+0.07}	0.08 _{-0.04} ^{+0.06}	0.05 _{-0.05} ^{+0.00}	7E-01	1E-02
74	4 ₋₂ ⁺³	0	3 ₋₁ ⁺³	0	2 ₋₂ ⁺⁰	5	-0.17 _{-0.83} ^{+0.00}	1	0.10 _{-0.04} ^{+0.07}	0.08 _{-0.04} ^{+0.06}	0.06 _{-0.06} ^{+0.00}	4E-01	6E-02
75	3 ₋₁ ⁺³	0	3 ₋₁ ⁺³	0	2 ₋₂ ⁺⁰	1	-0.26 _{-0.74} ^{+0.00}	1	0.08 _{-0.04} ^{+0.06}	0.08 _{-0.04} ^{+0.06}	0.05 _{-0.05} ^{+0.00}	-8E-02	1E+00
76	3 ₋₃ ⁺⁰	5	3 ₋₃ ⁺⁰	5	2 ₋₂ ⁺⁰	5	0.00 _{-0.00} ^{+0.00}	-2	0.06 _{-0.06} ^{+0.00}	0.07 _{-0.07} ^{+0.00}	0.05 _{-0.05} ^{+0.00}	4E-01	9E-02
77	3 ₋₁ ⁺³	0	4 ₋₁ ⁺³	0	2 ₋₂ ⁺⁰	1	-0.26 _{-0.74} ^{+0.00}	1	0.08 _{-0.04} ^{+0.06}	0.08 _{-0.04} ^{+0.06}	0.05 _{-0.05} ^{+0.00}	-5E-02	1E+00
78	6 ₋₂ ⁺³	0	2 ₋₂ ⁺⁰	5	3 ₋₂ ⁺³	0	0.16 _{-0.00} ^{+0.84}	-1	0.14 _{-0.05} ^{+0.08}	0.06 _{-0.06} ^{+0.00}	0.08 _{-0.04} ^{+0.06}	1E+00	4E-06
79	2 ₋₂ ⁺⁰	5	3 ₋₃ ⁺⁰	5	2 ₋₂ ⁺⁰	1	0.00 _{-0.00} ^{+0.00}	-2	0.05 _{-0.05} ^{+0.00}	0.06 _{-0.06} ^{+0.00}	0.05 _{-0.05} ^{+0.00}	-4E-02	1E+00
80	2 ₋₂ ⁺⁰	5	2 ₋₂ ⁺⁰	5	2 ₋₂ ⁺⁰	1	0.00 _{-0.00} ^{+0.00}	-2	0.05 _{-0.05} ^{+0.00}	0.06 _{-0.06} ^{+0.00}	0.05 _{-0.05} ^{+0.00}	-5E-02	1E+00
81	8 ₋₂ ⁺⁴	0	6 ₋₂ ⁺³	0	2 ₋₂ ⁺⁰	5	-0.45 _{-0.55} ^{+0.00}	1	0.17 _{-0.06} ^{+0.08}	0.13 _{-0.05} ^{+0.07}	0.05 _{-0.05} ^{+0.00}	7E-01	1E-01
82	3 ₋₃ ⁺⁰	5	4 ₋₄ ⁺⁰	5	2 ₋₂ ⁺⁰	1	0.00 _{-0.00} ^{+0.00}	-2	0.07 _{-0.07} ^{+0.00}	0.08 _{-0.08} ^{+0.00}	0.05 _{-0.05} ^{+0.00}	-7E-03	1E+00
83	20 ₋₄ ⁺⁵	0	15 ₋₃ ⁺⁵	0	5 ₋₂ ⁺³	0	-0.43 _{-0.21} ^{+0.25}	0	0.42 _{-0.09} ^{+0.11}	0.30 _{-0.08} ^{+0.10}	0.12 _{-0.05} ^{+0.07}	2E+00	1E-08
84	3 ₋₃ ⁺⁰	5	4 ₋₄ ⁺⁰	5	2 ₋₂ ⁺⁰	1	0.00 _{-0.00} ^{+0.00}	-2	0.07 _{-0.07} ^{+0.00}	0.08 _{-0.08} ^{+0.00}	0.05 _{-0.05} ^{+0.00}	-2E-02	1E+00
85C	7 ₋₂ ⁺³	0	3 ₋₁ ⁺³	0	3 ₋₁ ⁺³	0	0.01 _{-0.43} ^{+0.43}	0	0.16 _{-0.06} ^{+0.08}	0.08 _{-0.04} ^{+0.06}	0.08 _{-0.04} ^{+0.06}	1E+00	4E-06
86	16 ₋₄ ⁺⁵	0	2 ₋₂ ⁺⁰	5	15 ₋₃ ⁺⁵	0	0.74 _{-0.00} ^{+0.26}	-1	0.33 _{-0.08} ^{+0.10}	0.05 _{-0.05} ^{+0.00}	0.32 _{-0.08} ^{+0.10}	3E+00	1E-06
87	19 ₋₄ ⁺⁵	0	9 ₋₃ ⁺⁴	0	9 ₋₃ ⁺⁴	0	-0.01 _{-0.26} ^{+0.26}	0	0.40 _{-0.09} ^{+0.11}	0.20 _{-0.06} ^{+0.09}	0.20 _{-0.06} ^{+0.09}	2E+00	4E-12

TABLE 27:

Counts, count rates and AE detection significance and no-source probabilities for X-ray point sources in HCG 90 (online only).

88A	23361^{+153}_{-152}	0	528^{+24}_{-23}	0	22832^{+152}_{-151}	0	$0.95^{+0.00}_{-0.00}$	0	$471.64^{+3.11}_{-3.09}$	$10.66^{+0.48}_{-0.46}$	$460.98^{+3.07}_{-3.05}$	2E+02	0E+00
89	0^{+0}_{-0}	5	2^{+0}_{-2}	5	0^{+0}_{-0}	5	$0.00^{+0.00}_{-0.00}$	-2	$0.00^{+0.00}_{-0.00}$	$0.05^{+0.00}_{-0.05}$	$0.00^{+0.00}_{-0.00}$	2E-01	5E-01
90	8^{+4}_{-2}	0	2^{+0}_{-2}	1	8^{+4}_{-2}	0	$0.57^{+0.43}_{-0.00}$	-1	$0.17^{+0.08}_{-0.06}$	$0.05^{+0.00}_{-0.05}$	$0.17^{+0.08}_{-0.06}$	2E+00	6E-05
91C	4^{+3}_{-2}	0	4^{+3}_{-2}	0	2^{+0}_{-2}	1	$-0.36^{+0.00}_{-0.64}$	1	$0.10^{+0.07}_{-0.04}$	$0.10^{+0.07}_{-0.04}$	$0.05^{+0.00}_{-0.05}$	-6E-02	1E+00
92	10^{+4}_{-3}	0	2^{+0}_{-2}	5	9^{+4}_{-3}	0	$0.61^{+0.39}_{-0.00}$	-1	$0.21^{+0.09}_{-0.06}$	$0.05^{+0.00}_{-0.05}$	$0.20^{+0.09}_{-0.06}$	2E+00	7E-08
93	2^{+0}_{-2}	5	2^{+0}_{-2}	1	2^{+0}_{-2}	5	$0.00^{+0.00}_{-0.00}$	-2	$0.05^{+0.00}_{-0.05}$	$0.05^{+0.00}_{-0.05}$	$0.05^{+0.00}_{-0.05}$	1E+00	9E-03
94	9^{+4}_{-2}	0	2^{+0}_{-2}	5	8^{+4}_{-2}	0	$0.53^{+0.47}_{-0.00}$	-1	$0.18^{+0.08}_{-0.06}$	$0.05^{+0.00}_{-0.05}$	$0.16^{+0.08}_{-0.06}$	2E+00	5E-07
95	2^{+0}_{-2}	5	2^{+0}_{-2}	1	2^{+0}_{-2}	5	$0.00^{+0.00}_{-0.00}$	-2	$0.05^{+0.00}_{-0.05}$	$0.05^{+0.00}_{-0.05}$	$0.05^{+0.00}_{-0.05}$	6E-01	8E-02
96	2^{+0}_{-2}	5	2^{+0}_{-2}	1	2^{+0}_{-2}	5	$0.00^{+0.00}_{-0.00}$	-2	$0.05^{+0.00}_{-0.05}$	$0.05^{+0.00}_{-0.05}$	$0.05^{+0.00}_{-0.05}$	6E-01	9E-02
97	4^{+3}_{-2}	0	2^{+0}_{-2}	5	3^{+3}_{-1}	0	$0.14^{+0.86}_{-0.00}$	-1	$0.09^{+0.07}_{-0.04}$	$0.06^{+0.00}_{-0.06}$	$0.07^{+0.06}_{-0.04}$	1E+00	7E-04
98	2^{+0}_{-2}	5	2^{+0}_{-2}	1	2^{+0}_{-2}	5	$0.00^{+0.00}_{-0.00}$	-2	$0.05^{+0.00}_{-0.05}$	$0.05^{+0.00}_{-0.05}$	$0.05^{+0.00}_{-0.05}$	3E-01	3E-01
99	2^{+0}_{-2}	5	2^{+0}_{-2}	1	2^{+0}_{-2}	5	$0.00^{+0.00}_{-0.00}$	-2	$0.05^{+0.00}_{-0.05}$	$0.05^{+0.00}_{-0.05}$	$0.05^{+0.00}_{-0.05}$	6E-01	8E-02
100	4^{+3}_{-2}	0	4^{+3}_{-2}	0	2^{+0}_{-2}	1	$-0.36^{+0.00}_{-0.64}$	1	$0.10^{+0.07}_{-0.04}$	$0.10^{+0.07}_{-0.04}$	$0.05^{+0.00}_{-0.05}$	-2E-02	1E+00
101	2^{+0}_{-2}	5	2^{+0}_{-2}	5	2^{+0}_{-2}	1	$0.00^{+0.00}_{-0.00}$	-2	$0.05^{+0.00}_{-0.05}$	$0.06^{+0.00}_{-0.06}$	$0.05^{+0.00}_{-0.05}$	-1E-01	1E+00
102	2^{+0}_{-2}	5	2^{+0}_{-2}	5	2^{+0}_{-2}	1	$0.00^{+0.00}_{-0.00}$	-2	$0.05^{+0.00}_{-0.05}$	$0.05^{+0.00}_{-0.05}$	$0.05^{+0.00}_{-0.05}$	-1E-02	1E+00
103	3^{+0}_{-3}	5	2^{+0}_{-2}	1	3^{+0}_{-3}	5	$0.00^{+0.00}_{-0.00}$	-2	$0.06^{+0.00}_{-0.06}$	$0.05^{+0.00}_{-0.05}$	$0.08^{+0.00}_{-0.08}$	7E-01	9E-04
104	2^{+0}_{-2}	5	2^{+0}_{-2}	5	2^{+0}_{-2}	5	$0.00^{+0.00}_{-0.00}$	-2	$0.05^{+0.00}_{-0.05}$	$0.05^{+0.00}_{-0.05}$	$0.05^{+0.00}_{-0.05}$	4E-01	3E-01
105C	8^{+4}_{-2}	0	2^{+0}_{-2}	5	5^{+3}_{-2}	0	$0.40^{+0.60}_{-0.00}$	-1	$0.17^{+0.06}_{-0.06}$	$0.05^{+0.00}_{-0.05}$	$0.12^{+0.07}_{-0.05}$	2E+00	1E-08
106	2^{+0}_{-2}	5	2^{+0}_{-2}	5	2^{+0}_{-2}	1	$0.00^{+0.00}_{-0.00}$	-2	$0.05^{+0.00}_{-0.05}$	$0.05^{+0.00}_{-0.05}$	$0.05^{+0.00}_{-0.05}$	-5E-02	1E+00
107	24^{+6}_{-4}	0	14^{+4}_{-3}	0	9^{+4}_{-3}	0	$-0.20^{+0.23}_{-0.22}$	0	$0.48^{+0.12}_{-0.10}$	$0.29^{+0.10}_{-0.08}$	$0.19^{+0.09}_{-0.06}$	2E+00	3E-07
108C	23^{+5}_{-4}	0	15^{+5}_{-3}	0	7^{+3}_{-2}	0	$-0.33^{+0.23}_{-0.21}$	0	$0.47^{+0.12}_{-0.10}$	$0.31^{+0.10}_{-0.08}$	$0.16^{+0.08}_{-0.06}$	2E+00	1E-11
109C	10^{+4}_{-3}	0	6^{+3}_{-2}	0	3^{+3}_{-1}	0	$-0.24^{+0.38}_{-0.34}$	0	$0.21^{+0.09}_{-0.06}$	$0.13^{+0.07}_{-0.05}$	$0.08^{+0.06}_{-0.04}$	1E+00	4E-05
110	27^{+6}_{-5}	0	16^{+5}_{-4}	0	10^{+4}_{-3}	0	$-0.23^{+0.22}_{-0.20}$	0	$0.55^{+0.13}_{-0.10}$	$0.34^{+0.10}_{-0.08}$	$0.21^{+0.09}_{-0.06}$	2E+00	3E-11
111C	3^{+3}_{-1}	0	3^{+0}_{-3}	5	2^{+0}_{-2}	5	$0.00^{+0.00}_{-0.00}$	-2	$0.08^{+0.06}_{-0.04}$	$0.06^{+0.00}_{-0.06}$	$0.06^{+0.00}_{-0.06}$	4E-01	5E-02
112C	8^{+4}_{-2}	0	2^{+0}_{-2}	5	6^{+3}_{-2}	0	$0.47^{+0.53}_{-0.00}$	-1	$0.17^{+0.08}_{-0.06}$	$0.05^{+0.00}_{-0.05}$	$0.14^{+0.08}_{-0.05}$	2E+00	4E-10
113	3^{+3}_{-1}	0	3^{+3}_{-1}	0	2^{+0}_{-2}	1	$-0.25^{+0.00}_{-0.75}$	1	$0.08^{+0.06}_{-0.04}$	$0.08^{+0.06}_{-0.04}$	$0.05^{+0.00}_{-0.05}$	-3E-02	1E+00
114	3^{+0}_{-3}	5	3^{+0}_{-3}	5	2^{+0}_{-2}	1	$0.00^{+0.00}_{-0.00}$	-2	$0.06^{+0.00}_{-0.06}$	$0.08^{+0.00}_{-0.08}$	$0.05^{+0.00}_{-0.05}$	-2E-02	1E+00
115	2^{+0}_{-2}	5	2^{+0}_{-2}	5	2^{+0}_{-2}	1	$0.00^{+0.00}_{-0.00}$	-2	$0.05^{+0.00}_{-0.05}$	$0.05^{+0.00}_{-0.05}$	$0.05^{+0.00}_{-0.05}$	-5E-02	1E+00
116	5^{+3}_{-2}	0	3^{+3}_{-1}	0	2^{+0}_{-2}	5	$-0.18^{+0.00}_{-0.82}$	1	$0.12^{+0.07}_{-0.05}$	$0.08^{+0.06}_{-0.04}$	$0.06^{+0.00}_{-0.06}$	7E-01	1E-02
117	2^{+0}_{-2}	5	2^{+0}_{-2}	5	2^{+0}_{-2}	1	$0.00^{+0.00}_{-0.00}$	-2	$0.05^{+0.00}_{-0.05}$	$0.05^{+0.00}_{-0.05}$	$0.05^{+0.00}_{-0.05}$	-4E-02	1E+00
118	16^{+5}_{-4}	0	13^{+4}_{-3}	0	3^{+0}_{-3}	5	$-0.63^{+0.00}_{-0.37}$	1	$0.34^{+0.10}_{-0.08}$	$0.28^{+0.10}_{-0.07}$	$0.06^{+0.00}_{-0.06}$	1E+00	3E-04
119	2^{+0}_{-2}	5	4^{+0}_{-4}	5	2^{+0}_{-2}	1	$0.00^{+0.00}_{-0.00}$	-2	$0.06^{+0.00}_{-0.06}$	$0.09^{+0.00}_{-0.09}$	$0.05^{+0.00}_{-0.05}$	-6E-02	1E+00
120C	5^{+3}_{-2}	0	3^{+0}_{-3}	5	5^{+0}_{-5}	5	$0.00^{+0.00}_{-0.00}$	-2	$0.12^{+0.07}_{-0.05}$	$0.06^{+0.00}_{-0.06}$	$0.12^{+0.00}_{-0.12}$	1E+00	9E-06
121	3^{+3}_{-1}	0	4^{+3}_{-2}	0	2^{+0}_{-2}	1	$-0.33^{+0.00}_{-0.67}$	1	$0.08^{+0.06}_{-0.04}$	$0.09^{+0.07}_{-0.04}$	$0.05^{+0.00}_{-0.05}$	-2E-01	7E-01
122	2^{+0}_{-2}	5	2^{+0}_{-2}	5	2^{+0}_{-2}	1	$0.00^{+0.00}_{-0.00}$	-2	$0.05^{+0.00}_{-0.05}$	$0.05^{+0.00}_{-0.05}$	$0.05^{+0.00}_{-0.05}$	-2E-02	1E+00
123	2^{+0}_{-2}	5	2^{+0}_{-2}	5	2^{+0}_{-2}	1	$0.00^{+0.00}_{-0.00}$	-2	$0.05^{+0.00}_{-0.05}$	$0.05^{+0.00}_{-0.05}$	$0.05^{+0.00}_{-0.05}$	-4E-02	1E+00
124	4^{+3}_{-2}	0	2^{+0}_{-2}	5	3^{+3}_{-2}	0	$0.15^{+0.85}_{-0.00}$	-1	$0.10^{+0.07}_{-0.04}$	$0.06^{+0.00}_{-0.06}$	$0.08^{+0.06}_{-0.04}$	1E+00	5E-05
125C	3^{+3}_{-1}	0	3^{+3}_{-1}	0	2^{+0}_{-1}	1	$-0.25^{+0.00}_{-0.75}$	1	$0.08^{+0.06}_{-0.04}$	$0.08^{+0.06}_{-0.04}$	$0.05^{+0.00}_{-0.05}$	-2E-02	1E+00
126	2^{+0}_{-2}	5	3^{+0}_{-3}	5	2^{+0}_{-2}	1	$0.00^{+0.00}_{-0.00}$	-2	$0.06^{+0.00}_{-0.06}$	$0.07^{+0.00}_{-0.07}$	$0.05^{+0.00}_{-0.05}$	-4E-02	1E+00
127	3^{+3}_{-1}	0	3^{+3}_{-1}	0	2^{+0}_{-2}	1	$-0.24^{+0.00}_{-0.76}$	1	$0.07^{+0.06}_{-0.04}$	$0.08^{+0.06}_{-0.04}$	$0.05^{+0.00}_{-0.05}$	-4E-02	1E+00
128	4^{+3}_{-2}	0	2^{+0}_{-2}	1	5^{+3}_{-2}	0	$0.38^{+0.62}_{-0.00}$	-1	$0.10^{+0.07}_{-0.04}$	$0.05^{+0.00}_{-0.05}$	$0.10^{+0.07}_{-0.04}$	1E+00	3E-04
129D	4^{+3}_{-2}	0	4^{+3}_{-2}	0	2^{+0}_{-2}	1	$-0.36^{+0.00}_{-0.64}$	1	$0.10^{+0.07}_{-0.04}$	$0.10^{+0.07}_{-0.04}$	$0.05^{+0.00}_{-0.05}$	-1E-02	1E+00
130D	9^{+4}_{-3}	0	7^{+3}_{-2}	0	3^{+0}_{-3}	5	$-0.45^{+0.00}_{-0.55}$	1	$0.20^{+0.09}_{-0.06}$	$0.16^{+0.08}_{-0.06}$	$0.06^{+0.00}_{-0.06}$	7E-01	5E-03
131	11^{+4}_{-3}	0	5^{+3}_{-2}	0	5^{+3}_{-2}	0	$-0.01^{+0.35}_{-0.35}$	0	$0.23^{+0.09}_{-0.07}$	$0.12^{+0.07}_{-0.05}$	$0.12^{+0.07}_{-0.05}$	2E+00	2E-06
132	2^{+0}_{-2}	5	3^{+0}_{-3}	5	2^{+0}_{-2}	1	$0.00^{+0.00}_{-0.00}$	-2	$0.06^{+0.00}_{-0.06}$	$0.06^{+0.00}_{-0.06}$	$0.05^{+0.00}_{-0.05}$	-1E-02	1E+00

TABLE 27:

Counts, count rates and AE detection significance and no-source probabilities for X-ray point sources in HCG 90 (online only).

133D	6^{+3}_{-2}	0	5^{+3}_{-2}	0	3^{+0}_{-3}	5	$-0.23^{+0.00}_{-0.77}$	1	$0.14^{+0.08}_{-0.05}$	$0.10^{+0.07}_{-0.04}$	$0.06^{+0.00}_{-0.06}$	7E-01	3E-03
134	13^{+4}_{-3}	0	8^{+4}_{-2}	0	4^{+3}_{-2}	0	$-0.32^{+0.32}_{-0.29}$	0	$0.27^{+0.10}_{-0.07}$	$0.18^{+0.08}_{-0.06}$	$0.09^{+0.07}_{-0.04}$	1E+00	2E-04
135	5^{+3}_{-2}	0	3^{+3}_{-1}	0	2^{+0}_{-2}	5	$-0.22^{+0.00}_{-0.78}$	1	$0.11^{+0.07}_{-0.05}$	$0.08^{+0.06}_{-0.04}$	$0.05^{+0.00}_{-0.05}$	6E-01	5E-02
136	2^{+0}_{-2}	5	2^{+0}_{-2}	5	2^{+0}_{-2}	1	$0.00^{+0.00}_{-0.00}$	-2	$0.05^{+0.00}_{-0.05}$	$0.05^{+0.00}_{-0.05}$	$0.05^{+0.00}_{-0.05}$	-2E-02	1E+00
137	2^{+0}_{-2}	5	3^{+0}_{-3}	5	2^{+0}_{-2}	1	$0.00^{+0.00}_{-0.00}$	-2	$0.05^{+0.00}_{-0.05}$	$0.07^{+0.00}_{-0.07}$	$0.05^{+0.00}_{-0.05}$	-6E-02	1E+00
138	9^{+4}_{-3}	0	5^{+3}_{-2}	0	3^{+3}_{-1}	0	$-0.22^{+0.39}_{-0.36}$	0	$0.20^{+0.09}_{-0.06}$	$0.12^{+0.07}_{-0.05}$	$0.08^{+0.06}_{-0.04}$	1E+00	1E-04
139	4^{+3}_{-2}	0	3^{+0}_{-3}	5	2^{+0}_{-2}	5	$0.00^{+0.00}_{-0.00}$	-2	$0.10^{+0.07}_{-0.04}$	$0.06^{+0.00}_{-0.06}$	$0.05^{+0.00}_{-0.05}$	7E-01	2E-02
140	8^{+4}_{-2}	0	8^{+4}_{-2}	0	2^{+0}_{-2}	1	$-0.59^{+0.00}_{-0.41}$	1	$0.17^{+0.08}_{-0.06}$	$0.18^{+0.08}_{-0.06}$	$0.05^{+0.00}_{-0.05}$	-1E-01	1E+00
141	10^{+4}_{-3}	0	7^{+3}_{-2}	0	3^{+0}_{-3}	5	$-0.43^{+0.00}_{-0.57}$	1	$0.22^{+0.09}_{-0.07}$	$0.16^{+0.08}_{-0.06}$	$0.06^{+0.00}_{-0.06}$	1E+00	5E-04
142	2^{+0}_{-2}	5	2^{+0}_{-2}	5	2^{+0}_{-2}	1	$0.00^{+0.00}_{-0.00}$	-2	$0.05^{+0.00}_{-0.05}$	$0.06^{+0.00}_{-0.06}$	$0.05^{+0.00}_{-0.05}$	-3E-02	1E+00
143	13^{+4}_{-3}	0	11^{+4}_{-3}	0	3^{+0}_{-3}	5	$-0.55^{+0.00}_{-0.45}$	1	$0.28^{+0.10}_{-0.07}$	$0.22^{+0.09}_{-0.07}$	$0.06^{+0.00}_{-0.06}$	1E+00	3E-04
144	2^{+0}_{-2}	5	3^{+0}_{-3}	5	2^{+0}_{-2}	1	$0.00^{+0.00}_{-0.00}$	-2	$0.06^{+0.00}_{-0.06}$	$0.06^{+0.00}_{-0.06}$	$0.05^{+0.00}_{-0.05}$	-3E-02	1E+00
145	7^{+3}_{-2}	0	6^{+3}_{-2}	0	3^{+0}_{-3}	5	$-0.29^{+0.00}_{-0.71}$	1	$0.16^{+0.08}_{-0.06}$	$0.12^{+0.07}_{-0.05}$	$0.07^{+0.00}_{-0.07}$	7E-01	3E-03
146D	4^{+3}_{-2}	0	2^{+0}_{-2}	5	3^{+0}_{-3}	5	$0.00^{+0.00}_{-0.00}$	-2	$0.09^{+0.07}_{-0.04}$	$0.05^{+0.00}_{-0.05}$	$0.07^{+0.00}_{-0.07}$	1E+00	3E-04
147	5^{+3}_{-2}	0	2^{+0}_{-2}	1	5^{+3}_{-3}	0	$0.42^{+0.58}_{-0.00}$	-1	$0.11^{+0.07}_{-0.05}$	$0.05^{+0.00}_{-0.05}$	$0.11^{+0.07}_{-0.05}$	2E+00	2E-06
148	15^{+5}_{-3}	0	13^{+4}_{-3}	0	3^{+0}_{-3}	5	$-0.62^{+0.00}_{-0.38}$	1	$0.32^{+0.10}_{-0.08}$	$0.28^{+0.10}_{-0.07}$	$0.07^{+0.00}_{-0.07}$	7E-01	3E-03
149D	10^{+4}_{-3}	0	10^{+3}_{-3}	0	2^{+0}_{-2}	1	$-0.63^{+0.00}_{-0.37}$	1	$0.21^{+0.09}_{-0.06}$	$0.21^{+0.09}_{-0.06}$	$0.05^{+0.00}_{-0.05}$	-3E-02	1E+00
150	8^{+4}_{-2}	0	8^{+4}_{-2}	0	2^{+0}_{-2}	1	$-0.55^{+0.00}_{-0.45}$	1	$0.16^{+0.08}_{-0.06}$	$0.16^{+0.08}_{-0.06}$	$0.05^{+0.00}_{-0.05}$	-1E-02	1E+00
151	8^{+4}_{-2}	0	7^{+3}_{-2}	0	2^{+0}_{-2}	5	$-0.52^{+0.00}_{-0.48}$	1	$0.17^{+0.08}_{-0.06}$	$0.15^{+0.08}_{-0.06}$	$0.05^{+0.00}_{-0.05}$	4E-01	3E-01
152	6^{+3}_{-2}	0	3^{+0}_{-3}	5	4^{+3}_{-1}	0	$0.04^{+0.96}_{-0.00}$	-1	$0.14^{+0.08}_{-0.05}$	$0.07^{+0.00}_{-0.07}$	$0.08^{+0.06}_{-0.04}$	1E+00	4E-07
153D	9^{+4}_{-3}	0	8^{+4}_{-2}	0	2^{+0}_{-2}	5	$-0.50^{+0.00}_{-0.50}$	1	$0.19^{+0.08}_{-0.06}$	$0.17^{+0.08}_{-0.06}$	$0.06^{+0.00}_{-0.06}$	4E-01	5E-02
154	2^{+0}_{-2}	5	2^{+0}_{-2}	5	2^{+0}_{-2}	5	$0.00^{+0.00}_{-0.00}$	-2	$0.05^{+0.00}_{-0.05}$	$0.05^{+0.00}_{-0.05}$	$0.06^{+0.00}_{-0.06}$	4E-01	6E-02
155	5^{+3}_{-2}	0	3^{+3}_{-1}	0	3^{+0}_{-3}	5	$-0.06^{+0.00}_{-0.94}$	1	$0.12^{+0.07}_{-0.05}$	$0.08^{+0.06}_{-0.04}$	$0.07^{+0.00}_{-0.07}$	7E-01	2E-03
156	2^{+0}_{-2}	5	2^{+0}_{-2}	5	2^{+0}_{-2}	1	$0.00^{+0.00}_{-0.00}$	-2	$0.05^{+0.00}_{-0.05}$	$0.05^{+0.00}_{-0.05}$	$0.05^{+0.00}_{-0.05}$	-7E-02	1E+00
157	10^{+4}_{-3}	0	6^{+3}_{-2}	0	4^{+3}_{-1}	0	$-0.27^{+0.36}_{-0.33}$	0	$0.22^{+0.09}_{-0.07}$	$0.14^{+0.08}_{-0.05}$	$0.08^{+0.06}_{-0.04}$	1E+00	1E-07
158	2^{+0}_{-2}	5	2^{+0}_{-2}	1	2^{+0}_{-2}	5	$0.00^{+0.00}_{-0.00}$	-2	$0.05^{+0.00}_{-0.05}$	$0.05^{+0.00}_{-0.05}$	$0.05^{+0.00}_{-0.05}$	7E-01	3E-02
159B	54^{+8}_{-7}	0	32^{+6}_{-5}	0	21^{+5}_{-4}	0	$-0.20^{+0.15}_{-0.14}$	0	$1.09^{+0.17}_{-0.15}$	$0.65^{+0.14}_{-0.11}$	$0.44^{+0.12}_{-0.09}$	4E+00	1E-29
160B	5^{+3}_{-2}	0	4^{+3}_{-1}	0	2^{+0}_{-2}	5	$-0.24^{+0.00}_{-0.76}$	1	$0.11^{+0.07}_{-0.05}$	$0.08^{+0.06}_{-0.04}$	$0.05^{+0.00}_{-0.05}$	6E-01	5E-02
161	5^{+3}_{-2}	0	5^{+0}_{-5}	5	3^{+0}_{-3}	5	$0.00^{+0.00}_{-0.00}$	-2	$0.12^{+0.07}_{-0.05}$	$0.12^{+0.00}_{-0.12}$	$0.07^{+0.00}_{-0.07}$	1E+00	1E-04
162B	5^{+3}_{-2}	0	2^{+0}_{-2}	5	2^{+0}_{-2}	5	$0.00^{+0.00}_{-0.00}$	-2	$0.10^{+0.07}_{-0.04}$	$0.05^{+0.00}_{-0.05}$	$0.06^{+0.00}_{-0.06}$	9E-01	2E-03
163B	2^{+0}_{-2}	5	3^{+3}_{-1}	0	2^{+0}_{-2}	1	$0.00^{+0.00}_{-0.00}$	-2	$0.05^{+0.00}_{-0.05}$	$0.08^{+0.06}_{-0.04}$	$0.05^{+0.00}_{-0.05}$	-9E-02	1E+00
164B	31^{+6}_{-5}	0	25^{+6}_{-5}	0	5^{+3}_{-2}	0	$-0.64^{+0.18}_{-0.14}$	0	$0.63^{+0.13}_{-0.11}$	$0.52^{+0.12}_{-0.10}$	$0.11^{+0.07}_{-0.05}$	2E+00	2E-06
165	2^{+0}_{-2}	5	2^{+0}_{-2}	5	2^{+0}_{-2}	1	$0.00^{+0.00}_{-0.00}$	-2	$0.05^{+0.00}_{-0.05}$	$0.05^{+0.00}_{-0.05}$	$0.05^{+0.00}_{-0.05}$	-1E-01	1E+00
166B	7^{+3}_{-2}	0	4^{+3}_{-2}	0	2^{+0}_{-2}	5	$-0.23^{+0.00}_{-0.77}$	1	$0.14^{+0.08}_{-0.05}$	$0.09^{+0.07}_{-0.04}$	$0.06^{+0.00}_{-0.06}$	9E-01	2E-03
167	2^{+0}_{-2}	5	2^{+0}_{-2}	5	2^{+0}_{-2}	1	$0.00^{+0.00}_{-0.00}$	-2	$0.05^{+0.00}_{-0.05}$	$0.05^{+0.00}_{-0.05}$	$0.05^{+0.00}_{-0.05}$	-1E-01	7E-01
168	9^{+4}_{-3}	0	5^{+3}_{-2}	0	3^{+3}_{-1}	0	$-0.20^{+0.39}_{-0.36}$	0	$0.20^{+0.09}_{-0.06}$	$0.12^{+0.07}_{-0.05}$	$0.08^{+0.06}_{-0.04}$	1E+00	9E-06
169	2^{+0}_{-2}	5	2^{+0}_{-2}	5	2^{+0}_{-2}	1	$0.00^{+0.00}_{-0.00}$	-2	$0.05^{+0.00}_{-0.05}$	$0.05^{+0.00}_{-0.05}$	$0.05^{+0.00}_{-0.05}$	-6E-02	1E+00
170	2^{+0}_{-2}	5	2^{+0}_{-2}	5	2^{+0}_{-2}	1	$0.00^{+0.00}_{-0.00}$	-2	$0.05^{+0.00}_{-0.05}$	$0.05^{+0.00}_{-0.05}$	$0.05^{+0.00}_{-0.05}$	-1E-01	1E+00
171B	7^{+3}_{-2}	0	4^{+3}_{-2}	0	2^{+0}_{-2}	5	$-0.22^{+0.00}_{-0.78}$	1	$0.15^{+0.08}_{-0.05}$	$0.09^{+0.07}_{-0.04}$	$0.06^{+0.00}_{-0.06}$	1E+00	9E-04
172	23^{+5}_{-4}	0	8^{+4}_{-2}	0	14^{+4}_{-3}	0	$0.24^{+0.32}_{-0.24}$	0	$0.46^{+0.12}_{-0.10}$	$0.18^{+0.08}_{-0.06}$	$0.29^{+0.10}_{-0.08}$	3E+00	2E-14
173	2^{+0}_{-2}	5	2^{+0}_{-2}	5	2^{+0}_{-2}	5	$0.00^{+0.00}_{-0.00}$	-2	$0.05^{+0.00}_{-0.05}$	$0.05^{+0.00}_{-0.05}$	$0.05^{+0.00}_{-0.05}$	4E-01	9E-02
174	13^{+4}_{-3}	0	3^{+0}_{-3}	5	10^{+4}_{-3}	0	$0.55^{+0.45}_{-0.00}$	-1	$0.27^{+0.10}_{-0.07}$	$0.06^{+0.00}_{-0.06}$	$0.21^{+0.09}_{-0.06}$	2E+00	8E-12
175	15^{+5}_{-3}	0	11^{+4}_{-3}	0	3^{+3}_{-1}	0	$-0.51^{+0.28}_{-0.23}$	0	$0.32^{+0.10}_{-0.08}$	$0.24^{+0.09}_{-0.07}$	$0.08^{+0.06}_{-0.04}$	1E+00	4E-05
176	8^{+4}_{-2}	0	5^{+3}_{-2}	0	2^{+0}_{-2}	5	$-0.40^{+0.00}_{-0.60}$	1	$0.16^{+0.08}_{-0.06}$	$0.11^{+0.07}_{-0.05}$	$0.05^{+0.00}_{-0.05}$	8E-01	3E-02
177B	3^{+3}_{-1}	0	3^{+0}_{-3}	5	2^{+0}_{-2}	5	$0.00^{+0.00}_{-0.00}$	-2	$0.08^{+0.06}_{-0.04}$	$0.06^{+0.00}_{-0.06}$	$0.05^{+0.00}_{-0.05}$	4E-01	9E-02

TABLE 27:

Counts, count rates and AE detection significance and no-source probabilities for X-ray point sources in HCG 90 (online only).

178B	3^{+3}_{-1}	0	2^{+0}_{-2}	5	3^{+0}_{-3}	5	$0.00^{+0.00}_{-0.00}$	-2	$0.08^{+0.06}_{-0.04}$	$0.06^{+0.00}_{-0.06}$	$0.07^{+0.00}_{-0.07}$	4E-01	3E-02
179B	4^{+3}_{-2}	0	2^{+0}_{-2}	5	3^{+0}_{-3}	5	$0.00^{+0.00}_{-0.00}$	-2	$0.10^{+0.07}_{-0.04}$	$0.06^{+0.00}_{-0.06}$	$0.06^{+0.00}_{-0.06}$	7E-01	5E-03
180	6^{+3}_{-2}	0	3^{+0}_{-3}	5	3^{+3}_{-1}	0	$0.06^{+0.94}_{-0.00}$	-1	$0.14^{+0.08}_{-0.05}$	$0.07^{+0.00}_{-0.07}$	$0.08^{+0.06}_{-0.04}$	1E+00	2E-06
181	4^{+3}_{-2}	0	3^{+3}_{-1}	0	2^{+0}_{-2}	5	$-0.22^{+0.00}_{-0.78}$	1	$0.10^{+0.07}_{-0.04}$	$0.08^{+0.06}_{-0.04}$	$0.05^{+0.00}_{-0.05}$	4E-01	1E-01
182	2^{+0}_{-2}	5	2^{+0}_{-2}	5	2^{+0}_{-2}	1	$0.00^{+0.00}_{-0.00}$	-2	$0.05^{+0.00}_{-0.05}$	$0.06^{+0.00}_{-0.06}$	$0.05^{+0.00}_{-0.05}$	-2E-02	1E+00
183	2^{+0}_{-2}	5	3^{+0}_{-3}	5	2^{+0}_{-2}	1	$0.00^{+0.00}_{-0.00}$	-2	$0.06^{+0.00}_{-0.06}$	$0.06^{+0.00}_{-0.06}$	$0.05^{+0.00}_{-0.05}$	-1E-02	1E+00
184B	6^{+3}_{-2}	0	4^{+3}_{-2}	0	3^{+0}_{-3}	5	$-0.19^{+0.00}_{-0.81}$	1	$0.14^{+0.08}_{-0.05}$	$0.10^{+0.07}_{-0.04}$	$0.07^{+0.00}_{-0.07}$	7E-01	3E-03
185	3^{+0}_{-3}	5	3^{+0}_{-3}	5	2^{+0}_{-2}	1	$0.00^{+0.00}_{-0.00}$	-2	$0.06^{+0.00}_{-0.06}$	$0.07^{+0.00}_{-0.07}$	$0.05^{+0.00}_{-0.05}$	-3E-02	1E+00
186	8^{+4}_{-2}	0	5^{+3}_{-2}	0	3^{+0}_{-3}	5	$-0.23^{+0.00}_{-0.77}$	1	$0.18^{+0.08}_{-0.06}$	$0.12^{+0.07}_{-0.05}$	$0.07^{+0.00}_{-0.07}$	1E+00	1E-04
187	3^{+0}_{-3}	5	2^{+0}_{-2}	1	5^{+0}_{-5}	5	$0.00^{+0.00}_{-0.00}$	-2	$0.08^{+0.00}_{-0.08}$	$0.05^{+0.00}_{-0.05}$	$0.11^{+0.00}_{-0.10}$	8E-01	1E-04
188	3^{+3}_{-1}	0	4^{+0}_{-4}	5	2^{+0}_{-2}	5	$0.00^{+0.00}_{-0.00}$	-2	$0.08^{+0.06}_{-0.04}$	$0.08^{+0.00}_{-0.08}$	$0.05^{+0.00}_{-0.05}$	3E-01	2E-01
189	3^{+0}_{-3}	5	3^{+0}_{-3}	5	2^{+0}_{-2}	1	$0.00^{+0.00}_{-0.00}$	-2	$0.06^{+0.00}_{-0.06}$	$0.07^{+0.00}_{-0.07}$	$0.05^{+0.00}_{-0.05}$	-2E-02	1E+00
190	2^{+0}_{-2}	5	2^{+0}_{-2}	5	2^{+0}_{-2}	1	$0.00^{+0.00}_{-0.00}$	-2	$0.05^{+0.00}_{-0.05}$	$0.05^{+0.00}_{-0.05}$	$0.05^{+0.00}_{-0.05}$	-2E-01	1E+00
191	14^{+4}_{-3}	0	2^{+0}_{-2}	1	14^{+4}_{-3}	0	$0.73^{+0.27}_{-0.00}$	-1	$0.29^{+0.10}_{-0.08}$	$0.05^{+0.00}_{-0.05}$	$0.30^{+0.08}_{-0.08}$	3E+00	7E-19
192	3^{+3}_{-1}	0	2^{+0}_{-2}	1	3^{+1}_{-1}	0	$0.26^{+0.74}_{-0.00}$	-1	$0.08^{+0.06}_{-0.04}$	$0.05^{+0.00}_{-0.05}$	$0.08^{+0.06}_{-0.04}$	1E+00	2E-06
193	21^{+5}_{-4}	0	13^{+4}_{-3}	0	8^{+4}_{-2}	0	$-0.27^{+0.24}_{-0.23}$	0	$0.44^{+0.12}_{-0.09}$	$0.28^{+0.10}_{-0.07}$	$0.16^{+0.08}_{-0.06}$	2E+00	8E-15
194	6^{+3}_{-2}	0	2^{+0}_{-2}	5	2^{+0}_{-2}	5	$0.00^{+0.00}_{-0.00}$	-2	$0.13^{+0.07}_{-0.05}$	$0.05^{+0.00}_{-0.05}$	$0.05^{+0.00}_{-0.05}$	1E+00	1E-03
195	3^{+0}_{-3}	5	3^{+0}_{-3}	5	2^{+0}_{-2}	5	$0.00^{+0.00}_{-0.00}$	-2	$0.07^{+0.00}_{-0.07}$	$0.07^{+0.00}_{-0.07}$	$0.06^{+0.00}_{-0.06}$	4E-01	5E-02
196	3^{+3}_{-1}	0	2^{+0}_{-2}	5	2^{+0}_{-2}	5	$0.00^{+0.00}_{-0.00}$	-2	$0.08^{+0.06}_{-0.04}$	$0.05^{+0.00}_{-0.05}$	$0.05^{+0.00}_{-0.05}$	6E-01	2E-01
197	2^{+0}_{-2}	5	2^{+0}_{-2}	5	2^{+0}_{-2}	5	$0.00^{+0.00}_{-0.00}$	-2	$0.05^{+0.00}_{-0.05}$	$0.05^{+0.00}_{-0.05}$	$0.05^{+0.00}_{-0.05}$	4E-01	3E-01
198	4^{+3}_{-2}	0	4^{+3}_{-1}	0	2^{+0}_{-2}	5	$-0.20^{+0.00}_{-0.80}$	1	$0.10^{+0.07}_{-0.04}$	$0.08^{+0.06}_{-0.04}$	$0.05^{+0.00}_{-0.05}$	4E-01	9E-02
199	3^{+3}_{-1}	0	2^{+0}_{-2}	1	4^{+3}_{-2}	0	$0.30^{+0.70}_{-0.00}$	-1	$0.08^{+0.06}_{-0.04}$	$0.05^{+0.00}_{-0.05}$	$0.09^{+0.07}_{-0.04}$	1E+00	1E-03
200	3^{+3}_{-1}	0	2^{+0}_{-2}	1	3^{+3}_{-1}	0	$0.25^{+0.75}_{-0.00}$	-1	$0.08^{+0.06}_{-0.04}$	$0.05^{+0.00}_{-0.05}$	$0.08^{+0.06}_{-0.04}$	1E+00	3E-05
201	11^{+4}_{-3}	0	4^{+3}_{-2}	0	7^{+3}_{-2}	0	$0.19^{+0.33}_{-0.35}$	0	$0.24^{+0.09}_{-0.07}$	$0.10^{+0.07}_{-0.04}$	$0.14^{+0.08}_{-0.05}$	2E+00	2E-05
202	2^{+0}_{-2}	5	2^{+0}_{-2}	5	2^{+0}_{-2}	5	$0.00^{+0.00}_{-0.00}$	-2	$0.05^{+0.00}_{-0.05}$	$0.05^{+0.00}_{-0.05}$	$0.05^{+0.00}_{-0.05}$	2E-01	4E-01
203	6^{+3}_{-2}	0	3^{+3}_{-1}	0	3^{+0}_{-3}	5	$-0.03^{+0.00}_{-0.97}$	1	$0.14^{+0.08}_{-0.05}$	$0.08^{+0.06}_{-0.04}$	$0.07^{+0.00}_{-0.07}$	1E+00	1E-04
204	89^{+10}_{-9}	0	71^{+9}_{-8}	0	17^{+5}_{-4}	0	$-0.60^{+0.10}_{-0.09}$	0	$1.81^{+0.21}_{-0.19}$	$1.45^{+0.19}_{-0.17}$	$0.36^{+0.11}_{-0.08}$	3E+00	2E-29
205	12^{+4}_{-3}	0	7^{+3}_{-2}	0	4^{+3}_{-2}	0	$-0.24^{+0.33}_{-0.31}$	0	$0.26^{+0.09}_{-0.07}$	$0.16^{+0.08}_{-0.06}$	$0.10^{+0.07}_{-0.04}$	1E+00	2E-06
206	22^{+5}_{-4}	0	17^{+5}_{-4}	0	5^{+3}_{-2}	0	$-0.56^{+0.22}_{-0.18}$	0	$0.46^{+0.12}_{-0.10}$	$0.36^{+0.11}_{-0.08}$	$0.10^{+0.07}_{-0.04}$	1E+00	1E-02
207	70^{+9}_{-8}	0	47^{+8}_{-6}	0	22^{+5}_{-4}	0	$-0.35^{+0.12}_{-0.12}$	0	$1.43^{+0.19}_{-0.17}$	$0.97^{+0.16}_{-0.14}$	$0.46^{+0.12}_{-0.10}$	4E+00	1E-36
208	8^{+4}_{-2}	0	4^{+0}_{-4}	5	5^{+3}_{-2}	0	$0.14^{+0.86}_{-0.00}$	-1	$0.18^{+0.08}_{-0.06}$	$0.09^{+0.00}_{-0.09}$	$0.12^{+0.07}_{-0.05}$	2E+00	8E-08
209	3^{+3}_{-1}	0	2^{+0}_{-2}	5	3^{+0}_{-3}	5	$0.00^{+0.00}_{-0.00}$	-2	$0.08^{+0.06}_{-0.04}$	$0.05^{+0.00}_{-0.05}$	$0.06^{+0.00}_{-0.06}$	1E+00	7E-04
210	4^{+3}_{-2}	0	2^{+0}_{-2}	5	4^{+3}_{-1}	0	$0.25^{+0.75}_{-0.00}$	-1	$0.09^{+0.07}_{-0.04}$	$0.05^{+0.00}_{-0.05}$	$0.08^{+0.06}_{-0.04}$	1E+00	5E-03
211	3^{+3}_{-1}	0	2^{+0}_{-2}	1	3^{+3}_{-1}	0	$0.26^{+0.74}_{-0.00}$	-1	$0.08^{+0.06}_{-0.04}$	$0.05^{+0.00}_{-0.05}$	$0.08^{+0.06}_{-0.04}$	1E+00	2E-06
212	8^{+4}_{-2}	0	3^{+3}_{-1}	0	5^{+3}_{-2}	0	$0.15^{+0.39}_{-0.41}$	0	$0.18^{+0.08}_{-0.06}$	$0.08^{+0.06}_{-0.04}$	$0.10^{+0.07}_{-0.04}$	1E+00	6E-04
213	2^{+0}_{-2}	5	3^{+0}_{-3}	5	2^{+0}_{-2}	1	$0.00^{+0.00}_{-0.00}$	-2	$0.05^{+0.00}_{-0.05}$	$0.07^{+0.00}_{-0.07}$	$0.05^{+0.00}_{-0.05}$	-1E-01	1E+00
214	5^{+3}_{-2}	0	3^{+0}_{-3}	5	2^{+0}_{-2}	5	$0.00^{+0.00}_{-0.00}$	-2	$0.12^{+0.07}_{-0.05}$	$0.06^{+0.00}_{-0.06}$	$0.06^{+0.00}_{-0.06}$	1E+00	9E-04
215	36^{+7}_{-6}	0	26^{+6}_{-5}	0	9^{+4}_{-3}	0	$-0.46^{+0.18}_{-0.16}$	0	$0.74^{+0.14}_{-0.12}$	$0.54^{+0.13}_{-0.10}$	$0.20^{+0.09}_{-0.06}$	2E+00	2E-04
216	2^{+0}_{-2}	5	2^{+0}_{-2}	1	3^{+0}_{-3}	5	$0.00^{+0.00}_{-0.00}$	-2	$0.06^{+0.00}_{-0.06}$	$0.05^{+0.00}_{-0.05}$	$0.06^{+0.00}_{-0.06}$	1E+00	3E-04
217	6^{+3}_{-2}	0	3^{+0}_{-3}	5	3^{+3}_{-1}	0	$0.12^{+0.88}_{-0.00}$	-1	$0.14^{+0.08}_{-0.05}$	$0.06^{+0.00}_{-0.06}$	$0.08^{+0.06}_{-0.04}$	1E+00	4E-05
218	2^{+0}_{-2}	5	2^{+0}_{-2}	1	3^{+0}_{-3}	5	$0.00^{+0.00}_{-0.00}$	-2	$0.05^{+0.00}_{-0.05}$	$0.05^{+0.00}_{-0.05}$	$0.06^{+0.00}_{-0.06}$	7E-01	3E-03
219	4^{+3}_{-2}	0	3^{+3}_{-1}	0	2^{+0}_{-2}	5	$-0.23^{+0.00}_{-0.77}$	1	$0.09^{+0.07}_{-0.04}$	$0.08^{+0.06}_{-0.04}$	$0.05^{+0.00}_{-0.05}$	3E-01	2E-01
220	5^{+3}_{-2}	0	3^{+0}_{-3}	5	2^{+0}_{-2}	5	$0.00^{+0.00}_{-0.00}$	-2	$0.11^{+0.07}_{-0.05}$	$0.06^{+0.00}_{-0.06}$	$0.05^{+0.00}_{-0.05}$	9E-01	2E-02
221	4^{+3}_{-2}	0	3^{+0}_{-3}	5	2^{+0}_{-2}	5	$0.00^{+0.00}_{-0.00}$	-2	$0.09^{+0.07}_{-0.04}$	$0.07^{+0.00}_{-0.07}$	$0.05^{+0.00}_{-0.05}$	9E-01	4E-03
222	9^{+4}_{-3}	0	2^{+0}_{-2}	1	10^{+4}_{-3}	0	$0.63^{+0.37}_{-0.00}$	-1	$0.20^{+0.09}_{-0.06}$	$0.05^{+0.00}_{-0.05}$	$0.21^{+0.09}_{-0.06}$	2E+00	6E-10

TABLE 27:

Counts, count rates and AE detection significance and no-source probabilities for X-ray point sources in HCG 90 (online only).

223	4 ⁺³ ₋₂	0	3 ⁺⁰ ₋₃	5	2 ⁺⁰ ₋₂	5	0.00 ^{+0.00} _{-0.00}	-2	0.09 ^{+0.07} _{-0.04}	0.06 ^{+0.00} _{-0.06}	0.05 ^{+0.00} _{-0.05}	7E-01	2E-02
224	60 ⁺⁸ ₋₇	0	44 ⁺⁷ ₋₆	0	15 ⁺⁵ ₋₃	0	-0.48 ^{+0.13} _{-0.12}	0	1.22 ^{+0.18} _{-0.16}	0.90 ^{+0.16} _{-0.13}	0.32 ^{+0.10} _{-0.08}	3E+00	5E-21
225	6 ⁺³ ₋₂	0	2 ⁺⁰ ₋₂	5	3 ⁺³ ₋₁	0	0.20 ^{+0.80} _{-0.00}	-1	0.12 ^{+0.07} _{-0.05}	0.05 ^{+0.00} _{-0.05}	0.07 ^{+0.06} _{-0.04}	1E+00	1E-02
226	18 ⁺⁵ ₋₄	0	14 ⁺⁴ ₋₃	0	2 ⁺⁰ ₋₂	5	-0.70 ^{+0.00} _{-0.30}	1	0.37 ^{+0.11} _{-0.09}	0.30 ^{+0.10} _{-0.08}	0.05 ^{+0.00} _{-0.05}	1E+00	1E-03
227	16 ⁺⁵ ₋₄	0	9 ⁺⁴ ₋₃	0	6 ⁺³ ₋₂	0	-0.18 ^{+0.29} _{-0.27}	0	0.34 ^{+0.10} _{-0.08}	0.20 ^{+0.09} _{-0.06}	0.14 ^{+0.08} _{-0.05}	2E+00	2E-09
228	12 ⁺⁴ ₋₃	0	8 ⁺⁴ ₋₂	0	3 ⁺³ ₋₁	0	-0.40 ^{+0.33} _{-0.28}	0	0.26 ^{+0.09} _{-0.07}	0.18 ^{+0.08} _{-0.06}	0.08 ^{+0.06} _{-0.04}	1E+00	5E-05
229	3 ⁺³ ₋₁	0	2 ⁺⁰ ₋₂	1	3 ⁺³ ₋₁	0	0.25 ^{+0.75} _{-0.00}	-1	0.07 ^{+0.06} _{-0.04}	0.05 ^{+0.00} _{-0.05}	0.08 ^{+0.06} _{-0.04}	1E+00	6E-05
230	6 ⁺³ ₋₂	0	5 ⁺³ ₋₂	0	2 ⁺⁰ ₋₂	5	-0.39 ^{+0.00} _{-0.61}	1	0.12 ^{+0.07} _{-0.05}	0.11 ^{+0.07} _{-0.05}	0.05 ^{+0.00} _{-0.05}	3E-01	4E-01
231	17 ⁺⁵ ₋₄	0	11 ⁺⁴ ₋₃	0	6 ⁺³ ₋₂	0	-0.23 ^{+0.27} _{-0.26}	0	0.36 ^{+0.11} _{-0.08}	0.22 ^{+0.09} _{-0.07}	0.14 ^{+0.08} _{-0.05}	2E+00	5E-04
232	2 ⁺⁰ ₋₂	5	2 ⁺⁰ ₋₂	5	2 ⁺⁰ ₋₂	1	0.00 ^{+0.00} _{-0.00}	-2	0.05 ^{+0.00} _{-0.05}	0.06 ^{+0.00} _{-0.06}	0.05 ^{+0.00} _{-0.05}	-3E-01	1E+00
233	54 ⁺⁸ ₋₇	0	38 ⁺⁷ ₋₆	0	15 ⁺⁵ ₋₃	0	-0.43 ^{+0.14} _{-0.13}	0	1.10 ^{+0.17} _{-0.15}	0.78 ^{+0.15} _{-0.13}	0.31 ^{+0.10} _{-0.08}	3E+00	1E-17
234	2 ⁺⁰ ₋₂	5	3 ⁺³ ₋₁	0	2 ⁺⁰ ₋₂	1	0.00 ^{+0.00} _{-0.00}	-2	0.05 ^{+0.00} _{-0.05}	0.07 ^{+0.06} _{-0.04}	0.05 ^{+0.00} _{-0.05}	-2E-01	1E+00
235	2 ⁺⁰ ₋₂	5	2 ⁺⁰ ₋₂	5	2 ⁺⁰ ₋₂	5	0.00 ^{+0.00} _{-0.00}	-2	0.05 ^{+0.00} _{-0.05}	0.05 ^{+0.00} _{-0.05}	0.05 ^{+0.00} _{-0.05}	5E-01	2E-01
236	181 ⁺¹⁴ ₋₁₃	0	167 ⁺¹⁴ ₋₁₂	0	14 ⁺⁴ ₋₃	0	-0.85 ^{+0.05} _{-0.04}	0	3.67 ^{+0.29} _{-0.27}	3.39 ^{+0.28} _{-0.26}	0.28 ^{+0.10} _{-0.07}	3E+00	8E-10
237	14 ⁺⁴ ₋₃	0	8 ⁺⁴ ₋₂	0	5 ⁺³ ₋₂	0	-0.26 ^{+0.31} _{-0.29}	0	0.29 ^{+0.10} _{-0.08}	0.18 ^{+0.08} _{-0.06}	0.11 ^{+0.07} _{-0.04}	1E+00	2E-03
238	8 ⁺⁴ ₋₂	0	4 ⁺³ ₋₂	0	2 ⁺⁰ ₋₂	5	-0.30 ^{+0.00} _{-0.70}	1	0.16 ^{+0.06} _{-0.11}	0.09 ^{+0.04} _{-0.04}	0.05 ^{+0.00} _{-0.05}	1E+00	4E-03
239	2 ⁺⁰ ₋₂	5	2 ⁺⁰ ₋₂	1	2 ⁺⁰ ₋₂	5	0.00 ^{+0.00} _{-0.00}	-2	0.05 ^{+0.00} _{-0.05}	0.05 ^{+0.00} _{-0.05}	0.05 ^{+0.00} _{-0.05}	5E-01	2E-01
240	11 ⁺⁴ ₋₃	0	4 ⁺² ₋₂	0	7 ⁺³ ₋₂	0	0.21 ^{+0.33} _{-0.35}	0	0.23 ^{+0.07} _{-0.07}	0.09 ^{+0.07} _{-0.04}	0.14 ^{+0.08} _{-0.05}	2E+00	2E-05
241	12 ⁺⁴ ₋₃	0	9 ⁺⁴ ₋₃	0	2 ⁺⁰ ₋₂	5	-0.61 ^{+0.00} _{-0.39}	1	0.26 ^{+0.09} _{-0.07}	0.20 ^{+0.09} _{-0.06}	0.05 ^{+0.00} _{-0.05}	9E-01	5E-02
242	28 ⁺⁶ ₋₅	0	23 ⁺⁵ ₋₄	0	5 ⁺³ ₋₂	0	-0.63 ^{+0.19} _{-0.15}	0	0.58 ^{+0.13} _{-0.11}	0.47 ^{+0.12} _{-0.10}	0.11 ^{+0.07} _{-0.05}	1E+00	2E-03
243	27 ⁺⁶ ₋₅	0	17 ⁺⁵ ₋₄	0	9 ⁺⁴ ₋₃	0	-0.30 ^{+0.22} _{-0.20}	0	0.55 ^{+0.13} _{-0.10}	0.36 ^{+0.11} _{-0.08}	0.19 ^{+0.08} _{-0.06}	2E+00	8E-10
244	2 ⁺⁰ ₋₂	5	2 ⁺⁰ ₋₂	1	2 ⁺⁰ ₋₂	5	0.00 ^{+0.00} _{-0.00}	-2	0.05 ^{+0.00} _{-0.05}	0.05 ^{+0.00} _{-0.05}	0.05 ^{+0.00} _{-0.05}	9E-01	4E-02
245	5 ⁺³ ₋₂	0	2 ⁺⁰ ₋₂	1	5 ⁺³ ₋₂	0	0.42 ^{+0.58} _{-0.00}	-1	0.10 ^{+0.07} _{-0.04}	0.05 ^{+0.00} _{-0.05}	0.11 ^{+0.07} _{-0.05}	1E+00	8E-03
246	4 ⁺³ ₋₁	0	2 ⁺⁰ ₋₂	5	2 ⁺⁰ ₋₂	5	0.00 ^{+0.00} _{-0.00}	-2	0.08 ^{+0.06} _{-0.04}	0.05 ^{+0.00} _{-0.05}	0.05 ^{+0.00} _{-0.05}	5E-01	2E-01
247	2 ⁺⁰ ₋₂	5	2 ⁺⁰ ₋₂	5	2 ⁺⁰ ₋₂	5	0.00 ^{+0.00} _{-0.00}	-2	0.05 ^{+0.00} _{-0.05}	0.05 ^{+0.00} _{-0.05}	0.05 ^{+0.00} _{-0.05}	8E-01	4E-02
248	12 ⁺⁴ ₋₃	0	4 ⁺³ ₋₁	0	8 ⁺⁴ ₋₂	0	0.34 ^{+0.30} _{-0.34}	0	0.25 ^{+0.09} _{-0.07}	0.08 ^{+0.06} _{-0.04}	0.17 ^{+0.08} _{-0.06}	2E+00	2E-05
249	20 ⁺⁵ ₋₄	0	15 ⁺⁵ ₋₃	0	5 ⁺³ ₋₂	0	-0.48 ^{+0.25} _{-0.21}	0	0.41 ^{+0.11} _{-0.09}	0.30 ^{+0.10} _{-0.08}	0.11 ^{+0.07} _{-0.04}	1E+00	4E-02
250	10 ⁺⁴ ₋₃	0	10 ⁺⁴ ₋₃	0	2 ⁺⁰ ₋₂	1	-0.64 ^{+0.00} _{-0.36}	1	0.21 ^{+0.09} _{-0.06}	0.22 ^{+0.09} _{-0.06}	0.05 ^{+0.00} _{-0.05}	-4E-02	6E-01
251	335 ⁺¹⁹ ₋₁₈	0	246 ⁺¹⁶ ₋₁₅	0	89 ⁺¹⁰ ₋₉	0	-0.47 ^{+0.05} _{-0.05}	0	6.77 ^{+0.39} _{-0.37}	4.97 ^{+0.34} _{-0.32}	1.80 ^{+0.21} _{-0.19}	8E+00	0E+00
252	11 ⁺⁴ ₋₃	0	9 ⁺⁴ ₋₃	0	2 ⁺⁰ ₋₂	5	-0.58 ^{+0.00} _{-0.42}	1	0.24 ^{+0.09} _{-0.07}	0.18 ^{+0.08} _{-0.06}	0.05 ^{+0.00} _{-0.05}	8E-01	7E-02
253	81 ⁺¹⁰ ₋₉	0	63 ⁺⁹ ₋₈	0	17 ⁺⁵ ₋₄	0	-0.57 ^{+0.11} _{-0.09}	0	1.65 ^{+0.20} _{-0.18}	1.29 ^{+0.18} _{-0.16}	0.36 ^{+0.11} _{-0.08}	3E+00	2E-12
254	64 ⁺⁹ ₋₈	0	40 ⁺⁷ ₋₆	0	23 ⁺⁶ ₋₄	0	-0.26 ^{+0.13} _{-0.13}	0	1.30 ^{+0.18} _{-0.16}	0.82 ^{+0.15} _{-0.13}	0.48 ^{+0.12} _{-0.10}	4E+00	2E-18
255	32 ⁺⁶ ₋₅	0	23 ⁺⁵ ₋₄	0	9 ⁺⁴ ₋₃	0	-0.44 ^{+0.19} _{-0.17}	0	0.66 ^{+0.14} _{-0.11}	0.47 ^{+0.12} _{-0.10}	0.18 ^{+0.08} _{-0.06}	2E+00	7E-05
256	63 ⁺⁹ ₋₈	0	57 ⁺⁸ ₋₇	0	6 ⁺³ ₋₂	0	-0.80 ^{+0.10} _{-0.08}	0	1.29 ^{+0.18} _{-0.16}	1.16 ^{+0.17} _{-0.15}	0.13 ^{+0.07} _{-0.05}	2E+00	4E-03

TABLE 28:

Counts, count rates and AE detection significance and no-source probabilities for X-ray point sources in HCG 92 (online only).

ID (1)	c(FB) (2)	lim _F (3)	c(SB) (4)	lim _S (5)	c(HB) (6)	lim _S (7)	HR (8)	lim _{HR} (9)	cr(FB) (10)	cr(SB) (11)	cr(HB) (12)	AE(sig) (13)	AE(<i>P</i>) (14)
1	4 ⁺³ ₋₂	0	3 ⁺³ ₋₁	0	2 ⁺⁰ ₋₂	5	-0.24 ^{+0.00} _{-0.76}	1	0.04 ^{+0.03} _{-0.06}	0.03 ^{+0.03} _{-0.02}	0.02 ^{+0.00} _{-0.02}	3E-01	3E-01
2	2 ⁺⁰ ₋₂	5	3 ⁺³ ₋₁	0	2 ⁺⁰ ₋₂	1	0.00 ^{+0.00} _{-0.00}	-2	0.02 ^{+0.06} _{-0.02}	0.03 ^{+0.03} _{-0.02}	0.02 ^{+0.00} _{-0.02}	-2E-01	1E+00
3	6 ⁺³ ₋₂	0	3 ⁺³ ₋₁	0	2 ⁺⁰ ₋₂	5	-0.22 ^{+0.00} _{-0.78}	1	0.06 ^{+0.03} _{-0.02}	0.03 ^{+0.03} _{-0.02}	0.02 ^{+0.00} _{-0.02}	9E-01	1E-02
4	12 ⁺⁴ ₋₃	0	2 ⁺⁰ ₋₂	5	10 ⁺⁴ ₋₃	0	0.63 ^{+0.37} _{-0.00}	-1	0.11 ^{+0.04} _{-0.03}	0.02 ^{+0.00} _{-0.02}	0.09 ^{+0.04} _{-0.03}	2E+00	6E-12
5	4 ⁺³ ₋₂	0	3 ⁺³ ₋₁	0	2 ⁺⁰ ₋₂	5	-0.24 ^{+0.00} _{-0.76}	1	0.04 ^{+0.03} _{-0.02}	0.03 ^{+0.03} _{-0.02}	0.02 ^{+0.00} _{-0.02}	2E-01	4E-01
6	8 ⁺⁴ ₋₂	0	3 ⁺³ ₋₁	0	4 ⁺³ ₋₂	0	0.09 ^{+0.41} _{-0.43}	0	0.07 ^{+0.04} _{-0.02}	0.03 ^{+0.03} _{-0.02}	0.04 ^{+0.03} _{-0.02}	1E+00	3E-04
7	6 ⁺³ ₋₂	0	2 ⁺⁰ ₋₂	5	4 ⁺³ ₋₂	0	0.27 ^{+0.73} _{-0.00}	-1	0.06 ^{+0.03} _{-0.02}	0.02 ^{+0.00} _{-0.02}	0.04 ^{+0.03} _{-0.02}	1E+00	1E-03
8	2 ⁺⁰ ₋₂	5	2 ⁺⁰ ₋₂	5	2 ⁺⁰ ₋₂	1	0.00 ^{+0.00} _{-0.00}	-2	0.02 ^{+0.00} _{-0.02}	0.02 ^{+0.00} _{-0.02}	0.02 ^{+0.00} _{-0.02}	-1E-01	1E+00
9	7 ⁺³ ₋₂	0	6 ⁺³ ₋₂	0	2 ⁺⁰ ₋₂	5	-0.47 ^{+0.00} _{-0.53}	1	0.07 ^{+0.03} _{-0.02}	0.06 ^{+0.03} _{-0.02}	0.02 ^{+0.00} _{-0.02}	5E-01	2E-01
10	33 ⁺⁶ ₋₅	0	20 ⁺⁵ ₋₄	0	12 ⁺⁴ ₋₃	0	-0.25 ^{+0.19} _{-0.18}	0	0.29 ^{+0.06} _{-0.05}	0.18 ^{+0.05} _{-0.04}	0.11 ^{+0.04} _{-0.03}	3E+00	4E-14
11	6 ⁺³ ₋₂	0	5 ⁺³ ₋₂	0	2 ⁺⁰ ₋₂	5	-0.42 ^{+0.00} _{-0.58}	1	0.06 ^{+0.03} _{-0.02}	0.05 ^{+0.03} _{-0.02}	0.02 ^{+0.00} _{-0.02}	3E-01	3E-01
12	2 ⁺⁰ ₋₂	5	2 ⁺⁰ ₋₂	1	2 ⁺⁰ ₋₂	5	0.00 ^{+0.00} _{-0.00}	-2	0.02 ^{+0.00} _{-0.02}	0.02 ^{+0.00} _{-0.02}	0.02 ^{+0.00} _{-0.02}	9E-01	2E-03
13	13 ⁺⁴ ₋₃	0	7 ⁺³ ₋₂	0	5 ⁺³ ₋₂	0	-0.15 ^{+0.32} _{-0.31}	0	0.12 ^{+0.03} _{-0.02}	0.07 ^{+0.03} _{-0.02}	0.05 ^{+0.03} _{-0.02}	2E+00	2E-06
14	5 ⁺³ ₋₂	0	2 ⁺⁰ ₋₂	5	4 ⁺³ ₋₂	0	0.33 ^{+0.67} _{-0.00}	-1	0.05 ^{+0.03} _{-0.02}	0.02 ^{+0.00} _{-0.02}	0.04 ^{+0.03} _{-0.02}	1E+00	2E-05
15	2 ⁺⁰ ₋₂	5	2 ⁺⁰ ₋₂	1	2 ⁺⁰ ₋₂	5	0.00 ^{+0.00} _{-0.00}	-2	0.02 ^{+0.00} _{-0.02}	0.02 ^{+0.00} _{-0.02}	0.02 ^{+0.00} _{-0.02}	9E-01	1E-02
16	2 ⁺⁰ ₋₂	5	2 ⁺⁰ ₋₂	1	2 ⁺⁰ ₋₂	5	0.00 ^{+0.00} _{-0.00}	-2	0.02 ^{+0.00} _{-0.02}	0.02 ^{+0.00} _{-0.02}	0.02 ^{+0.00} _{-0.02}	9E-01	4E-03
17	4 ⁺³ ₋₂	0	2 ⁺⁰ ₋₂	5	2 ⁺⁰ ₋₂	5	0.00 ^{+0.00} _{-0.00}	-2	0.04 ^{+0.03} _{-0.02}	0.02 ^{+0.00} _{-0.02}	0.02 ^{+0.00} _{-0.02}	6E-01	8E-02
18	16 ⁺⁵ ₋₄	0	10 ⁺⁴ ₋₃	0	6 ⁺³ ₋₂	0	-0.22 ^{+0.29} _{-0.27}	0	0.15 ^{+0.05} _{-0.04}	0.09 ^{+0.04} _{-0.03}	0.06 ^{+0.03} _{-0.02}	2E+00	3E-04
19	35 ⁺⁷ ₋₆	0	19 ⁺⁵ ₋₄	0	16 ⁺⁵ ₋₄	0	-0.10 ^{+0.19} _{-0.18}	0	0.32 ^{+0.06} _{-0.05}	0.17 ^{+0.05} _{-0.04}	0.14 ^{+0.05} _{-0.04}	3E+00	3E-16
20	4 ⁺³ ₋₂	0	4 ⁺³ ₋₂	0	2 ⁺⁰ ₋₂	1	-0.30 ^{+0.00} _{-0.70}	1	0.04 ^{+0.03} _{-0.02}	0.04 ^{+0.03} _{-0.02}	0.02 ^{+0.00} _{-0.02}	-6E-02	7E-01
21	347 ⁺¹⁹ ₋₁₈	0	276 ⁺¹⁷ ₋₁₆	0	70 ⁺⁹ ₋₈	0	-0.59 ^{+0.05} _{-0.04}	0	3.08 ^{+0.17} _{-0.17}	2.45 ^{+0.16} _{-0.15}	0.63 ^{+0.08} _{-0.07}	7E+00	0E+00
22E	40 ⁺⁷ ₋₆	0	33 ⁺⁶ ₋₅	0	6 ⁺³ ₋₂	0	-0.69 ^{+0.15} _{-0.12}	0	0.36 ^{+0.07} _{-0.06}	0.30 ^{+0.06} _{-0.05}	0.06 ^{+0.03} _{-0.02}	2E+00	2E-05
23E	6 ⁺³ ₋₂	0	5 ⁺³ ₋₂	0	2 ⁺⁰ ₋₂	5	-0.35 ^{+0.00} _{-0.65}	1	0.06 ^{+0.03} _{-0.02}	0.04 ^{+0.03} _{-0.02}	0.02 ^{+0.00} _{-0.02}	5E-01	2E-01
24	2 ⁺⁰ ₋₂	5	2 ⁺⁰ ₋₂	5	2 ⁺⁰ ₋₂	5	0.00 ^{+0.00} _{-0.00}	-2	0.02 ^{+0.00} _{-0.02}	0.02 ^{+0.00} _{-0.02}	0.02 ^{+0.00} _{-0.02}	5E-01	1E-01
25	22 ⁺⁵ ₋₄	0	14 ⁺⁴ ₋₃	0	7 ⁺³ ₋₂	0	-0.30 ^{+0.24} _{-0.22}	0	0.20 ^{+0.05} _{-0.04}	0.13 ^{+0.04} _{-0.03}	0.07 ^{+0.03} _{-0.02}	2E+00	9E-06
26	159 ⁺¹³ ₋₁₂	0	106 ⁺¹¹ ₋₁₀	0	52 ⁺⁸ ₋₇	0	-0.34 ^{+0.08} _{-0.08}	0	1.41 ^{+0.12} _{-0.11}	0.95 ^{+0.10} _{-0.09}	0.47 ^{+0.07} _{-0.06}	6E+00	0E+00
27	20 ⁺⁵ ₋₄	0	12 ⁺⁴ ₋₃	0	7 ⁺³ ₋₂	0	-0.28 ^{+0.26} _{-0.24}	0	0.18 ^{+0.05} _{-0.04}	0.11 ^{+0.04} _{-0.03}	0.06 ^{+0.03} _{-0.02}	2E+00	3E-06
28	15 ⁺⁵ ₋₃	0	12 ⁺⁴ ₋₃	0	2 ⁺⁰ ₋₂	5	-0.68 ^{+0.00} _{-0.32}	1	0.13 ^{+0.04} _{-0.03}	0.11 ^{+0.04} _{-0.03}	0.02 ^{+0.00} _{-0.02}	8E-01	2E-02
29	9 ⁺⁴ ₋₃	0	8 ⁺⁴ ₋₂	0	2 ⁺⁰ ₋₂	5	-0.57 ^{+0.00} _{-0.43}	1	0.08 ^{+0.04} _{-0.03}	0.08 ^{+0.04} _{-0.03}	0.02 ^{+0.00} _{-0.02}	3E-01	2E-01
30	2 ⁺⁰ ₋₂	5	2 ⁺⁰ ₋₂	1	2 ⁺⁰ ₋₂	5	0.00 ^{+0.00} _{-0.00}	-2	0.02 ^{+0.00} _{-0.02}	0.02 ^{+0.00} _{-0.02}	0.02 ^{+0.00} _{-0.02}	9E-01	3E-03
31	525 ⁺²³ ₋₂₂	0	390 ⁺²⁰ ₋₁₉	0	135 ⁺¹² ₋₁₁	0	-0.48 ^{+0.04} _{-0.04}	0	4.66 ^{+0.21} _{-0.20}	3.46 ^{+0.18} _{-0.17}	1.20 ^{+0.11} _{-0.10}	1E+01	0E+00
32	7 ⁺³ ₋₂	0	7 ⁺³ ₋₂	0	2 ⁺⁰ ₋₂	1	-0.52 ^{+0.00} _{-0.48}	1	0.06 ^{+0.03} _{-0.02}	0.07 ^{+0.03} _{-0.02}	0.02 ^{+0.00} _{-0.02}	-1E-01	1E+00
33	2 ⁺⁰ ₋₂	5	2 ⁺⁰ ₋₂	5	2 ⁺⁰ ₋₂	1	0.00 ^{+0.00} _{-0.00}	-2	0.02 ^{+0.00} _{-0.02}	0.02 ^{+0.00} _{-0.02}	0.02 ^{+0.00} _{-0.02}	-1E-01	1E+00
34	5 ⁺³ ₋₂	0	3 ⁺³ ₋₁	0	2 ⁺⁰ ₋₂	5	-0.21 ^{+0.00} _{-0.79}	1	0.05 ^{+0.03} _{-0.02}	0.03 ^{+0.03} _{-0.02}	0.02 ^{+0.00} _{-0.02}	6E-01	7E-02
35	15 ⁺⁵ ₋₃	0	11 ⁺⁴ ₋₃	0	4 ⁺³ ₋₂	0	-0.45 ^{+0.29} _{-0.24}	0	0.14 ^{+0.05} _{-0.03}	0.10 ^{+0.04} _{-0.03}	0.04 ^{+0.03} _{-0.02}	1E+00	6E-04
36D	75 ⁺⁹ ₋₈	0	67 ⁺⁹ ₋₈	0	8 ⁺⁴ ₋₂	0	-0.78 ^{+0.09} _{-0.07}	0	0.67 ^{+0.09} _{-0.08}	0.60 ^{+0.08} _{-0.07}	0.07 ^{+0.04} _{-0.02}	2E+00	9E-08
37	4 ⁺³ ₋₂	0	2 ⁺⁰ ₋₂	5	2 ⁺⁰ ₋₂	5	0.00 ^{+0.00} _{-0.00}	-2	0.04 ^{+0.03} _{-0.02}	0.02 ^{+0.00} _{-0.02}	0.02 ^{+0.00} _{-0.02}	1E+00	1E-03
38	6 ⁺³ ₋₂	0	2 ⁺⁰ ₋₂	5	4 ⁺³ ₋₂	0	0.33 ^{+0.67} _{-0.00}	-1	0.06 ^{+0.03} _{-0.02}	0.02 ^{+0.00} _{-0.02}	0.04 ^{+0.03} _{-0.02}	1E+00	2E-05
39	12 ⁺⁴ ₋₃	0	10 ⁺⁴ ₋₃	0	2 ⁺⁰ ₋₂	5	-0.63 ^{+0.00} _{-0.37}	1	0.11 ^{+0.04} _{-0.03}	0.09 ^{+0.04} _{-0.03}	0.02 ^{+0.00} _{-0.02}	6E-01	6E-02
40D	17 ⁺⁵ ₋₄	0	16 ⁺⁵ ₋₄	0	2 ⁺⁰ ₋₂	5	-0.75 ^{+0.00} _{-0.25}	1	0.15 ^{+0.05} _{-0.04}	0.15 ^{+0.05} _{-0.04}	0.02 ^{+0.00} _{-0.02}	2E-01	5E-01
41	17 ⁺⁵ ₋₄	0	15 ⁺⁵ ₋₃	0	2 ⁺⁰ ₋₂	5	-0.73 ^{+0.00} _{-0.27}	1	0.15 ^{+0.05} _{-0.04}	0.14 ^{+0.04} _{-0.03}	0.02 ^{+0.00} _{-0.02}	6E-01	8E-02
42	75 ⁺⁹ ₋₈	0	50 ⁺⁸ ₋₇	0	24 ⁺⁶ ₋₄	0	-0.35 _{-0.11}	0	0.67 _{-0.08}	0.45 _{-0.06}	0.22 _{-0.04}	4E+00	2E-32

TABLE 28:

Counts, count rates and AE detection significance and no-source probabilities for X-ray point sources in HCG 92 (online only).

43	4 ⁺³ ₋₂	0	4 ⁺³ ₋₂	0	2 ⁺⁰ ₋₂	1	-0.34 ^{+0.00} _{-0.66}	1	0.04 ^{+0.03} _{-0.02}	0.04 ^{+0.03} _{-0.02}	0.02 ^{+0.00} _{-0.02}	-3E-01	1E+00
44	12 ⁺⁴ ₋₃	0	2 ⁺⁰ ₋₂	5	8 ⁺⁴ ₋₂	0	0.55 ^{+0.45} _{-0.00}	-1	0.11 ^{+0.04} _{-0.03}	0.02 ^{+0.00} _{-0.02}	0.08 ^{+0.04} _{-0.03}	2E+00	2E-06
45B	12 ⁺⁴ ₋₃	0	11 ⁺⁴ ₋₃	0	2 ⁺⁰ ₋₂	5	-0.66 ^{+0.00} _{-0.34}	1	0.11 ^{+0.04} _{-0.03}	0.10 ^{+0.04} _{-0.03}	0.02 ^{+0.00} _{-0.02}	2E-01	4E-01
46B	19 ⁺⁵ ₋₄	0	14 ⁺⁴ ₋₃	0	4 ⁺³ ₋₂	0	-0.53 ^{+0.25} _{-0.21}	0	0.17 ^{+0.05} _{-0.04}	0.13 ^{+0.04} _{-0.03}	0.04 ^{+0.03} _{-0.02}	1E+00	2E-04
47	4 ⁺³ ₋₂	0	2 ⁺⁰ ₋₂	5	2 ⁺⁰ ₋₂	5	0.00 ^{+0.00} _{-0.00}	-2	0.04 ^{+0.03} _{-0.02}	0.02 ^{+0.00} _{-0.02}	0.02 ^{+0.00} _{-0.02}	8E-01	5E-02
48	2 ⁺⁰ ₋₂	5	3 ⁺³ ₋₁	0	2 ⁺⁰ ₋₂	1	0.00 ^{+0.00} _{-0.00}	-2	0.02 ^{+0.00} _{-0.02}	0.03 ^{+0.03} _{-0.02}	0.02 ^{+0.00} _{-0.02}	-2E-01	1E+00
49	21 ⁺⁵ ₋₄	0	16 ⁺⁵ ₋₄	0	5 ⁺³ ₋₂	0	-0.50 ^{+0.24} _{-0.20}	0	0.19 ^{+0.05} _{-0.04}	0.14 ^{+0.05} _{-0.04}	0.05 ^{+0.03} _{-0.02}	1E+00	7E-05
50	4 ⁺³ ₋₂	0	2 ⁺⁰ ₋₂	5	2 ⁺⁰ ₋₂	5	0.00 ^{+0.00} _{-0.00}	-2	0.04 ^{+0.03} _{-0.02}	0.02 ^{+0.00} _{-0.02}	0.02 ^{+0.00} _{-0.02}	6E-01	8E-02
51	18 ⁺⁵ ₋₄	0	9 ⁺⁴ ₋₃	0	8 ⁺⁴ ₋₂	0	-0.04 ^{+0.27} _{-0.27}	0	0.16 ^{+0.05} _{-0.04}	0.08 ^{+0.04} _{-0.03}	0.08 ^{+0.04} _{-0.03}	2E+00	5E-10
52	32 ⁺⁶ ₋₅	0	11 ⁺⁴ ₋₃	0	21 ⁺⁵ ₋₄	0	0.30 ^{+0.18} _{-0.19}	0	0.29 ^{+0.06} _{-0.05}	0.10 ^{+0.04} _{-0.03}	0.19 ^{+0.05} _{-0.04}	4E+00	3E-25
53	9 ⁺⁴ ₋₃	0	8 ⁺³ ₋₂	0	2 ⁺⁰ ₋₂	5	-0.47 ^{+0.00} _{-0.53}	1	0.08 ^{+0.04} _{-0.03}	0.07 ^{+0.03} _{-0.02}	0.03 ^{+0.00} _{-0.03}	5E-01	1E-01
54	9 ⁺⁴ ₋₃	0	8 ⁺⁴ ₋₂	0	2 ⁺⁰ ₋₂	5	-0.50 ^{+0.00} _{-0.50}	1	0.08 ^{+0.04} _{-0.03}	0.07 ^{+0.04} _{-0.02}	0.02 ^{+0.00} _{-0.02}	5E-01	1E-01
55	2 ⁺⁰ ₋₂	5	2 ⁺⁰ ₋₂	5	2 ⁺⁰ ₋₂	1	0.00 ^{+0.00} _{-0.00}	-2	0.02 ^{+0.00} _{-0.02}	0.02 ^{+0.00} _{-0.02}	0.02 ^{+0.00} _{-0.02}	-4E-01	1E+00
56	9 ⁺⁴ ₋₃	0	2 ⁺⁰ ₋₂	5	6 ⁺³ ₋₂	0	0.46 ^{+0.54} _{-0.00}	-1	0.09 ^{+0.04} _{-0.03}	0.02 ^{+0.00} _{-0.02}	0.06 ^{+0.03} _{-0.02}	2E+00	4E-06
57	8 ⁺⁴ ₋₂	0	8 ⁺⁴ ₋₂	0	2 ⁺⁰ ₋₂	5	-0.52 ^{+0.00} _{-0.48}	1	0.07 ^{+0.04} _{-0.02}	0.07 ^{+0.04} _{-0.02}	0.02 ^{+0.00} _{-0.02}	1E-01	5E-01
58	7 ⁺³ ₋₂	0	6 ⁺³ ₋₂	0	2 ⁺⁰ ₋₂	5	-0.46 ^{+0.00} _{-0.54}	1	0.06 ^{+0.03} _{-0.02}	0.06 ^{+0.03} _{-0.02}	0.02 ^{+0.00} _{-0.02}	2E-01	4E-01
59	7 ⁺² ₋₂	0	8 ⁺⁴ ₋₂	0	2 ⁺⁰ ₋₂	1	-0.57 ^{+0.00} _{-0.43}	1	0.07 ^{+0.03} _{-0.02}	0.07 ^{+0.04} _{-0.02}	0.02 ^{+0.00} _{-0.02}	-4E-01	1E+00
60	24 ⁺⁶ ₋₄	0	24 ⁺⁶ ₋₄	0	2 ⁺⁰ ₋₂	5	-0.82 ^{+0.00} _{-0.18}	1	0.22 ^{+0.05} _{-0.04}	0.21 ^{+0.05} _{-0.04}	0.02 ^{+0.00} _{-0.02}	1E-01	5E-01
61	7 ⁺³ ₋₂	0	8 ⁺⁴ ₋₂	0	2 ⁺⁰ ₋₂	1	-0.55 ^{+0.00} _{-0.45}	1	0.07 ^{+0.03} _{-0.02}	0.07 ^{+0.04} _{-0.02}	0.02 ^{+0.00} _{-0.02}	-2E-01	1E+00
62	8 ⁺⁴ ₋₂	0	7 ⁺³ ₋₂	0	2 ⁺⁰ ₋₂	5	-0.43 ^{+0.00} _{-0.57}	1	0.08 ^{+0.04} _{-0.03}	0.06 ^{+0.03} _{-0.02}	0.03 ^{+0.00} _{-0.03}	6E-01	1E-01
63	2 ⁺⁰ ₋₂	5	2 ⁺⁰ ₋₂	5	2 ⁺⁰ ₋₂	1	0.00 ^{+0.00} _{-0.00}	-2	0.02 ^{+0.00} _{-0.02}	0.02 ^{+0.00} _{-0.02}	0.02 ^{+0.00} _{-0.02}	-2E-01	1E+00
64	13 ⁺⁴ ₋₃	0	12 ⁺⁴ ₋₃	0	2 ⁺⁰ ₋₂	5	-0.68 ^{+0.00} _{-0.32}	1	0.12 ^{+0.04} _{-0.03}	0.11 ^{+0.04} _{-0.03}	0.02 ^{+0.00} _{-0.02}	1E-01	5E-01
65	11 ⁺⁴ ₋₃	0	11 ⁺⁴ ₋₃	0	2 ⁺⁰ ₋₂	5	-0.63 ^{+0.00} _{-0.37}	1	0.10 ^{+0.04} _{-0.03}	0.10 ^{+0.04} _{-0.03}	0.02 ^{+0.00} _{-0.02}	2E-01	4E-01
66	2 ⁺⁰ ₋₂	5	2 ⁺⁰ ₋₂	1	2 ⁺⁰ ₋₂	5	0.00 ^{+0.00} _{-0.00}	-2	0.02 ^{+0.00} _{-0.02}	0.02 ^{+0.00} _{-0.02}	0.02 ^{+0.00} _{-0.02}	1E+00	2E-03
67	5 ⁺³ ₋₂	0	2 ⁺⁰ ₋₂	5	2 ⁺⁰ ₋₂	5	0.00 ^{+0.00} _{-0.00}	-2	0.05 ^{+0.03} _{-0.02}	0.02 ^{+0.00} _{-0.02}	0.02 ^{+0.00} _{-0.02}	9E-01	1E-02
68	13 ⁺⁴ ₋₃	0	12 ⁺⁴ ₋₃	0	2 ⁺⁰ ₋₂	5	-0.64 ^{+0.00} _{-0.36}	1	0.12 ^{+0.04} _{-0.03}	0.11 ^{+0.04} _{-0.03}	0.02 ^{+0.00} _{-0.02}	5E-01	2E-01
69	17 ⁺⁵ ₋₄	0	3 ⁺³ ₋₁	0	13 ⁺⁴ ₋₃	0	0.58 ^{+0.21} _{-0.27}	0	0.15 ^{+0.05} _{-0.04}	0.03 ^{+0.03} _{-0.02}	0.12 ^{+0.04} _{-0.03}	3E+00	6E-16
70	9 ⁺⁴ ₋₃	0	10 ⁺⁴ ₋₃	0	2 ⁺⁰ ₋₂	1	-0.63 ^{+0.00} _{-0.37}	1	0.09 ^{+0.04} _{-0.03}	0.09 ^{+0.04} _{-0.03}	0.02 ^{+0.00} _{-0.02}	-3E-01	1E+00
71	8 ⁺⁴ ₋₂	0	7 ⁺³ ₋₂	0	2 ⁺⁰ ₋₂	5	-0.51 ^{+0.00} _{-0.49}	1	0.08 ^{+0.04} _{-0.03}	0.07 ^{+0.03} _{-0.02}	0.02 ^{+0.00} _{-0.02}	4E-01	3E-01
72	4 ⁺³ ₋₂	0	2 ⁺⁰ ₋₂	5	2 ⁺⁰ ₋₂	5	0.00 ^{+0.00} _{-0.00}	-2	0.04 ^{+0.03} _{-0.02}	0.02 ^{+0.00} _{-0.02}	0.02 ^{+0.00} _{-0.02}	9E-01	3E-02
73	113 ⁺¹¹ ₋₁₀	0	85 ⁺¹⁰ ₋₉	0	27 ⁺⁶ ₋₅	0	-0.52 ^{+0.09} _{-0.08}	0	1.00 ^{+0.10} _{-0.09}	0.76 ^{+0.09} _{-0.08}	0.24 ^{+0.06} _{-0.05}	4E+00	4E-29
74	22 ⁺⁵ ₋₄	0	17 ⁺⁵ ₋₄	0	4 ⁺³ ₋₂	0	-0.59 ^{+0.22} _{-0.18}	0	0.20 ^{+0.05} _{-0.04}	0.16 ^{+0.05} _{-0.04}	0.04 ^{+0.03} _{-0.02}	1E+00	3E-04
75	5 ⁺³ ₋₂	0	2 ⁺⁰ ₋₂	5	5 ⁺³ ₋₂	0	0.40 ^{+0.60} _{-0.00}	-1	0.05 ^{+0.03} _{-0.02}	0.02 ^{+0.00} _{-0.02}	0.05 ^{+0.03} _{-0.02}	1E+00	2E-03
76	6 ⁺³ ₋₂	0	5 ⁺³ ₋₂	0	2 ⁺⁰ ₋₂	5	-0.37 ^{+0.00} _{-0.63}	1	0.05 ^{+0.03} _{-0.02}	0.05 ^{+0.02} _{-0.02}	0.02 ^{+0.00} _{-0.02}	3E-01	3E-01
77	12 ⁺⁴ ₋₃	0	13 ⁺⁴ ₋₃	0	2 ⁺⁰ ₋₂	1	-0.71 ^{+0.00} _{-0.29}	1	0.11 ^{+0.04} _{-0.03}	0.12 ^{+0.04} _{-0.03}	0.02 ^{+0.00} _{-0.02}	-3E-01	1E+00
78	5 ⁺³ ₋₂	0	2 ⁺⁰ ₋₂	5	2 ⁺⁰ ₋₂	5	0.00 ^{+0.00} _{-0.00}	-2	0.05 ^{+0.03} _{-0.02}	0.02 ^{+0.00} _{-0.02}	0.02 ^{+0.00} _{-0.02}	7E-01	5E-02
79	2 ⁺⁰ ₋₂	5	2 ⁺⁰ ₋₂	5	2 ⁺⁰ ₋₂	5	0.00 ^{+0.00} _{-0.00}	-2	0.02 ^{+0.00} _{-0.02}	0.02 ^{+0.00} _{-0.02}	0.02 ^{+0.00} _{-0.02}	2E-01	4E-01
80	4 ⁺³ ₋₁	0	2 ⁺⁰ ₋₂	5	2 ⁺⁰ ₋₂	5	0.00 ^{+0.00} _{-0.00}	-2	0.04 ^{+0.03} _{-0.02}	0.02 ^{+0.00} _{-0.02}	0.02 ^{+0.00} _{-0.02}	8E-01	2E-02
81	8 ⁺⁴ ₋₂	0	2 ⁺⁰ ₋₂	5	5 ⁺³ ₋₂	0	0.38 ^{+0.62} _{-0.00}	-1	0.07 ^{+0.04} _{-0.03}	0.02 ^{+0.00} _{-0.02}	0.05 ^{+0.03} _{-0.02}	1E+00	1E-04
82	7 ⁺³ ₋₂	0	7 ⁺³ ₋₂	0	2 ⁺⁰ ₋₂	5	-0.49 ^{+0.00} _{-0.51}	1	0.07 ^{+0.03} _{-0.02}	0.06 ^{+0.03} _{-0.02}	0.02 ^{+0.00} _{-0.02}	2E-01	4E-01
83	4 ⁺³ ₋₂	0	2 ⁺⁰ ₋₂	5	2 ⁺⁰ ₋₂	5	0.00 ^{+0.00} _{-0.00}	-2	0.04 ^{+0.03} _{-0.02}	0.02 ^{+0.00} _{-0.02}	0.02 ^{+0.00} _{-0.02}	4E-01	2E-01
84	8 ⁺⁴ ₋₂	0	5 ⁺³ ₋₂	0	2 ⁺⁰ ₋₂	5	-0.40 ^{+0.00} _{-0.60}	1	0.07 ^{+0.04} _{-0.03}	0.05 ^{+0.03} _{-0.02}	0.02 ^{+0.00} _{-0.02}	9E-01	1E-02
85	3 ⁺³ ₋₁	0	2 ⁺⁰ ₋₂	1	5 ⁺³ ₋₂	0	0.37 ^{+0.63} _{-0.00}	-1	0.03 ^{+0.03} _{-0.02}	0.02 ^{+0.00} _{-0.02}	0.04 ^{+0.03} _{-0.02}	1E+00	6E-03
86	9 ⁺⁴ ₋₃	0	9 ⁺⁴ ₋₃	0	2 ⁺⁰ ₋₂	5	-0.60 ^{+0.00} _{-0.40}	1	0.09 ^{+0.04} _{-0.03}	0.08 ^{+0.04} _{-0.03}	0.02 ^{+0.00} _{-0.02}	2E-02	6E-01
87	4 ⁺³ ₋₁	0	2 ⁺⁰ ₋₂	5	2 ⁺⁰ ₋₂	5	0.00 ^{+0.00} _{-0.00}	-2	0.04 ^{+0.03} _{-0.02}	0.02 ^{+0.00} _{-0.02}	0.02 ^{+0.00} _{-0.02}	2E-01	4E-01

TABLE 28:

Counts, count rates and AE detection significance and no-source probabilities for X-ray point sources in HCG 92 (online only).

88	2^{+0}_{-2}	5	2^{+0}_{-2}	5	2^{+0}_{-2}	5	$0.00^{+0.00}_{-0.00}$	-2	$0.02^{+0.00}_{-0.02}$	$0.02^{+0.00}_{-0.02}$	$0.02^{+0.00}_{-0.02}$	4E-01	2E-01
89	76^{+9}_{-8}	0	52^{+8}_{-7}	0	23^{+6}_{-4}	0	$-0.37^{+0.12}_{-0.11}$	0	$0.68^{+0.09}_{-0.08}$	$0.46^{+0.07}_{-0.06}$	$0.21^{+0.05}_{-0.04}$	4E+00	7E-24
90	32^{+6}_{-5}	0	32^{+6}_{-5}	0	2^{+0}_{-2}	5	$-0.87^{+0.00}_{-0.13}$	1	$0.29^{+0.06}_{-0.05}$	$0.29^{+0.06}_{-0.05}$	$0.02^{+0.00}_{-0.02}$	3E-02	6E-01
91	52^{+8}_{-7}	0	39^{+7}_{-6}	0	12^{+4}_{-3}	0	$-0.51^{+0.14}_{-0.13}$	0	$0.46^{+0.07}_{-0.06}$	$0.35^{+0.06}_{-0.06}$	$0.11^{+0.04}_{-0.03}$	3E+00	4E-11
92	4^{+3}_{-2}	0	2^{+0}_{-2}	5	3^{+3}_{-1}	0	$0.21^{+0.79}_{-0.00}$	-1	$0.04^{+0.03}_{-0.02}$	$0.02^{+0.00}_{-0.02}$	$0.03^{+0.03}_{-0.02}$	1E+00	1E-02
93	4^{+3}_{-2}	0	2^{+0}_{-2}	5	2^{+0}_{-2}	5	$0.00^{+0.00}_{-0.00}$	-2	$0.04^{+0.03}_{-0.02}$	$0.02^{+0.00}_{-0.02}$	$0.02^{+0.00}_{-0.02}$	5E-01	2E-01
94C	3375^{+59}_{-58}	0	430^{+21}_{-20}	0	2944^{+55}_{-54}	0	$0.74^{+0.01}_{-0.01}$	0	$29.91^{+0.52}_{-0.51}$	$3.82^{+0.19}_{-0.18}$	$26.09^{+0.49}_{-0.48}$	5E+01	0E+00
95C	138^{+12}_{-11}	0	103^{+11}_{-10}	0	35^{+7}_{-5}	0	$-0.49^{+0.08}_{-0.08}$	0	$1.23^{+0.11}_{-0.10}$	$0.91^{+0.10}_{-0.09}$	$0.31^{+0.06}_{-0.05}$	5E+00	2E-27
96	2^{+0}_{-2}	5	2^{+0}_{-2}	5	2^{+0}_{-2}	5	$0.00^{+0.00}_{-0.00}$	-2	$0.02^{+0.00}_{-0.02}$	$0.02^{+0.00}_{-0.02}$	$0.02^{+0.00}_{-0.02}$	1E-01	5E-01
97	13^{+4}_{-3}	0	8^{+4}_{-2}	0	5^{+3}_{-2}	0	$-0.24^{+0.32}_{-0.29}$	0	$0.12^{+0.04}_{-0.03}$	$0.07^{+0.04}_{-0.03}$	$0.05^{+0.03}_{-0.02}$	1E+00	2E-04
98	4^{+3}_{-2}	0	4^{+3}_{-2}	0	2^{+0}_{-2}	5	$-0.30^{+0.00}_{-0.70}$	1	$0.04^{+0.03}_{-0.02}$	$0.04^{+0.03}_{-0.02}$	$0.02^{+0.00}_{-0.02}$	7E-02	6E-01
99	5^{+3}_{-2}	0	2^{+0}_{-2}	5	4^{+3}_{-2}	0	$0.34^{+0.66}_{-0.00}$	-1	$0.05^{+0.03}_{-0.02}$	$0.02^{+0.00}_{-0.02}$	$0.04^{+0.03}_{-0.02}$	1E+00	2E-03
100	10^{+4}_{-3}	0	9^{+4}_{-3}	0	2^{+0}_{-2}	5	$-0.59^{+0.00}_{-0.41}$	1	$0.09^{+0.04}_{-0.03}$	$0.08^{+0.04}_{-0.03}$	$0.02^{+0.00}_{-0.02}$	5E-01	2E-01
101	2^{+0}_{-2}	5	2^{+0}_{-2}	5	2^{+0}_{-2}	1	$0.00^{+0.00}_{-0.00}$	-2	$0.02^{+0.00}_{-0.02}$	$0.02^{+0.00}_{-0.02}$	$0.02^{+0.00}_{-0.02}$	-4E-01	1E+00
102	26^{+6}_{-5}	0	9^{+4}_{-3}	0	17^{+5}_{-4}	0	$0.30^{+0.20}_{-0.22}$	0	$0.24^{+0.06}_{-0.05}$	$0.08^{+0.04}_{-0.03}$	$0.15^{+0.05}_{-0.04}$	3E+00	7E-18
103	58^{+22}_{-17}	0	35^{+7}_{-5}	0	23^{+5}_{-4}	0	$-0.21^{+0.14}_{-0.14}$	0	$0.52^{+0.08}_{-0.07}$	$0.31^{+0.06}_{-0.05}$	$0.21^{+0.05}_{-0.04}$	4E+00	3E-27
104	12^{+4}_{-3}	0	10^{+4}_{-3}	0	2^{+0}_{-2}	5	$-0.63^{+0.00}_{-0.37}$	1	$0.11^{+0.04}_{-0.03}$	$0.10^{+0.04}_{-0.03}$	$0.02^{+0.00}_{-0.02}$	3E-01	4E-01
105	43^{+7}_{-6}	0	29^{+20}_{-15}	0	13^{+4}_{-3}	0	$-0.37^{+0.16}_{-0.15}$	0	$0.39^{+0.07}_{-0.06}$	$0.26^{+0.05}_{-0.05}$	$0.12^{+0.04}_{-0.03}$	3E+00	8E-09
106	104^{+11}_{-10}	0	79^{+9}_{-8}	0	25^{+6}_{-5}	0	$-0.51^{+0.10}_{-0.09}$	0	$0.93^{+0.10}_{-0.09}$	$0.70^{+0.09}_{-0.08}$	$0.23^{+0.05}_{-0.04}$	4E+00	3E-11
107	390^{+20}_{-19}	0	295^{+18}_{-17}	0	95^{+10}_{-9}	0	$-0.51^{+0.05}_{-0.04}$	0	$3.46^{+0.18}_{-0.18}$	$2.61^{+0.16}_{-0.15}$	$0.85^{+0.10}_{-0.09}$	9E+00	0E+00
108	25^{+6}_{-5}	0	20^{+5}_{-4}	0	5^{+3}_{-2}	0	$-0.57^{+0.21}_{-0.17}$	0	$0.23^{+0.05}_{-0.04}$	$0.18^{+0.05}_{-0.04}$	$0.05^{+0.03}_{-0.02}$	1E+00	8E-04
109	16^{+5}_{-4}	0	12^{+4}_{-3}	0	3^{+3}_{-1}	0	$-0.52^{+0.28}_{-0.23}$	0	$0.14^{+0.05}_{-0.04}$	$0.11^{+0.04}_{-0.03}$	$0.03^{+0.03}_{-0.02}$	1E+00	6E-03
110	162^{+13}_{-12}	0	114^{+11}_{-10}	0	48^{+8}_{-6}	0	$-0.41^{+0.08}_{-0.07}$	0	$1.44^{+0.12}_{-0.11}$	$1.01^{+0.10}_{-0.09}$	$0.43^{+0.07}_{-0.06}$	6E+00	0E+00
111	2^{+0}_{-2}	5	2^{+0}_{-2}	5	2^{+0}_{-2}	1	$0.00^{+0.00}_{-0.00}$	-2	$0.02^{+0.00}_{-0.02}$	$0.02^{+0.00}_{-0.02}$	$0.02^{+0.00}_{-0.02}$	-6E-01	1E+00
112	8^{+4}_{-2}	0	2^{+0}_{-2}	5	4^{+3}_{-2}	0	$0.33^{+0.67}_{-0.00}$	-1	$0.07^{+0.04}_{-0.02}$	$0.02^{+0.00}_{-0.02}$	$0.04^{+0.03}_{-0.02}$	1E+00	1E-03
113	11^{+4}_{-3}	0	2^{+0}_{-2}	5	9^{+4}_{-2}	0	$0.56^{+0.44}_{-0.00}$	-1	$0.10^{+0.04}_{-0.03}$	$0.02^{+0.00}_{-0.02}$	$0.08^{+0.04}_{-0.03}$	2E+00	1E-05
114	2^{+0}_{-2}	5	2^{+0}_{-2}	5	2^{+0}_{-2}	1	$0.00^{+0.00}_{-0.00}$	-2	$0.02^{+0.00}_{-0.02}$	$0.02^{+0.00}_{-0.02}$	$0.02^{+0.00}_{-0.02}$	-2E-01	8E-01
115	9^{+4}_{-2}	0	10^{+4}_{-3}	0	2^{+0}_{-2}	1	$-0.62^{+0.00}_{-0.38}$	1	$0.08^{+0.04}_{-0.03}$	$0.09^{+0.04}_{-0.03}$	$0.02^{+0.00}_{-0.02}$	-4E-01	9E-01
116	13^{+4}_{-3}	0	10^{+4}_{-3}	0	2^{+0}_{-2}	5	$-0.61^{+0.00}_{-0.39}$	1	$0.12^{+0.04}_{-0.03}$	$0.09^{+0.04}_{-0.03}$	$0.02^{+0.00}_{-0.02}$	7E-01	2E-01
117	2^{+0}_{-2}	5	2^{+0}_{-2}	1	2^{+0}_{-2}	5	$0.00^{+0.00}_{-0.00}$	-2	$0.02^{+0.00}_{-0.02}$	$0.02^{+0.00}_{-0.02}$	$0.02^{+0.00}_{-0.02}$	8E-01	7E-02
118	2^{+0}_{-2}	5	2^{+0}_{-2}	1	2^{+0}_{-2}	5	$0.00^{+0.00}_{-0.00}$	-2	$0.02^{+0.00}_{-0.02}$	$0.02^{+0.00}_{-0.02}$	$0.02^{+0.00}_{-0.02}$	4E-01	3E-01
119	5^{+3}_{-2}	0	2^{+0}_{-2}	1	5^{+3}_{-2}	0	$0.42^{+0.58}_{-0.00}$	-1	$0.04^{+0.03}_{-0.02}$	$0.02^{+0.00}_{-0.02}$	$0.05^{+0.03}_{-0.02}$	2E+00	4E-04
120	2^{+0}_{-2}	1	2^{+0}_{-2}	5	2^{+0}_{-2}	1	$0.00^{+0.00}_{-0.00}$	-2	$0.02^{+0.00}_{-0.02}$	$0.02^{+0.00}_{-0.02}$	$0.02^{+0.00}_{-0.02}$	-1E+00	1E+00
121	11^{+4}_{-3}	0	2^{+0}_{-2}	5	7^{+3}_{-2}	0	$0.50^{+0.50}_{-0.00}$	-1	$0.10^{+0.04}_{-0.03}$	$0.02^{+0.00}_{-0.02}$	$0.07^{+0.03}_{-0.02}$	2E+00	3E-04
122	2^{+0}_{-2}	5	2^{+0}_{-2}	5	2^{+0}_{-2}	5	$0.00^{+0.00}_{-0.00}$	-2	$0.02^{+0.00}_{-0.02}$	$0.02^{+0.00}_{-0.02}$	$0.02^{+0.00}_{-0.02}$	8E-01	7E-02
123	17^{+5}_{-4}	0	2^{+0}_{-2}	5	16^{+5}_{-4}	0	$0.73^{+0.27}_{-0.00}$	-1	$0.16^{+0.05}_{-0.04}$	$0.02^{+0.00}_{-0.02}$	$0.14^{+0.05}_{-0.04}$	3E+00	7E-10
124	2^{+0}_{-2}	5	2^{+0}_{-2}	5	2^{+0}_{-2}	5	$0.00^{+0.00}_{-0.00}$	-2	$0.02^{+0.00}_{-0.02}$	$0.02^{+0.00}_{-0.02}$	$0.02^{+0.00}_{-0.02}$	1E-01	5E-01
125	6^{+3}_{-2}	0	5^{+3}_{-2}	0	2^{+0}_{-2}	5	$-0.42^{+0.00}_{-0.58}$	1	$0.05^{+0.03}_{-0.02}$	$0.05^{+0.03}_{-0.02}$	$0.02^{+0.00}_{-0.02}$	5E-02	5E-01
126	2^{+0}_{-2}	5	2^{+0}_{-2}	5	2^{+0}_{-2}	5	$0.00^{+0.00}_{-0.00}$	-2	$0.02^{+0.00}_{-0.02}$	$0.02^{+0.00}_{-0.02}$	$0.02^{+0.00}_{-0.02}$	4E-01	3E-01
127	8^{+4}_{-2}	0	3^{+3}_{-1}	0	5^{+3}_{-2}	0	$0.17^{+0.38}_{-0.41}$	0	$0.08^{+0.04}_{-0.03}$	$0.03^{+0.03}_{-0.02}$	$0.05^{+0.03}_{-0.02}$	1E+00	3E-03
128	6^{+3}_{-2}	0	2^{+0}_{-2}	5	3^{+3}_{-1}	0	$0.17^{+0.83}_{-0.00}$	-1	$0.06^{+0.03}_{-0.02}$	$0.02^{+0.00}_{-0.02}$	$0.03^{+0.03}_{-0.02}$	1E+00	4E-02
129	7^{+3}_{-2}	0	7^{+3}_{-2}	0	2^{+0}_{-2}	1	$-0.52^{+0.00}_{-0.48}$	1	$0.07^{+0.03}_{-0.02}$	$0.07^{+0.03}_{-0.02}$	$0.02^{+0.00}_{-0.02}$	-4E-02	6E-01
130	2^{+0}_{-2}	5	2^{+0}_{-2}	5	2^{+0}_{-2}	1	$0.00^{+0.00}_{-0.00}$	-2	$0.02^{+0.00}_{-0.02}$	$0.02^{+0.00}_{-0.02}$	$0.02^{+0.00}_{-0.02}$	-2E-02	6E-01
131	2^{+0}_{-2}	5	2^{+0}_{-2}	1	4^{+3}_{-2}	0	$0.00^{+0.00}_{-0.00}$	-2	$0.02^{+0.00}_{-0.02}$	$0.02^{+0.00}_{-0.02}$	$0.04^{+0.03}_{-0.02}$	1E+00	3E-02
132	7^{+3}_{-2}	0	7^{+3}_{-2}	0	2^{+0}_{-2}	5	$-0.51^{+0.00}_{-0.49}$	1	$0.07^{+0.03}_{-0.02}$	$0.07^{+0.03}_{-0.02}$	$0.02^{+0.00}_{-0.02}$	2E-02	6E-01

TABLE 28:

Counts, count rates and AE detection significance and no-source probabilities for X-ray point sources in HCG 92 (online only).

133	9^{+4}_{-3}	0	2^{+0}_{-2}	1	10^{+4}_{-3}	0	$0.61^{+0.39}_{-0.00}$	-1	$0.09^{+0.04}_{-0.03}$	$0.02^{+0.00}_{-0.02}$	$0.09^{+0.04}_{-0.03}$	2E+00	6E-04
134	22^{+5}_{-4}	0	15^{+5}_{-3}	0	7^{+3}_{-2}	0	$-0.37^{+0.24}_{-0.21}$	0	$0.20^{+0.05}_{-0.04}$	$0.14^{+0.04}_{-0.03}$	$0.06^{+0.03}_{-0.02}$	1E+00	2E-02
135	16^{+5}_{-4}	0	10^{+4}_{-3}	0	6^{+3}_{-2}	0	$-0.26^{+0.29}_{-0.27}$	0	$0.14^{+0.05}_{-0.04}$	$0.09^{+0.04}_{-0.03}$	$0.05^{+0.03}_{-0.02}$	1E+00	8E-02
136	2^{+0}_{-2}	5	2^{+0}_{-2}	5	2^{+0}_{-2}	1	$0.00^{+0.00}_{-0.00}$	-2	$0.02^{+0.00}_{-0.02}$	$0.02^{+0.00}_{-0.02}$	$0.02^{+0.00}_{-0.02}$	-5E-01	9E-01
137	2^{+0}_{-2}	5	2^{+0}_{-2}	5	2^{+0}_{-2}	1	$0.00^{+0.00}_{-0.00}$	-2	$0.02^{+0.00}_{-0.02}$	$0.02^{+0.00}_{-0.02}$	$0.02^{+0.00}_{-0.02}$	-7E-01	9E-01
138	7^{+3}_{-2}	0	9^{+4}_{-3}	0	2^{+0}_{-2}	1	$-0.60^{+0.00}_{-0.40}$	1	$0.07^{+0.03}_{-0.02}$	$0.09^{+0.04}_{-0.03}$	$0.02^{+0.00}_{-0.02}$	-7E-01	8E-01
139	15^{+5}_{-3}	0	2^{+0}_{-2}	5	12^{+4}_{-3}	0	$0.65^{+0.35}_{-0.00}$	-1	$0.14^{+0.04}_{-0.03}$	$0.02^{+0.00}_{-0.02}$	$0.11^{+0.04}_{-0.03}$	2E+00	2E-05
140	24^{+6}_{-4}	0	13^{+4}_{-3}	0	10^{+4}_{-3}	0	$-0.13^{+0.23}_{-0.22}$	0	$0.22^{+0.05}_{-0.04}$	$0.12^{+0.04}_{-0.03}$	$0.09^{+0.04}_{-0.03}$	2E+00	6E-03
141	2^{+0}_{-2}	5	2^{+0}_{-2}	1	2^{+0}_{-2}	5	$0.00^{+0.00}_{-0.00}$	-2	$0.02^{+0.00}_{-0.02}$	$0.02^{+0.00}_{-0.02}$	$0.02^{+0.00}_{-0.02}$	6E-01	2E-01
142	2^{+0}_{-2}	1	2^{+0}_{-2}	5	2^{+0}_{-2}	1	$0.00^{+0.00}_{-0.00}$	-2	$0.02^{+0.00}_{-0.02}$	$0.02^{+0.00}_{-0.02}$	$0.02^{+0.00}_{-0.02}$	-2E+00	1E+00
143	4^{+3}_{-2}	0	2^{+0}_{-2}	5	2^{+0}_{-2}	5	$0.00^{+0.00}_{-0.00}$	-2	$0.04^{+0.03}_{-0.02}$	$0.02^{+0.00}_{-0.02}$	$0.02^{+0.00}_{-0.02}$	1E+00	8E-03
144	2^{+0}_{-2}	1	2^{+0}_{-2}	1	2^{+0}_{-2}	1	$0.00^{+0.00}_{-0.00}$	-2	$0.02^{+0.00}_{-0.02}$	$0.02^{+0.00}_{-0.02}$	$0.02^{+0.00}_{-0.02}$	-2E-01	1E+00
145F	30^{+6}_{-5}	0	27^{+6}_{-5}	0	2^{+0}_{-2}	5	$-0.83^{+0.00}_{-0.17}$	1	$0.27^{+0.06}_{-0.05}$	$0.25^{+0.06}_{-0.05}$	$0.02^{+0.00}_{-0.02}$	7E-01	2E-01
146	21^{+4}_{-4}	0	4^{+3}_{-2}	0	17^{+5}_{-4}	0	$0.61^{+0.18}_{-0.23}$	0	$0.19^{+0.05}_{-0.04}$	$0.04^{+0.03}_{-0.02}$	$0.15^{+0.05}_{-0.04}$	3E+00	5E-06
147	10^{+4}_{-3}	0	9^{+4}_{-3}	0	2^{+0}_{-2}	5	$-0.59^{+0.00}_{-0.41}$	1	$0.10^{+0.04}_{-0.03}$	$0.09^{+0.04}_{-0.03}$	$0.02^{+0.00}_{-0.02}$	3E-01	4E-01
148	58^{+8}_{-7}	0	44^{+7}_{-6}	0	14^{+4}_{-3}	0	$-0.51^{+0.13}_{-0.12}$	0	$0.52^{+0.08}_{-0.07}$	$0.39^{+0.07}_{-0.06}$	$0.13^{+0.04}_{-0.03}$	2E+00	3E-04
149	2^{+0}_{-2}	1	2^{+0}_{-2}	1	2^{+0}_{-2}	5	$0.00^{+0.00}_{-0.00}$	-2	$0.02^{+0.00}_{-0.02}$	$0.02^{+0.00}_{-0.02}$	$0.02^{+0.00}_{-0.02}$	5E-01	3E-01